



Title	Mechanochemical Synthesis of Organometallic Compounds and Their Applications to Organic Synthesis
Author(s)	Takahashi, Rina
Citation	北海道大学. 博士(工学) 甲第14917号
Issue Date	2022-03-24
DOI	10.14943/doctoral.k14917
Doc URL	http://hdl.handle.net/2115/85287
Type	theses (doctoral)
File Information	TAKAHASHI_Rina.pdf



[Instructions for use](#)

Ph.D. thesis

**Mechanochemical Synthesis of
Organometallic Compounds and Their
Applications to Organic Synthesis**

有機金属化合物のメカノケミカル合成と有機合成への応用

Hokkaido University

Graduate School of Chemical Sciences and Engineering

Organoelement Laboratory

Rina Takahashi

2022

Contents

General Introduction	2
Chapter 1. Mechanochemical Synthesis of Palladium Oxidative Addition Complexes in Air via Air-sensitive Pd(0) Intermediates	15
Chapter 2. Development of Air- and Moisture-stable Xantphos-ligated Palladium Precatalyst for Cross-Coupling Reactions	49
Chapter 3. Mechanochemical Synthesis of Magnesium-based Carbon Nucleophiles and Their Application to Organic Synthesis	85
List of publications	155
Acknowledgements	156

General Introduction

Mechanochemistry is a diverse and broad research area. It can be divided into several regions depending on mechanical stimuli or target materials. For example, trituration (chemistry induced by grinding and milling), tribochemistry (the chemistry of surfaces in contact), sonochemistry (chemistry induced by ultrasound), macromolecular mechanochemistry (single molecule AFM, polymer chain breakage, shape memory, biological motion, etc.), and shock-induced solid-state chemistry (Figure 1).¹ According to the Gold Book of the International Union of Pure and Applied Chemistry (IUPAC), “mechano-chemical reaction” is defined as “a chemical reaction that is induced by the direct absorption of mechanical energy.”² Such mechanochemical reactions using ball milling have received increasing attention from the area of organic synthesis as an alternative activation method which complements heat, photoirradiation, and electric current.^{3–11} In this thesis, I focus on mechanochemical organic reactions induced by grinding or milling using automated ball mills.

Research area of mechanochemistry

Trituration: grinding, milling

- solid-liquid
 - solid-solid
 - hard solids (inorganic)
 - hard-soft solids (MOFs)
 - soft solids (organic)
- *topic in this thesis

Tribochemistry: surface friction

- surface electrification
- surface modification
- Lubrication

Sonochemistry: ultrasound

- liquid/gas
- liquid/liquid
- liquid/solid

Macromolecular mechanochemistry

- breakage of polymer chains
- mechanophores
- single molecular AFM
- shape memory
- biological motion

Shock-induced solid-state chemistry

Figure 1. Categorized research area of mechanochemistry.

The earliest mechanochemical reactions were conducted using a mortar and a pestle. These reactions highly depended on operators and the conditions of the apparatus they used. It was difficult to control mechanical impact precisely and conduct reactions for a long reaction time. Therefore, automated ball mills are recently used and reagents are ground in a closed reaction vessel (jar) charged with balls. Ball mills conduct grinding in a reproducible manner and allow long-time reactions. The common types of automated ball mills for laboratory-scale experiments are a mixer mill (a vibrational mill) and a planetary ball mill. In the case of a mixer mill, the reaction jars are mounted horizontally and rapidly shaken from side to side at the desired frequency. The main mechanical

energy applied to the reaction mixture is an impact force. In the case of a planetary mill, the reaction jars rotate at high speed in the reverse direction to that of the main sun wheel, which results in the balls grinding the solids in the jars. Importantly, the main mechanical energy in a planetary mill is a shear force. Additionally, for pilot and manufacture scales, stirred media ball mills are used. The Outotec HIGMill, for example, has a volume of 30 000 L and can be used at >1000 kg scales.¹²

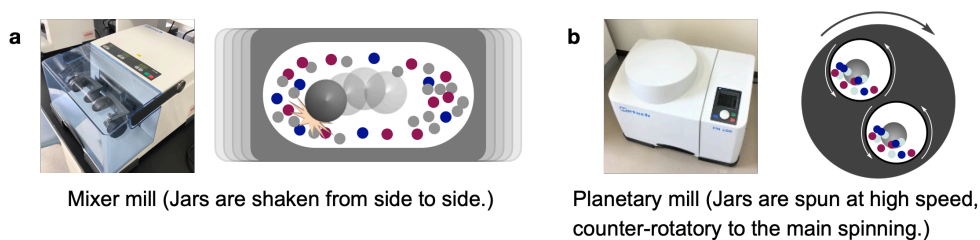


Figure 2. Common types of automated ball mills for laboratory-scale synthesis.

In addition to reaction time and temperature, various parameters can be tuned for organic reactions with ball mills: milling frequency, jar size, ball diameter, number of balls, volume of reactants, and volume ratio of balls/reactants/vacant space in the jar. The materials of jars and balls are an important factor in many cases because the hardness and density of the material affect the strength of the mechanical force. One of the most common materials is stainless steel. Other easily available materials for the jars and balls are for example, ceramics (tungsten carbide, zirconium oxide, sintered aluminum oxide, and silicon nitride), plastics (Teflon, PMMA, etc.), and agate.

There is another critical parameter for mechanochemical reactions. The addition of a small amount of liquid sometimes enhances the reactivity or changes their selectivity. This is termed “liquid-assisted grinding (LAG)”. A LAG parameter (η) was defined as the ratio of liquid (μL) to the combined weights of solid reactants (mg).¹³ A value of $\eta = 0$ corresponds to neat grinding without any liquid additive, and a value in the range of $0 < \eta \leq 1$ corresponds to LAG. Reaction mixtures with higher η values would form a slurry ($1 < \eta$) or homogenous dissolved solutions ($10 \leq \eta$). These do not fall under the category of LAGs.

Important parameters for mechanochemical reactions using ball mills

- Milling frequency: 0.3–30 Hz
- Jar size: 1.5 mL, 5 mL, 10 mL, 50 mL, ...
- Ball diameter
- Number of balls
- Volume of reactants
- Volume ratio of balls : reactants : vacant space
- Materials of jars and balls
 - stainless steel (common)
 - tungsten carbide
 - zirconium oxide
 - aluminum oxide
 - silicon nitride
 - plastics (Teflon, PMMA)
 - agate



- Liquid assisted grinding (LAG)

$$\text{parameter } \eta = \frac{\text{volume of liquid additive } [\mu\text{L}]}{\text{weights of solid reactants } [\text{mg}]}$$

$\eta = 0$ neat grinding
 $0 < \eta \leq 1$ liquid assisted grinding
 $1 < \eta < 10$ slurry
 $10 \leq \eta$ homogenous dissolved solution

Figure 3. Key parameters for mechanochemical reactions.

A representative procedure of the mechanochemical reactions using a mixer mill is shown in Figure 4. One or more balls are placed in a milling jar and reagents are added. The jar is tightly closed and placed in a mixer mill. The reactants are ground for a preset time at a preset milling frequency. In most cases, mechanochemical reactions do not require special operating conditions such as glove box operation under inert gas. The main reason for the low impact of the presence of moisture and oxygen would be explained by the low diffusion efficiency of gaseous water and oxygen in crystalline or amorphous solid-state reaction mixtures in a milling jar.

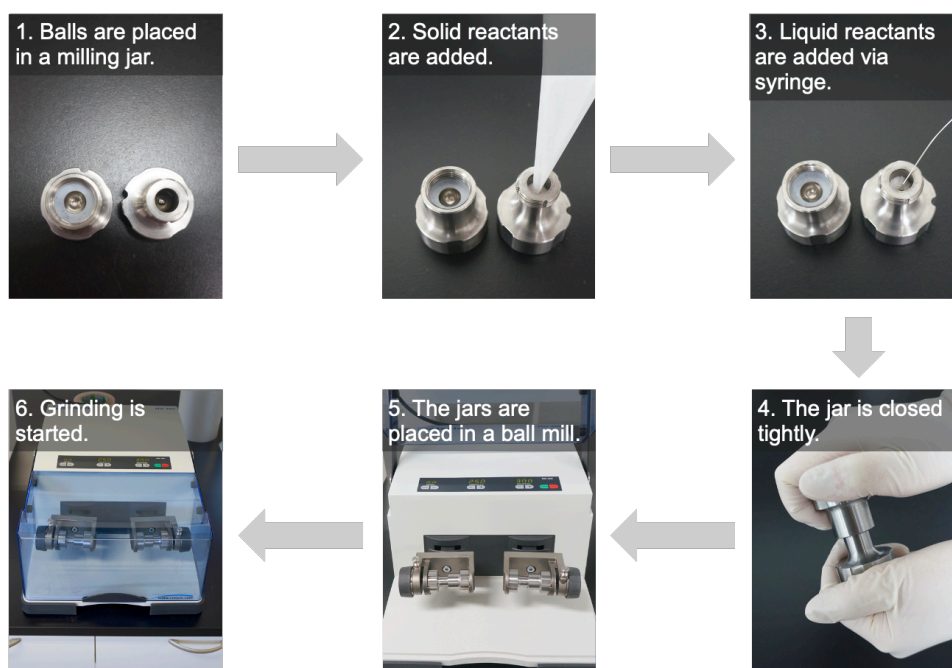


Figure 4. Setting up procedure for mechanochemical reactions using automated ball mills.

In order to understand how mechanochemical reactions proceed, a variety of solid-state characterization techniques are employed for *ex-situ* and *in-situ* analysis. Powder X-ray diffraction (PXRD) is a powerful tool for the *ex-situ* characterization of crystalline powders. Reaction mixtures can be analyzed quickly and quantitatively without preparing single crystals by comparing the reagents and product diffraction patterns. PXRD is also useful to characterize the structure of unstable or unobtainable compounds in solution. However, the reaction mixtures often become amorphous by prolonged grinding, and their diffraction signals are lost. Fourier-transform infrared spectroscopy (FTIR) and Raman spectroscopy are applicable to both crystalline and amorphous compounds. These techniques can measure the relative energies of chemical bonds. Therefore these techniques qualitatively assess changes in covalent bond interactions. In addition, solid-state nuclear magnetic resonance spectroscopy (solid-state NMR) is also useful to analyze the chemical structure of solid materials independent of compound crystallinity.¹⁴

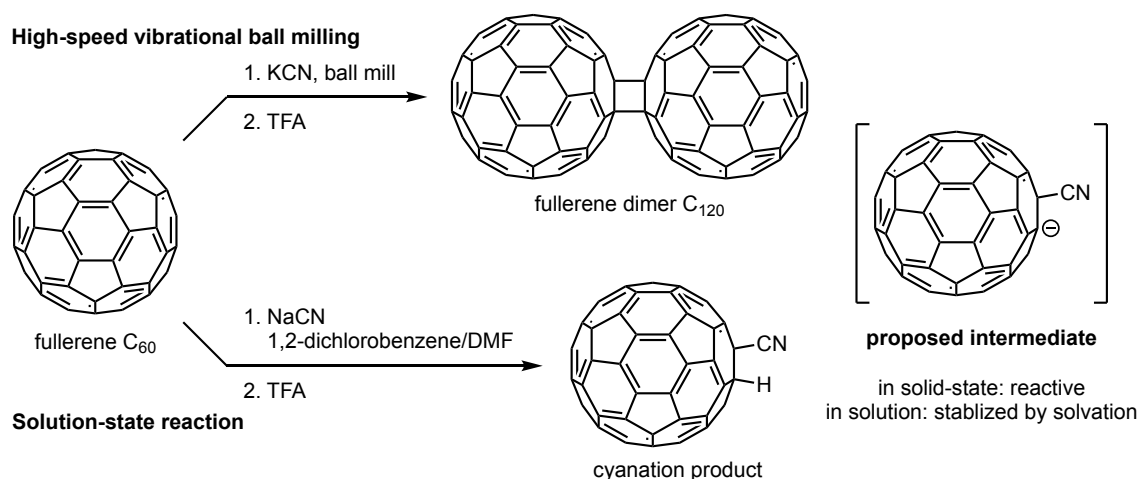
Electron dispersive X-ray spectroscopy (EDS) introduced to a scanning electron microscope (SEM) enables the elemental analysis of the material surface. This method can evaluate the dispersion of reagents or catalysts and contamination from milling materials.¹⁵ SEM and transmission electron microscope (TEM) are also used to measure particle size of materials.

Recently, several methods for *in-situ* monitoring of mechanochemical reactions have been developed. For example, temperature monitoring,¹⁶ pressure monitoring,¹⁷ PXRD,¹⁸⁻²⁰ and Raman spectroscopy²⁰⁻²² can be performed during mechanochemical reactions. Such *in situ* monitoring methods allow to analyze reaction progress of the mechanochemical reactions without any interruption of the ball milling process and provide important insights into the reaction mechanisms of ball mill reactions. However, the *in situ* monitoring of mechanochemical reactions is still limited because the preparation of special equipment is required.

By these developments, a variety of organic transformations have been performed under mechanochemical conditions as an environmentally friendly alternative to conventional solution-based reactions in the past two decades.³⁻¹¹ Mechanochemical organic reactions are conducted using solid reactants under solvent-less conditions and do not require the bulk dissolution of reactants. This method can avoid harmful organic solvents and shorten reaction times compared to conventional solution-based reactions using a large amount of organic solvents.

Organic reactions that do not require the use of solvents have other advantages. The

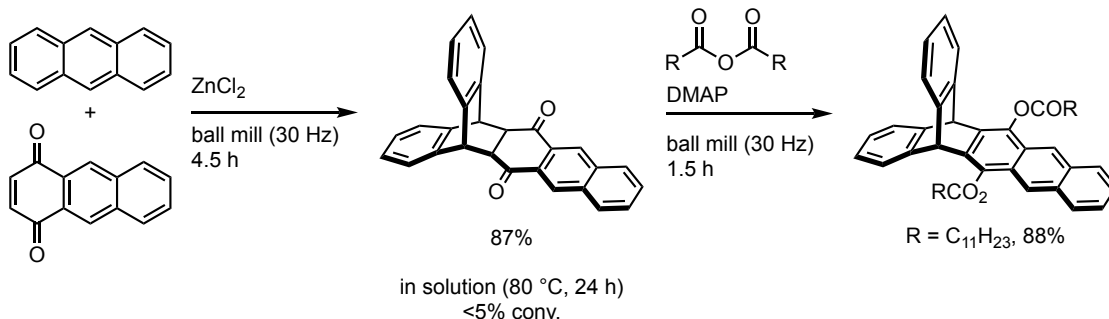
mechanochemical synthesis that is not affected by solubility issues allows access to unexplored chemical space to discover new organic materials. In addition, the unique reactivities caused by characteristic environments of the solid-state mechanochemical reactions have been reported. For example, Komatsu and co-workers investigated the modification of fullerene, which is low-soluble to organic solvents, by using high-speed vibration milling.^{23–26} In 1997, they reported the first synthesis of fullerene dimer, C₁₂₀ (Scheme 1).²⁴ The reaction of fullerene with KCN was carried out using high-speed vibration ball milling for 30 minutes under nitrogen atmosphere to give unexpected fullerene dimer, C₁₂₀, in 18% yield after quenching the reaction with trifluoroacetic acid. On the other hand, the reaction of fullerene with NaCN in a solvent mixture of 1,2-dichlorobenzene and DMF provided cyanated fullerene in 29% yield. The difference of the product selectivity would come from the close location of the reactants in the solid-state and the stabilization of anionic intermediates by solvation in the solution-state.



Scheme 1. Difference in reactivity of fullerene C₆₀ under ball milling conditions and solution-state conditions.

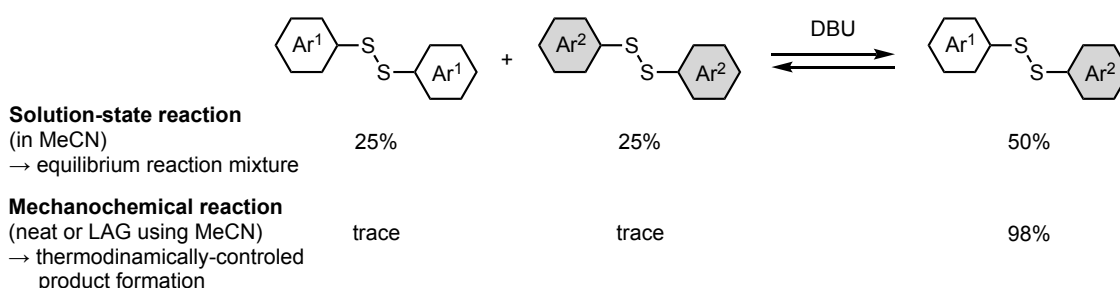
Strong reaction promoting effects of mechanochemical techniques sometimes lead to shorter reaction time and lower reaction temperature even when conventional solution-state chemistry suffers from solubility issues. In 2016, Swager and co-workers reported the preparation of highly rigid iptycenes via Diels-Alder reactions under solvent-free mechanochemical conditions (Scheme 2).²⁷ The preparation of iptycenes in solution-state reactions is often problematic due to their limited solubility and the requirement of harsh reaction conditions.^{28,29} In contrast, Diels-Alder reactions under solvent-free mechanochemical conditions proceeded in shorter reaction times to afford the desired products in excellent yield (>80%). Furthermore, the researchers demonstrated the

synthesis of molecular cage based on high order iptycene prepared by the developed mechanochemical reaction.



Scheme 2. Mechanochemical synthesis of an extended iptycene via Diels-Alder reaction.

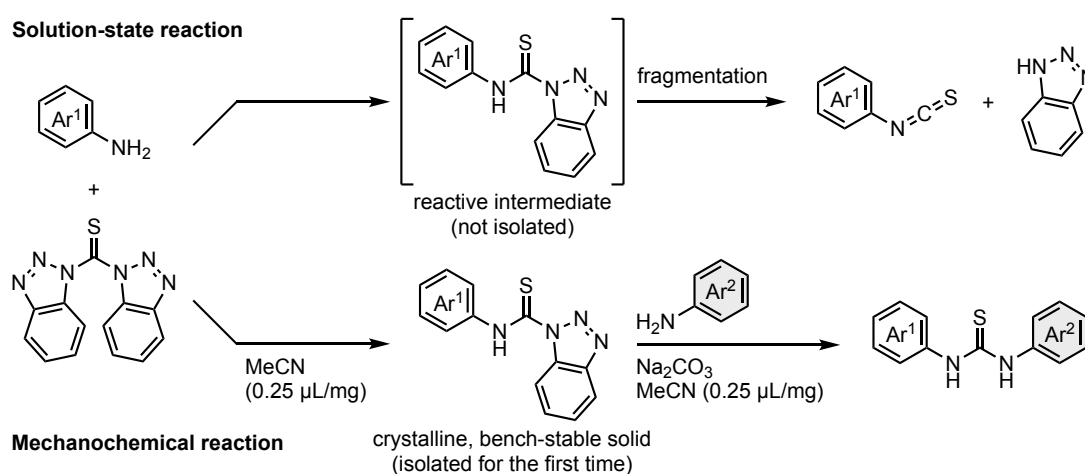
Neat grinding and LAG sometimes lead to different outcomes compared to conventional solution-state reactions. In 2011, Belenguer, Frišćić, and co-workers studied reversibility and thermodynamic product selectivity in mechanochemical reactions by using the disulfide metathesis reactions as the model reaction.³⁰ Mixing of two different aromatic disulfides provides a nonsymmetric heterodimer in the presence of a base catalyst. In solution-state reaction, the disulfide metathesis reaction provided the product mixture of two initial homodimeric disulfides and heterodimer with a statistical ratio of 1:1:2. In contrast, neat grinding or LAG afforded almost pure heterodimer in 98% yield. Probably, these selectivities were due to differences in the stabilities of the homodimers and heterodimers in solution and in the solid state.



Scheme 3. Difference in product ratio of disulfide metathesis reactions under solution-based and mechanochemical conditions.

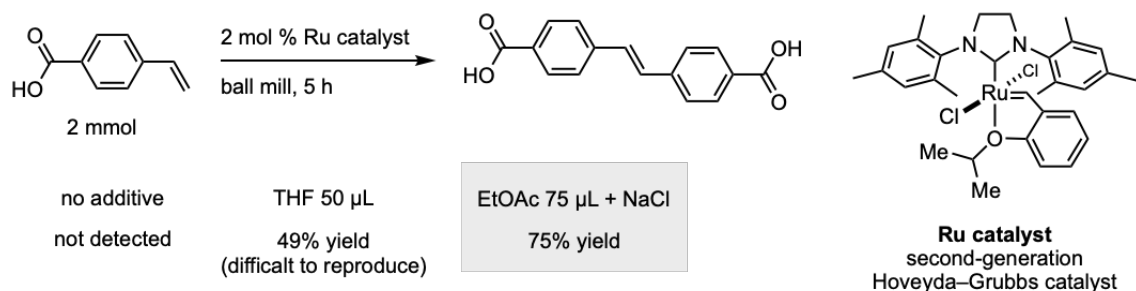
The crystallinity of compounds is also involved in product selectivity of mechanochemical synthesis. In 2015, Štrukil, Frišćić, and co-workers investigated the reaction between anilines and bis(benzotriazole)methanethione under the mechanochemical condition (Scheme 3).³¹ This reaction generally provided

corresponding isothiocyanates and benzotriazole via the formation of *N*-thiocarbamoyl benzotriazoles as reactive intermediates under conventional solution-state conditions. However, the mechanochemical reaction using LAG approach afforded *N*-thiocarbamoylbenzotriazoles as crystalline solids in high yields (>98%). The products were identified by solution- and solid-state NMR spectroscopy, PXRD, thermogravimetric analysis, and differential scanning calorimetry. Notably, the researchers found that these *N*-thiocarbamoylbenzotriazole products are bench-stable crystalline solids and can be stored for one year or more.



Scheme 4. Reactions between anilines and bis(benzotriazole)methanethione under solution-based and mechanochemical conditions.

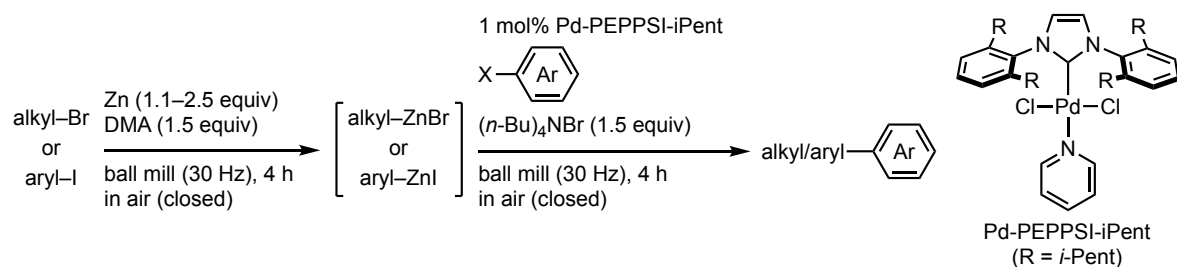
Mechanochemical reactions have been applied to more sensitive organic reactions involving transition-metal catalysts. In 2015, Frišćić and co-workers reported the mechanochemical approach for ruthenium-catalyzed olefin-metathesis including cross-metathesis and ring-closing metathesis.³³ This mechanochemical method can be applied to the reactions using a wide variety of solid and liquid olefins as substrates. A multigram scale synthesis is also reported. In this reaction system, the addition of solid auxiliaries such as NaCl or KCl was necessary for the high reaction efficiency and reproducibility. These additives were required to improve the mixing efficiency of the sticky reaction mixtures.



Scheme 5. Ruthenium-catalyzed olefin metathesis reaction under mechanochemical conditions.

Among various mechanochemical organic syntheses using transition metal catalysts, palladium-catalyzed cross-coupling reactions have actively been investigated.¹¹ Many researchers have developed the mechanochemical methods for Suzuki–Miyaura cross-coupling reactions, Mizoroki–Heck reactions, Sonogashira coupling reactions, Negishi coupling reactions, Buchwald–Hartwig amination, C–H arylation, and cross-coupling polymerization.

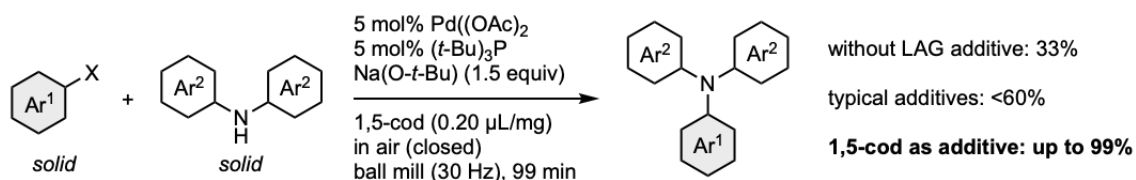
In 2018, Browne and co-workers reported the first example of the mechanochemical Negishi coupling reaction that was carried out in a one-pot, two-step process.³⁴ Various organozinc reagents were generated from alkyl bromides and aryl iodides using zinc granular under the mechanochemical condition. After the preparation of organozinc reagents, a coupling partner and a Pd catalyst were added to the reaction vessel and the reaction mixture was milled again. The desired products of Negishi coupling reaction were obtained in moderate to excellent yields in the presence of dimethylacetamide for the first step and tetrabutylammonium bromide for the second step.



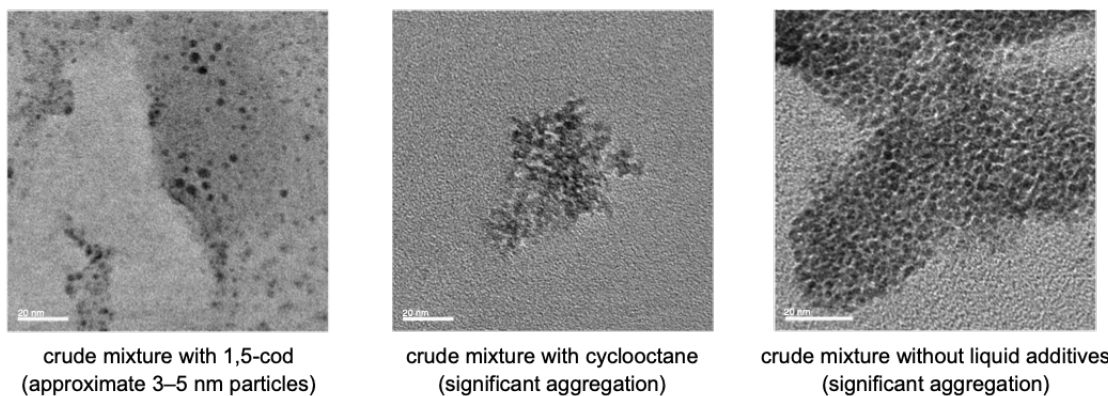
Scheme 6. Mechanochemical synthesis of organozinc reagents and palladium-catalyzed Negishi coupling reaction in a one-pot fashion.

Although the substrate scope of the pioneering studies in this area was mostly limited to liquid aryl halides, the cross-coupling reactions applicable to solid aryl halides have been developed. In 2019, Ito, Kubota, and co-workers reported the mechanochemical

Buchwald–Hartwig amination under the solid-state condition.³⁵ The performance of the mechanochemical reaction was dramatically improved by addition of olefins, in particular, 1,5-cyclooctadiene (cod). The olefin additives might act as dispersants for the palladium catalysts to suppress aggregation and as a stabilizer for the catalytically active Pd(0) species.



TEM images of palladium nanoparticles in the crude reaction mixtures



Scheme 7. Mechanochemical Buchwald–Hartwig amination of solid substrates in the presence of olefin additive as a dispersant.

Even though these cross-coupling reactions involved air- and moisture-sensitive species, such as palladium(0) intermediates and zinc-based carbon nucleophiles, most of these reactions can be carried out in the air. In the case of conventional solution-state reactions, however, many organometallic reagents and catalysts are highly reactive and therefore incompatible with exposure to the ambient atmosphere which includes oxygen and moisture. Preparation of such organometallic compounds usually requires the use of glove-box or high-vacuum Schlenk-lines and a large amount of dry and degassed solvents. These requirements are costly and demand special training for the operations. In this context, chemical processes that do not require such precautions are likely to substantially increase the practical utility of the targeted organic molecules. However, the benefits of mechanochemistry in the context of organometallic chemistry have not yet been explored systematically, and the potential applicability of highly sensitive reagents or intermediates

toward mechanochemical organometallic transformations under ambient conditions remains elusive.

In this context, I focused on the mechanochemical synthesis of organometallic reagents and transition-metal complexes to develop compelling alternatives to conventional synthetic procedures in solution. Compared to conventional solution-state reactions, air and moisture in reaction vessels would have little impact on mechanochemical reactions due to the low diffusion efficiency of oxygen and moisture in crystalline or amorphous solid-state reaction mixtures, composed by solid substrates and a small amount of liquid additives (Figure 5a). A small empty volume of the reaction vessels should also minimize the detrimental effect of air and moisture in the vessel on organometallic reactions (Figure 5b).

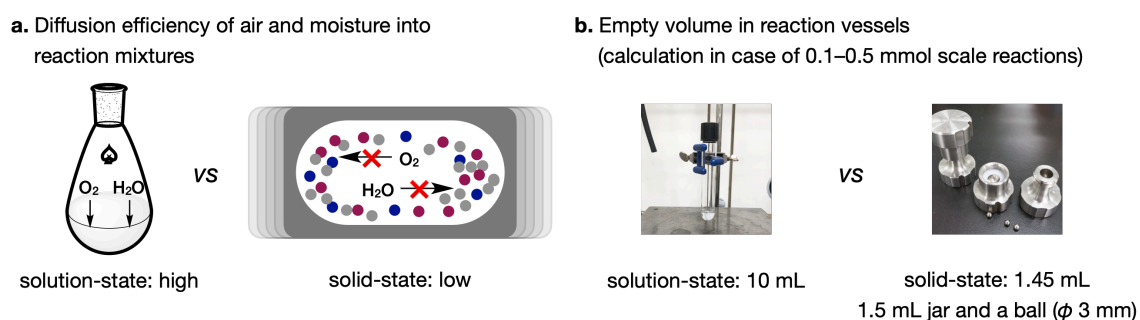


Figure 5. Comparison between conventional solution-based protocol and mechanochemical protocol in point of effects of air and moisture.

Chapter 1 describes the mechanochemical synthesis of palladium oxidative addition complexes with dialkylbiaryl phosphine ligands using highly oxygen-sensitive palladium(0) species in air. Palladium oxidative addition complexes obtained from oxidative addition reactions of aryl halides with palladium(0) have been widely used as catalyst precursors, in mechanistic studies of several cross-coupling reactions, and as aryl-group transfer reagents for modification of biomolecules and pharmaceuticals. The reported preparation of these complexes generally requires glove-box techniques because the formation of air-sensitive palladium(0) intermediates are involved before the oxidative addition, but the author demonstrated the mechanochemical synthesis of dialkylbiaryl phosphine-ligated palladium oxidative addition complexes using highly oxygen-sensitive palladium(0) species proceeded efficiently under ambient conditions.

Chapter 2 describes that the diphosphine-ligated palladium dialkyl complexes serve as powerful precatalysts for cross-coupling reactions. Xantphos-ligated palladium dialkyl complex, (Xantphos)Pd(CH₂TMS)₂, was unexpectedly obtained during the study of

chapter 1 and the author found that the palladium complex shows the high catalytic activity in carbon–carbon and carbon–heteroatom bond-forming reactions. The precatalyst can be activated thermally via rapid reductive elimination to form the catalytically active Pd(0) species and 1,2-bis(trimethylsilyl)ethane as a sole byproduct, which does not interfere with the catalyst.

Chapter 3 describes the mechanochemical synthesis of magnesium-based carbon nucleophiles and their application to organic synthesis. Grignard reagents in paste form were synthesized from magnesium turnings and a wide variety of organic halides by using ball milling techniques in the presence of a stoichiometric amount of ethers. The present mechanochemical synthesis of magnesium-based carbon nucleophiles and their reactions with various electrophiles can be carried out in air without the need for large amounts of dry and degassed solvents, special precautions, or synthetic techniques. The generation of the magnesium-based carbon nucleophiles under mechanochemical conditions was confirmed by near-edge X-ray absorption fine structure (NEXAFS) spectroscopy. In addition, the author achieved the synthesis of novel magnesium-based carbon nucleophiles from poorly soluble aryl halides that are incompatible with conventional solution-based conditions.

Reference

- 1) Suslick, K. S. Mechanochemistry and sonochemistry: concluding remarks. *Faraday Discuss.* **2014**, *170*, 411.
- 2) (a) McNaught, A. D.; Wilkinson, A. *Compendium of Chemical Terminology*, 2nd ed.; Blackwell Scientific Publications: Oxford, 1997. Online version (2019-) created by S. J. Chalk. ISBN 0-9678550-9-8. <https://doi.org/10.1351/goldbook> (accessed October 27, 2021). (b) Horie, K.; Barón, M.; Fox, R. B.; He, J.; Hess, M.; Kahovec, J.; Kitayama, T.; Kubisa, P.; Maréchal, E.; Mormann, W.; Stepto, R. F. T.; Tabak, D.; Vohlídal, J.; Wilks, E. S.; Work, W. J. *Pure Appl. Chem.* **2004**, *76*, 889.
- 3) Kaupp, G. *CrystEngComm.* **2009**, *11*, 388.
- 4) James, S. L.; Adams, C. J.; Bolm, C.; Braga, D.; Collier, P.; Frišćić, T.; Grepioni, F.; Harris, K. D. M.; Hyett, G.; Jones, W.; Krebs, A.; Mack, J.; Maini, L.; Orpen, A. G.; Parkin, I. P.; Shearouse, W. C.; Steed, J. W.; Waddell, D. C. *Chem. Soc. Rev.* **2012**, *41*, 413.
- 5) Do, J.-L.; Frišćić, T. *ACS Cent. Sci.* **2017**, *3*, 13.
- 6) Hernández, J. G.; Bolm, C. *J. Org. Chem.* **2017**, *82*, 4007.
- 7) Howard, J. L.; Cao, Q.; Browne, D. L. *Chem. Sci.* **2018**, *9*, 3080.
- 8) Tan, D.; García, F. *Chem. Soc. Rev.* **2019**, *48*, 2274.
- 9) Bolm, C.; Hernández, J. G. *Angew. Chem., Int. Ed.* **2019**, *58*, 3285.
- 10) Porcheddu, A.; Colacino, E.; De Luca, L.; Delogu, F. *ACS Catal.* **2020**, *10*, 8344.
- 11) Kubota, K.; Ito, H. *Trends Chem.* **2020**, *2*, 1066.
- 12) <https://www.mogroup.com/portfolio/higmill-high-intensity-grinding-mill/>, accessed October 2021.
- 13) Frišćić, T.; Childs, S. L.; Rizvi, S. A. A.; Jones, W. *CrystEngComm* **2009**, *11*, 418.
- 14) Seo, T.; Ishiyama, T.; Kubota, K.; Ito, H. *Chem. Sci.* **2019**, *10*, 8202.
- 15) Vogt, C. G.; Grätz, S.; Lukin, S.; Halasz, I.; Etter, M.; Evans, J. D.; Borchardt, L. *Angew. Chem., Int. Ed.* **2019**, *58*, 18942.
- 16) Takacs, L. *Prog. Mater. Sci.* **2002**, *47*, 355.
- 17) Urakaev, F. Kh.; Boldyrev, V. V. *Powder Technol.* **2000**, *107*, 93.
- 18) Frišćić, T.; Halasz, I.; Beldon, P. J.; Belenguer, A. M.; Adams, F.; Kimber, S. A. J.; Honkimäki, V.; Dinnebier, R. E. *Nat. Chem.* **2013**, *5*, 66.
- 19) Halasz, I.; Puskaric, A.; Kimber, S. A. J.; Beldon, P. J.; Belenguer, A. M.; Adams, F.; Honkimäki, V.; Dinnebier, R. E.; Patel, B.; Jones, W.; Strukil, V.; Frišćić, T. *Angew. Chem. Int. Ed.* **2013**, *52*, 11538.
- 20) Batzdorf, L.; Fischer, F.; Wilke, M.; Wenzel, K. J.; Emmerling, F. *Angew. Chem., Int.*

- Ed.* **2015**, *54*, 1799.
- 21) Gracin, D.; Strukil, V.; Frišćić, T.; Halasz, I.; Užarević, K. *Angew. Chem., Int. Ed.* **2014**, *53*, 6193.
 - 22) Kulla, H.; Wilke, M.; Fischer, F.; Röllig, M.; Maierhofer, C.; Emmerling, F. *Chem. Commun.* **2017**, *53*, 1664.
 - 23) Wang, G.-W.; Murata, Y.; Komatsu, K.; Wan, T. S. M. *Chem. Commun.* **1996**, 2059.
 - 24) Komatsu, K.; Wang, G.-W.; Murata, Y.; Shiro, M. *Nature* **1997**, *387*, 583.
 - 25) Komatsu, K.; Wang, G.-W.; Murata, Y.; Tanaka, T.; Fujiwara, K.; Yamamoto, K.; Saunders, M. *J. Org. Chem.* **1998**, *63*, 9358.
 - 26) Komatsu, K.; Fujiwara, K.; Murata, Y. *Chem. Lett.* **2000**, *29*, 1016.
 - 27) Zhao, Y.; Rocha, S. V.; Swager, T. M. *J. Am. Chem. Soc.* **2016**, *138*, 13834–13837.
 - 28) Patney, H. K. *Synthesis* **1991**, *1991*, 694.
 - 29) Hua, D. H.; Tamura, M.; Huang, X.; Stephany, H. A.; Helfrich, B. A.; Perchellet, E. M.; Sperflage, B. J.; Perchellet, J.-P.; Jiang, S.; Kyle, D. E.; Chiang, P. K. *J. Org. Chem.* **2002**, *67*, 2907.
 - 30) Belenguer, A. M.; Frišćić, T.; Day, G. M.; Sanders, J. K. M. *Chem. Sci.* **2011**, *2*, 696.
 - 31) Štrukil, V.; Gracin, D.; Magdysyuk, V. O.; Dinnebier, R. E.; Frišćić, T. *Angew. Chem., Int. Ed.* **2015**, *54*, 8440.
 - 32) Larsen, C.; Steliou, K.; Harpp, D. N. *J. Org. Chem.* **1978**, *43*, 337.
 - 33) Do, J. L.; Mottillo, C.; Tan, D.; Štrukil, V.; Frišćić, T. *J. Am. Chem. Soc.* **2015**, *137*, 2476.
 - 34) Cao, Q.; Howard, J. L.; Wheatley, E.; Browne, D. L. *Angew. Chem., Int. Ed.* **2018**, *57*, 11339.
 - 35) Kubota, K.; Seo, T.; Koide, K.; Hasegawa, Y.; Ito, H. *Nat. Commun.* **2019**, *10*, 111.

Chapter 1.

Mechanochemical Synthesis of Palladium Oxidative Addition Complexes in Air via Air-sensitive Pd(0) Intermediates

Abstract

Organic reactions that employ moisture- and/or oxygen-sensitive reagents or intermediates usually require the use of glove-box or Schlenk-line techniques as well as dry and degassed solvents. Unfortunately, these requirements may greatly reduce the utility of the targeted organic molecules. Herein, I demonstrate the synthesis of palladium(II) complexes under the ambient atmosphere via oxidative addition to highly oxygen-sensitive palladium(0) species using solvent-free mechanochemical synthetic techniques. The low diffusion efficiency of gaseous oxygen in crystalline or amorphous solid-state reaction mixtures should be the main reason for the low impact of the presence of atmospheric oxygen on the sensitive oxidative addition reactions under the applied conditions. This study thus illustrates the outstanding potential of mechanochemistry to serve as an operationally simple synthetic route to organometallic compounds and other valuable synthetic targets, even when sensitive reagents or intermediates are involved.

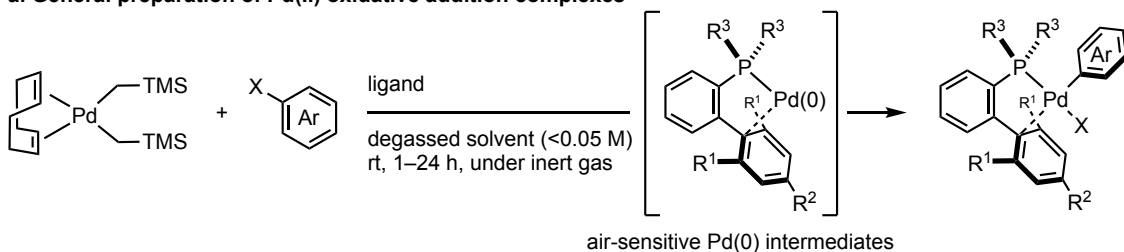
Introduction

Many useful reagents and catalysts employed in the preparation of organic compounds and organometallic complexes are highly reactive and therefore incompatible with exposure to the ambient atmosphere.¹ The techniques for organic synthesis with these sensitive compounds usually require gloveboxes and high-vacuum Schlenk lines and are thus costly and demand special training. In addition, a large amount of dry and degassed organic solvents are required for these reactions. Chemical processes that do not require such precautions are therefore likely to substantially increase the practical utility of the targeted organic molecules.

Palladium complexes obtained from oxidative addition reactions have been widely used in mechanistic studies,² as catalyst precursors for several cross-coupling reactions³ and as stoichiometric aryl-group transfer reagents for the diversification of biomolecules and pharmaceuticals (Scheme 1-1).⁴ Dialkylbiaryl phosphine-ligated palladium(II) complexes developed by Buchwald and co-workers are particularly useful reagents in these applications due to their high stability and ease of handling.^{2a-e,3a,4} One of the most common synthetic routes to these oxidative addition complexes involves reactions between the palladium(0) precursor (COD)Pd(CH₂TMS)₂ (COD = 1,5-cyclooctadiene; TMS = trimethylsilyl) (**1**)⁵ and aryl halides **2** in the presence of appropriate Buchwald-type ligands (Figure 1).^{2a-e,3a,4} According to the developed protocol reported by Buchwald and co-workers, this procedure generally requires glove-box techniques, given that highly air-sensitive palladium(0) species are involved.^{3a,4c} These restrictions may greatly reduce the practical utility of the obtained palladium complexes. The development of scalable,

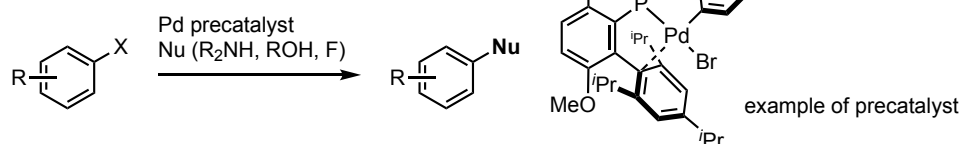
operationally simple and glove-box-and-Schlenk-line-free synthetic methods should therefore be highly beneficial.

a. General preparation of Pd(II) oxidative addition complexes

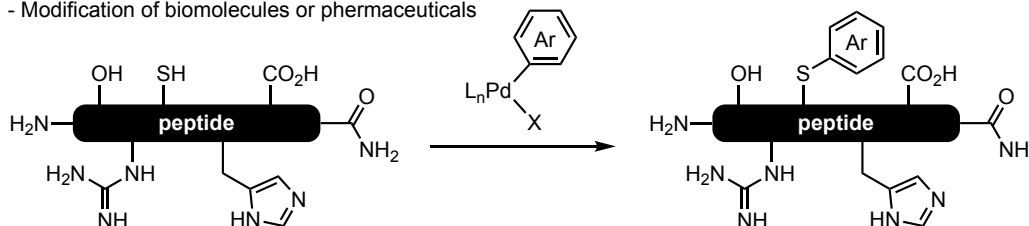


b. Application of Pd oxidative addition complexes

- Mechanistic studies for coupling reactions
- On-cycle precatalyst



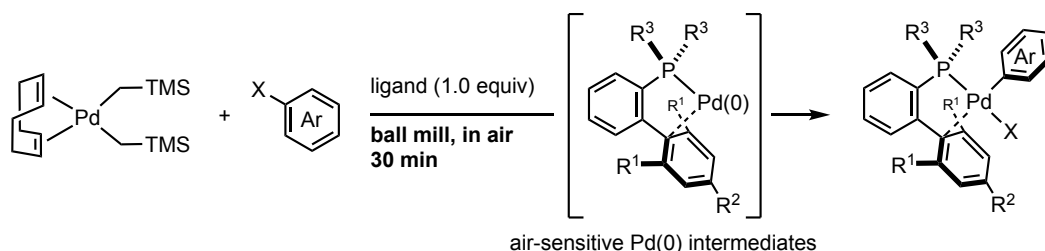
- Modification of biomolecules or pharmaceuticals



Scheme 1-1. Palladium oxidative addition complexes in organic synthesis. (a) Preparation of palladium oxidative addition complexes. (b) Application of palladium oxidative addition complexes in organic synthesis.

Mechanochemical solvent-free organic reactions using ball milling have emerged as powerful alternatives to synthetic procedures in solution.⁶ However, the benefits of mechanochemistry in the context of organometallic chemistry have not yet been explored systematically,^{6m,7-19} and the potential applicability of highly sensitive reagents or intermediates toward mechanochemical organometallic transformations under ambient conditions remains elusive.¹⁴ Herein, I demonstrate that mechanochemistry enables glove-box-and-Schlenk-line-free synthesis of palladium complexes by oxidative additions using readily available starting materials (Scheme 1-2).²⁰ This reaction is operationally simple and proceeds efficiently in air to afford a variety of synthetically useful palladium complexes in moderate to high yields. I anticipate that the method presented herein could be readily transferred to the development of glove-box-and-Schlenk-line-free synthetic routes to other valuable organometallic complexes and

synthetic targets, even when sensitive reagents or intermediates are involved.



Conventional solution-state reaction

- glove-box operation or Schlenk-line techniques under inert atmosphere
- use of degassed solvents
- complex reaction set up



This work: mechanochemical reaction

- proceeds efficiently in air
- without solvents
- operationally simple (just milling in air)

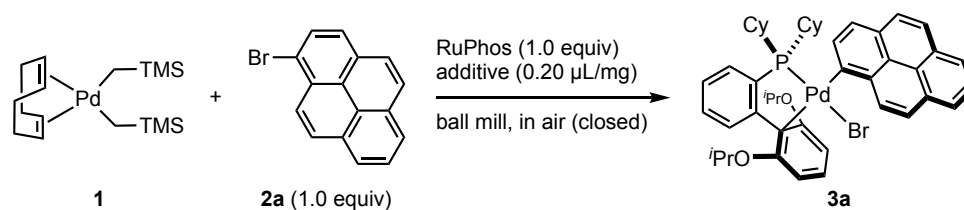
Scheme 1-2. Mechanochemical synthesis of palladium oxidative addition complexes in air.

Results and Discussion

All mechanochemical reactions were conducted in a Retsch MM 400 mill (stainless-steel milling jar; 30 Hz or 25 Hz; stainless-steel balls). To probe the effectiveness of this mechanochemical approach for the preparation of palladium-based oxidative addition complexes, I initially tested the reaction between **1** and 1-bromopyrene (**2a**) in the presence of 2-dicyclohexylphosphino-2',6'-diisopropoxybiphenyl (RuPhos), which is a commonly used Buchwald-type ligand (Table 1-1).²¹ The corresponding oxidative addition complex (**3a**) was obtained in moderate yield upon grinding for 30 minutes in air (40% yield; entry 1). Prolonging the reaction time did not improve the yield (43% yield; entry 2). Subsequently, I attempted LAG to improve the performance (entries 3–12).²² Unless otherwise noted, the following reactions with liquid additives are all characterized by the addition of 0.20 μL of liquid per mg of reactant. I found that the addition of a small amount of tetrahydrofuran (THF) greatly improved the yield of **3a** (71% yield; entry 3). Other commonly used organic solvents in palladium-catalyzed cross-coupling reactions such as toluene, acetonitrile (CH_3CN), dioxane, dimethyl formamide (DMF), and diethyl ether (Et_2O) also improved the efficiency of the reaction (entries 4–8). The use of highly polar solvents such as dimethyl sulfoxide (DMSO) or simple alkanes (pentane and cyclohexane) slightly accelerated the oxidative addition (entries 9–11). Protic solvents such as methanol (MeOH) did not promote the reaction (entry 12). Next, I focused on the identification of the optimal milling parameters for this mechanochemical oxidative addition reaction (entries 13–15). The milling frequency can

be reduced to 25 Hz (78% yield; entry 13), while increasing the number of stainless-steel balls did not improve the yield (entries 14 and 15). Notably, the reaction time can be reduced to 10 min without affecting the yield when THF was used as a LAG additive (71% yield; entry 16).

Table 1-1. Optimization of reaction conditions.

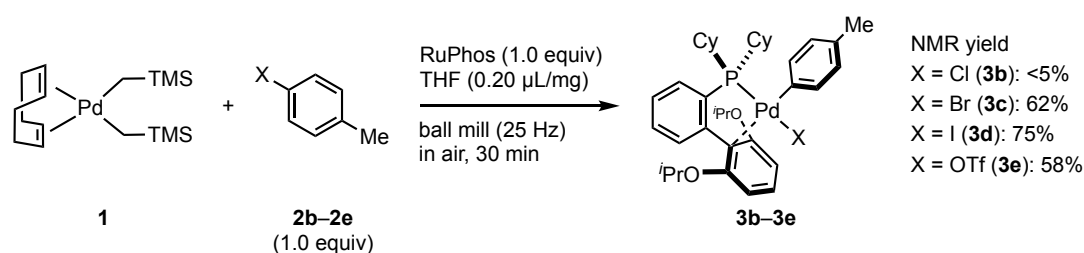


entry	additive	Milling frequency (Hz)	time (min)	yield (%) ^b
1	None	30	30	40
2	None	30	60	43
3	THF	30	30	71
4	toluene	30	30	61
5	CH ₃ CN	30	30	71
6	1,4-dioxane	30	30	64
7	DMF	30	30	64
8	Et ₂ O	30	30	66
9	DMSO	30	30	55
10	pentane	30	30	58
11	cyclohexane	30	30	47
12	MeOH	30	30	48
13	THF	25	30	78 ^e
14 ^c	THF	25	30	55
15 ^d	THF	25	30	67
16	THF	25	10	71

^aConditions: **1** (0.05 mmol), **2a** (0.05 mmol), RuPhos (0.05 mmol), LAG additives (0.2 μL/mg) in a stainless-steel ball-milling jar (1.5 mL) with a stainless-steel ball (diameter: 3 mm). ^bDetermined by ¹H NMR analysis of the crude reaction mixture with an internal standard. ^cTwo stainless-steel balls (diameter: 3 mm) were used. ^dThree stainless-steel balls (diameter: 3 mm) were used. ^eIsolated yield.

With the optimized conditions in hand, I investigated the effect of different halides and a pseudohalide on the oxidative addition of palladium complexes (Scheme 1-3). Even though the corresponding aryl chloride (**2b**) undergoes oxidative addition in solution, the desired oxidative addition complex (**3b**) was not formed under mechanochemical

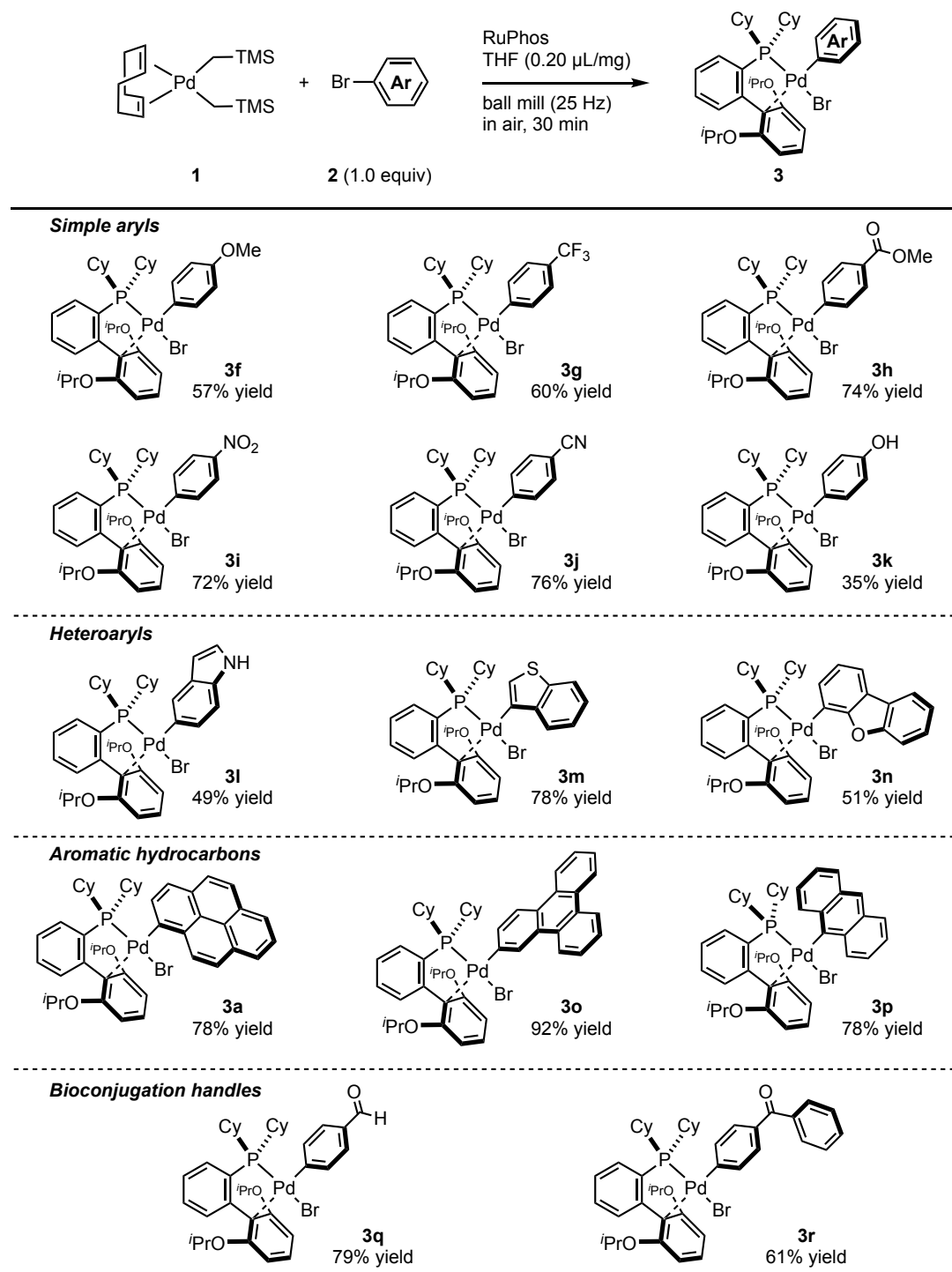
conditions.⁴ When 4-bromotoluene (**2c**) and 4-iodotoluene (**2d**) were used, the products were obtained in 62% and 75% yields, respectively. Although Ondruschka and co-workers reported that aryl bromides were more reactive than aryl iodides in mechanochemical palladium-catalyzed Suzuki–Miyaura coupling reactions,²³ the iodide substrate (**2d**) provided higher yield in the mechanochemical stoichiometric oxidative addition process. The aryl triflate (**2e**) afforded the corresponding palladium complex (**3e**) in moderate yield (58%).



Scheme 1-3. Mechanochemical synthesis of palladium oxidative addition complexes from various aryl halides and pseudohalide.

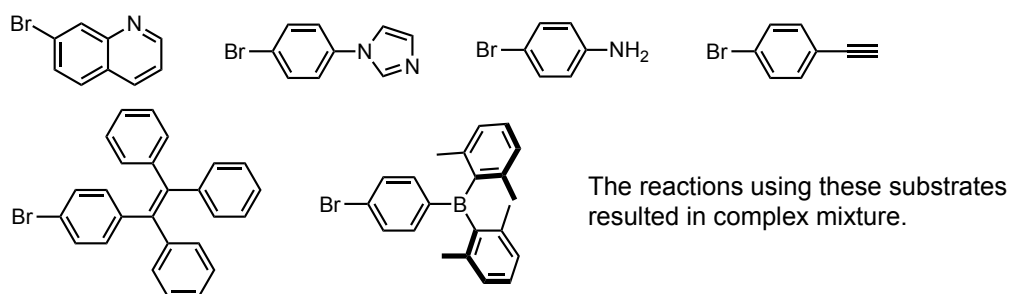
The aforementioned optimized conditions were used for further evaluation of the substrate scope (Table 1-2). The reaction of both electron-rich and -poor aryl bromides (**2f–2j**) proceeded smoothly to give the corresponding oxidative addition complexes (**3f–3j**) in good yields (57–76% yields). 4-Bromophenol (**2k**) also afforded the desired product (**3k**) in moderate yield (35% yield). The present protocol could also be applied to heteroaryl bromides such as indole (**2l**), thiophene (**2m**), and dibenzofuran (**2n**) derivatives. Palladium(II) complexes containing aromatic hydrocarbon cores (**3a**, **3o**, and **3p**) were obtained in 78–92% yields. The reaction of aryl bromides bearing aldehyde **2q** and benzophenone moieties **2r** afforded the desired palladium(II) complexes (**3q** and **3r**), which are used in bioconjugation applications,⁴ in 79% and 61% yields, respectively. Unfortunately, the reactions resulted in complex mixture when the substrates that can coordinate on palladium were used (Table 1-3).

Table 1-2. Scope of aryl bromides.



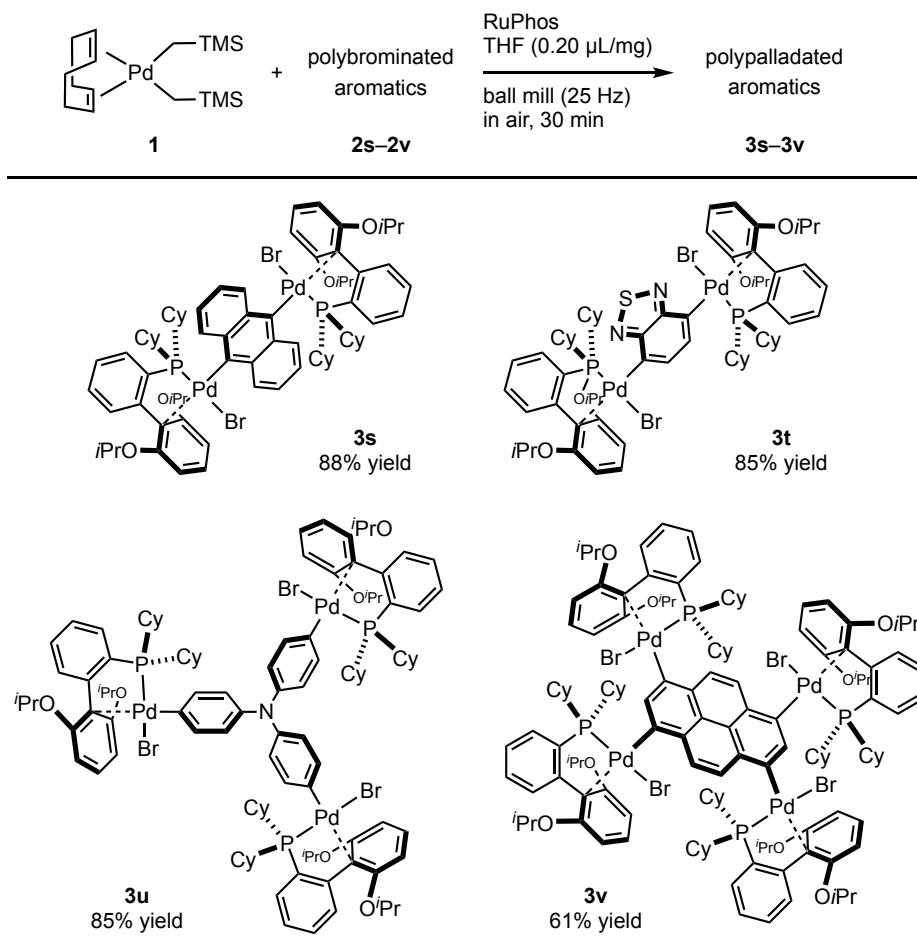
^aConditions: **1** (0.12 mmol), **2a** (0.12 mmol), RuPhos (0.12 mmol), THF (0.20 μL/mg) in a stainless-steel ball-milling jar (1.5 mL) with a stainless-steel ball (diameter: 3 mm).

Table 1-3. List of unsuccessful substrates.



Polymetalated transition-metal complexes have attracted considerable attention due to their unique reactivity and physical properties.^{4e,24} The developed mechanochemical oxidative addition protocol can be applied to the synthesis of polymetalated palladium complexes (Table 1-4). The reaction of dibromides **2s** and **2t** in the presence of 2 equivalents of **1** and RuPhos afforded di-palladated **3s** and **3t**, which are useful reagents for macrocyclization of peptides,^{4e} in 88% and 85% yields, respectively. The tri-palladated arylamine **3u** and the tetra-palladated pyrene **3v** were synthesized in 91% and 61% yields, respectively under the applied mechanochemical conditions in air. The molecular structure of **3v** in the solid state was unequivocally determined by a single-crystal X-ray diffraction analysis (Figure 1-1). The results revealed that two of the four palladium atoms in **3v** adopt a C-bound conformation, while the other two adopt an O-bound conformation in the solid state. The orientation of the phosphine ligands on adjacent palladium atoms is in opposing directions relative to each other, which is probably due to the steric congestion between substituents on the phosphine ligands in the solid state.

Table 1-4. Scope of polybrominated aromatics.



^aConditions: **1** (0.05 mmol), **2** (0.05 mmol), RuPhos (0.05 mmol), THF (0.20 $\mu\text{L/mg}$) in a stainless-steel ball-milling jar (1.5 mL) with a stainless-steel ball (3 mm).

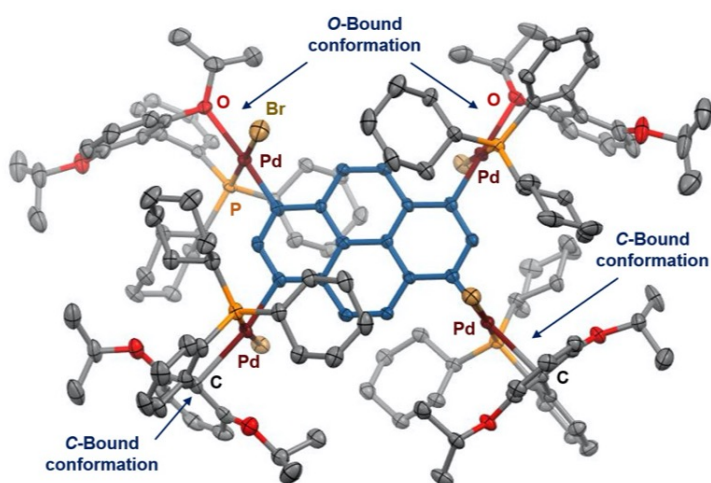
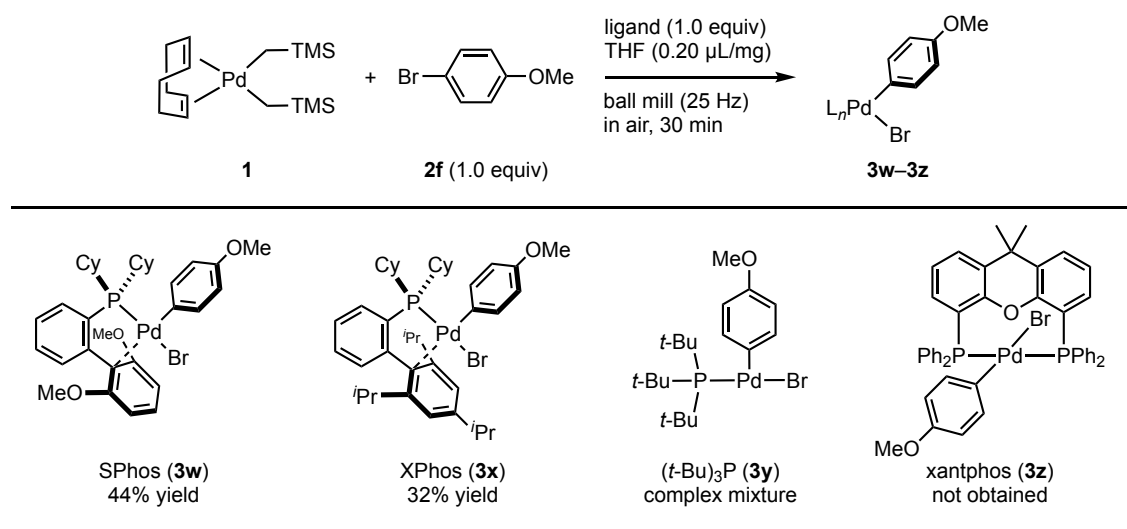


Figure 1-1. Molecular structure of **3v** in the solid state (thermal ellipsoids at 50% probability; hydrogen atoms and CH_2Cl_2 are omitted for clarity).

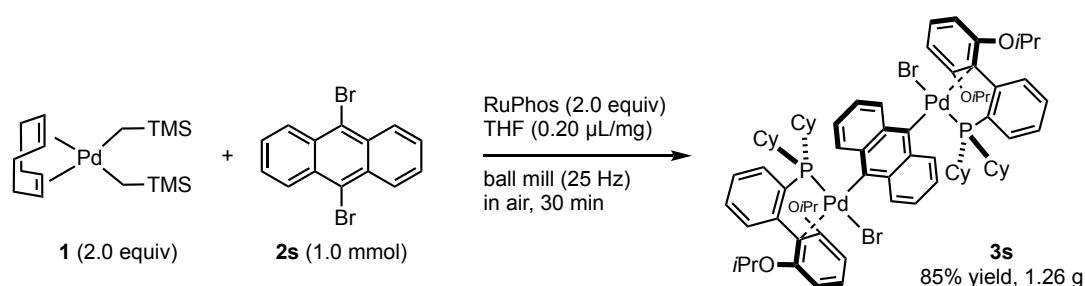
Subsequently, I investigated the effect of the phosphine ligand on the mechanochemical palladium-mediated oxidative addition of **2f** (Table 1-5). The reactions using 2-dicyclohexylphosphino-2',6'-dimethoxybiphenyl (SPhos) and 2-dicyclohexylphosphino-2',4',6'-triisopropylbiphenyl (XPhos) furnished **3w** and **3x** in 44% and 32% yields, respectively. Unfortunately, the reaction using Xantphos and *t*-Bu₃P did not afford the desired palladium complexes under this mechanochemical condition.

Table 1-5. Scope of phosphine ligands.



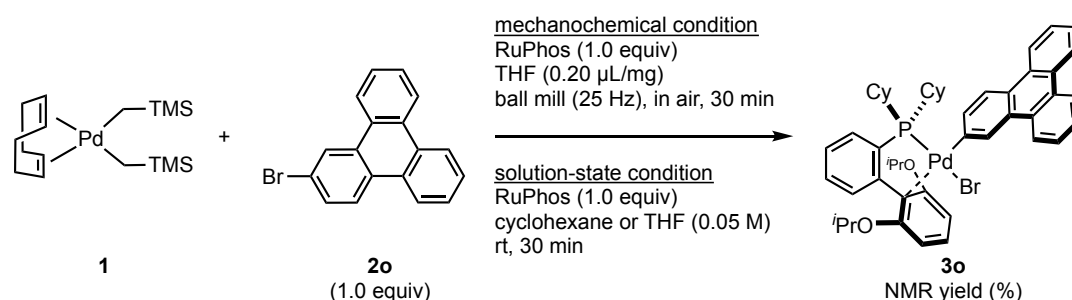
^aConditions: **1** (0.12 mmol), **2f** (0.12 mmol), ligand (0.12 mmol), THF (0.20 μL/mg) in a stainless-steel ball-milling jar (1.5 mL) with a stainless-steel ball (3 mm).

These palladium-based oxidative addition complexes can be prepared on the gram-scale in air using mechanochemistry (Scheme 1-4). The reaction of **2s** (1 mmol) was carried out in a larger stainless-steel ball-milling jar (25 mL) with two stainless-steel balls (10 mm) in air, and the desired oxidative addition complex (**3s**) was obtained in 85% yield (1.26 g). This result clearly demonstrates the potential utility of the present mechanochemical protocol for large-scale preparation of synthetically useful palladium reagents without any special operational skills or precautions.



Scheme 1-4. Gram-scale synthesis of **3s**. Conditions: **1** (2.0 mmol), **2s** (1.0 mmol), RuPhos (2.0 mmol), and THF (0.20 mL/mg) in a stainless-steel ball-milling jar (25 mL) with two stainless-steel balls (diameter: 10 mm).

In order to further explore the practical utility of this protocol, the efficiency of the mechanochemical reactions was compared to that of the conventional solution-based reactions (Scheme 1-5). The oxidative addition of **2o** under the reported solution-based conditions using cyclohexane or THF as solvents^{3a,4} provided **3o** in 61% and 87% yields, respectively. However, when the reactions were conducted in air, significantly lower yields were obtained (8% and 46%, respectively). In contrast, under the aforementioned mechanochemical conditions, the oxidative addition proceeded efficiently, even in air, providing **3o** in 92% yield. These results suggest that gaseous oxygen does not efficiently diffuse through crystalline or amorphous solid-state reaction mixtures,^{25,26} which results in little to no impact on the air-sensitive palladium(0)-mediated oxidative addition reactions. Related to this finding, Mack and co-workers have described that the gaseous nature of water and oxygen does not significantly influence moisture-sensitive organic transformations under mechanochemical conditions.²⁵



Solution-state condition

under N₂ in air
 - Cyclohexane: 61% - Cyclohexane: 8%
 - THF: 87% - THF: 46%

Mechanochemistry

in air, 92% yield

Scheme 1-5. Comparison of the performance of solution-based and mechanochemical reactions.

Summary

I have demonstrated that mechanochemistry allows synthesizing a wide range of Buchwald-type-phosphine-ligated palladium(II)-based oxidative addition complexes in air. The main reason for the low impact of atmospheric oxygen on these sensitive organometallic reactions would be the low diffusion efficiency of gaseous oxygen in the solid-state reaction mixture. This study illustrates the outstanding potential of mechanochemistry as an operationally simple glove-box-and-Schlenk-line-free synthetic route to valuable organometallic compounds and other attractive synthetic targets, even when highly sensitive reagents or intermediates are involved.

Reference

- 1) *The Manipulations of Air-Sensitive Compounds*, 2nd ed.; D. F. Shriver, M. A. Drezdon, Eds.; John Wiley and Sons: New York, 1986.
- 2) For selected examples of mechanistic studies using palladium-based oxidative addition complexes, see: (a) Watson, D. A.; Su, M.; Teverovskiy, G.; Zhang, Y.; García-Fortanet, J.; Kinzel, T.; Buchwald, S. L. *Science* **2009**, *325*, 1661. (b) Maimone, T. J.; Milner, R. J.; Kinzel, T.; Zhang, Y.; Takase, M. K.; Buchwald, S. L. *J. Am. Chem. Soc.* **2011**, *133*, 18106. (c) Sather, A. C.; Lee, H. G.; De La Rosa, V. Y.; Yang, Y.; Müller, P.; Buchwald, S. L. *J. Am. Chem. Soc.* **2015**, *137*, 13433. (d) Arrechea, P. L.; Buchwald, S. L. *J. Am. Chem. Soc.* **2016**, *138*, 12486. (e) Dennis, J. M.; White, N. A.; Liu, R. Y.; Buchwald, S. L. *J. Am. Chem. Soc.* **2018**, *140*, 4721. (f) Roy, A. H.; Hartwig, J. F. *J. Am. Chem. Soc.* **2001**, *123*, 1232. (g) Roy, A. H.; Hartwig, J. F. *J. Am. Chem. Soc.* **2003**, *125*, 13944. (i) Fujita, K.; Yamashita, M.; Puschmann, F.; Alvarez-Falcon, M. M.; Incarvito, C. D.; Hartwig, J. F. *J. Am. Chem. Soc.* **2006**, *128*, 9044. (j) Yamashita, M.; Hartwig, J. F. *J. Am. Chem. Soc.* **2004**, *126*, 5344. (k) Peacock, D. M.; Jiang, Q.; Hanley, P. S.; Cundari, T. R.; Hartwig, J. F. *J. Am. Chem. Soc.* **2018**, *140*, 4893. (l) Maleckis, A.; Sanford, M. S. *Organometallics* **2014**, *33*, 2653. (m) Maleckis, A.; Kampf, J. W.; Sanford, M. S. *J. Am. Chem. Soc.* **2013**, *135*, 6618. (n) Racowski, J. M.; Ball, N. D.; Sanford, M. S. *J. Am. Chem. Soc.* **2011**, *133*, 18022. (o) Hartwig, J. F.; Paul, F. *J. Am. Chem. Soc.* **1995**, *117*, 5373. (p) Portnoy, M.; Milstein, D. *Organometallics* **1993**, *12*, 1665. (q) Amatore, C.; Pflüger, F. *Organometallics* **1990**, *9*, 2276. (r) Moser, W. R.; Wang, A. W.; Kildahl, N. K. *J. Am. Chem. Soc.* **1988**, *110*, 2816. (s) Andersen, T. L.; Kramer, S.; Overgaard, J.; Skrydstrup, T. *Organometallics* **2017**, *36*, 2058.
- 3) For selected examples of the use of palladium-based oxidative addition complexes as catalyst precursors, see: (a) Ingoglia, B. T.; Buchwald, S. L. *Org. Lett.* **2017**, *19*,

2853. (b) Vicente, J.; Arcas, A.; Juliá-Hernández, F.; Bautista, D. *Angew. Chem., Int. Ed.* **2011**, *50*, 6896. (c) Yokoyama, A.; Suzuki, H.; Kubota, Y.; Ohuchi, K.; Higashimura, H.; Yokozawa, T. *J. Am. Chem. Soc.* **2007**, *129*, 7236.
- 4) For selected examples of the use of palladium-based oxidative addition complexes as stoichiometric aryl-group-transfer reagents for the diversification of biomolecules and pharmaceuticals, see: (a) Vinogradova, E. V.; Zhang, C.; Spokoyny, A. M.; Pentelute, B. L. *Nature* **2015**, *526*, 687. (b) Zhao, W.; Lee, H. G.; Buchwald, S. L. Hooker, J. M. *J. Am. Chem. Soc.* **2017**, *139*, 7152. (c) Rojas, A. J.; Pentelute, B. L.; Buchwald, S. L. *Org. Lett.* **2017**, *19*, 4263. (d) Lee, H. G.; Lautrette, G.; Pentelute, B. L.; Buchwald, S. L. *Angew. Chem., Int. Ed.* **2017**, *56*, 3177. (e) Rojas, A. J.; Zhang, C.; Vinogradova, E. V.; Buchwald, N.; Reilly, J.; Pentelute, B. L.; Buchwald, S. L. *Chem. Sci.* **2017**, *8*, 4257. (f) Kubota, K.; Dai, P.; Pentelute, B. L.; Buchwald, S. L. *J. Am. Chem. Soc.* **2018**, *140*, 3128. (g) Uehling, M. R.; King, R. P.; Krska, S. W.; Cernak, T.; Buchwald, S. L. *Science* **2019**, *363*, 405.
- 5) (a) Pan, Y.; Young, G. B. *J. Organomet. Chem.* **1999**, *577*, 257. (b) McAtee, J. R.; Martin, S. E. S.; Ahneman, D. T.; Johnson, K. A.; Watson, D. A. *Angew. Chem., Int. Ed.* **2012**, *51*, 3663.
- 6) For recent reviews on organic syntheses using mechanochemistry, see: (a) James, S. L.; Adams, C. J.; Bolm, C.; Braga, D.; Collier, P.; Friščić, T.; Grepioni, F.; Harris, K. D. M.; Hyett, G.; Jones, W.; Krebs, A.; Mack, J.; Maini, L.; Orpen, A. G.; Parkin, I. P.; Shearouse, W. C.; Steed, J. W.; Waddell, D. C. *Chem. Soc. Rev.* **2012**, *41*, 413. (b) Wang, G.-W. *Chem. Soc. Rev.* **2013**, *42*, 7668. (c) Friščić, T.; Halasz, I.; Štrukil, V.; Eckert-Maksić, M.; Dinnebier, R. E. *ACS Cent. Sci.* **2017**, *3*, 13. (d) Hernández, J. G.; Bolm, C. *J. Org. Chem.* **2017**, *82*, 4007. (e) Hernández, J. G. *Chem.-Eur. J.* **2017**, *23*, 17157. (f) Métro, T.-X.; Martinez, J.; Lamaty, F. *ACS Sustainable Chem. Eng.* **2017**, *5*, 9599. (g) Achar, T. K.; Bose, A.; Mal, P. *Beilstein J. Org. Chem.* **2017**, *13*, 1907. (h) Do, J.-L.; Friščić, T. *Synlett* **2017**, *28*, 2066. (i) Tan, D.; Friščić, T. *Eur. J. Org. Chem.* **2018**, *18*. (j) Eguaoie, O.; Vyle, J. S.; Conlon, P. F.; Gílea, M. A.; Liang, Y. *Beilstein J. Org. Chem.* **2018**, *14*, 955. (k) Howard, J. L.; Cao, Q.; Browne, D. L. *Chem. Sci.* **2018**, *9*, 3080. (l) Andersen, J.; Mack, J. *Green Chem.* **2018**, *20*, 1435. (m) Rightmire, N. R.; Hanusa, T. P. *Dalton Trans.* **2016**, *45*, 2352.
- 7) For the mechanochemical synthesis of gold complexes, see: (a) Zhdanko, A.; Ströbele, M.; Maier, M. E. *Chem.-Eur. J.* **2012**, *18*, 14732. (b) Egbert, J. D.; Slawin, A. M. Z.; Nolan, S. P. *Organometallics* **2013**, *32*, 2271.
- 8) For the mechanochemical synthesis of ferrocene, see: Makhaev, V. D.; Borisov, A. P.; Petrova, L. A. *J. Organomet. Chem.* **1999**, *590*, 222.

- 9) For the mechanochemical synthesis of rhenium and manganese complexes, see: Hernández, J. G.; Butler, I. S.; Friščić, T. *Chem. Sci.* **2014**, *5*, 3576.
- 10) For the mechanochemical oxidative addition of rhenium complexes, see: Hernández, J. G.; Macdonald, N. A. J.; Mottillo, C.; Butler, I. S.; Friščić, T. *Green Chem.* **2014**, *16*, 1087.
- 11) For the mechanochemical synthesis of nickel and cobalt complexes, see: Gomes, C. S. B.; Gomes, P. T.; Duarte, M. T. *J. Organomet. Chem.* **2014**, *760*, 101.
- 12) For the mechanochemical synthesis of palladium complexes, see: (a) Cinčić, D.; Juribašić, M.; Babić, D.; Molčanov, K.; Šket, P.; Ćurić, M. *Chem. Commun.* **2011**, *47*, 11543. (b) Juribašić, M.; Užarević, K.; Gracin, D.; Ćurić, M. *Chem. Commun.* **2014**, *50*, 10287.
- 13) For the mechanochemical synthesis of zinc complexes, see: (a) Lewiński, J.; Dutkiewicz, M.; Lesiuk, M.; Śliwiński, W.; Zelga, K.; Justyniak, I.; Lipkowski, J. *Angew. Chem., Int. Ed.* **2010**, *49*, 8266.
- 14) Browne and co-workers have reported the mechanochemical synthesis of organozinc species in air; see: Cao, Q.; Howard, J. L.; Wheatley, E.; Browne, D. L. *Angew. Chem., Int. Ed.* **2018**, *57*, 11339.
- 15) For the mechanochemical synthesis of gold-silver honeycomb aggregates, see: Blanco, M. C.; Cámara, J.; Gimeno, M. C.; Laguna, A.; James, S. T.; Lagunas, M. C.; Villacampa, M. D. *Angew. Chem., Int. Ed.* **2012**, *51*, 9777.
- 16) For the mechanochemical synthesis of aluminium complexes, see: Rightmire, N. R.; Hanusa, T. P.; Rheingold, A. L. *Organometallics* **2014**, *33*, 5952.
- 17) For the mechanochemical synthesis of Grignard reagents, see: Harrowfield, J. M.; Hart, R. J.; Whitaker, C. R. *Aust. J. Chem.* **2001**, *54*, 423.
- 18) For selected recent examples of palladium-catalyzed cross-coupling reactions in air using mechanochemistry, see: (a) Cao, Q.; Howard, J. L.; Wheatley, E.; Browne, D. L. *Angew. Chem., Int. Ed.* **2018**, *57*, 11339. (b) Shao, Q.-L.; Jiang, Z.-J.; Su, W.-K. *Tetrahedron Lett.* **2018**, *59*, 2277. (c) Kubota, K.; Seo, T.; Koide, K.; Hasegawa, Y.; Ito, H. *Nat. Commun.* **2019**, *10*, 111. (d) Declerck, V.; Colacino, E.; Bantreil, X.; Martinez, J.; Lamaty, F. *Chem. Commun.* **2012**, *48*, 11778. (e) Cravotto, G.; Garella, D.; Tagliapietra, S.; Stolle, A.; Schüßler, S.; Leonhardt, S. E. S.; Ondruschka, B. *New J. Chem.* **2012**, *36*, 1304. (f) Jiang, Z.-J.; Li, Z.-H.; Yu, J.-B.; Su, W.-K. *J. Org. Chem.* **2016**, *81*, 10049.
- 19) (a) Old, D. W.; Wolfe, J. P.; Buchwald, S. L. *J. Am. Chem. Soc.* **1998**, *120*, 9722. (b) Martin, R.; Buchwald, S. L. *Acc. Chem. Res.* **2008**, *41*, 1461.
- 20) Friščić, T.; Childs, S. L.; Rizvi, S. A. A.; Jones, W. *CrystEngComm* **2009**, *11*, 418.

- 21) (a) Vicente, J.; Lyakhovych, M. *Organometallics* **2001**, *20*, 4695. (b) Vicente, J.; Shenoy, R. V.; Martínez-Viviente, E. *Organometallics* **2009**, *28*, 6101. (c) Vicente, J.; Shenoy, R. V.; Martínez-Viviente, E.; Jones, P. G. *Inorg. Chem.* **2011**, *50*, 7189.
- 22) Waddell, D. C.; Clark, T. D.; Mack, J. *Tetrahedron Lett.* **2012**, *53*, 4510.
- 23) Bolm, C.; Hernández, J. D. *Angew. Chem., Int Ed.* **2019**, *58*, 3285.

Experimental Section

Table of Contents

General and Materials	31
General Procedure for Synthesis of Palladium Oxidative Addition Complexes	32
Single Crystal X-Ray Analysis	33
Characterization of Palladium Oxidative Addition Complexes	35
References	48

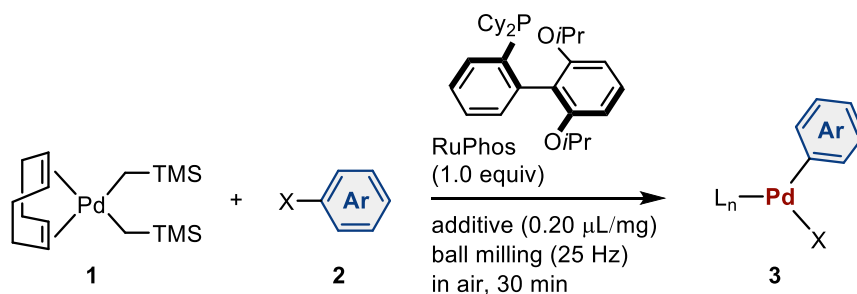
1. General and Materials.

The starting materials were obtained from commercial suppliers and used as received unless otherwise noted. Solvents were also purchased from commercial suppliers, and dried over molecular sieves (MS 4Å). All mechanochemical reactions were carried out using grinding vessels in a Retsch MM400 mill (Supplementary Figure 1). Both jars (1.5 mL or 25 mL) and balls (diameter: 3 mm or 10 mm) are made of stainless (Supplementary Figure 1). NMR spectra were recorded on JEOL JNM-ECX400P and JNM-ECS400 spectrometers (^1H : 392, 396 or 401 MHz, ^{13}C : 99 MHz, ^{31}P : 160 MHz). Tetramethylsilane (^1H), CDCl_3 (^{13}C) and H_3PO_4 (^{31}P) were employed as external standards, respectively. Multiplicity was recorded as follows: s = singlet, br, s = broad singlet, d = doublet, t = triplet, q = quartet, quin = quintet, sext = sextet, sep = septet, m = multiplet. Dibromomethane was used as an internal standard to determine NMR yields. High-resolution mass spectra were recorded at the Global Facility Center, Hokkaido University. Single crystal X-ray structural analyses were carried out on a Rigaku XtaLAB PRO MM007 diffractometer using graphite monochromated $\text{Cu-K}\alpha$ radiation. The structure was solved by direct methods and expanded using Frontier techniques. Non-hydrogen atoms were refined anisotropically. Hydrogen atoms were refined using the riding model. All calculations were performed using Olex crystallographic software package except for refinement, which was performed using SHELXL.¹



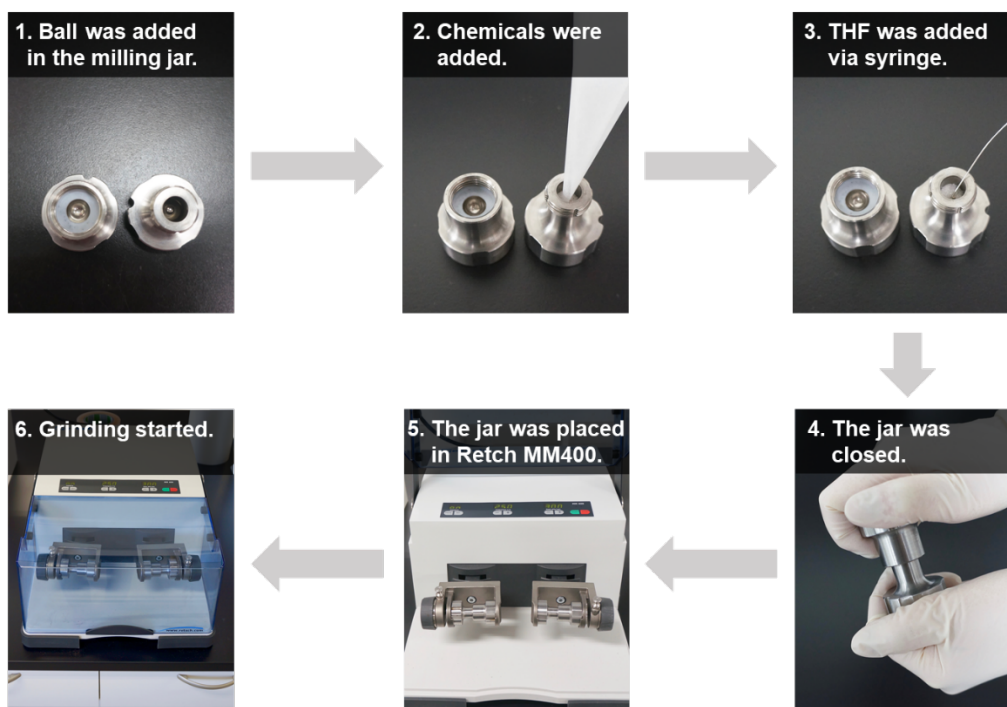
Supplementary Figure 1. Retsch MM400 mill (left) and ball milling vessels (right).

2. General Procedure for Synthesis of Palladium Oxidative Addition Complexes



$(\text{COD})\text{Pd}(\text{CH}_2\text{TMS})_2$ **1** was prepared by according to the procedure.² The material **1** is thermo-sensitive and must be stored at a temperature of -20 °C or lower to avoid decomposition, while the material can be stored out of glovebox and used in air.

$(\text{COD})\text{Pd}(\text{CH}_2\text{TMS})_2$ **1** (0.12 mmol), arylhalide **2** (0.12 mmol, 1.0 equiv), a phosphine ligand (0.12 mmol, 1.0 equiv) were placed in a ball milling vessel (stainless, 1.5 mL) loaded with one grinding ball (stainless, diameter: 3 mm), then THF (0.20 $\mu\text{L mg}^{-1}$) was added via syringe. After the vessel was closed in air without the purge with inert gas, the vessel was placed in the ball mill (Retch MM400, 30 min at 25Hz). After passing through a short silica gel column eluting with EtOAc, the crude mixture was concentrated, washed with pentane three times and dried under reduced pressure to afford the oxidative addition complex **3**.

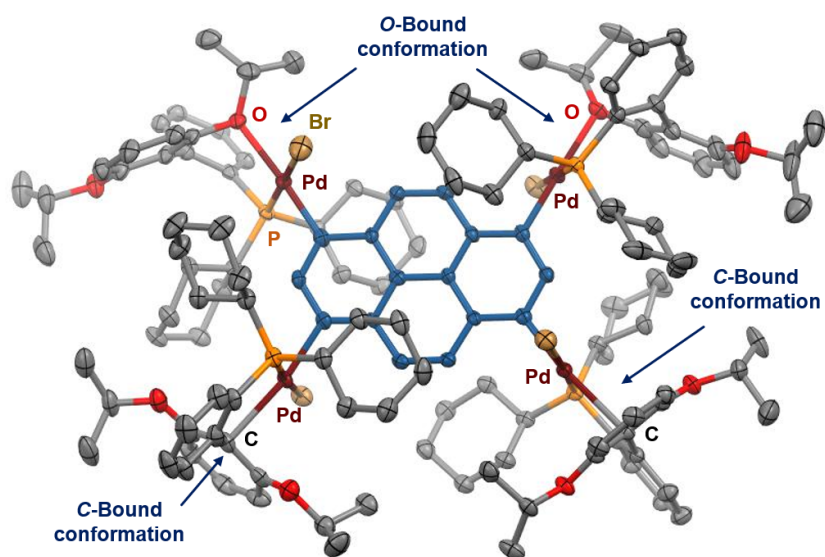


Supplementary Figure 2. How to set up the mechanochemical reactions.

3. Single Crystal X-Ray Analysis

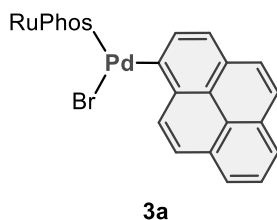
Supplementary Table 1. Summary of X-ray crystallographic data for **3v**.

CCDC number	1908179
Empirical Formula	C ₁₄₁ H ₁₈₈ Br ₄ Cl ₁₀ O ₈ P ₄ Pd ₄
Formula Weight	3234.52
Crystal System	triclinic
Crystal Size / mm	0.18 × 0.17 × 0.02
a / Å	13.8478(2)
b / Å	18.2868(2)
c / Å	28.8141(2)
α / °	95.321(1)
β / °	96.590(1)
γ / °	92.188(1)
V / Å ³	7208.41(14)
Space Group	<i>P</i> -1
Z value	2
D _{calc} / g·cm ⁻³	1.490
Temperature / K	123
No. of Reflections	Total: 66930
Measured	27857 (<i>R</i> _{int} = 0.0455)
Residuals: <i>R</i> _I	5.38
(<i>I</i> > 2.00σ(<i>I</i>)) / %	
Residuals: <i>wR</i> ₂	15.39
(All reflections) / %	
Goodness of Fit (GOF)	1.095
Maximum peak in Final Diff. Map / Å ³	1.71 e ⁻
Minimum peak in Final Diff. Map / Å ³	-1.67 e ⁻



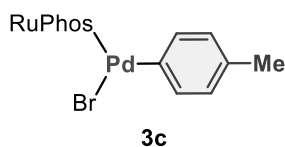
Supplementary Figure 3. Single-crystal structure of **3v** (thermal ellipsoids set at 50% probability; hydrogen atoms and CH₂Cl₂ omitted for clarity).

4. Characterization of Palladium Oxidative Addition Complexes



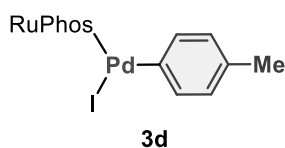
The reaction was carried out with **1** (47.2 mg, 0.12 mmol), **2a** (33.5 mg, 0.12 mmol) and RuPhos (57.0 mg, 0.12 mmol). The product **3a** was obtained as an off-white solid by washing with hexane (79.5 mg, 0.093 mmol, 78% yield).

^1H NMR (392 MHz, CDCl_3 , δ): -0.68--0.49 (m, 1H), 0.08--0.25 (m, 1H), 0.51--0.67 (m, 1H), 0.69--0.91 (m, 3H), 1.01 (d, $J = 5.9$ Hz, 3H), 1.13 (d, $J = 6.3$ Hz, 3H), 0.94--1.30 (m, 4H), 1.42 (d, $J = 5.9$ Hz, 3H), 1.46--1.56 (m, 4H), 1.61 (d, $J = 5.9$ Hz, 3H), 1.65--2.00 (m, 6H), 2.16--2.27 (m, 1H), 2.55 (t, $J = 9.6$ Hz, 1H), 4.65 (hept, $J = 5.9$ Hz, 1H), 4.75 (hept, $J = 6.1$ Hz, 1H), 6.66 (d, $J = 8.2$ Hz, 1H), 6.78 (d, $J = 8.6$ Hz, 1H), 6.88 (dd, $J = 2.4, 7.4$ Hz, 1H), 7.36 (t, $J = 7.4$ Hz, 1H), 7.44 (t, $J = 7.6$ Hz, 1H), 7.54 (t, $J = 7.1$ Hz, 1H), 7.74--7.94 (m, 7H), 8.02 (d, $J = 7.8$ Hz, 2H), 8.77 (d, $J = 8.6$ Hz, 1H). ^{13}C NMR (99 MHz, CDCl_3 , δ): 21.7 (CH₃), 22.1 (CH₃), 22.5 (CH₃), 24.9 (CH₂), 25.0 (CH₂), 26.2 (CH₂), 26.3 (CH₂), 26.4 (CH₂), 27.0 (CH₂), 27.1 (CH₂), 27.19 (CH₂), 27.23 (CH₂), 27.29 (CH₂), 27.33 (CH₂), 27.8 (CH₂), 29.8 (CH₂), 29.9 (CH₂), 32.8 (CH), 33.0 (CH), 34.7 (CH), 34.9 (CH), 70.2 (CH), 71.5 (CH), 106.8 (CH), 106.9 (CH), 109.61 (C), 109.65 (C), 123.4 (CH), 123.5 (CH), 123.7 (CH), 124.4 (CH), 124.67 (C), 124.74 (C), 125.1 (CH), 126.3 (CH), 126.4 (CH), 127.4 (CH), 127.9 (C), 130.5 (CH), 130.6 (CH), 131.3 (C), 131.4 (C), 132.0 (CH), 132.1 (CH), 133.9 (CH), 134.0 (CH), 134.5 (C), 134.6 (CH), 134.8 (C), 135.8 (CH), 136.71 (C), 136.73 (C), 137.7 (C), 145.1 (C), 145.3 (C), 160.1 (C), 160.4 (C) (observed complexity is due to C-P coupling). ^{31}P NMR (160 MHz, CDCl_3 , δ): 32.0. HRMS-ESI (m/z): $[\text{M}+\text{Na}]^+$ calcd for $\text{C}_{46}\text{H}_{52}\text{BrNaO}_2\text{PPd}$, 877.1825; found, 877.1817.



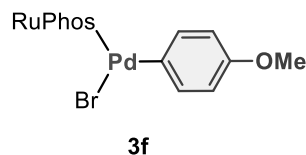
The reaction was carried out with **1** (49.0 mg, 0.12 mmol), **2c** (20.1 mg, 0.12 mmol) and RuPhos (56.3 mg, 0.12 mmol). The product **3c** was obtained as an off-white solid (54.2 mg, 0.073 mmol, 62% yield). ^1H NMR (396 MHz, CDCl_3 , δ): 0.69--0.86 (m, 2H), 1.01 (d, $J = 5.9$ Hz, 6H), 1.06--1.29 (m, 6H), 1.37 (d, $J = 5.9$ Hz, 6H), 1.51--1.71 (m, 6H), 1.71--1.87 (m, 6H), 2.08--2.17 (m, 2H), 2.19 (s, 3H), 4.60 (hept,

$J = 6.1$ Hz, 2H), 6.64 (d, $J = 8.7$ Hz, 2H), 6.75 (d, $J = 7.9$ Hz, 2H), 6.86 (ddd, $J = 1.3, 3.1, 7.4$ Hz, 1H), 6.95 (dd, $J = 1.8, 8.1$ Hz, 2H), 7.33–7.38 (m, 1H), 7.41 (tt, $J = 1.6, 7.3$ Hz, 1H), 7.56–7.62 (m, 1H), 7.65 (t, $J = 8.5$ Hz, 1H). ^{13}C NMR (99 MHz, CDCl_3 , δ): 20.5 (CH_3), 21.5 (CH_3), 22.1 (CH_3), 25.9 (CH_2), 26.7 (CH_2), 26.8 (CH_2), 27.1 (CH_2), 27.2 (CH_2), 27.4 (CH_2), 28.0 (CH_2), 33.4 (CH), 33.7 (CH), 70.6 (CH), 107.2 (CH), 111.5 (C), 126.1 (CH), 126.2 (CH), 127.9 (CH), 130.3 (CH), 130.4 (CH), 130.7 (CH), 132.2 (CH), 132.3 (CH), 132.4 (C), 133.2 (C), 133.6 (C), 134.4 (CH), 136.7 (CH), 136.8 (CH), 144.6 (C), 144.7 (C), 158.6 (C). ^{31}P NMR (160 MHz, CDCl_3 , δ): 31.1. HRMS-ESI (m/z): $[\text{M}+\text{Na}]^+$ calcd for $\text{C}_{37}\text{H}_{50}\text{BrNaO}_2\text{PPd}$, 767.1665; found, 767.1634.



The reaction was carried out with **1** (47.8 mg, 0.12 mmol), **2d** (26.3 mg, 0.12 mmol) and RuPhos (56.0 mg, 0.12 mmol). The product **3d** was obtained as a yellow solid (72.0 mg, 0.091 mmol, 75% yield).

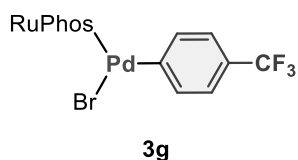
^1H NMR (392 MHz, CDCl_3 , δ): 0.69–0.83 (m, 2H), 1.01 (d, $J = 5.9$ Hz, 6H), 1.05–1.27 (m, 6H), 1.39 (d, $J = 6.3$ Hz, 6H), 1.52–1.70 (m, 6H), 1.70–1.85 (m, 6H), 2.09–2.18 (m, 2H), 2.20 (s, 3H), 4.57 (hept, $J = 5.9$ Hz, 2H), 6.64 (d, $J = 8.2$ Hz, 2H), 6.73 (d, $J = 8.2$ Hz, 2H), 6.83 (ddd, $J = 1.2, 3.1, 7.4$ Hz, 1H), 6.92 (dd, $J = 1.8, 8.0$ Hz, 2H), 7.32–7.37 (m, 1H), 7.40 (tt, $J = 0.8, 6.8$ Hz, 1H), 7.57–7.62 (m, 1H), 7.63 (t, $J = 8.4$ Hz, 1H). ^{13}C NMR (99 MHz, CDCl_3 , δ): 20.5 (CH_3), 21.6 (CH_3), 22.1 (CH_3), 25.9 (CH_2), 26.7 (CH_2), 26.8 (CH_2), 27.1 (CH_2), 27.3 (CH_2), 27.9 (CH_2), 33.5 (CH), 33.7 (CH), 70.6 (CH), 107.5 (CH), 111.4 (C), 125.2 (C), 126.10 (CH), 126.15 (CH), 127.5 (CH), 130.3 (CH), 130.8 (CH), 131.9 (C), 132.3 (CH), 132.4 (C), 133.3 (C), 133.6 (C), 134.5 (CH), 138.00 (CH), 138.03 (CH), 144.4 (C), 144.6 (C), 158.9 (C). ^{31}P NMR (160 MHz, CDCl_3 , δ): 27.0. HRMS-ESI (m/z): $[\text{M}-\text{I}]^+$ calcd for $\text{C}_{37}\text{H}_{50}\text{O}_2\text{PPd}$, 663.2597; found, 663.2584.



The reaction was carried out with **1** (48.3 mg, 0.12 mmol), **2f** (23.0 mg, 0.12 mmol) and RuPhos (56.1 mg, 0.12 mmol). The product **3f** was obtained as an off-white solid (52.0 mg, 0.068 mmol, 57% yield).

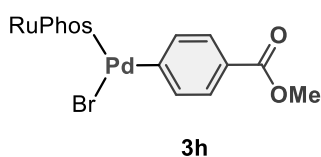
^1H NMR (392 MHz, CDCl_3 , δ): 0.72–0.87 (m, 2H), 1.01 (d, $J = 5.9$ Hz, 6H), 1.06–1.30 (m, 6H), 1.37 (d, $J = 5.9$ Hz, 6H), 1.51–1.71 (m, 6H), 1.71–1.98 (m, 6H), 2.05–2.26 (m, 2H), 3.71 (s, 3H), 4.60 (hept,

$J = 5.9$ Hz, 2H), 6.61 (d, $J = 8.6$ Hz, 2H), 6.65 (d, $J = 8.6$ Hz, 2H), 6.83–6.89 (m, 1H), 6.96 (d, $J = 8.6$ Hz, 2H), 7.32–7.48 (m, 2H), 7.59 (t, $J = 7.2$ Hz, 1H), 7.65 (t, $J = 8.2$ Hz, 1H). ^{13}C NMR (99 MHz, CDCl_3 , δ): 21.5 (CH_3), 22.1 (CH_3), 26.0 (CH_2), 26.8 (CH_2), 26.9 (CH_2), 27.1 (CH_2), 27.2 (CH_2), 27.5 (CH_2), 28.1 (CH_2), 33.5 (CH), 33.8 (CH), 55.1 (CH_3), 70.7 (CH), 107.3 (CH), 111.5 (C), 113.2 (CH), 122.8 (C), 126.2 (CH), 126.3 (CH), 130.4 (CH), 130.7 (CH), 132.3 (CH), 132.5 (CH), 133.2 (C), 133.6 (C), 134.5 (CH), 136.9 (CH), 137.0 (CH), 144.6 (C), 144.8 (C), 156.6 (C), 158.7 (C) (observed complexity is due to C–P coupling). ^{31}P NMR (160 MHz, CDCl_3 , δ): 31.3. HRMS-ESI (m/z): $[\text{M}+\text{Na}]^+$ calcd for $\text{C}_{37}\text{H}_{50}\text{BrNaO}_3\text{PPd}$, 783.1615; found, 783.1610.



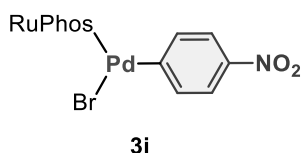
2g was distilled before the use. The reaction was carried out with **1** (46.4 mg, 0.12 mmol), **2g** (26.9 mg, 0.12 mmol) and RuPhos (55.9 mg, 0.12 mmol). The product **3g** was obtained as an off-white solid (57.5 mg, 0.072 mmol, 60% yield).

^1H NMR (392 MHz, CDCl_3 , δ): 0.63–0.77 (m, 2H), 1.02 (d, $J = 6.3$ Hz, 6H), 1.05–1.29 (m, 6H), 1.38 (d, $J = 5.9$ Hz, 6H), 1.48–1.86 (m, 12H), 2.03–2.17 (m, 2H), 4.61 (hept, $J = 6.1$ Hz, 2H), 6.66 (d, $J = 7.8$ Hz, 2H), 6.88 (ddd, $J = 1.4, 3.1, 7.6$ Hz, 1H), 7.15 (d, $J = 8.2$ Hz, 2H), 7.27 (d, $J = 5.1$ Hz, 2H), 7.34–7.41 (m, 1H), 7.44 (tt, $J = 1.5, 7.5$ Hz, 1H), 7.54–7.62 (m, 1H), 7.67 (t, $J = 8.2$ Hz, 1H). ^{13}C NMR (99 MHz, CDCl_3 , δ): 21.5 (CH_3), 22.1 (CH_3), 25.9 (CH_2), 26.6 (CH_2), 26.7 (CH_2), 27.0 (CH_2), 27.1 (CH_2), 27.4 (CH_2), 28.0 (CH_2), 33.5 (CH), 33.7 (CH), 70.9 (CH), 107.4 (CH), 110.86 (C), 110.90 (C), 122.7 (CH), 123.3 (C), 125.4 (C), 125.7 (C), 126.1 (C), 126.4 (CH), 126.5 (CH), 130.66 (CH), 130.70 (CH), 132.4 (CH), 132.5 (CH), 132.8 (C), 134.9 (CH), 137.40 (CH), 137.44 (CH), 143.0 (C), 144.4 (C), 144.6 (C), 159.0 (C) (observed complexity is due to C–P and C–F coupling). ^{31}P NMR (160 MHz, CDCl_3 , δ): 31.4. HRMS-ESI (m/z): $[\text{M}+\text{Na}]^+$ calcd for $\text{C}_{37}\text{H}_{47}\text{BrF}_3\text{NaO}_2\text{PPd}$, 821.1383; found, 821.1381.



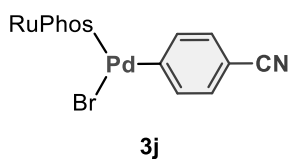
The reaction was carried out with **1** (46.2 mg, 0.12 mmol), **2h** (26.1 mg, 0.12 mmol) and RuPhos (60.0 mg, 0.12 mmol). The product **3h** was obtained as a pale yellow solid (69.1 mg, 0.088 mmol, 74% yield).

^1H NMR (401 MHz, CDCl_3 , δ): 0.70–0.84 (m, 2H), 1.02 (d, $J = 6.4$ Hz, 6H), 1.05–1.30 (m, 6H), 1.38 (d, $J = 6.0$ Hz, 6H), 1.50–1.87 (m, 12H), 2.04–2.20 (m, 2H), 3.84 (s, 3H), 4.61 (hept, $J = 5.9$ Hz, 2H), 6.66 (d, $J = 8.4$ Hz, 2H), 6.84–6.91 (m, 1H), 7.21–7.31 (m, 2H), 7.40 (dt, $J = 7.6, 22.8$ Hz, 2H), 7.53–7.62 (m, 3H), 7.66 (t, $J = 8.4$ Hz, 1H). ^{13}C NMR (99 MHz, CDCl_3 , δ): 21.4 (CH_3), 22.1 (CH_3), 25.9 (CH_2), 26.6 (CH_2), 26.7 (CH_2), 26.9 (CH_2), 27.1 (CH_2), 27.5 (CH_2), 28.0 (CH_2), 33.5 (CH), 33.8 (CH), 51.6 (CH_3), 70.9 (CH), 107.4 (CH), 111.0 (C), 111.1 (C), 125.1 (C), 126.36 (CH), 126.40 (CH), 127.0 (CH), 130.55 (CH), 130.64 (CH), 132.4 (CH), 132.5 (CH), 132.8 (C), 134.8 (CH), 137.31 (CH), 137.34 (CH), 144.3 (C), 144.5 (C), 146.9 (C), 158.9 (C), 168.0 (C) (observed complexity is due to C–P coupling). ^{31}P NMR (160 MHz, CDCl_3 , δ): 31.2. HRMS-ESI (m/z): $[\text{M}+\text{Na}]^+$ calcd for $\text{C}_{38}\text{H}_{50}\text{BrNaO}_4\text{PPd}$, 811.1564; found, 811.1570.

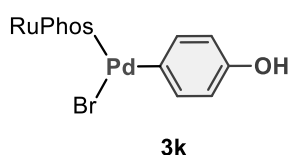


The reaction was carried out with **1** (47.6 mg, 0.12 mmol), **2i** (23.9 mg, 0.12 mmol) and RuPhos (57.5 mg, 0.12 mmol). The product **3i** was obtained as an off-white solid (66.4 mg, 0.086 mmol, 72% yield).

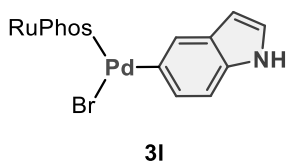
^1H NMR (392 MHz, CDCl_3 , δ): 0.72–0.88 (m, 2H), 1.03 (d, $J = 6.3$ Hz, 6H), 1.06–1.30 (m, 6H), 1.38 (d, $J = 5.5$ Hz, 6H), 1.49–1.64 (m, 2H), 1.64–1.86 (m, 10H), 2.03–2.16 (m, 2H), 4.62 (hept, $J = 6.1$ Hz, 2H), 6.67 (d, $J = 8.6$ Hz, 2H), 6.88 (ddd, $J = 1.3, 2.8, 7.7$ Hz, 1H), 7.35–7.42 (m, 3H), 7.45 (tt, $J = 1.6, 7.4$ Hz, 1H), 7.55–7.62 (m, 1H), 7.68 (t, $J = 8.4$ Hz, 1H), 7.79 (d, $J = 8.6$ Hz, 2H). ^{13}C NMR (99 MHz, CDCl_3 , δ): 21.4 (CH_3), 22.1 (CH_3), 25.9 (CH_2), 26.6 (CH_2), 26.7 (CH_2), 26.9 (CH_2), 27.0 (CH_2), 27.7 (CH_2), 28.1 (CH_2), 33.7 (CH), 34.0 (CH), 71.1 (CH), 107.5 (CH), 110.4 (C), 120.2 (CH), 126.58 (CH), 126.62 (CH), 130.7 (CH), 130.9 (CH), 132.0 (C), 132.4 (C), 132.5 (CH), 132.6 (CH), 135.3 (CH), 137.56 (CH), 137.60 (CH), 144.3 (C), 144.5 (C), 144.9 (C), 152.2 (C), 159.3 (C) (observed complexity is due to C–P coupling). ^{31}P NMR (160 MHz, CDCl_3 , δ): 31.6. HRMS-ESI (m/z): $[\text{M}-\text{Br}]^+$ calcd for $\text{C}_{38}\text{H}_{50}\text{BrNaO}_4\text{PPd}$, 694.2291; found, 694.2292.



The reaction was carried out with **1** (46.9 mg, 0.12 mmol), **2j** (21.8 mg, 0.12 mmol) and RuPhos (56.0 mg, 0.12 mmol). The product **3j** was obtained as an off-white solid (68.4 mg, 0.091 mmol, 76% yield). ^1H NMR (392 MHz, CDCl_3 , δ): 0.67–0.82 (m, 2H), 1.02 (d, $J = 5.8$ Hz, 6H), 1.03–1.30 (m, 6H), 1.37 (d, $J = 6.3$ Hz, 6H), 1.48–1.64 (m, 2H), 1.65–1.84 (m, 10H), 2.01–2.16 (m, 2H), 4.56–4.67 (m, 2H), 6.66 (d, $J = 8.5$ Hz, 2H), 6.85–6.92 (m, 1H), 7.14–7.21 (m, 2H), 7.28–7.36 (m, 2H), 7.39 (t, $J = 7.4$ Hz, 1H), 7.45 (t, $J = 7.4$ Hz, 1H), 7.58 (t, $J = 7.2$ Hz, 1H), 7.67 (t, $J = 8.3$ Hz, 1H). ^{13}C NMR (99 MHz, CDCl_3 , δ): 21.5 (CH₃), 22.1 (CH₃), 25.9 (CH₂), 26.6 (CH₂), 26.7 (CH₂), 27.0 (CH₂), 27.1 (CH₂), 27.6 (CH₂), 28.1 (CH₂), 33.6 (CH), 33.9 (CH), 71.0 (CH), 106.5 (C), 107.4 (CH), 110.4 (C), 119.9 (C), 126.5 (CH), 126.6 (CH), 129.0 (CH), 129.2 (CH), 130.7 (CH), 130.8 (CH), 132.5 (CH), 132.6 (CH), 135.2 (CH), 138.3 (CH), 144.4 (C), 144.6 (C), 147.6 (C), 159.2 (C) (observed complexity is due to C–P coupling). ^{31}P NMR (160 MHz, CDCl_3 , δ): 31.5, 32.6. HRMS-ESI (m/z): $[\text{M}–\text{Br}]^+$ calcd for C₃₇H₄₇NaO₂PPd, 674.2393; found, 674.2391.

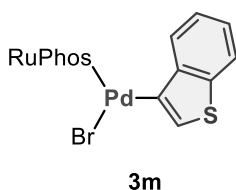


The reaction was carried out with **1** (47.2 mg, 0.12 mmol), **2k** (20.9 mg, 0.12 mmol) and RuPhos (56.4 mg, 0.12 mmol). The product **3k** was obtained as an off-white solid (31.3 mg, 0.042 mmol, 35% yield). ^1H NMR (396 MHz, CDCl_3 , δ): 0.71–0.85 (m, 2H), 1.01 (d, $J = 6.3$ Hz, 6H), 1.04–1.34 (m, 6H), 1.37 (d, $J = 5.9$ Hz, 6H), 1.49–1.96 (m, 12H), 2.06–2.23 (m, 2H), 4.59 (hept, $J = 6.0$ Hz, 2H), 6.48 (d, $J = 8.7$ Hz, 2H), 6.62 (d, $J = 7.9$ Hz, 2H), 6.80–6.90 (m, 3H), 7.33–7.47 (m, 2H), 7.55–7.61 (m, 1H), 7.64 (t, $J = 8.5$ Hz, 1H) (a proton of hydroxyl group cannot be detected). ^{13}C NMR (99 MHz, CDCl_3 , δ): 21.6 (CH₃), 22.1 (CH₃), 26.0 (CH₂), 26.8 (CH₂), 26.9 (CH₂), 27.1 (CH₂), 27.2 (CH₂), 27.6 (CH₂), 28.1 (CH₂), 33.6 (CH), 33.9 (CH), 70.6 (CH), 107.1 (CH), 110.00 (C), 115.1 (CH), 121.3 (C), 126.17 (CH), 126.21 (CH), 130.4 (CH), 130.7 (CH), 132.3 (CH), 132.4 (CH), 133.6 (C), 134.0 (C), 134.7 (CH), 136.7 (CH), 136.8 (CH), 144.8 (C), 144.9 (C), 152.9 (C), 158.9 (C) (observed complexity is due to C–P coupling). ^{31}P NMR (160 MHz, CDCl_3 , δ): 31.6. HRMS-ESI (m/z): $[\text{M}+\text{Na}]^+$ calcd for C₃₆H₄₈BrNaO₃PPd, 769.1458; found, 769.1442.



The reaction was carried out with **1** (46.7 mg, 0.12 mmol), **2l** (23.6 mg, 0.12 mmol) and RuPhos (56.1 mg, 0.12 mmol). The product **3l** was obtained as an off-white solid by reprecipitation with CH₂Cl₂/hexane (45.8 mg, 0.060 mmol, 49% yield).

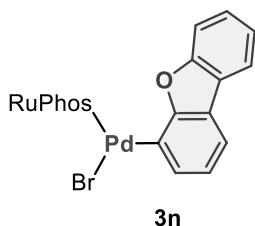
¹H NMR (392 MHz, CDCl₃, δ): 0.62 (br, s, 1H), 0.78–1.32 (m, 12H), 1.40 (d, *J* = 5.9 Hz, 6H), 1.46–1.86 (m, 12H), 1.98 (br, s, 1H), 2.07–2.24 (m, 2H), 4.56–4.69 (m, 2H), 6.29 (t, *J* = 2.4 Hz, 1H), 6.67 (dd, *J* = 8.0, 22.1 Hz, 2H), 6.88 (ddd, *J* = 1.3, 3.2, 7.5 Hz, 1H), 6.97 (t, *J* = 2.7 Hz, 1H), 6.94–7.05 (m, 2H), 7.17 (d, *J* = 1.6 Hz, 1H), 7.32–7.45 (m, 2H), 7.56–7.62 (m, 1H), 7.65 (t, *J* = 8.4 Hz, 1H), 7.88 (s, 1H). ¹³C NMR (99 MHz, CDCl₃, δ): 21.4 (CH₃), 21.6 (CH₃), 22.2 (CH₃), 25.9 (CH₂), 26.0 (CH₂), 26.5 (CH₂), 26.6 (CH₂), 26.8 (CH₂), 26.9 (CH₂), 27.0 (CH₂), 27.1 (CH₂), 27.3 (CH₂), 27.7 (CH₂), 28.2 (CH₂), 28.3 (CH₂), 30.9 (CH), 32.9 (CH), 33.2 (CH), 34.1 (CH), 34.3 (CH), 70.3 (CH), 70.9 (CH), 100.8 (CH), 106.9 (CH), 107.6 (CH), 109.3 (CH), 112.03 (C), 112.06 (C), 121.7 (C), 122.5 (CH), 126.07 (CH), 126.13 (CH), 126.9 (CH), 127.0 (CH), 128.46 (C), 128.49 (C), 130.2 (CH), 130.46 (CH), 130.49 (CH), 130.7 (CH), 132.3 (CH), 132.4 (CH), 133.5 (C), 133.8 (C), 134.2 (CH), 144.6 (C), 144.8 (C), 158.2 (C), 158.7 (C) (observed complexity is due to C–P coupling). ³¹P NMR (160 MHz, CDCl₃, δ): 31.2. HRMS-ESI (*m/z*): [M–Br]⁺ calcd for C₃₈H₄₉NO₂PPd, 688.2550; found, 688.2527.



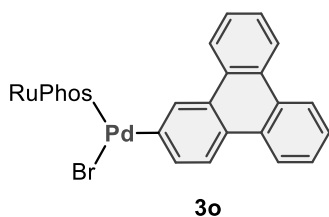
The reaction was carried out with **1** (46.6 mg, 0.12 mmol), **2m** (25.9 mg, 0.12 mmol) and RuPhos (55.9 mg, 0.12 mmol). The product **3m** was obtained as an off-white solid (73.6 mg, 0.094 mmol, 78% yield).

¹H NMR (392 MHz, CDCl₃, δ): 0.66 (br, s, 1H), 0.77–0.93 (m, 1H), 0.95–1.30 (m, 12H), 1.34–1.45 (m, 6H), 1.47–1.85 (m, 11H), 1.93 (br, s, 1H), 2.12 (br, s, 2H), 4.63 (br, s, 2H), 6.68 (dd, *J* = 8.2, 18.0 Hz, 2H), 6.89 (ddd, *J* = 1.4, 3.1, 7.6 Hz, 1H), 7.10 (d, *J* = 5.1 Hz, 1H), 7.17–7.24 (m, 2H), 7.33–7.49 (m, 4H), 7.59 (t, *J* = 6.7 Hz, 1H), 7.66 (t, *J* = 8.4 Hz, 1H). ¹³C NMR (99 MHz, CDCl₃, δ): 21.4 (CH₃), 21.5 (CH₃), 22.1 (CH₃), 25.9 (CH₂), 26.8 (CH₂), 27.1 (CH₂), 27.2 (CH₂), 27.7 (CH₂), 28.0 (CH₂), 28.3 (CH₂), 33.0 (CH), 33.3 (CH), 33.9 (CH), 34.2 (CH), 70.5 (CH), 71.1 (CH), 107.2 (CH), 107.7 (CH),

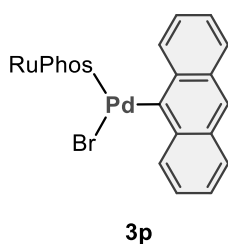
111.7 (C), 119.7 (CH), 123.0 (CH), 124.5 (CH), 126.2 (CH), 126.23 (CH), 130.0 (C), 130.4 (CH), 130.7 (CH), 130.89 (CH), 130.93 (CH), 132.4 (CH), 132.5 (CH), 132.8 (C), 133.1 (C), 133.67 (CH), 133.71 (CH), 134.4 (CH), 135.5 (C), 139.3 (C), 139.4 (C), 144.4 (C), 144.6 (C), 158.3 (C), 158.9 (C) (observed complexity is due to C–P coupling). ^{31}P NMR (160 MHz, CDCl_3 , δ): 31.2. HRMS-ESI (m/z): $[\text{M}+\text{Na}]^+$ calcd for $\text{C}_{38}\text{H}_{48}\text{BrNaO}_2\text{PPdS}$, 809.1401; found, 809.1218.



The reaction was carried out with **1** (46.9 mg, 0.12 mmol), **2n** (29.7 mg, 0.12 mmol) and RuPhos (56.0 mg, 0.12 mmol). The product **3n** was obtained as an off-white solid (50.2 mg, 0.061 mmol, 51% yield). ^1H NMR (392 MHz, CDCl_3 , δ): -0.22–0.03 (m, 1H), 0.20–0.41 (m, 1H), 0.79–1.40 (m, 18H), 1.41–1.85 (m, 10H), 1.86–2.24 (m, 3H), 2.30–2.42 (m, 1H), 4.55–4.76 (m, 2H), 6.58 (d, $J = 8.5$ Hz, 1H), 6.69 (d, $J = 8.5$ Hz, 1H), 6.86 (d, $J = 6.7$ Hz, 1H), 7.00–7.15 (m, 2H), 7.18–7.27 (m, 1H), 7.29–7.39 (m, 2H), 7.43 (d, $J = 8.1$ Hz, 2H), 7.49 (d, $J = 7.2$ Hz, 1H), 7.57 (t, $J = 7.2$ Hz, 1H), 7.77 (t, $J = 8.3$ Hz, 1H), 7.85 (d, $J = 7.6$ Hz, 1H). ^{13}C NMR (99 MHz, CDCl_3 , δ): 21.7 (CH_3), 21.9 (CH_3), 22.0 (CH_3), 22.5 (CH_2), 25.4 (CH_2), 25.6 (CH_2), 26.1 (CH_2), 26.3 (CH_2), 26.5 (CH_2), 26.7 (CH_2), 26.8 (CH_2), 26.9 (CH_2), 27.0 (CH_2), 27.1 (CH_2), 27.3 (CH_2), 27.5 (CH_2), 28.1 (CH_2), 29.41 (CH_2), 29.44 (CH_2), 33.0 (CH), 33.3 (CH), 35.1 (CH), 35.3 (CH), 70.2 (CH), 70.9 (CH), 106.3 (CH), 106.8 (CH), 108.1 (C), 113.3 (CH), 115.5 (C), 115.6 (CH), 120.5 (CH), 121.5 (C), 121.7 (CH), 122.7 (CH), 125.3 (C), 125.8 (CH), 126.28 (CH), 126.34 (CH), 130.6 (CH), 130.8 (CH), 132.1 (CH), 132.2 (CH), 134.7 (CH), 136.1 (CH), 145.3 (C), 145.5 (C), 155.8 (C), 159.9 (C), 160.0 (C), 161.0 (C) (observed complexity is due to C–P coupling). ^{31}P NMR (160 MHz, CDCl_3 , δ): 36.2, 37.4. HRMS-ESI (m/z): $[\text{M}-\text{Br}]^+$ calcd for $\text{C}_{42}\text{H}_{50}\text{O}_3\text{PPd}$, 739.2548; found, 739.2547.

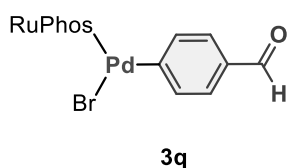


The reaction was carried out with **1** (48.1 mg, 0.12 mmol), **2o** (37.1 mg, 0.12 mmol) and RuPhos (56.3 mg, 0.12 mmol). The product **3o** was obtained as an off-white solid (98.3 mg, 0.11 mmol, 92% yield). ¹H NMR (392 MHz, CDCl₃, δ): 0.62–0.77 (m, 1H), 0.90–1.36 (m, 6H), 1.02 (d, *J* = 5.9 Hz, 3H), 1.11 (d, *J* = 5.9 Hz, 3H), 1.46 (d, *J* = 5.9 Hz, 6H), 1.50–1.85 (m, 12H), 1.98–2.23 (m, 3H), 4.63–4.75 (m, 2H), 6.74 (q, *J* = 6.8 Hz, 2H), 6.90–6.95 (m, 1H), 7.38 (t, *J* = 6.3 Hz, 1H), 7.45 (t, *J* = 7.1 Hz, 1H), 7.51–7.64 (m, 6H), 7.70 (t, *J* = 8.4 Hz, 1H), 8.20 (d, *J* = 8.6 Hz, 1H), 8.30 (s, 1H), 8.51–8.63 (m, 4H). ¹³C NMR (99 MHz, CDCl₃, δ): 21.5 (CH₃), 21.6 (CH₃), 22.3 (CH₃), 26.0 (CH₂), 26.1 (CH₂), 26.7 (CH₂), 26.8 (CH₂), 27.0 (CH₂), 27.1 (CH₂), 27.3 (CH₂), 28.0 (CH₂), 28.2 (CH₂), 28.4 (CH₂), 33.2 (CH), 33.5 (CH), 34.1 (CH), 34.4 (CH), 70.7 (CH), 71.2 (CH), 107.3 (CH), 108.0 (CH), 111.9 (C), 120.8 (CH), 122.8 (CH), 123.0 (CH), 123.1 (CH), 123.3 (CH), 126.1 (CH), 126.2 (C), 126.3 (CH), 126.39 (CH), 126.43 (CH), 126.7 (CH), 126.8 (CH), 128.7 (C), 129.0 (C), 129.66 (C), 129.74 (C), 130.5 (CH), 130.56 (C), 130.64 (CH), 130.7 (CH), 130.8 (CH), 132.5 (CH), 132.7 (CH), 132.8 (C), 133.1 (CH), 134.6 (CH), 136.1 (C), 137.49 (CH), 137.52 (CH), 144.6 (C), 144.7 (C), 158.4 (C), 159.0 (C) (observed complexity is due to C–P coupling). ³¹P NMR (160 MHz, CDCl₃, δ): 31.2. HRMS-ESI (*m/z*): [M–Br]⁺ calcd for C₄₈H₅₄O₂PPd, 799.2914; found, 799.2904.

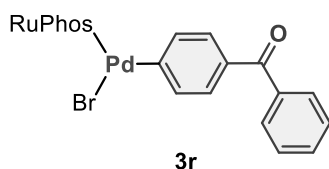


The reaction was carried out with **1** (47.5 mg, 0.12 mmol), **2p** (31.1 mg, 0.12 mmol) and RuPhos (56.0 mg, 0.12 mmol). The product **3p** was obtained as a yellow solid (77.7 mg, 0.094 mmol, 78% yield). ¹H NMR (392 MHz, CDCl₃, δ): –0.43––0.26 (m, 2H), 0.50 (q, *J* = 13.1 Hz, 2H), 0.72–0.85 (m, 2H), 0.97 (q, *J* = 12.3 Hz, 2H), 1.06 (d, *J* = 6.3 Hz, 6H), 1.26–1.57 (m, 12H), 1.50 (d, *J* = 5.9 Hz, 6H), 1.58–1.74 (m, 2H), 4.72 (hept, *J* = 6.1 Hz, 2H), 6.71 (d, *J* = 8.6 Hz, 2H), 6.84 (ddd, *J* = 1.0, 2.7, 7.6 Hz, 1H), 7.27–7.36 (m, 5H), 7.38–7.48 (m, 2H), 7.72–7.80 (m, 2H), 7.87 (t, *J* = 8.6 Hz, 1H), 7.95 (s, 1H), 8.66–8.73 (m, 2H). ¹³C NMR (99 MHz, CDCl₃, δ): 21.7 (CH₃), 22.3 (CH₃), 25.5 (CH₂), 26.3 (CH₂),

26.4 (CH₂), 26.6 (CH₂), 26.7 (CH₂), 26.9 (CH₂), 27.0 (CH₂), 34.2 (CH), 34.5 (CH), 70.8 (CH), 106.7 (CH), 109.0 (CH), 109.1 (CH), 122.4 (CH), 122.8 (CH), 124.3 (CH), 126.30 (CH), 126.35 (CH), 127.7 (CH), 129.9 (CH), 130.6 (CH), 131.7 (C), 131.8 (CH), 131.9 (CH), 134.7 (CH), 135.8 (C), 136.2 (C), 136.3 (CH), 137.20 (C), 137.24 (C), 142.21 (C), 142.25 (C), 145.1 (C), 145.3 (C), 161.0 (C). ³¹P NMR (160 MHz, CDCl₃, δ): 31.7. HRMS-ESI (m/z): [M+Na]⁺ calcd for C₄₄H₅₂BrNaO₂PPd, 853.1824; found, 853.1819.

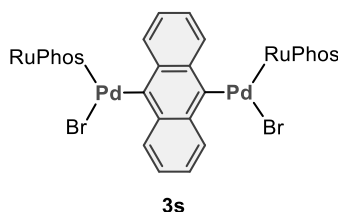


The reaction was carried out with **1** (46.8 mg, 0.12 mmol), **2q** (22.5 mg, 0.12 mmol) and RuPhos (56.1 mg, 0.12 mmol). The product **3q** was obtained as an off-white solid (71.7 mg, 0.095 mmol, 79% yield). ¹H NMR (392 MHz, CDCl₃, δ): 0.70–0.83 (m, 2H), 1.03 (d, *J* = 6.3 Hz, 6H), 1.05–1.31 (m, 6H), 1.39 (d, *J* = 6.3 Hz, 6H), 1.50–1.86 (m, 12H), 2.04–2.20 (m, 2H), 4.62 (hept, *J* = 5.9 Hz, 2H), 6.67 (d, *J* = 8.2 Hz, 2H), 6.88 (ddd, *J* = 1.5, 3.2, 7.5 Hz, 1H), 7.36–7.50 (m, 6H), 7.59 (t, *J* = 7.1 Hz, 1H), 7.67 (t, *J* = 8.2 Hz, 1H), 9.83 (s, 1H). ¹³C NMR (99 MHz, CDCl₃, δ): 21.4 (CH₃), 22.0 (CH₃), 25.9 (CH₂), 26.6 (CH₂), 26.7 (CH₂), 26.9 (CH₂), 27.1 (CH₂), 27.5 (CH₂), 28.0 (CH₂), 33.6 (CH), 33.8 (CH), 70.9 (CH), 107.4 (CH), 110.72 (C), 110.74 (C), 126.4 (CH), 126.5 (CH), 126.9 (CH), 130.6 (CH), 132.3 (C), 132.4 (CH), 132.5 (CH), 132.6 (C), 135.0 (CH), 137.98 (CH), 138.01 (CH), 144.3 (C), 144.5 (C), 151.3 (C), 159.0 (C), 192.7 (C) (observed complexity is due to C–P coupling). ³¹P NMR (160 MHz, CDCl₃, δ): 31.4. HRMS-ESI (m/z): [M+Na]⁺ calcd for C₃₇H₄₈BrNaO₃PPd, 781.1458; found, 781.1458.



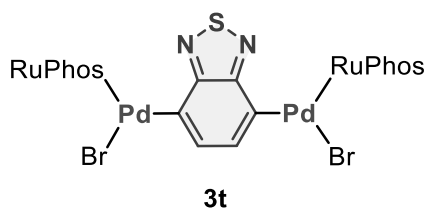
The reaction was carried out with **1** (47.3 mg, 0.12 mmol), **2r** (31.7 mg, 0.12 mmol) and RuPhos (57.0 mg, 0.12 mmol). The product **3r** was obtained as an off-white solid (61.8 mg, 0.074 mmol, 61% yield). ¹H NMR (396 MHz, CDCl₃, δ): 0.72–0.87 (m, 2H), 1.02 (d, *J* = 5.9 Hz, 6H), 1.05–1.28 (m, 6H), 1.39 (d, *J* = 5.9 Hz, 6H), 1.51–1.84 (m, 12H), 2.07–2.19 (m, 2H), 4.62 (hept, *J* = 6.0 Hz, 2H), 6.68 (d, *J* = 8.7 Hz, 2H), 6.88 (ddd, *J* = 1.4, 3.2, 7.7 Hz, 1H), 7.29–7.47 (m, 8H), 7.53 (tt, *J* = 1.6, 7.5 Hz, 1H), 7.56–7.62 (m, 1H), 7.68 (t, *J* = 5.1 Hz, 1H), 7.73–7.78 (m, 2H). ¹³C NMR (99 MHz, CDCl₃, δ): 21.5

(CH₃), 22.0 (CH₃), 25.8 (CH₂), 26.6 (CH₂), 26.7 (CH₂), 27.0 (CH₂), 27.1 (CH₂), 27.5 (CH₂), 28.0 (CH₂), 33.5 (CH), 33.8 (CH), 70.9 (CH), 107.4 (CH), 110.97 (C), 111.01 (C), 126.38 (CH), 126.43 (CH), 127.8 (CH), 127.9 (CH), 129.8 (CH), 130.6 (CH), 130.7 (CH), 131.6 (CH), 132.37 (CH), 132.42 (CH), 132.5 (C), 132.7 (C), 134.8 (CH), 137.2 (CH), 137.3 (CH), 138.4 (C), 144.4 (C), 144.5 (C), 147.5 (C), 158.9 (C), 197.0 (C) (observed complexity is due to C–P coupling). ³¹P NMR (160 MHz, CDCl₃, δ): 31.3. HRMS-ESI (m/z): [M+Na]⁺ calcd for C₄₃H₅₂BrNaO₃PPd, 857.1773; found, 857.1756.



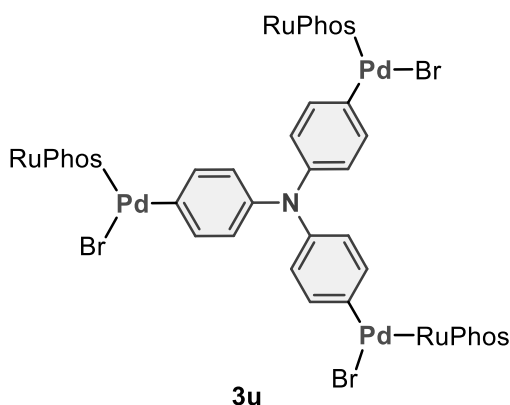
The reaction was carried out with **1** (779.1 mg, 2.0 mmol), **2s** (336.2 mg, 1.0 mmol) and RuPhos (933.3 mg, 2.0 mmol). The product **3s** was obtained as an orange solid (1.261 g, 0.85 mmol, 85% yield).

¹H NMR (392 MHz, CDCl₃, δ): -0.44–-0.22 (m, 4H), 0.37–0.54 (m, 4H), 0.69–0.83 (m, 4H), 0.84–0.98 (m, 4H), 1.04 (d, *J* = 5.8 Hz, 12H), 1.18–1.60 (m, 36H), 1.71–1.85 (m, 4H), 4.70 (quin, *J* = 5.8 Hz, 4H), 6.68 (d, *J* = 8.5 Hz, 4H), 6.78–6.83 (m, 2H), 7.17 (dd, *J* = 3.1, 6.3 Hz, 4H), 7.23–7.29 (m, 2H), 7.34 (t, *J* = 6.7 Hz, 2H), 7.41 (t, *J* = 7.2 Hz, 2H), 7.78 (t, *J* = 8.1 Hz, 2H), 8.57 (dd, *J* = 3.1, 6.3 Hz, 4H). ¹³C NMR (99 MHz, CDCl₃, δ): 21.7 (CH₃), 22.6 (CH₃), 26.0 (CH₂), 26.6 (CH₂), 26.7 (CH₂), 26.8 (CH₂), 26.95 (CH₂), 26.99 (CH₂), 27.7 (CH₂), 34.7 (CH₂), 35.0 (CH₂), 71.0 (CH), 107.3 (CH), 111.1 (C), 121.9 (CH), 126.1 (CH), 130.1 (CH), 130.3 (CH), 131.8 (CH), 132.0 (CH), 134.5 (CH), 135.5 (CH), 136.7 (C), 137.5 (C), 145.2 (C), 160.7 (C) (observed complexity is due to C–P coupling). ³¹P NMR (160 MHz, CDCl₃, δ): 31.4 (s). HRMS-ESI (m/z): [M–Br]⁺ calcd for C₇₄H₉₄BrO₄P₂Pd₂, 1401.3906; found, 1401.3888.



The reaction was carried out with **1** (93.5 mg, 0.24 mmol), **2t** (35.3 mg, 0.12 mmol) and RuPhos (112.1 mg, 0.12 mmol). The product **3t** was obtained as a yellow solid (146.9 mg, 0.10 mmol, 85% yield).

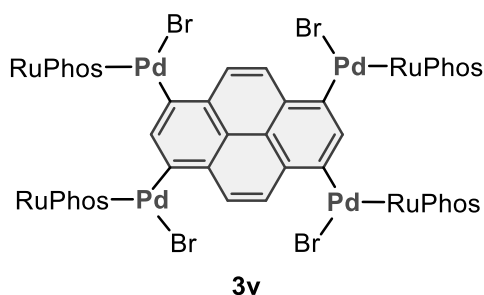
^1H NMR (392 MHz, CDCl_3 , δ): -0.59 (q, $J = 12.7$ Hz, 2H), 0.16 (q, $J = 12.9$ Hz, 2H), 0.66 (q, $J = 12.4$ Hz, 2H), 0.80–1.95 (m, 56H), 1.99–2.11 (m, 2H), 2.20–2.35 (m, 2H), 2.44–2.53 (m, 2H), 4.57 (quin, $J = 5.8$ Hz, 2H), 4.69 (quin, $J = 6.0$ Hz, 2H), 6.54 (d, $J = 8.5$ Hz, 2H), 6.62 (s, 2H), 6.77 (d, $J = 8.1$ Hz, 2H), 6.85 (d, $J = 6.3$ Hz, 2H), 7.33 (t, $J = 7.4$ Hz, 2H), 7.40 (t, $J = 7.4$ Hz, 2H), 7.54 (t, $J = 7.4$ Hz, 2H), 7.65 (t, $J = 8.3$ Hz, 2H). ^{13}C NMR (99 MHz, CDCl_3 , δ): 21.5 (CH_3), 21.6 (CH_3), 22.2 (CH_3), 22.8 (CH_3), 25.7 (CH_2), 26.0 (CH_2), 26.3 (CH_2), 26.56 (CH_2), 26.62 (CH_2), 26.7 (CH_2), 27.3 (CH_2), 27.4 (CH_2), 27.6 (CH_2), 27.8 (CH_2), 30.2 (CH_2), 31.8 (CH), 32.1 (CH), 34.8 (CH), 35.1 (CH), 70.0 (CH), 72.0 (CH), 106.4 (CH), 107.9 (CH), 106.4 (CH), 107.9 (CH), 110.90 (C), 110.91 (C), 123.1 (C), 126.05 (CH), 126.10 (CH), 130.3 (CH), 130.9 (CH), 132.3 (C), 132.4 (C), 134.3 (C), 134.8 (CH), 144.9 (C), 145.1 (C), 158.9 (C), 160.2 (C), 160.4 (C) (observed complexity is due to C–P coupling). ^{31}P NMR (160 MHz, CDCl_3 , δ): 35.4. HRMS-ESI (m/z): $[\text{M}-\text{Br}]^+$ calcd for $\text{C}_{66}\text{H}_{88}\text{BrN}_2\text{O}_4\text{P}_2\text{Pd}_2\text{S}$, 1359.3214; found, 1359.3198.



The reaction was carried out with **1** (140.1 mg, 0.36 mmol), **2u** (57.8 mg, 0.12 mmol) and RuPhos (168.1 mg, 0.36 mmol). The product **3u** was obtained as an orange solid (240.4 mg, 0.11 mmol, 91% yield).

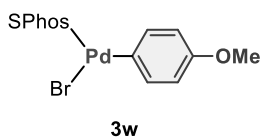
^1H NMR (392 MHz, CDCl_3 , δ): 0.64–0.82 (m, 6H), 0.95–1.30 (m, 36H), 1.35 (d, $J = 2.7$ Hz, 9H), 1.37 (d, $J = 2.9$ Hz, 9H), 1.45–1.92 (m, 33H), 2.20 (q, $J = 10.5$ Hz, 6H), 4.53–4.64 (m, 6H), 6.62 (dd, $J =$

2.2, 8.5 Hz, 6H), 6.68–6.76 (m, 6H), 6.78–6.97 (m, 11H), 7.14 (d, $J = 8.5$ Hz, 1H), 7.32–7.45 (m, 6H), 7.59 (t, $J = 7.0$ Hz, 3H), 7.67 (td, $J = 4.0, 8.3$ Hz, 3H). ^{13}C NMR (99 MHz, CDCl_3 , δ): 21.6 (CH_3), 22.0 (CH_3), 25.9 (CH_2), 26.8 (CH_2), 26.9 (CH_2), 27.2 (CH_2), 27.3 (CH_2), 27.5 (CH_2), 27.9 (CH_2), 33.4 (CH), 33.6 (CH), 70.4 (CH), 70.6 (CH), 106.97 (CH), 107.01 (CH), 110.68 (C), 110.72 (C), 111.0 (C), 111.1 (C), 112.4 (C), 122.7 (CH), 123.5 (CH), 123.6 (CH), 124.6 (C), 126.1 (CH), 126.19 (CH), 126.23 (CH), 127.4 (C), 130.3 (CH), 130.5 (CH), 130.7 (CH), 130.8 (CH), 131.3 (CH), 132.2 (CH), 132.27 (CH), 132.33 (CH), 132.4 (CH), 133.4 (C), 133.7 (C), 133.8 (C), 134.1 (C), 134.6 (CH), 134.9 (CH), 136.56 (CH), 136.60 (CH), 137.2 (CH), 137.3 (CH), 143.2 (C), 144.0 (C), 144.8 (C), 144.9 (C), 145.9 (C), 147.5 (C), 158.8 (C), 159.0 (C) (observed complexity is due to C–P coupling). ^{31}P NMR (160 MHz, CDCl_3 , δ): 31.5, 31.6, 32.4, 32.7. HRMS-ESI (m/z): $[\text{M}-\text{Br}]^+$ calcd for $\text{C}_{108}\text{H}_{141}\text{Br}_2\text{NO}_6\text{P}_3\text{Pd}_3$, 2120.5480; found, 2120.5469.

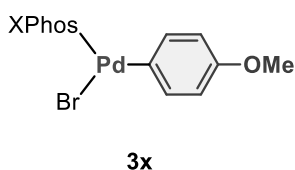


The reaction was carried out with **1** (124.7 mg, 0.32 mmol), **2v** (41.5 mg, 0.08 mmol) and RuPhos (149.3 mg, 0.32 mmol). The product **3v** was obtained as an orange solid (137.5 mg, 0.05 mmol, 61% yield).

^1H NMR (392 MHz, CDCl_3 , δ): -0.40–0.25 (m, 3H), 0.32–0.69 (m, 8H), 0.72–1.37 (m, 62H), 1.42–2.01 (m, 55H), 2.29–2.54 (m, 8H), 4.50–4.62 (m, 4H), 4.70–4.83 (m, 4H), 6.54–6.65 (m, 4H), 6.82–6.95 (m, 8H), 7.01–7.13 (m, 2H), 7.25–7.40 (m, 8H), 7.48–7.61 (m, 8H), 8.36–8.45 (m, 4H). ^{13}C NMR (99 MHz, CDCl_3 , δ): 21.47 (CH_3), 22.05 (CH_3), 25.84 (CH_2), 26.60 (CH_2), 26.72 (CH_2), 26.95 (CH_2), 27.08 (CH_2), 27.52 (CH_2), 28.04 (CH_2), 33.53 (CH), 33.80 (CH), 70.90 (CH), 107.41 (CH), 110.97 (C), 111.01 (C), 126.38 (CH), 126.43 (CH), 127.84 (CH), 127.89 (CH), 129.81 (CH), 130.61 (CH), 130.68 (CH), 131.57 (CH), 132.37 (CH), 132.42 (CH), 132.52 (C), 132.73 (C), 134.85 (CH), 137.23 (CH), 137.27 (CH), 138.38 (C), 144.36 (C), 144.54 (C), 147.46 (C), 158.92 (C), 197.00 (C) (observed complexity is due to C–P coupling). ^{31}P NMR (160 MHz, CDCl_3 , δ): 28.8, 29.2, 29.3, 30.4. HRMS-ESI (m/z): $[\text{M}]^+$ calcd for $\text{C}_{136}\text{H}_{178}\text{Br}_4\text{O}_8\text{P}_4\text{Pd}_4$, 2809.5383; found, 2809.5324.



The reaction was carried out with **1** (46.8 mg, 0.12 mmol), **2f** (22.4 mg, 0.12 mmol) and SPhos (49.4 mg, 0.12 mmol). The product **3w** was obtained as an off-white solid (37.2 mg, 0.053 mmol, 44% yield). ^1H NMR (392 MHz, CDCl_3 , δ): 0.60–0.73 (m, 2H), 1.01–1.31 (m, 7H), 1.51–1.82 (m, 9H), 1.83–1.98 (m, 2H), 2.17 (q, $J = 11.4$ Hz, 2H), 3.72 (s, 3H), 3.78 (s, 6H), 6.59–6.69 (m, 4H), 6.83–6.88 (m, 1H), 6.94 (dd, $J = 2.0, 8.7$ Hz, 2H), 7.42 (t, $J = 7.6$ Hz, 1H), 7.48 (t, $J = 7.4$ Hz, 1H), 7.65 (t, $J = 6.7$ Hz, 1H), 7.79 (t, $J = 8.3$ Hz, 1H). ^{13}C NMR (99 MHz, CDCl_3 , δ): 25.9 (CH_2), 27.0 (CH_2), 27.2 (CH_2), 27.4 (CH_2), 27.5 (CH_2), 27.7 (CH_2), 34.1 (CH), 34.4 (CH), 55.1 (CH_3), 55.9 (CH_3), 106.1 (CH), 107.97 (C), 108.00 (C), 113.4 (CH), 121.9 (C), 126.7 (CH), 126.8 (CH), 131.3 (CH), 131.4 (CH), 131.6 (CH), 131.7 (CH), 135.8 (CH), 136.7 (CH), 136.8 (CH), 144.2 (C), 156.8 (C), 160.4 (C) (observed complexity is due to C–P coupling). ^{31}P NMR (160 MHz, CDCl_3 , δ): 34.3, 35.2. HRMS-ESI (m/z): $[\text{M}-\text{Br}]^+$ calcd for $\text{C}_{33}\text{H}_{42}\text{O}_3\text{PPd}$, 623.1919; found, 623.1904.



The reaction was carried out with **1** (46.9 mg, 0.12 mmol), **2f** (22.4 mg, 0.12 mmol) and XPhos (57.2 mg, 0.12 mmol). The product **3x** was obtained as a pale-yellow solid (29.6 mg, 0.038 mmol, 44% yield). ^1H NMR (392 MHz, CDCl_3 , δ): 0.60–0.75 (m, 2H), 0.90 (d, $J = 6.7$ Hz, 6H), 1.05–1.29 (m, 8H), 1.39 (d, $J = 7.2$ Hz, 6H), 1.59 (d, $J = 6.7$ Hz, 6H), 1.62–1.85 (m, 8H), 1.91–2.01 (m, 2H), 2.22 (q, $J = 11.4$ Hz, 2H), 2.44 (sep, $J = 6.5$ Hz, 2H), 3.12 (sep, $J = 6.7$ Hz, 1H), 3.70 (s, 3H), 6.61 (d, $J = 8.5$ Hz, 2H), 6.85–6.92 (m, 3H), 7.13 (s, 2H), 7.38–7.44 (m, 2H), 7.64–7.71 (m, 1H). ^{13}C NMR (99 MHz, CDCl_3 , δ): 24.1 (CH_3), 24.4 (CH_3), 24.6 (CH_3), 25.5 (CH_3), 25.8 (CH_2), 27.2 (CH_2), 27.3 (CH_2), 27.5 (CH_2), 27.6 (CH_2), 28.2 (CH_2), 31.4 (CH), 34.1 (CH), 35.0 (CH), 35.3 (CH), 55.2 (CH_3), 113.5 (CH), 121.6 (C), 124.6 (CH), 125.56 (C), 125.60 (C), 126.68 (CH), 126.73 (CH), 130.3 (CH), 131.8 (CH), 133.3 (CH), 133.4 (CH), 134.3 (C), 134.6 (C), 136.38 (CH), 136.42 (CH), 147.4 (C), 147.6 (C), 149.1 (C), 155.8 (C), 156.7 (C) (observed complexity is due to C–P coupling). ^{31}P NMR (160 MHz, CDCl_3 , δ): 26.7. HRMS-ESI (m/z): $[\text{M}-\text{Br}]^+$ calcd for $\text{C}_{40}\text{H}_{56}\text{OPPd}$, 689.3119; found, 689.3118.

5. References

- 1) Sheldrick, G. M. *Acta Crystallogr., Sect. A* **2008**, *64*, 112.
- 2) Kubota, K.; Dai, P.; Pentelute, B. L.; Buchwald, S. L. *J. Am. Chem. Soc.* **2018**, *140*, 3128–3133.

Chapter 2.

Development of Air- and Moisture-stable Xantphos- ligated Palladium Precatalyst for Cross-Coupling Reactions

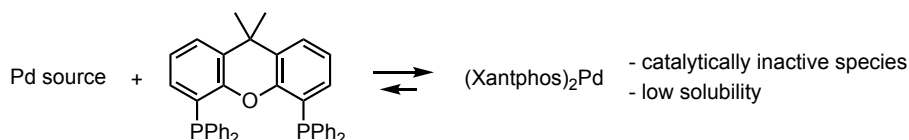
Abstract

Xantphos has been employed in a variety of palladium-catalyzed cross-coupling reactions, but there has been little progress in developing Xantphos-ligated palladium precatalysts for these reactions. Herein I describe a Xantphos-ligated palladium dialkyl complex that acts as a powerful precatalyst for C–N, C–S, and C–C cross-coupling reactions. This precatalyst is air- and moisture stable but can be thermally activated in the absence of external reagents. Additionally, potential catalyst inhibitors are not generated during the precatalyst activation. This complex thus represents a convenient alternative to previously reported classes of Xantphos-ligated precatalysts.

Introduction

Palladium-catalyzed cross-coupling reactions have become one of the most powerful and versatile methods for the formation of carbon–carbon and carbon–heteroatom bonds in academic and industrial settings.¹ The development of specialized phosphine- and N-heterocyclic-carbene-(NHC)-based ligands, which promote fundamental steps in the catalytic cycle such as oxidative addition, transmetalation, and reductive elimination, has led to significant advances in this field.¹ Furthermore, recent studies have revealed that the generation of catalytically active and coordinatively unsaturated monoligated Pd(0) species is crucial for the success of cross-coupling reactions.^{1,2} In this context, the development of readily available and bench-stable palladium precatalysts that form catalytically-active monoligated Pd(0) species has attracted considerable interest in the synthetic-chemistry community.¹

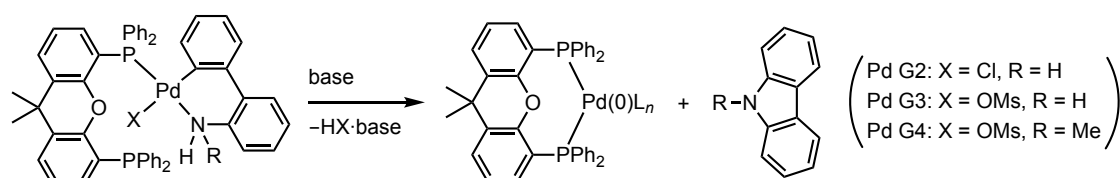
Xantphos, a diphosphine ligand with a large bite angle, has been employed in a variety of palladium-catalyzed carbon–carbon- and carbon–heteroatom-bond-forming reactions.³ However, Buchwald and co-workers have reported that the catalytically inactive bis-ligated palladium species Pd(Xantphos)₂ is readily formed during such reactions, which significantly decreases the reaction rate due to the very high binding constant for the ligand in the bis-ligated species (Scheme 2-1).⁴ Thus, the development of a Xantphos-ligated precatalyst that does not form bis-ligated palladium species should be highly desirable.



Scheme 2-1. Formation of catalytically inactive species during palladium-catalyzed cross-coupling reactions using Xantphos as a ligand.

Buchwald and co-workers have developed a series of highly active palladacyclic precatalysts that bear a variety of phosphine ligands.⁵ These complexes are commonly referred to as Buchwald precatalysts and have become a valuable tool for palladium-catalyzed cross-coupling reactions. Moreover, such Xantphos-ligated palladacyclic precatalysts are now commercially available as Xantphos Pd G2 (Aldrich, product no. 763047), Xantphos Pd G3 (Aldrich, product no. 763039) and Xantphos Pd G4 (Aldrich, product no. 900329) (Scheme 2-2). However, these precatalysts form carbazole-based byproducts upon catalyst activation, which could potentially lead to subsequent catalyst inhibition and complicate the purification step.

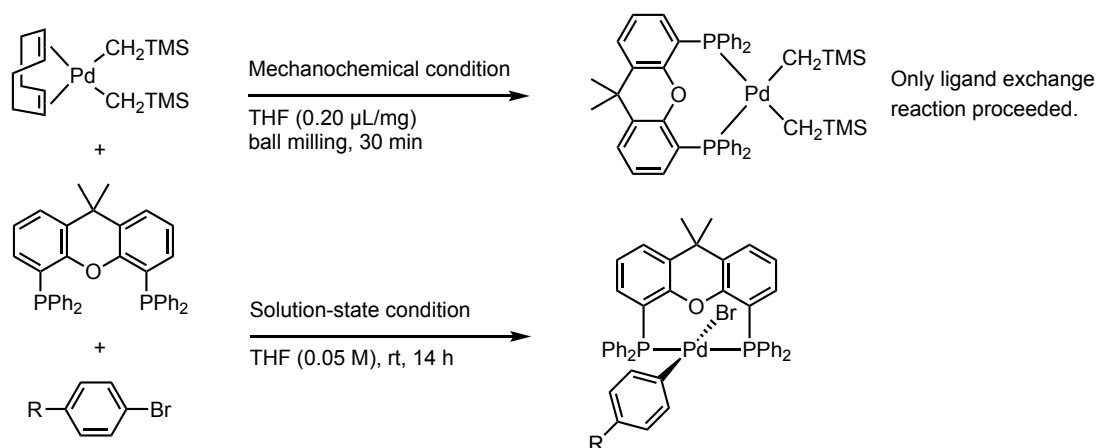
Buchwald palladacycle precatalysts bearing Xantphos



- + high-performance precatalysts
- + can be synthesized in 3 steps
- + commercially available
- carbazole-based byproducts are potential catalyst inhibitors

Scheme 2-2. Xantphos-ligated palladacyclic precatalysts developed by Buchwald and co-workers.

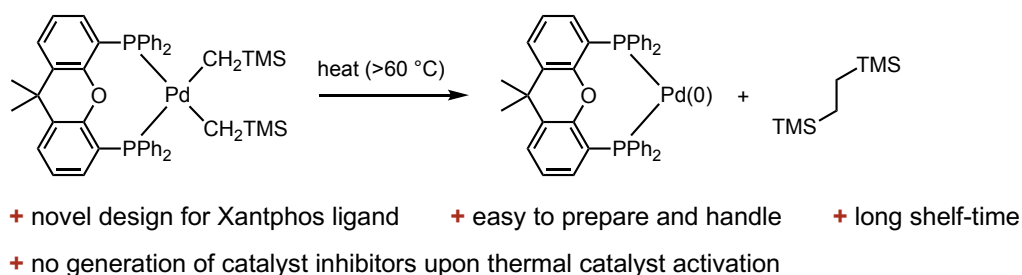
During the study described in the chapter 1, Xantphos-ligated palladium dialkyl complex, (Xantphos)Pd(CH₂TMS)₂, was unexpectedly obtained under mechanochemical conditions by ligand exchange reaction of (COD)Pd(CH₂TMS)₂ with Xantphos, even in the presence of aryl halides (Scheme 2-3). On the other hand, when the reactions using (COD)Pd(CH₂TMS)₂, Xantphos, and aryl halides were carried out in common organic solvents at room temperature, the corresponding palladium(II) oxidative addition complexes were obtained in moderate yield. These results indicate that Xantphos-ligated palladium dialkyl complex would be stable in the solid-state and the reductive elimination from this palladium complex proceeds smoothly in the solution-state. Therefore, I expected that this palladium complex may be suitable as a precatalyst for palladium-catalyzed cross-coupling reactions.



Scheme 2-3. Attempted synthesis of Xantphos-ligated palladium oxidative addition complexes under mechanochemical condition.

Herein, I describe the synthesis of air- and moisture-stable palladium dialkyl complex bearing Xantphos ligand and its application as a precatalyst for cross-coupling reactions (Scheme 2-4).^{6,7} This precatalyst can be thermally activated via a reductive elimination to form a catalytically active, coordinatively unsaturated $L_nPd(0)$ species. The sole byproduct of this activation process is 1,2-bis(trimethylsilyl)ethane, which does not interfere with the catalyst. Notably, this newly developed precatalyst is easy to handle and exhibit a long shelf-life. The strict exclusion of air and water is not necessary.

Xantphos-ligated dialkyl complex as precatalyst

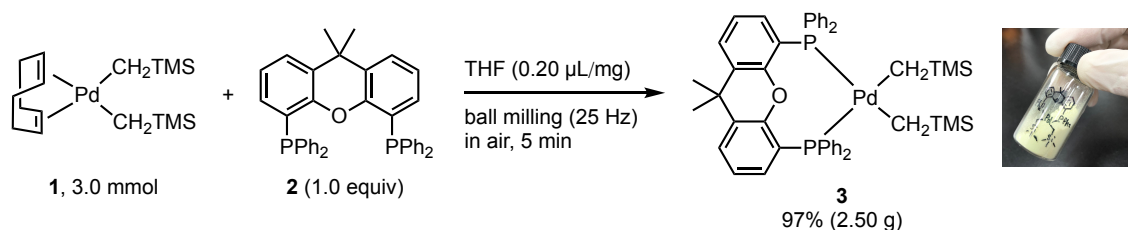


Scheme 2-4. New design of a Xantphos-ligated palladium(II) precatalyst for cross-coupling reactions.

Results and Discussion

To prepare a Xantphos-ligated palladium dialkyl complex, a ligand-exchange reaction between (COD)Pd(CH₂TMS)₂ (**1**) and Xantphos (**2**) was carried out in a stainless-steel ball-milling jar (25 mL) with two stainless-steel balls (diameter: 10 mm) under the solid-state mechanochemical condition. The reaction completed within 5 minutes and afforded the corresponding palladium complex (Xantphos)Pd(CH₂TMS)₂ (**3**)

in 97% yield (2.5 g) (Scheme 2-5). The molecular structure of **3** was determined by a single-crystal X-ray diffraction analysis, which revealed a square-planar *cis* geometry around the Pd center (Figure 2-1).



Scheme 2-5. Synthesis of **3** under the mechanochemical condition.

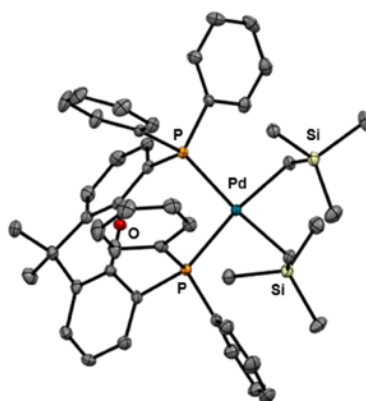
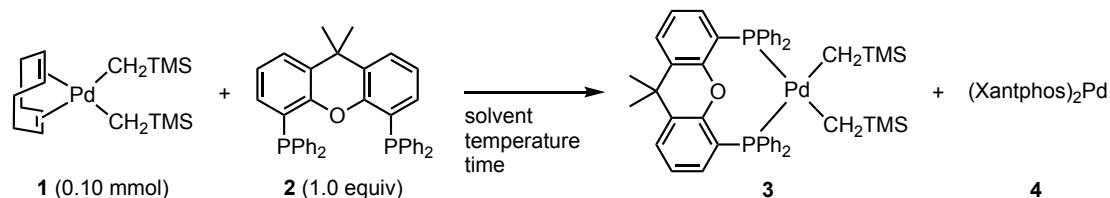


Figure 2-1. Single-crystal structure of **3** (thermal ellipsoids set at 50% probability; hydrogen atoms have been omitted for clarity).

I also investigated the synthesis of **3** in a solution-state (Table 2-1).⁸ Unfortunately, when the reaction was carried out in tetrahydrofuran (THF) at room temperature, the desired product **3** was not obtained. Instead, an insoluble compound, which was identified as the bis-ligated palladium species, Pd(Xantphos)₂ (**4**), was obtained (entry 1).^{4,9} Reactions in simple alkane solvents also failed to generate **3** (entries 2 and 3). Pleasingly, the reaction in acetonitrile (CH₃CN) provided **3** in moderate yield (52% yield; entry 4), and **3** was obtained in high yield when the reaction time was shortened to 20 minutes (84% yield; entry 5). These results indicate that shorter reaction times may suppress the undesired reductive elimination from **3** that decreases the yield of **3**. I also found that lowering the reaction temperature avoided the formation of **4** in favor of **3** in THF or diethyl ether (entries 6 and 7). Pd complex **3** was obtained as an air- and moisture-stable solid that can be handled at room temperature. For the long-term storage, low temperatures (−30 °C) are required in order to avoid decomposition (see the experimental

section for details).

Table 2-1. Preparation of Xantphos-ligated palladium dialkyl complex **3**^a



entry	solvent	temperature (°C)	time	yield (%) of 3 ^b
1	THF	rt	16 h	-
2	cyclohexane	rt	16 h	-
3	pentane	rt	16 h	-
4	CH ₃ CN	rt	16 h	52
5	CH ₃ CN	rt	20 min	84
6	THF	0	16 h	43
7	Et ₂ O	0	20 min	89

^aConditions: **1** (0.10 mmol) and **2** (0.10 mmol) in the specified solvent (0.10 M) were stirred under nitrogen atmosphere. ^bIsolated yields based on the amount of **2**.

To determine the conditions required for the thermal activation of **3** to generate the catalytically active species, the progress of the reductive elimination reaction was monitored at different reaction temperatures using ¹H NMR spectroscopy (Figure 2-2). The reductive elimination of **3** proceeded rapidly at 80 °C and 60 °C to form 1,2-bis(trimethylsilyl)ethane (**5**) quantitatively within 60 minutes. In contrast, the reductive elimination was slow at 40 °C. These results indicate that **3** could potentially be used as a precatalyst for a number of cross-coupling reactions, as palladium-catalyzed cross-coupling reactions are typically carried out at 60 °C or higher.

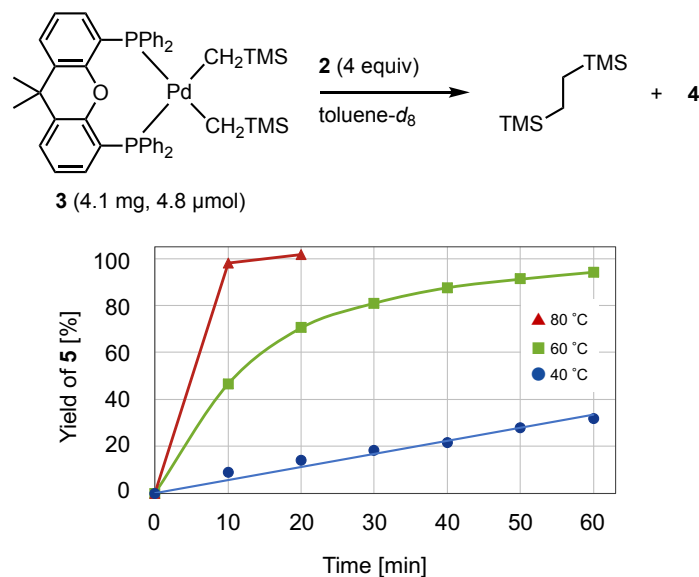


Figure 2-2. Monitoring the reductive elimination of 1,2-bis(trimethylsilyl)ethane (**5**) from **3** at various temperature.

To evaluate the performance of **3** as a precatalyst, I examined its efficacy in promoting C–N cross-coupling reactions between aryl halides and amides (Figure 2-3).¹⁰ 1-Bromo-2-methylbenzene (**6a**) reacted with benzamide (**7a**) in the presence of **3** to afford the desired product (**8a**) in high yield. For comparison, I also tested the Buchwald palladacycle precatalyst G3 (Xantphos Pd G3) instead of **3** for this coupling reaction, which provided the almost same product yield. These results show that the catalytic activity of **3** is comparable to that of the Buchwald precatalyst G3.^{1c} Moreover, **3** showed significantly higher catalytic activity than conventional catalyst precursors such as Pd(OAc)₂/Xantphos or Pd(dba)₂/Xantphos in these C–N coupling reactions.

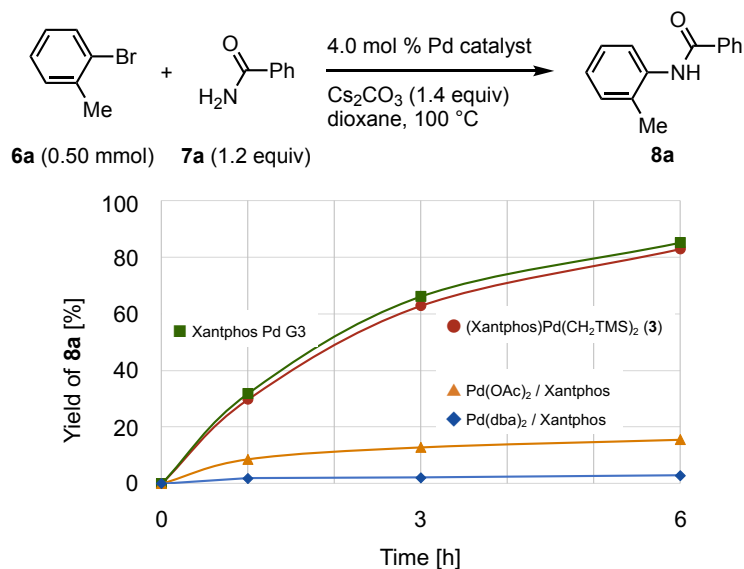
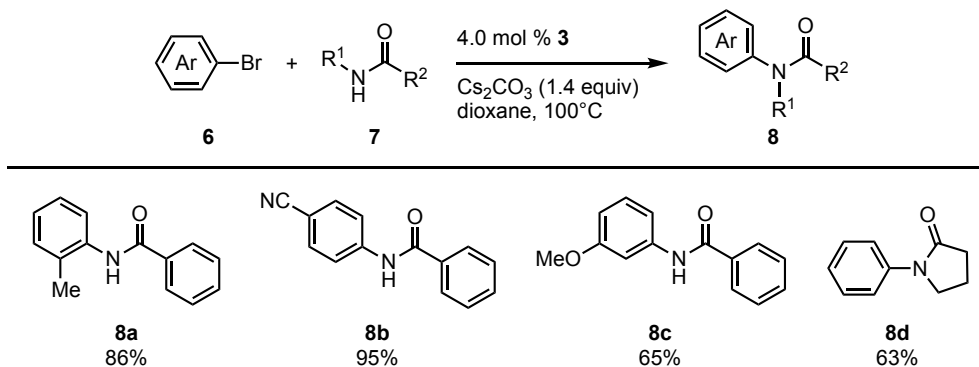


Figure 2-3. Comparison of the catalytic performance of **3** in C–N cross-coupling reaction with those of other catalyst precursors.

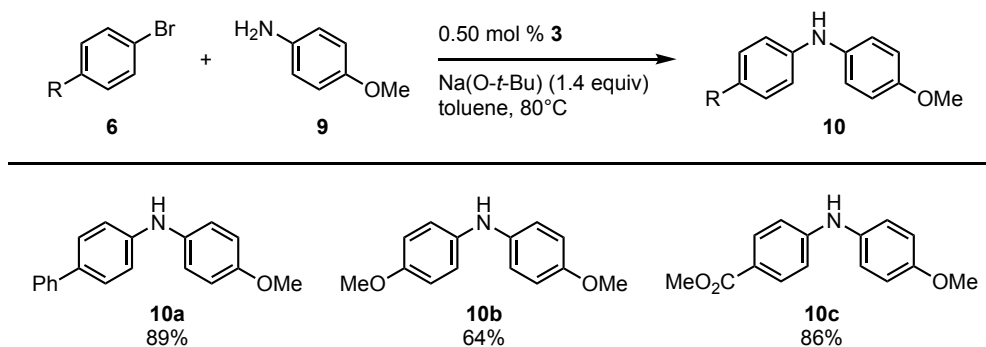
Next, I investigated the catalytic performance of **3** in C–N coupling reactions using various amine nucleophiles (Tables 2-2 and 2-3).^{10,11} A variety of aryl halides reacted with benzamide to give the desired products (**8a–8c**) in good to excellent yields (Table 2-2). The reaction using 2-pyrrolidone also proceeded efficiently to form **8d** in good yield (63% yield). 4-Methoxy-substituted aniline (**9**) reacted with aryl halides that bear electron-donating and -withdrawing groups to afford the desired products (**10a–10c**) in good to high yields (Table 2-3). The performance of **3** was further evaluated in C–S coupling reactions with thiol as nucleophiles (Table 2-4).¹² The reaction of 4-methoxybenzyl thiol proceeded to afford the desired products (**12a–12c**) in high yields, and the reaction with thiophenol provided the corresponding diaryl sulfide (**12d**) in high yield.

Table 2-2. Evaluation of the catalytic activity of **3** in C–N coupling with amides.^a



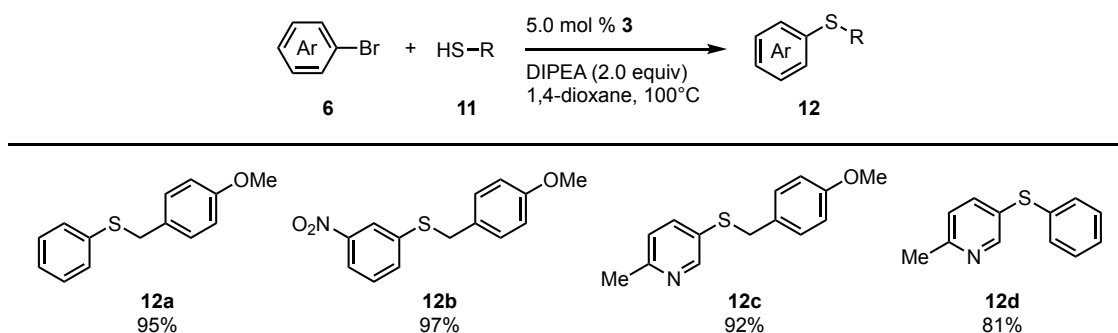
^aConditions: **3** (0.02 mmol), aryl bromides (**6**; 0.50 mmol), amides (**7**; 0.60 mmol), and Cs₂CO₃ (0.70 mmol) in 1,4-dioxane (0.50 M).

Table 2-3. Evaluation of the catalytic activity of **3** in C–N coupling with aryl amines.^a



^aConditions: **3** (0.005 mmol), aryl bromides (**6**; 1.0 mmol), amines (**9**; 1.2 mmol), and Na(O-*t*-Bu) (1.4 mmol) in toluene (0.50 M).

Table 2-4. Evaluation of the catalytic activity of **3** in C–S coupling with thiols.^a

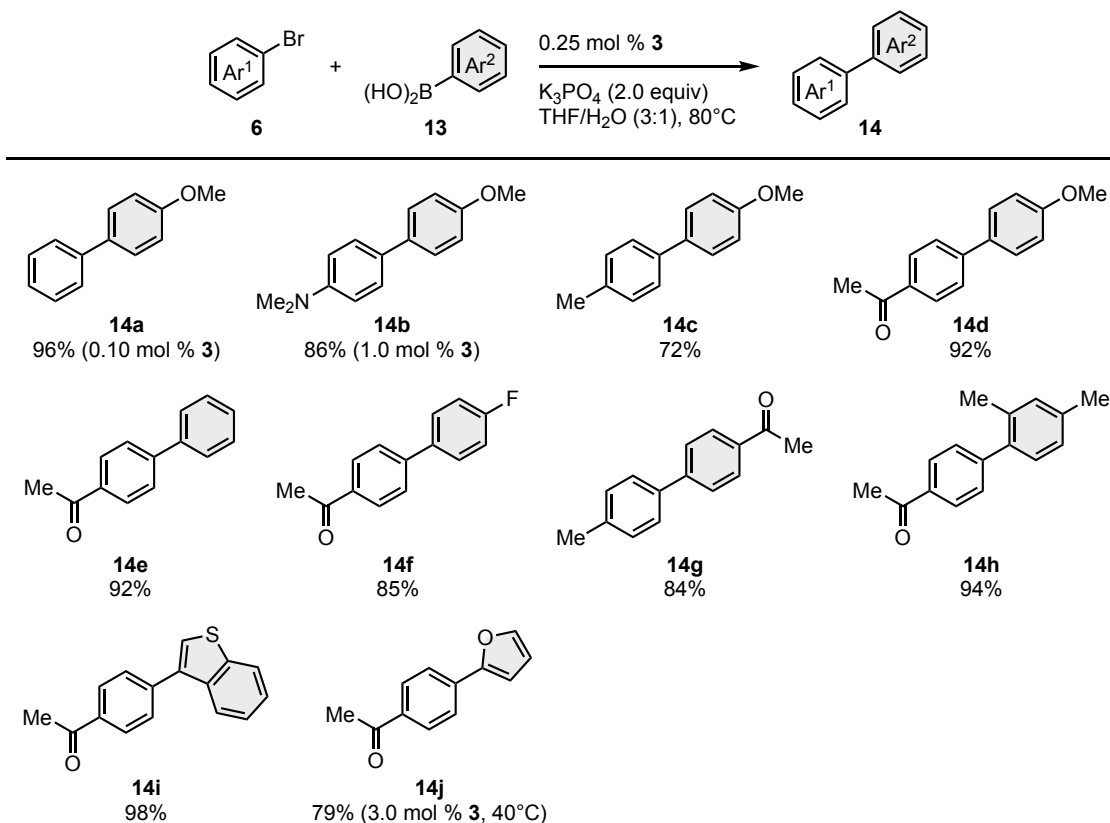


^aConditions: **3** (0.025 mmol), aryl bromides (**6**; 0.50 mmol), thiols (**11**; 0.50 mmol), and DIPEA (1.0 mmol) in 1,4-dioxane (0.50 M).

I also confirmed that the developed precatalyst **3** was applicable to Suzuki–Miyaura cross-coupling reactions with a variety of arylboronic acids (**13**) (Table 2-5). Notably, the use of 0.1 mol% of the catalyst provided **14a** in excellent yield (96% yield). The reaction

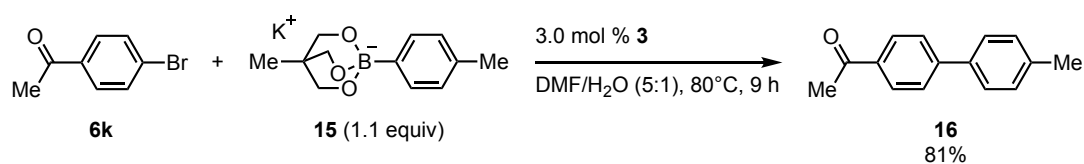
of base-sensitive 2-furylboronic acid (**13j**) proceeded smoothly to give the desired coupling product (**14j**) in good yield (79% yield).

Table 2-5. Evaluation of catalytic activity of **3** in Suzuki–Miyaura cross-coupling.^a



^aConditions: **3** (0.0125 mmol), aryl bromides (**6**; 0.50 mmol), arylboronic acids (**13**; 0.60 mmol), and K_3PO_4 (1.0 mmol) in THF/H₂O (3:1, 0.38 M).

I speculated that **3** might also be suitable as a precatalyst for base-free Suzuki–Miyaura cross-coupling reactions, as **3** can be activated thermally without bases. To this end, the coupling reactions between aryl halide (**6k**) and triol borate (**15**) in the presence of **3** as a precatalyst was carried out (Scheme 2-6).¹³ The targeted coupling product (**16**) was obtained in high yield (81% yield).



Scheme 2-6. Base-free Suzuki–Miyaura cross-coupling reaction using **3** as a precatalyst.

Summary

I have demonstrated that a Xantphos-ligated palladium dialkyl complex can serve as a high-performance precatalyst for various cross-coupling reactions. This study provides a convenient alternative to previously reported classes of precatalysts. Notably, this palladium complex can be easily prepared, stored for several months, and easily activated under thermal conditions without the formation of any potential catalyst inhibitors. I expect that the design of this precatalyst will find wide-spread applications in cross-coupling chemistry.

Reference

- 1) Li, H.; Johansson Seechurn, C. C. C.; Colacot, T. J. *ACS Catal.* **2012**, *2*, 1147. (b) Biffis, A.; Centomo, P.; Del Zotto, A.; Zecca, M. *Chem. Rev.* **2018**, *118*, 2249. (c) Ruiz-Castillo, P. Buchwald, S. L. *Chem. Rev.* **2016**, *116*, 12564. (d) Korch, K. M. Watson, D. A. *Chem. Rev.* **2019**, *119*, 8192. (e) Dorel, R.; Grugel, M. Sc. C. P. Haydl, A. M. *Angew. Chem., Int. Ed.* **2019**, *58*, 17118. (f) Roy, D.; Uozumi, Y. *Adv. Synth. Catal.* **2019**, *360*, 602. (g) Li, J.; Yang, S.; Wu, W.; Jiang, H. *Eur. J. Org. Chem.* **2018**, *2018*, 1284. (h) Shi, S.; Nolan, S. P.; Szostak, M. *Acc. Chem. Res.* **2018**, *51*, 2589. (i) Campeau, L.-C.; Hazari, N. *Organometallics* **2019**, *38*, 3. (j) Johansson Seechurn, C. C. C.; Kitching, M. O.; Colacot, T. J.; Snieckus, V. *Angew. Chem., Int. Ed.* **2012**, *51*, 5062. (k) *Palladium-catalyzed coupling reactions: Practical aspects and future developments*, 2nd revised ed.; Molnár, Á. ed.; Wiley-VCH: Weinheim, 2013. (l) *Metal-catalyzed cross-coupling reactions*; Meijere, A., Diederich, F., Eds.; Wiley-VCH: Weinheim, 2008. (m) Miyaura, N.; Suzuki, A. *Chem. Rev.* **1995**, *95*, 2457. (n) Hazari, N.; Melvin, P. R.; Beromi, M. M. *Nat. Rev. Chem.* **2017**, *1*, 0025.
- 2) Christmann, U.; Vilar, R. *Angew. Chem., Int. Ed.* **2005**, *44*, 366.
- 3) van Leeuwen, P. W. N. M.; Kamer, P. C. J. *Catal. Sci. Technol.* **2018**, *8*, 26.
- 4) Klingensmith, L. M.; Strieter, E. R.; Barder, T. E. Buchwald, S. L. *Organometallics* **2006**, *25*, 82.
- 5) (a) Biscoe, M. R.; Fors, B. P.; Buchwald, S. L. *J. Am. Chem. Soc.* **2008**, *130*, 6686. (b) Kinzel, T.; Zhang, Y.; Buchwald, S. L. *J. Am. Chem. Soc.* **2010**, *132*, 14073. (c) Bruno, N. C.; Tudge, M. T.; Buchwald, S. L. *Chem. Sci.* **2013**, *4*, 916. (d) Bruno, N. C.; Niljianskul, N.; Buchwald, S. L. *J. Org. Chem.* **2014**, *79*, 4161.
- 6) Seligson, A. L.; Troglér, W. C. *Organometallics* **1993**, *12*, 744.
- 7) Yang, Y.; Zhou, Q.; Cai, J.; Xue, T.; Liu, Y.; Jiang, Y.; Su, Y.; Chung, L.; Vicic, D. A. *Chem. Sci.* **2019**, *10*, 5275.
- 8) Pan, Y.; Young, G. B. *J. Organomet. Chem.* **1999**, *577*, 257.
- 9) The ESI-MS analysis of the insoluble compound suggested that it is Pd(Xantphos)₂

(4). The poor solubility of **4** in organic solvents hampered an examination by NMR spectroscopy.

- 10) Yin, J.; Buchwald, S. L. *J. Am. Chem. Soc.* **2002**, *124*, 6043.
- 11) (a) Sadighi, J. P.; Harris, M. C.; Buchwald, S. L. *Tetrahedron Lett.* **1998**, *39*, 5327;
(b) Hamann, B. C.; Hartwig, J. F. *J. Am. Chem. Soc.* **1998**, *120*, 3694.
- 12) Itoh, T.; Mase, T. *Org. Lett.* **2004**, *6*, 4587.
- 13) Yamamoto, Y.; Takizawa, M.; Yu, X. Q.; Miyaura, N. *Angew. Chem., Int. Ed.* **2008**, *47*, 928.

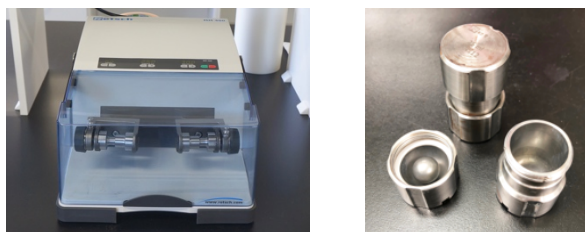
Experimental Section

Table of Contents

General and Materials	62
General Procedure for Synthesis of Palladium Dialkyl Complex 3	63
Single Crystal X-Ray Analysis of 3	64
General Procedure for Cross-Coupling Reactions	66
Monitoring the Progress of the Reductive Elimination from 3	79
Stability of 3 for the Long-Term Storage	80
Comparison of the Catalytic Performance of 3 with Those of Other Catalyst Precursors	81
Investigation of C-Heteroatom Cross-Coupling Reactions with Low Catalyst Loading	84
References	84

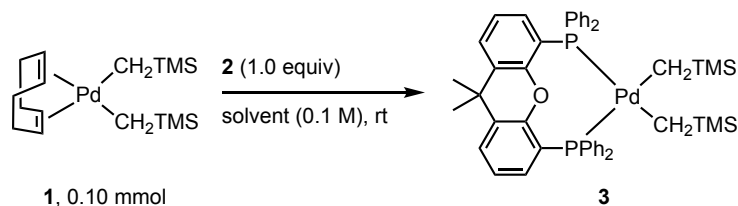
General and Materials.

The starting materials were obtained from commercial suppliers and used as received unless otherwise noted. Solvents were also purchased from commercial suppliers, and dried over molecular sieves (MS 4Å). Mechanochemical reaction was carried out using grinding vessels in a Retsch MM400 mill (Supplementary Figure 1, left photograph). Both jar (25 mL) and ball (diameter: 10 mm) are made of stainless (Supplementary Figure 1, right photograph). NMR spectra were recorded on JEOL JNM-ECX400P and JNM-ECS400 spectrometers (^1H : 392, 396, 400 or 401 MHz, ^{13}C : 99, 100 or 101 MHz, ^{31}P : 160 MHz). Tetramethylsilane (^1H), CDCl_3 (^1H , ^{13}C) and H_3PO_4 (^{31}P) were employed as external standards, respectively. Multiplicity was recorded as follows: s = singlet, br, s = broad singlet, d = doublet, t = triplet, quint = quintet, sext = sextet, sep = septet, m = multiplet. Dibromomethane or 1,2-diphenylethane were used as an internal standard to determine NMR yields. High-resolution mass spectra were recorded at the Global Facility Center, Hokkaido University. Single crystal X-ray structural analyses were carried out on a Rigaku XtaLAB PRO MM007 diffractometer using graphite monochromated Mo-K_α radiation. The structure was solved by direct methods and expanded using Frontier techniques. Non-hydrogen atoms were refined anisotropically. Hydrogen atoms were refined using the riding model. All calculations were performed using Olex crystallographic software package except for refinement, which was performed using SHELXL.¹



Supplementary Figure 1. Retsch MM400 mill (left) and ball milling vessels (right).

General Procedure for Synthesis of Palladium Dialkyl Complex **3**.

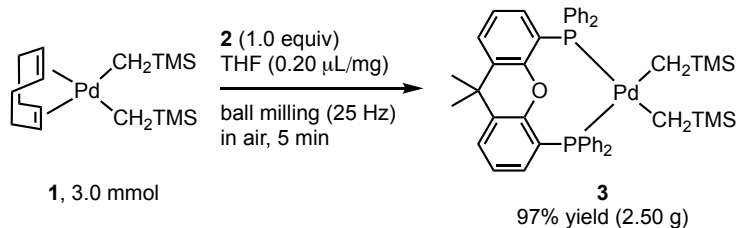


(COD)Pd(CH₂TMS)₂ **1** was prepared by according to the reported procedure.² The material **1** is thermo-sensitive and must be stored at a temperature of $-20\text{ }^{\circ}\text{C}$ or lower to avoid decomposition, while the material can be stored out of glovebox and used in air.

1 (38.9 mg, 0.10 mmol) and Xantphos (**2**) (57.9 mg, 0.10 mmol, 1.0 equiv) were placed in an oven-dried reaction vial, then MeCN (1.0 mL) was added. The reaction mixture was stirred at room temperature for 20 minutes, then the solvent was removed under reduced pressure. The crude product was washed with pentane and Et₂O and dried under reduced pressure to afford the palladium complex **3** as a yellow solid (66.5 mg, 0.0773 mmol, 78% yield).

¹H NMR (396 MHz, CDCl₃, δ): -0.34 (s, 18H), $0.37\text{--}0.54$ (m, 4H), 1.68 (s, 6H), $6.90\text{--}7.42$ (m, 24H), 7.51 (dd, $J = 1.6, 7.1$ Hz, 2H). ¹³C NMR was not assigned due to poor resolution and peak broadening in several common NMR-solvents; spectrum recorded in CDCl₃ is shown in appendix. ³¹P NMR (160 MHz, CDCl₃, δ): 8.9. HRMS-ESI (m/z): $[\text{M-TMSCH}_2]^+$ calcd for C₄₃H₄₃OP₂PdSi, 771.1593; found, 771.1587.

Gram-scale synthesis of palladium complex **3** by mechanochemistry

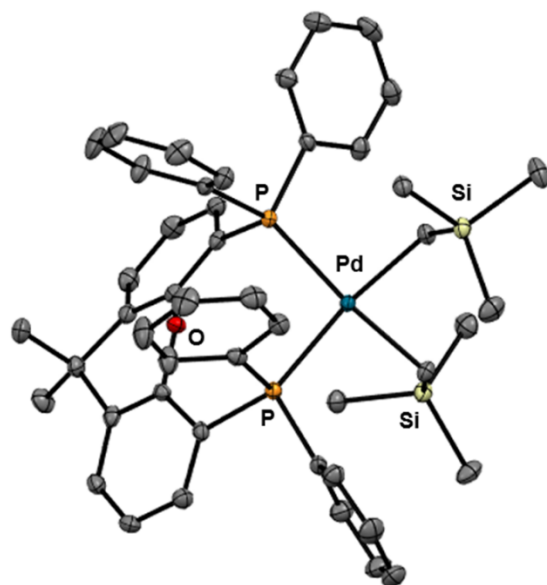


1 (3.0 mmol) and **2** (3.0 mmol, 1.0 equiv) were placed in a ball milling vessel (stainless, 25 mL) loaded with two grinding balls (stainless, diameter: 10 mm), then THF ($0.58\text{ mL}, 0.20\text{ }\mu\text{L mg}^{-1}$) was added via syringe. After the vessel was closed in air without the purge with inert gas, the vessel was placed in the ball mill (Retch MM400, 5 min at 25Hz). The crude product was washed with pentane and Et₂O and dried under reduced pressure to afford the corresponding palladium complex **3** as a yellow solid (2.50 g, 2.9 mmol, 97% yield).

Single Crystal X-Ray Analysis of 3.

Supplementary Table 1. Summary of X-ray crystallographic data for 3.

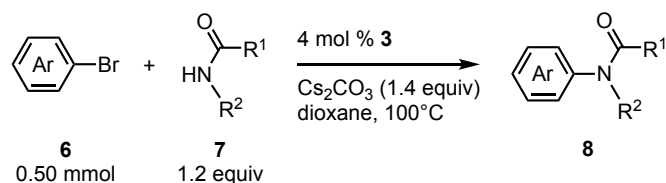
CCDC number	1938978
Empirical Formula	C ₄₇ H ₅₄ OP ₂ PdSi ₂
Formula Weight	859.42
Crystal System	monoclinic
Crystal Size / mm ³	0.55 × 0.08 × 0.09
a / Å	20.6034(4)
b / Å	11.5855(2)
c / Å	35.7054(8)
α / °	90
β / °	97.7204(19)
γ / °	90
V / Å ³	8445.6(3)
Space Group	C2/c
Z value	8
D _{calc} / g·cm ⁻³	1.352
Temperature / K	123(2)
No. of Reflections	53737
Measured	7717 (R _{int} = 0.0720)
Residuals: R _I	0.0337
(I > 2.00σ(I)) / %	
Residuals: wR ₂	0.0821
(All reflections) / %	
Goodness of Fit (GOF)	1.075
Maximum peak in Final Diff. Map / Å ³	0.76 e ⁻
Minimum peak in Final Diff. Map / Å ³	-0.60 e ⁻



Supplementary Figure 2. Single-crystal structure of **3** (thermal ellipsoids set at 50% probability; hydrogen atoms have been omitted for clarity).

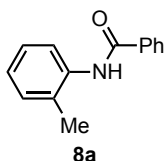
General Procedure for Cross-Coupling Reactions.

C–N Coupling with amides



3 (0.015 mmol), **6** (0.50 mmol), **7** (0.60 mmol) and Cs₂CO₃ (0.70 mmol) were placed in an oven-dried reaction vial. After being sealed with a screw cap containing a Teflon-coated rubber septum, the vial was connected to a nitrogen line through a needle. After 1,4-dioxane (1.0 mL) was added, the reaction mixture was heated to 100 °C for the specified time. After cooling to room temperature, the reaction mixture was passed through a short silica gel column. The crude mixture was purified by flash column chromatography (SiO₂, EtOAc/hexane, 0:100–30:70).

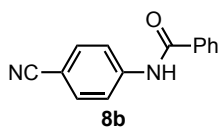
N-(o-Tolyl)benzamide (8a)



The reaction was carried out for 8 h with **3** (19.1 mg, 0.02 mmol), 1-bromo-2-methylbenzene (85.1 mg, 0.50 mmol), benzamide (72.7 mg, 0.60 mmol) and Cs₂CO₃ (135.1 mg, 0.70 mmol). The product **8a** was obtained in 86% yield (90.6 mg, 0.43 mmol) as a white solid (m.p. = 145–146 °C).

¹H NMR (401 MHz, CDCl₃, δ): 2.35 (s, 3H), 7.13 (td, *J* = 1.1, 7.4 Hz, 1H), 7.21–7.31 (m, 2H), 7.48–7.54 (m, 2H), 7.58 (tt, *J* = 1.8, 7.3 Hz, 1H), 7.66 (br, s, 1H), 7.90 (d, *J* = 7.2 Hz, 2H), 7.98 (d, *J* = 7.6 Hz, 1H). ¹³C NMR (100 MHz, CDCl₃, δ): 17.8 (CH₃), 123.1 (CH), 125.3 (CH), 126.9 (CH), 127.0 (CH), 128.8 (CH), 129.3 (C), 130.5 (CH), 131.8 (CH), 135.0 (C), 135.7 (C), 165.6 (C). HRMS-EI (m/z): [M] calcd for C₁₄H₁₃NO, 211.0997; found, 211.1002.

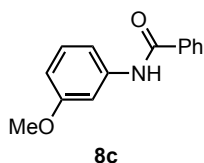
***N*-(4-Cyanophenyl)benzamide (8b)**



The reaction was carried out for 7 h with **3** (21.5 mg, 0.025 mmol), 4-bromobenzonitrile (91.3 mg, 0.50 mmol), benzamide (72.5 mg, 0.60 mmol) and Cs₂CO₃ (134.7 mg, 0.70 mmol). The product **8b** was obtained in 95% yield (105.9 mg, 0.48 mmol) as a white solid (m.p. = 171–172 °C).

¹H NMR (392 MHz, CDCl₃, δ): 7.50–7.56 (m, 2H), 7.61 (tt, *J* = 1.6, 7.4 Hz, 1H), 7.68 (dt, *J* = 2.0, 9.0 Hz, 2H), 7.80 (dt, *J* = 2.2, 9.0 Hz, 2H), 7.85–7.90 (m, 2H), 7.94 (br, s, 1H). ¹³C NMR (100 MHz, CDCl₃, δ): 107.3 (C), 118.8 (C), 119.9 (CH), 127.1 (CH), 129.0 (CH), 132.5 (CH), 133.3 (CH), 134.1 (C), 142.0 (C), 165.9 (C). HRMS-EI (*m/z*): [*M*] calcd for C₁₄H₁₀N₂O, 222.0793; found, 222.0796.

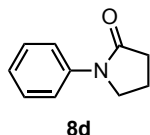
***N*-(3-Methoxyphenyl)benzamide (8c)**



The reaction was carried out for 3 h with **3** (21.4 mg, 0.025 mmol), 1-bromo-2-methylbenzene (93.5 mg, 0.50 mmol), benzamide (72.7 mg, 0.65 mmol) and Cs₂CO₃ (135.2 mg, 0.70 mmol). The product **8c** was obtained in 65% yield (74.1 mg, 0.33 mmol) as a white solid (m.p. = 113–114 °C).

¹H NMR (392 MHz, CDCl₃, δ): 3.84 (s, 3H), 6.72 (dd, *J* = 2.4, 8.2 Hz, 1H), 7.09 (dt, *J* = 0.9, 8.0 Hz, 1H), 7.22–7.32 (m, 1H), 7.45 (t, *J* = 2.2 Hz, 1H), 7.47–7.59 (m, 3H), 7.78 (br, s, 1H), 7.87 (d, *J* = 8.2 Hz, 2H). ¹³C NMR (100 MHz, CDCl₃, δ): 55.2 (CH₃), 105.8 (CH), 110.4 (CH), 112.4 (CH), 127.0 (CH), 128.6 (CH), 129.6 (CH), 131.7 (CH), 134.8 (C), 139.2 (C), 160.0 (C), 166.0 (C). HRMS-EI (*m/z*): [*M*] calcd for C₁₄H₁₃NO₂, 227.0946; found, 227.0949.

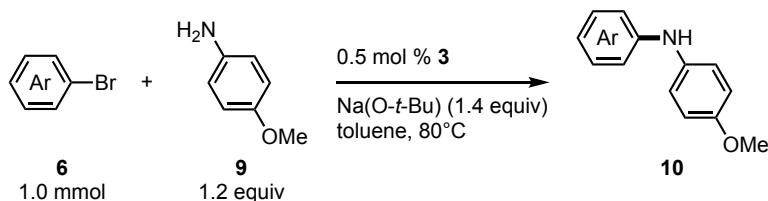
1-Phenylpyrrolidin-2-one (8d)



The reaction was carried out for 20 h with **3** (21.4 mg, 0.025 mmol), bromobenzene (78.1 mg, 0.50 mmol), pyrrolidin-2-one (51.1 mg, 0.60 mmol) and Cs₂CO₃ (135.4 mg, 0.70 mmol). The product **8d** was obtained in 63% yield (50.6 mg, 0.31 mmol) as a beige solid (m.p. = 67–68 °C).

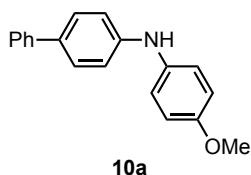
¹H NMR (396 MHz, CDCl₃, δ): 2.17 (quint, *J* = 7.6 Hz, 2H), 2.62 (t, *J* = 7.9 Hz, 2H), 3.87 (t, *J* = 6.9 Hz, 2H), 7.12–7.18 (m, 1H), 7.34–7.41 (m, 2H), 7.58–7.64 (m, 2H). ¹³C NMR (100 MHz, CDCl₃, δ): 17.9 (CH₂), 32.6 (CH₂), 48.6 (CH₂), 119.8 (CH), 124.3 (CH), 128.7 (CH), 139.2 (C), 174.1 (C). HRMS-EI (*m/z*): [M] calcd for C₁₀H₁₁NO, 161.0841; found, 161.0847.

C–N Coupling with aryl amines



3 (0.005 mmol), **6** (1.0 mmol), **9** (1.2 mmol) and Na(O-*t*-Bu) (1.4 mmol) were placed in an oven-dried reaction vial. After being sealed with a screw cap containing a Teflon-coated rubber septum, the vial was connected to a nitrogen line through a needle. After toluene (2.0 mL) was added, the reaction mixture was heated to 80 °C for the specified time. After cooling to room temperature, the reaction mixture was passed through a short silica gel column. The crude mixture was purified by flash column chromatography (SiO₂, EtOAc/hexane, 0:100–10:90).

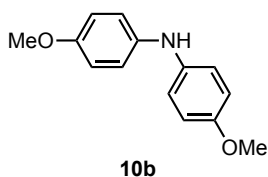
N-(4-Methoxyphenyl)-(1,1'-biphenyl)-4-amine (**10a**)



The reaction was carried out for 2 h with **3** (4.2 mg, 0.005 mmol), 4-bromo-1,1'-biphenyl (233.2 mg, 1.0 mmol), **9** (148.2 mg, 1.2 mmol) and Na(O-*t*-Bu) (134.2 mg, 1.4 mmol). The product **10a** was obtained in 89% yield (244.3 mg, 0.89 mmol) as a white solid (m.p. =126 °C).

¹H NMR (401 MHz, CDCl₃, δ): 3.81 (s, 3H), 5.58 (s, 1H), 6.85–6.92 (m, 2H), 6.94–7.01 (m, 2H), 7.08–7.15 (m, 2H), 7.27–7.31 (m, 1H), 7.40 (t, *J* = 7.8 Hz, 2H), 7.47 (d, *J* = 8.0 Hz, 2H), 7.55 (d, *J* = 7.6 Hz, 2H). ¹³C NMR (100 MHz, CDCl₃, δ): 55.6 (CH₃), 114.7 (CH), 115.7 (CH), 122.4 (CH), 126.3 (CH), 126.4 (CH), 127.9 (CH), 128.7 (CH), 132.3 (C), 135.4 (C), 141.0 (C), 144.6 (C), 155.4 (C). HRMS-EI (*m/z*): [M] calcd for C₁₉H₁₇NO, 275.1310; found, 275.1311.

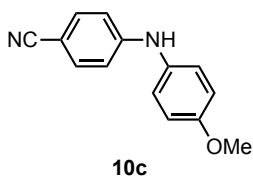
Bis(4-methoxyphenyl)amine (10b)



The reaction was carried out for 24 h with **3** (4.3 mg, 0.005 mmol), 1-bromo-4-methoxybenzene (187.1 mg, 1.0 mmol), **9** (148.1 mg, 1.2 mmol) and Na(O-*t*-Bu) (134.1 mg, 1.4 mmol). The product **10b** was obtained in 64% yield (147.3 mg, 0.64 mmol) as an off-white solid (103–104 °C).

¹H NMR (396 MHz, CDCl₃, δ): 3.78 (s, 6H), 5.28 (br, s, 1H), 6.82 (dt, *J* = 2.8, 9.8 Hz, 4H), 6.94 (dt, *J* = 2.9, 9.5 Hz, 4H). ¹³C NMR (99 MHz, CDCl₃, δ): 55.4 (CH₃), 114.6 (CH), 119.3 (CH), 137.8 (C), 154.0 (C). HRMS-EI (*m/z*): [M] calcd for C₁₄H₁₅NO₂, 229.1103; found, 229.1106.

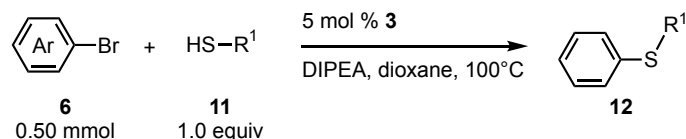
4-[(4-Methoxyphenyl)amino]benzonitrile (10c)



The reaction was carried out for 1 h with **3** (4.3 mg, 0.005 mmol), 4-bromobenzonitrile (182.2 mg, 1.0 mmol), **9** (148.4 mg, 1.2 mmol) and Na(O-*t*-Bu) (134.6 mg, 1.4 mmol). The product **10c** was obtained in 86% yield (210.7 mg, 0.86 mmol) as a white solid (m.p. = 102–103 °C).

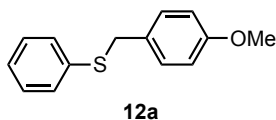
¹H NMR (396 MHz, CDCl₃, δ): 3.82 (s, 3H), 5.87 (br, s, 1H), 6.79 (dt, *J* = 2.3, 9.1 Hz, 2H), 6.91 (dt, *J* = 2.8, 9.8 Hz, 2H), 7.12 (dt, *J* = 2.7, 9.7 Hz, 2H), 7.43 (dt, *J* = 2.3, 9.1 Hz, 2H). ¹³C NMR (100 MHz, CDCl₃, δ): 55.3 (CH₃), 99.6 (C), 113.5 (CH), 114.6 (CH), 120.2 (C), 124.6 (CH), 132.4 (C), 133.5 (CH), 149.6 (C), 156.7 (C). HRMS-EI (*m/z*): [M] calcd for C₁₄H₁₂N₂O, 224.0950; found, 224.0952.

C–S Coupling with thiols



3 (0.015 mmol), **6** (0.50 mmol) were placed in an oven-dried reaction vial. After being sealed with a screw cap containing a Teflon-coated rubber septum, the vial was connected to a nitrogen line through a needle. 1,4-Dioxane (1.0 mL), DIPEA (174 μ L, 2.0 mmol) and **11** (0.50 mmol) were added to the mixture, then the reaction mixture was heated to 100 $^\circ$ C for 1 h. After cooling to room temperature, the reaction mixture was passed through a short silica gel column. The crude mixture was purified by flash column chromatography (SiO₂, EtOAc/hexane, 0:100–10:90).

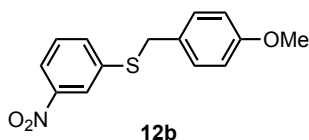
(4-Methoxybenzyl)(phenyl)sulfane (**12a**)



The reaction was carried out for 1 h with **3** (21.4 mg, 0.025 mmol), bromobenzene (79.5 mg, 0.50 mmol) and (4-methoxyphenyl)methanethiol (69 μ L, 0.50 mmol). The product **12a** was obtained in 95% yield (110.2 mg, 0.48 mmol) as a white solid (m.p. = 86–87 $^\circ$ C).

¹H NMR (396 MHz, CDCl₃, δ): 3.79 (s, 3H), 4.08 (s, 2H), 6.82 (dt, J = 2.6, 9.2 Hz, 2H), 7.15–7.34 (m, 7H). ¹³C NMR (100 MHz, CDCl₃, δ): 38.4 (CH₂), 55.2 (CH₃), 113.8 (CH), 126.2 (CH), 128.8 (CH), 129.3 (C), 129.7 (CH), 129.9 (CH), 136.5 (C), 158.7 (C). HRMS-EI (m/z): [M] calcd for C₁₄H₁₄OS, 230.0765; found, 230.0769.

(4-Methoxybenzyl)(3-nitrophenyl)sulfane (**12b**)

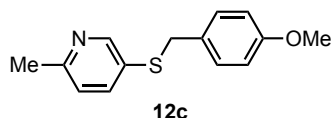


The reaction was carried out for 1 h with **3** (21.5 mg, 0.025 mmol), 1-bromo-3-nitrobenzene (101.0 mg, 0.50 mmol) and (4-methoxyphenyl)methanethiol (69 μ L, 0.50 mmol). The product **12b** was obtained in 97% yield (133.2 mg, 0.48 mmol) as a yellow solid (m.p. = 58–59 $^\circ$ C).

¹H NMR (396 MHz, CDCl₃, δ): 3.79 (s, 3H), 4.17 (s, 2H), 6.84 (dt, J = 2.4, 9.4 Hz, 2H), 7.21–7.29 (m, 2H), 7.40 (t, J = 7.9 Hz, 1H), 7.54 (dt, J = 1.0, 7.7 Hz, 1H), 7.99 (dd, J = 2.2, 8.1 Hz, 1H), 8.12 (t, J = 2.2 Hz, 1H). ¹³C NMR (100 MHz, CDCl₃, δ): 37.5 (CH₂), 55.1 (CH₃), 114.0 (CH), 120.5 (CH),

122.8 (CH), 127.7 (C), 129.3 (CH), 129.9 (CH), 134.3 (CH), 139.5 (C), 148.2 (C), 158.9 (C). HRMS-EI (m/z): [M] calcd for C₁₄H₁₃NO₃S, 275.0616; found, 275.0616.

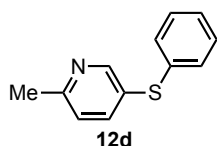
5-[(4-Methoxybenzyl)thio]-2-methylpyridine (**12c**)



The reaction was carried out for 1 h with **3** (21.5 mg, 0.025 mmol), 5-bromo-2-methylpyridine (85.9 mg, 0.50 mmol) and (4-methoxyphenyl)methanethiol (69 μ L, 0.50 mmol). The product **12c** was obtained in 92% yield (112.4 mg, 0.46 mmol) as a white solid (m.p. = 58–59 °C).

¹H NMR (396 MHz, CDCl₃, δ): 2.51 (s, 3H), 3.78 (s, 3H), 4.00 (s, 2H), 6.80 (dt, J = 2.5, 9.2 Hz, 2H), 7.02 (d, J = 8.2 Hz, 1H), 7.14 (dt, J = 2.6, 9.4 Hz, 2H), 7.45 (dd, J = 2.3, 8.2 Hz, 1H), 8.41 (d, J = 2.3 Hz, 1H). ¹³C NMR (100 MHz, CDCl₃, δ): 24.0 (CH₃), 39.3 (CH₂), 55.2 (CH₃), 113.8 (CH), 123.1 (CH), 129.1 (C), 129.9 (CH), 139.4 (CH), 151.3 (CH), 156.9 (C), 158.8 (C). HRMS-EI (m/z): [M] calcd for C₁₄H₁₅NOS, 245.0874; found, 245.0875.

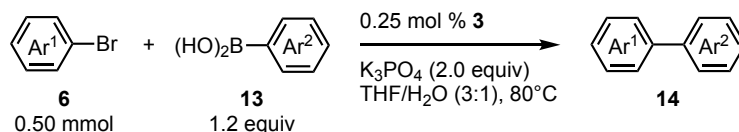
2-Methyl-5-(phenylthio)pyridine (**12d**)



The reaction was carried out for 1 h with **3** (21.5 mg, 0.025 mmol), 5-bromo-2-methylpyridine (85.7 mg, 0.50 mmol) and benzenethiol (51 μ L, 0.50 mmol). The product **12d** was obtained in 81% yield (81.0 mg, 0.40 mmol) as a pale yellow liquid.

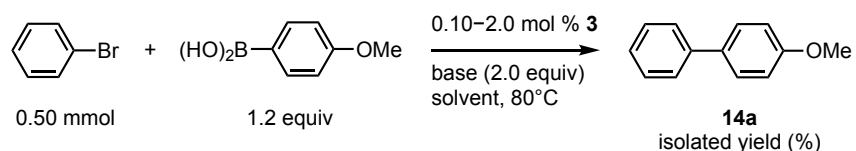
¹H NMR (396 MHz, CDCl₃, δ): 2.55 (s, 3H), 7.11 (d, J = 8.3 Hz, 1H), 7.21–7.31 (m, 5H), 7.57 (dd, J = 2.2, 8.1 Hz, 1H), 8.51 (d, J = 2.4 Hz, 1H). ¹³C NMR (100 MHz, CDCl₃, δ): 24.0 (CH₃), 123.6 (CH), 127.0 (CH), 128.8 (C), 129.2 (CH), 130.2 (CH), 135.4 (C), 139.6 (CH), 151.6 (CH), 157.5 (C). HRMS-EI (m/z): [M] calcd for C₁₂H₁₁NS, 201.0612; found, 201.0618.

Suzuki-Miyaura Cross-Coupling Reaction



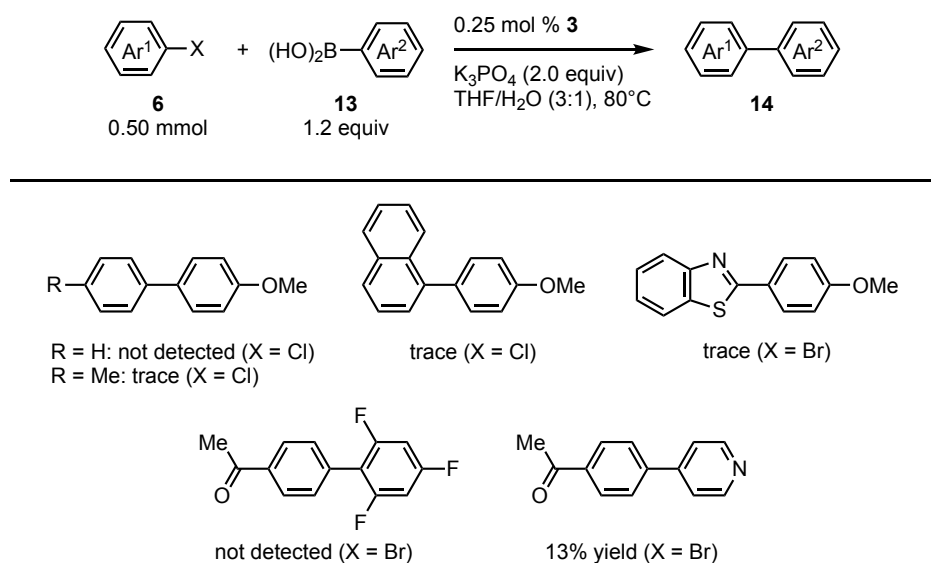
3 (1.25 μ mol), **6** (0.50 mmol), **13** (0.60 mmol) and K₃PO₄ (1.0 mmol) were placed in an oven-dried reaction vial. After being sealed with a screw cap containing a Teflon-coated rubber septum, the vial was connected to a nitrogen line through a needle. THF (1.0 mL) and H₂O (0.33 mL) were added, then the reaction mixture was heated to 80 °C for 3–24 h. After cooling to room temperature, the reaction mixture was extracted three times with CH₂Cl₂, washed with brine and dried over MgSO₄. The crude mixture was purified by flash column chromatography.

Supplementary Table 2. Optimization of reaction conditions for Suzuki-Miyaura cross-coupling reaction.



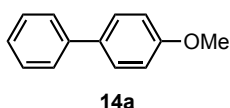
Entry	Base	Solvent (mL)	Catalyst (mol %)	Time (h)	Yield of 14a (%)
1	K ₂ CO ₃	DMF (1.0)	2.0	6	78
2	K ₃ PO ₄	DMF (1.0)	2.0	24	92
3	K ₃ PO ₄	THF (1.0)	2.0	1	88
4	K ₃ PO ₄	THF (1.0)	1.0	1	94
5	K ₃ PO ₄	THF (1.0)	0.50	7	92
6	K ₃ PO ₄	THF (1.0) + H ₂ O (0.33)	0.50	1.5	94
7	K ₃ PO ₄	THF (1.0) + H ₂ O (0.33)	0.25	1	95
8 ^a	K ₃ PO ₄	THF (3.0) + H ₂ O (1.0)	0.10	6	96

^aThe reaction was conducted in 1.5 mmol scale.



Supplementary Figure 3. Unsuccessful substrates in C-C coupling reaction.

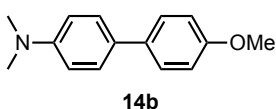
4-Methoxy-1,1'-biphenyl (**14a**)



The reaction was carried out for 1 h with **3** (1.1 mg, 1.25 μ mol), 1-bromo-4-methoxybenzene (78.9 mg, 0.50 mmol), (4-methoxyphenyl)boronic acid (91.2 mg, 0.60 mmol) and K_3PO_4 (212.5 mg, 1.0 mmol). The product **14a** was obtained in 95% yield (88.3 mg, 0.48 mmol) as a white solid (m.p. = 89 $^{\circ}C$) by flash chromatography (SiO_2 , hexane/ CH_2Cl_2 , 100:0 to 80:20).

1H NMR (396 MHz, $CDCl_3$, δ): 3.85 (s, 3H), 6.98 (dt, $J = 2.4, 9.2$ Hz, 2H), 7.30 (tt, $J = 1.4, 7.3$ Hz, 1H), 7.42 (tt, $J = 1.7, 7.7$ Hz, 2H), 7.54 (tt, $J = 2.1, 8.3$ Hz, 4H). ^{13}C NMR (101 MHz, $CDCl_3$, δ): 55.2 (CH₃), 114.1 (CH), 126.59 (CH), 126.65 (CH), 128.1 (CH), 128.7 (CH), 133.6 (C), 140.7 (C), 159.1 (C). HRMS-EI (m/z): [M] calcd for $C_{13}H_{12}O$, 184.0888; found, 184.0887.

4'-Methoxy-*N,N*-dimethyl-(1,1'-biphenyl)-4-amine (**14b**)

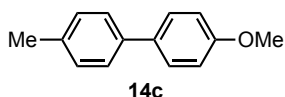


The reaction was carried out for 24 h with **3** (4.3 mg, 5.0 μ mol), 4-bromo-*N,N*-dimethylaniline (100.2 mg, 0.50 mmol), (4-methoxyphenyl)boronic acid (91.5 mg, 0.60 mmol) and K_3PO_4 (211.4 mg, 1.0 mmol). The product **14b** was obtained in 86% yield (97.4 mg, 0.43 mmol) as a white solid (m.p. = 158–159 $^{\circ}C$) by flash chromatography (SiO_2 , hexane/ CH_2Cl_2 , 90:10 to 0:100).

1H NMR (400 MHz, $CDCl_3$, δ): 2.98 (s, 6H), 3.84 (s, 3H), 6.80 (dt, $J = 2.7, 9.2$ Hz, 2H), 6.95 (dt, $J =$

2.3, 9.3 Hz, 2H), 7.43–7.51 (m, 4H). ^{13}C NMR (101 MHz, CDCl_3 , δ): 40.6 (CH_3), 55.2 (CH_3), 112.8 (CH), 114.0 (CH), 127.2 (CH), 129.0 (C), 133.8 (C), 149.5 (C), 158.1 (C). HRMS-ESI (m/z): $[\text{M}+\text{H}]^+$ calcd for $\text{C}_{15}\text{H}_{18}\text{NO}$, 228.1383; found, 228.1381.

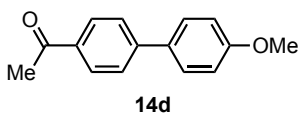
4-Methoxy-4'-methyl-1,1'-biphenyl (14c)



The reaction was carried out for 3 h with **3** (1.1 mg, 1.25 μmol), 1-bromo-4-methylbenzene (85.9 mg, 0.50 mmol), (4-methoxyphenyl)boronic acid (91.6 mg, 0.60 mmol) and K_3PO_4 (212.3 mg, 1.0 mmol). The product **14c** was obtained in 72% yield (71.6 mg, 0.36 mmol) as a white solid (m.p. = 110–111 $^\circ\text{C}$) by flash chromatography (SiO_2 , hexane/ CH_2Cl_2 , 50:50).

^1H NMR (400 MHz, CDCl_3 , δ): 2.39 (s, 3H), 3.85 (s, 3H), 6.97 (dt, $J = 2.7, 9.5$ Hz, 2H), 7.23 (d, $J = 7.6$ Hz, 2H), 7.45 (dt, $J = 1.8, 8.3$ Hz, 2H), 7.51 (dt, $J = 2.7, 9.5$ Hz, 2H). ^{13}C NMR (101 MHz, CDCl_3 , δ): 21.0 (CH_3), 55.2 (CH_3), 114.1 (CH), 126.5 (CH), 127.9 (CH), 129.4 (CH), 133.6 (C), 136.3 (C), 137.9 (C), 158.8 (C). HRMS-EI (m/z): $[\text{M}]$ calcd for $\text{C}_{14}\text{H}_{14}\text{O}$, 198.1045; found, 198.1043.

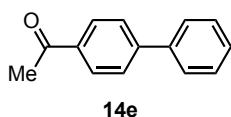
1-[4'-Methoxy-(1,1'-biphenyl)-4-yl]ethan-1-one (14d)



The reaction was carried out for 3 h with **3** (1.1 mg, 1.25 μmol), 4'-bromoacetophenone (99.2 mg, 0.50 mmol), (4-methoxyphenyl)boronic acid (91.0 mg, 0.60 mmol) and K_3PO_4 (212.0 mg, 1.0 mmol). The product **14d** was obtained in 92% yield (104.3 mg, 0.46 mmol) as a white solid (m.p. = 158–159 $^\circ\text{C}$) by flash chromatography (SiO_2 , hexane/ EtOAc , 97:3 to 60:40).

^1H NMR (400 MHz, CDCl_3 , δ): 2.64 (s, 3H), 3.87 (s, 3H), 7.01 (dt, $J = 2.5, 9.5$ Hz, 2H), 7.59 (dt, $J = 2.7, 9.5$ Hz, 2H), 7.65 (dt, $J = 1.9, 8.5$ Hz, 2H), 8.01 (dt, $J = 1.5, 8.8$ Hz, 2H). ^{13}C NMR (101 MHz, CDCl_3 , δ): 26.6 (CH_3), 55.3 (CH_3), 114.3 (CH), 126.5 (CH), 128.3 (CH), 128.9 (CH), 132.1 (C), 135.1 (C), 145.2 (C), 159.8 (C), 197.7 (C). HRMS-EI (m/z): $[\text{M}]$ calcd for $\text{C}_{15}\text{H}_{14}\text{O}_2$, 226.0994; found, 226.0994.

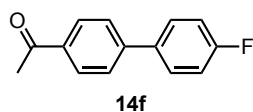
1-[(1,1'-Biphenyl)-4-yl]ethan-1-one (14e)



The reaction was carried out for 3 h with **3** (1.1 mg, 1.25 μmol), 4'-bromoacetophenone (99.6 mg, 0.50 mmol), phenylboronic acid (73.2 mg, 0.60 mmol) and K_3PO_4 (212.3 mg, 1.0 mmol). The product **14e** was obtained in 92% yield (90.6 mg, 0.46 mmol) as a white solid (m.p. = 122–123 $^\circ\text{C}$) by flash chromatography (SiO_2 , hexane/EtOAc, 100:0 to 85:15).

^1H NMR (400 MHz, CDCl_3 , δ): 2.65 (s, 3H), 7.41 (tt, $J = 1.6, 7.3$ Hz, 1H), 7.48 (tt, $J = 1.7, 7.3$ Hz, 2H), 7.61–7.66 (m, 2H), 7.70 (dt, $J = 1.9, 8.5$ Hz, 2H), 8.04 (dt, $J = 1.9, 8.5$ Hz, 2H). ^{13}C NMR (101 MHz, CDCl_3 , δ): 26.5 (CH_3), 127.06 (CH), 127.13 (CH), 128.1 (CH), 128.80 (CH), 128.83 (CH), 135.7 (C), 139.7 (C), 145.6 (C), 197.6 (C). HRMS-EI (m/z): [M] calcd for $\text{C}_{14}\text{H}_{12}\text{O}$, 196.0888; found, 196.0889.

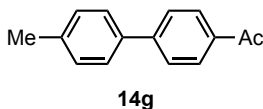
1-[4'-Fluoro-(1,1'-biphenyl)-4-yl]ethan-1-one (14f)



The reaction was carried out for 24 h with **3** (1.1 mg, 1.25 μmol), 4'-bromoacetophenone (99.3 mg, 0.50 mmol), (4-fluorophenyl)boronic acid (83.2 mg, 0.60 mmol) and K_3PO_4 (212.2 mg, 1.0 mmol). The product **14f** was obtained in 85% yield (79.4 mg, 0.43 mmol) as a white solid (m.p. = 105–106 $^\circ\text{C}$) by flash chromatography (SiO_2 , hexane/EtOAc, 98:2 to 60:40).

^1H NMR (400 MHz, CDCl_3 , δ): 2.65 (s, 3H), 7.17 (tt, $J = 2.4, 9.1$ Hz, 2H), 7.57–7.62 (m, 2H), 7.64 (dt, $J = 2.0, 8.5$ Hz, 2H), 8.03 (dt, $J = 1.9, 8.7$ Hz, 2H). ^{13}C NMR (101 MHz, CDCl_3 , δ): 26.5 (CH_3), 115.8 (d, $J = 21.2$ Hz, CH), 126.9 (CH), 128.8 (CH), 128.9 (CH), 135.7 (d, $J = 13.5$ Hz, C), 144.5 (C), 161.6 (C), 164.1 (C), 197.6 (C). HRMS-EI (m/z): [M] calcd for $\text{C}_{14}\text{H}_{11}\text{FO}$, 214.0794; found, 214.0794.

1-[4'-Methyl-(1,1'-biphenyl)-4-yl]ethan-1-one (14g)

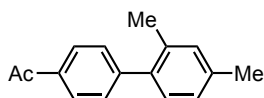


The reaction was carried out for 24 h with **3** (1.1 mg, 1.25 μmol), 1-bromo-4-methylbenzene (85.1 mg, 0.50 mmol), (4-acetylphenyl)boronic acid (98.6 mg, 0.60 mmol) and K_3PO_4 (212.3 mg, 1.0 mmol).

The product **14g** was obtained in 84% yield (88.3 mg, 0.42 mmol) as a white solid (m.p. = 122–123 °C) by flash chromatography (SiO₂, hexane/ CH₂Cl₂, 100:0 to 0:100).

¹H NMR (400 MHz, CDCl₃, δ): 2.42 (s, 3H), 2.64 (s, 3H), 7.29 (d, *J* = 8.0 Hz, 2H), 7.54 (d, *J* = 8.0 Hz, 2H), 7.68 (d, *J* = 8.8 Hz, 2H), 8.02 (d, *J* = 8.8 Hz, 2H). ¹³C NMR (101 MHz, CDCl₃, δ): 21.0 (CH₃), 26.5 (CH₃), 126.8 (CH), 126.9 (CH), 128.8 (CH), 129.6 (CH), 135.4 (C), 136.7 (C), 138.1 (C), 145.5 (C), 197.6 (C). HRMS-EI (m/z): [M] calcd for C₁₅H₁₄O, 210.1045; found, 210.1043.

1-[2',4'-Dimethyl-(1,1'-biphenyl)-4-yl]ethan-1-one (**14h**)

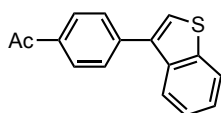


14h

The reaction was carried out for 24 h with **3** (1.1 mg, 1.25 μmol), 4'-bromoacetophenone (99.8 mg, 0.50 mmol), (2,4-dimethylphenyl)boronic acid (90.0 mg, 0.60 mmol) and K₃PO₄ (212.4 mg, 1.0 mmol). The product **14h** was obtained in 94% yield (105.7 mg, 0.47 mmol) as a colorless liquid by flash chromatography (SiO₂, hexane/CH₂Cl₂, 100:0 to 0:100).

¹H NMR (400 MHz, CDCl₃, δ): 2.25 (s, 3H), 2.38 (s, 3H), 2.65 (s, 3H), 7.06–7.15 (m, 3H), 7.42 (dt, *J* = 1.9, 8.3 Hz, 2H), 8.00 (dt, *J* = 2.0, 8.4 Hz, 2H). ¹³C NMR (101 MHz, CDCl₃, δ): 20.2 (CH₃), 21.0 (CH₃), 26.5 (CH₃), 126.6 (CH), 128.1 (CH), 129.35 (CH), 129.39 (CH), 131.2 (CH), 134.8 (C), 135.2 (C), 137.5 (C), 137.7 (C), 146.8 (C), 197.7 (C). HRMS-EI (m/z): [M] calcd for C₁₆H₁₆O, 224.1201; found, 224.1201.

1-[4-(Benzo[*b*]thiophen-3-yl)phenyl]ethan-1-one (**14i**)

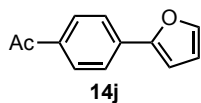


14i

The reaction was carried out for 24 h with **3** (1.1 mg, 1.25 μmol), 4'-bromoacetophenone (99.8 mg, 0.50 mmol), benzo[*b*]thiophene-3-boronic acid (106.7 mg, 0.60 mmol) and K₃PO₄ (212.3 mg, 1.0 mmol). The product **14i** was obtained in 98% yield (124.6 mg, 0.49 mmol) as a pale pink solid (m.p. = 92–93 °C) by flash chromatography (SiO₂, hexane/CH₂Cl₂, 90:10 to 0:100).

¹H NMR (400 MHz, CDCl₃, δ): 2.67 (s, 3H), 7.39–7.46 (m, 2H), 7.51 (s, 1H), 7.71 (dt, *J* = 1.9, 8.7 Hz, 2H), 7.89–7.97 (m, 2H), 8.09 (dt, *J* = 1.8, 8.4 Hz, 2H). ¹³C NMR (101 MHz, CDCl₃, δ): 26.5 (CH₃), 122.5 (CH), 122.9 (CH), 124.49 (CH), 124.54 (CH), 124.7(CH), 128.5 (CH), 128.7(CH), 135.8 (C), 136.7 (C), 137.2 (C), 140.5 (C), 140.6 (C), 197.5 (C). HRMS-EI (m/z): [M] calcd for C₁₆H₁₂OS, 252.0609; found, 252.0602.

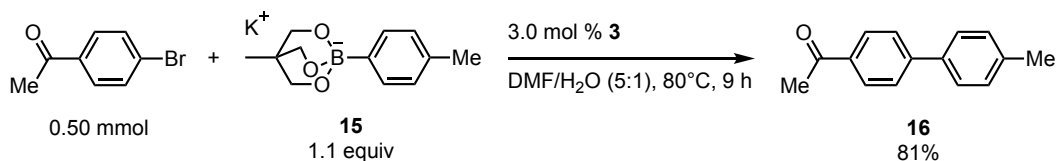
1-[4-(Furan-2-yl)phenyl]ethan-1-one (**14j**)



The reaction was carried out for 24 h at 40 °C with **3** (12.9 mg, 0.015 mmol), 4'-bromoacetophenone (99.2 mg, 0.50 mmol), 2-furylboronic acid (67.1 mg, 0.60 mmol) and K₃PO₄ (212.0 mg, 1.0 mmol). The product **14j** was obtained in 79% yield (73.5 mg, 0.39 mmol) as a white solid (m.p. = 104–105 °C) by flash chromatography (SiO₂, hexane/ CH₂Cl₂, 90:10 to 0:100).

¹H NMR (400 MHz, CDCl₃, δ): 2.62 (s, 3H), 6.52 (q, *J* = 1.7 Hz, 1H), 6.81 (dd, *J* = 0.8, 3.6 Hz, 1H), 7.54 (dd, *J* = 0.8, 2.0 Hz, 1H), 7.75 (dt, *J* = 1.9, 8.7 Hz, 2H), 7.98 (dt, *J* = 1.8, 8.5 Hz, 2H). ¹³C NMR (101 MHz, CDCl₃, δ): 26.4 (CH₃), 107.4 (CH), 112.0 (CH), 123.4 (CH), 128.8 (CH), 134.7 (C), 135.3 (C), 143.2 (CH), 152.7 (C), 197.2 (C). HRMS-EI (*m/z*): [M] calcd for C₁₂H₁₀O₂, 186.0681; found, 186.0675.

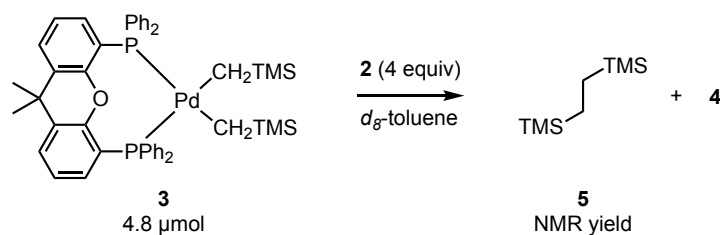
Base-Free Suzuki-Miyaura Cross-Coupling



3 (13.0 mg, 0.015 mmol), 4'-bromoacetophenone (99.6 mg, 0.50 mmol) and **15** (142.0 mg, 0.55 mmol) were placed in an oven-dried reaction vial. After being sealed with a screw cap containing a Teflon-coated rubber septum, the vial was connected to a nitrogen line through a needle. DMF (1.25 mL) and water (0.25 mL) were added, then the reaction mixture was heated to 80 °C for 9 hours. After cooling to room temperature, the reaction mixture was extracted three times with EtOAc, washed with brine and dried over MgSO₄. The crude mixture was purified by flash column chromatography (SiO₂, EtOAc/hexane, 0:100–6:94). The product **16** was obtained in 81% yield (85.7 mg, 0.41 mmol) as a white solid (m.p. = 122–123 °C).

¹H NMR (392 MHz, CDCl₃, δ): 2.41 (s, 3H), 2.64 (s, 3H), 7.28 (d, *J* = 8.1 Hz, 2H), 7.54 (dt, *J* = 2.0, 8.4 Hz, 2H), 7.68 (dt, *J* = 1.9, 8.7 Hz, 2H), 8.02 (dt, *J* = 1.9, 8.4 Hz, 2H). ¹³C NMR (99 MHz, CDCl₃, δ): 21.1 (CH₃), 26.5 (CH₃), 126.8 (CH), 127.0 (CH), 128.8 (CH), 129.6 (CH), 135.4 (C), 136.8 (C), 138.1 (C), 145.5 (C), 197.6 (C). HRMS-EI (*m/z*): [M] calcd for C₁₅H₁₄O, 210.1045; found, 210.1037.

Monitoring the Progress of the Reductive Elimination from **3**.



2 (11.0 mg, 19 μmol), **3** (4.1 mg, 4.8 μmol) and 1,2-diphenylethane (3.0 mg) as an internal standard were placed in the NMR test tube, then d_8 -toluene was added. The mixture was heated to 40, 60 or 80 °C and the yield of **5** was determined by ^1H NMR analysis.

Supplementary Table 3. Monitoring the reductive elimination at different reaction temperatures.

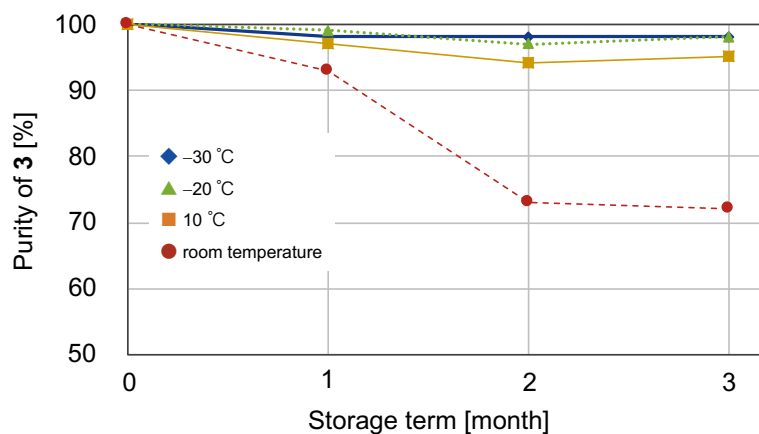
Temperature	NMR yield of 5 (%)					
	10 min	20 min	30 min	40 min	50 min	60 min
40 °C	9	14	18	22	28	32
60 °C	47	71	81	88	91	94
80 °C	98	102	-	-	-	-

Stability of 3 for the Long-Term Storage.

3 in the nitrogen purged vials were stored at room temperature (desiccator), 10 °C (refrigerator), –20 °C and –30 °C (freezer) respectively. The purity of them were determined by ¹H NMR analysis using dibromomethane as an internal standard.

Supplementary Table 4. Purity of 3 for three months from the synthesis.

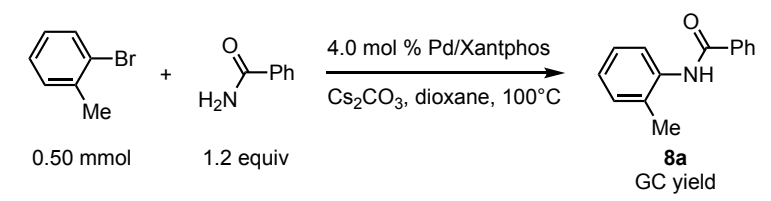
Storage conditions	Purity of 3 (%)		
	1 month	2 months	3 months
–30 °C	98	98	98
–20 °C	99	97	98
10 °C	97	94	95
room temperature	93	73	72



Supplementary Figure 4. Monitoring the purity of 3 depending on the storage temperature.

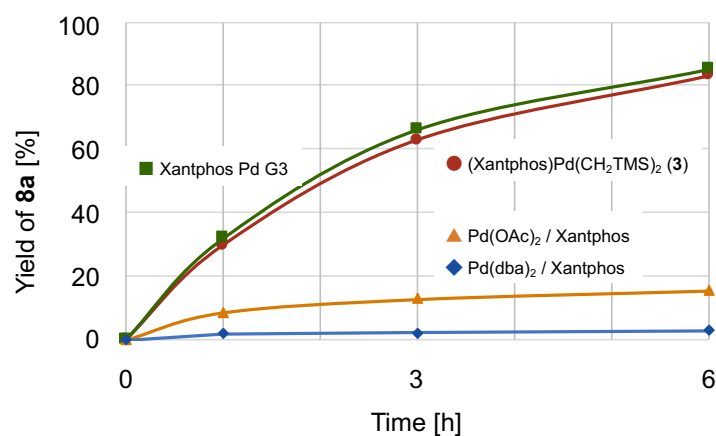
Comparison of the Catalytic Performance of **3** with Those of Other Catalyst Precursors.

Supplementary Table 5. Results of C–N coupling with various catalyst precursors.



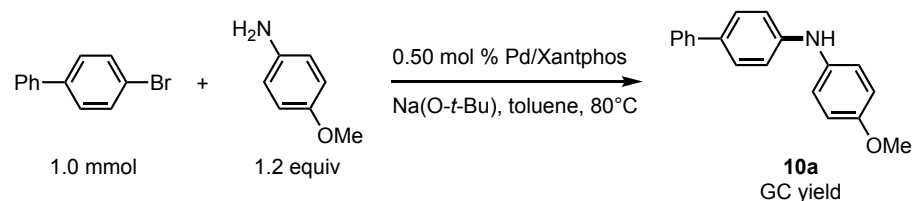
Precursor	GC yield of 8a (%) ^a		
	1 h	3 h	6 h
3	30	63	83
Xantphos Pd G3	32	66	85
Pd(OAc) ₂ / Xantphos	9	13	16
Pd(dba) ₂ / Xantphos	4	6	5

^aDetermined by GC analysis using 4,4'-di-tert-butyl-1,1'-biphenyl as an internal standard.



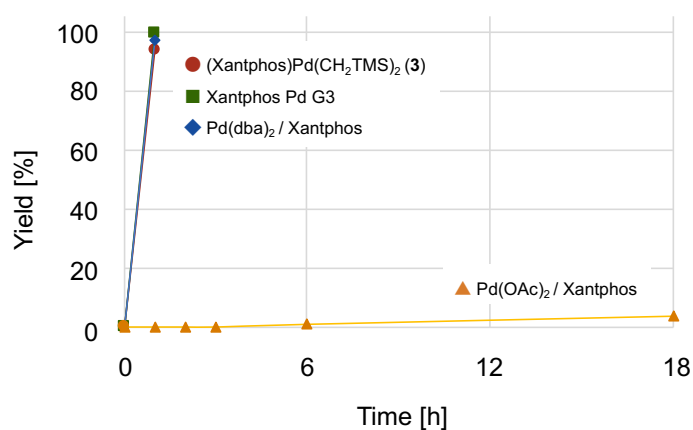
Supplementary Figure 5. Comparison of the catalytic performance of **3** with those of other catalyst precursors in C–N coupling.

Supplementary Table 6. Results of C–N coupling with various catalyst precursors.



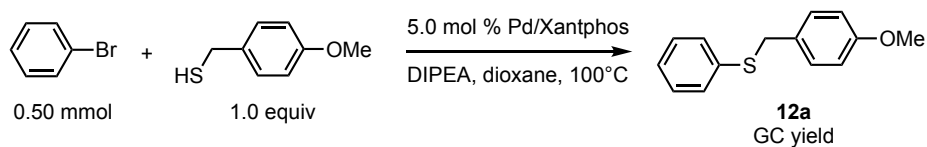
Precursor	GC yield of 10a (%) ^a			
	1 h	3 h	6 h	18 h
3	94	-	-	-
Xantphos Pd G3	99	-	-	-
Pd(OAc) ₂ / Xantphos	0	0	1	4
Pd(dba) ₂ / Xantphos	97	-	-	-

^aDetermined by GC analysis using 1,4-di-*tert*-butylbenzene as an internal standard.



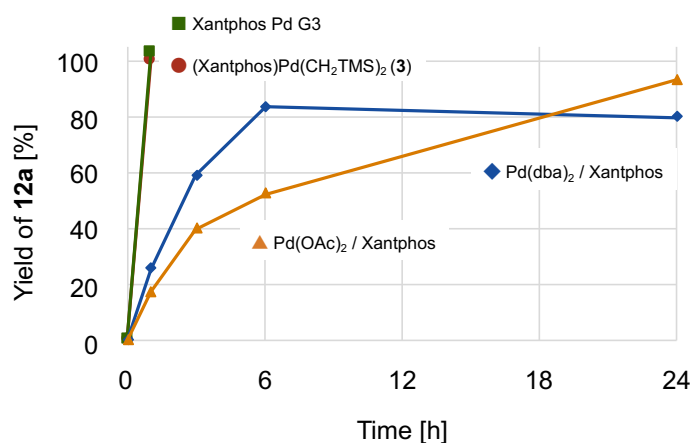
Supplementary Figure 6. Comparison of the catalytic performance of **3 with those of other catalyst precursors in C–N coupling.**

Supplementary Table 7. Result of C–S coupling of with various catalyst precursors.



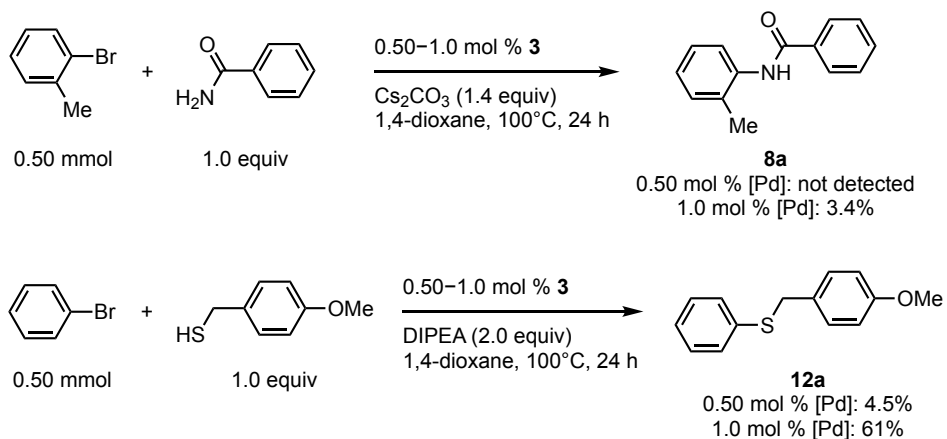
Precursor	GC yield of 12a (%) ^a			
	1 h	3 h	6 h	24 h
3	100	-	-	-
Xantphos Pd G3	103	-	-	-
Pd(OAc) ₂ / Xantphos	17	40	52	93
Pd(dba) ₂ / Xantphos	26	59	84	80

^aDetermined by GC analysis using 4,4'-di-tert-butyl-1,1'-biphenyl as an internal standard.



Supplementary Figure 7. Comparison of the catalytic performance of **3** with those of other catalyst precursors in C–S coupling.

Investigation of C-Heteroatom Cross-coupling Reaction with Low Catalyst Loading^a.



^aYields were determined by ¹H NMR analysis using dibromomethane as an internal standard.

9. References

- 1) Sheldrick, G. M. *Acta Crystallogr., Sect. A* **2008**, *64*, 112.
- 2) Kubota, K.; Dai, P.; Pentelute, B. L.; Buchwald, S. L. *J. Am. Chem. Soc.* **2018**, *140*, 3128–3133.
- 3) Andersen, T. L.; Kramer, S.; Overgaard, J.; Skrydstrup, T. *Organometallics* **2017**, *36*, 2058–2066.

Chapter 3.

Mechanochemical Synthesis of Magnesium-based Carbon Nucleophiles and Their Application to Organic Synthesis

Abstract

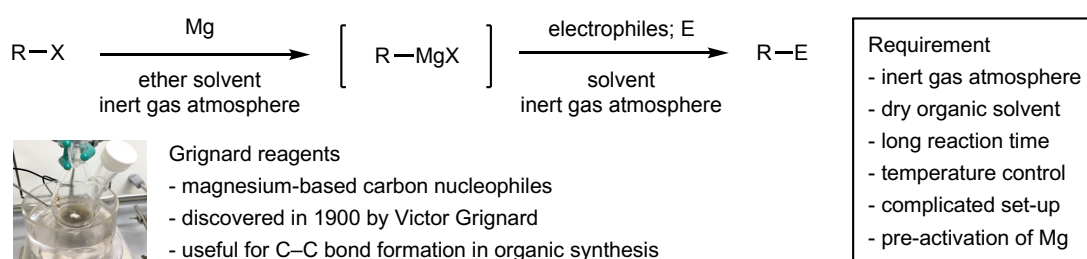
Since the discovery of Grignard reagents in 1900 by Victor Grignard, the nucleophilic addition of magnesium-based carbon nucleophiles to various electrophiles has become one of the most powerful, versatile, and well-established methods for the formation of carbon–carbon bonds in organic synthesis. Grignard reagents are typically prepared via reactions between organic halides and magnesium metal in a solvent. However, this method usually requires the use of dry organic solvents, long reaction times, strict control of the reaction temperature, and inert-gas-line techniques. Despite the widespread utility of Grignard reagents in organic chemistry, these requirements still represent major drawbacks from both an environmental and an economic perspective, and often cause reproducibility problems for unreactive organic halides. In addition, poorly soluble substrates are not readily applicable to conventional solution-based protocols. Herein, I report the first general mechanochemical synthesis of magnesium-based carbon nucleophiles (Grignard reagents in paste form) in air using a ball milling technique. These nucleophiles can be used directly for one-pot nucleophilic addition reactions with various electrophiles, nickel-catalyzed Kumada–Tamao–Corriu cross-coupling reactions, and metal-catalyzed selective addition reactions to conjugated enones under solvent-free conditions. Importantly, solid-state mechanochemical conditions enabled the formation of novel magnesium-based carbon nucleophiles from poorly soluble aryl halides, which are not suitable for conventional solution-based protocols. The generation of the magnesium-based carbon nucleophiles under mechanochemical conditions was examined by near-edge X-ray absorption fine structure (NEXAFS) spectroscopy. Beyond the immediate utility of this protocol, this method clearly demonstrates significant potential for the development of industrial applications given its operational simplicity and cost-effectiveness.

Introduction

The discovery of what later became commonly known as the ‘Grignard reagents’ and their use as carbon nucleophiles was first reported in 1900 by Victor Grignard.¹ Since then, Grignard reagents have occupied an important place in organic chemistry, as they have been used to produce numerous synthetic intermediates and valuable functional molecules in the materials, pharmaceutical, food, polymer, and related chemical industries.^{2–5} Thus, the development of efficient methods for their preparation has attracted considerable interest.^{6–8} The direct insertion of magnesium metal into organic halides is one of the most established routes, as it is an atom-economical process with low toxicity (Scheme 3-1).⁹ However, this method usually requires the use of dry organic

solvents, long reaction times, strict control of the reaction temperature, and inert-gas-line techniques. Moreover, the surface of the magnesium metal may be covered with an unreactive oxide layer,¹⁰ which requires a pre-activation process involving heating, ultrasound,¹¹ or microwave¹² treatment and/or the addition of activating reagents.^{13–15} Unfortunately, these requirements still represent major drawbacks from both an environmental and an economic perspective, and often cause reproducibility problems for unreactive organic halides.

Preparation of Grignard reagents by direct Mg insertion to organic halides



Scheme 3-1. Conventional-solution based method for the preparation of Grignard reagents.

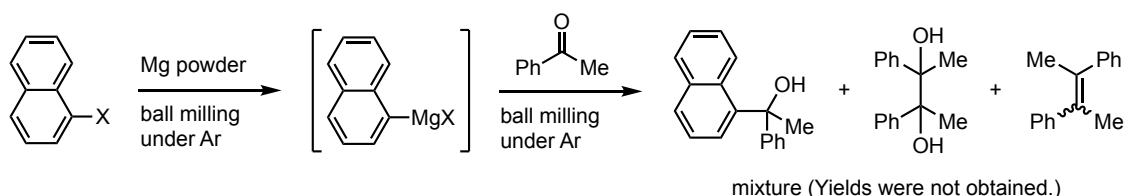
In this context, the use of ball milling techniques^{16–24} for the solvent-free preparation of Grignard reagents via reactions between aryl halides and magnesium metal has been studied by several research groups (Scheme 3-2). In 2001, Harrowfield and co-workers first attempted mechanochemical reactions of 1-chloro- or 1-bromo-naphthalenes with magnesium metal in a glovebox.²⁵ Unfortunately, their subsequent one-pot nucleophilic addition to ketones resulted in complex product mixtures. As part of a search for dehalogenation reactions of harmful organic compounds, Birke and co-workers reported that the complete protonation of aryl chlorides could be achieved by milling them with magnesium and n-butyl amine in a glovebox.²⁶ More recently, Hanusa and co-workers reported the mechanochemical reactions of bromo- or fluoroarenes with magnesium metal in a glovebox.²⁷ Subsequent addition of FeCl₃ to the reaction mixture gave the corresponding homo-coupling products in moderate to low yield. However, one-pot mechanochemical reactions with carbonyl electrophiles did not provide the corresponding nucleophilic addition products. More recently, Yang, Dai, and co-workers also reported magnesium-mediated reductive radical homo-coupling reactions of polyhaloarenes.²⁸ Although these pioneering studies are highly remarkable, neither successful examples of the use of magnesium-based carbon nucleophiles prepared by ball milling for the formation of carbon – carbon bonds with various electrophiles,²⁹ nor direct spectroscopic evidence for the formation of carbon – magnesium bonds under

mechanochemical conditions have been reported so far.

Attempts at mechanochemical synthesis of Grignard reagents

- Nucleophilic reactions were unsuccessful. - No direct evidence for the formation of Grignard reagents.

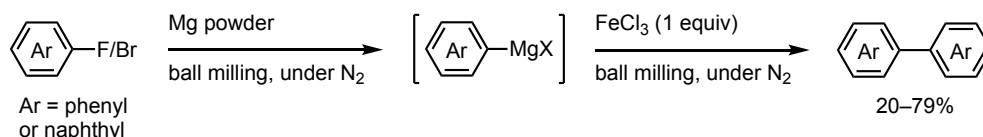
1. Grignard and McNarry reaction (Harrowfield, 2001)



2. Dehalogenation of organic halides (Birke, 2009, 2011)



3. Mg- and Fe-mediated homo-coupling reaction (Hanusa, 2020)

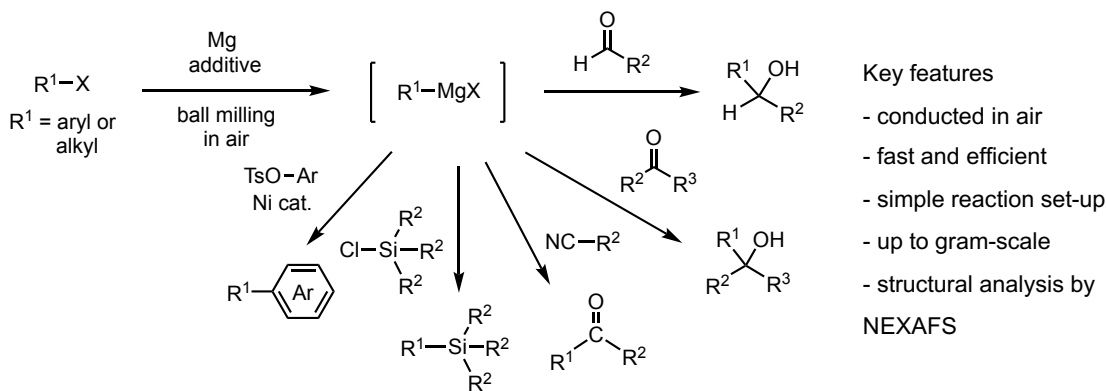


Scheme 3-2. Previous attempts to synthesize Grignard reagents by mechanochemistry.

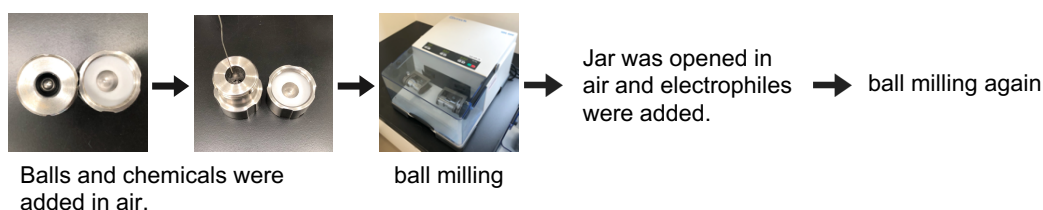
Herein, I report that a mechanochemical approach using ball milling allows for a highly efficient, general, and robust method for the preparation of magnesium-based carbon nucleophiles in air and their application to various organic transformations under mechanochemical conditions (Scheme 3-3). The key to the success of this protocol is the addition of small amounts of tetrahydrofuran (THF) or cyclopentyl methyl ether (CPME), which facilitates the formation of organomagnesium nucleophiles and their addition to electrophiles. The carbon nucleophiles thus formed can be used for various transformations including carbonyl addition, carbon–silicon bond formation, nickel-catalyzed Kumada–Tamao–Corriu cross-coupling reactions, and metal-catalyzed selective addition reactions to conjugated enones under mechanochemical conditions. Notably, the developed protocol does not require the use of inert gas or dry organic solvents, allowing the entire procedure to be conducted in air without necessitating any special precautions or synthetic techniques. I also succeeded in the preparation of an organomagnesium reagent from a poorly soluble aryl halide, and it should be noted here that this reagent cannot be synthesized via conventional solution-based protocols. Near edge X-ray absorption fine structure (NEXAFS) spectroscopy was used to analyze the

generation of the magnesium-based carbon nucleophiles under mechanochemical conditions. The present study thus provides a new platform centered on magnesium-based carbon nucleophiles, which has the potential to update modern organic synthesis with a more cost-effective and environmental-friendly procedure for Grignard reactions.

This work: mechanochemical synthesis of magnesium-based carbon nucleophiles



Reaction set-up



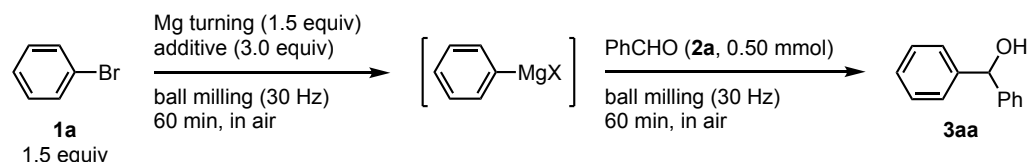
Scheme 3-3. Mechanochemical synthesis of magnesium-based carbon nucleophiles and their application to organic synthesis.

Results and Discussion

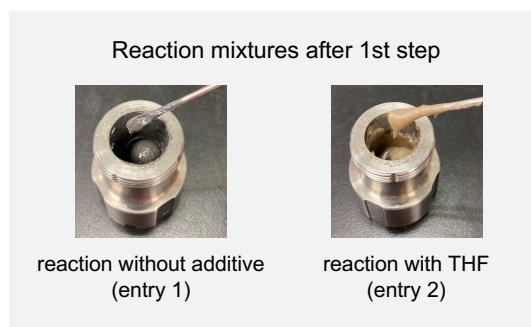
I first attempted the synthesis of organomagnesium species from bromobenzene [**1a**, 1.5 equiv for benzaldehyde (**2a**)] and magnesium turnings [1.5 equiv for benzaldehyde (**2a**)] and a subsequent nucleophilic addition to benzaldehyde (**2a**). Otherwise noted, mechanochemical reactions were conducted in a Retsch MM 400 mill (5 mL stainless-steel milling jar; 30 Hz; stainless-steel balls, diameter 10 mm) (Table 3-1). After the ball milling of **1a** and magnesium turnings for 60 minutes, the jar was opened in air, and a gray oil was obtained (Table 3-1, left photograph). Visible magnesium metal grains or powder were not observed in the mixture. Then, **2a** was added to the jar and ball milling was continued for 60 minutes. The desired nucleophilic addition product (**3aa**) was obtained, albeit in only 6% NMR yield (entry 1). Next, I attempted to improve the reactivity by using liquid ethers as additives in order to facilitate the formation of the magnesium-based carbon nucleophiles and their addition to the electrophiles. The use of

2.0 equivalents of tetrahydrofuran (THF) relative to the amount of magnesium afforded a muddy light-orange mixture (Table 3-1, right photograph). Then, this mixture was ball-milled with **2a**, which dramatically improved the yield of **3aa** to 94% yield (entry 2). I also tested other liquid ethers, such as diethyl ether (Et₂O) and cyclopentyl methyl ether (CPME), but the resulting yields were lower than that obtained using THF (entries 3 and 4). The use of liquid additives that are not used as solvents for the preparation of Grignard reagents, such as 1,4-dioxane, toluene or hexane, did not improve the yield of **3aa** (entries 5–7). The protocol using THF as an additive was applied to the synthesis of magnesium-based carbon nucleophiles from iodobenzene (**1a'**) and chlorobenzene (**1a''**), and the desired alcohol **3aa** was obtained in good yields of 74% and 84%, respectively (for details, see the experimental section). Notably, the reaction of **1a** and magnesium was also carried out on a gram scale in a 10-mL stainless-steel ball-milling jar with two 15-mm-diameter stainless-steel balls to afford **3aa** in 93% yield (1.03 g; Scheme 3-4). This result underscores the high practical utility of this protocol. Even when the reaction was carried out under a nitrogen atmosphere, the product yield was not improved. This indicates that air (oxygen and CO₂) in the reaction vessel does not significantly affect the efficiency of this protocol.

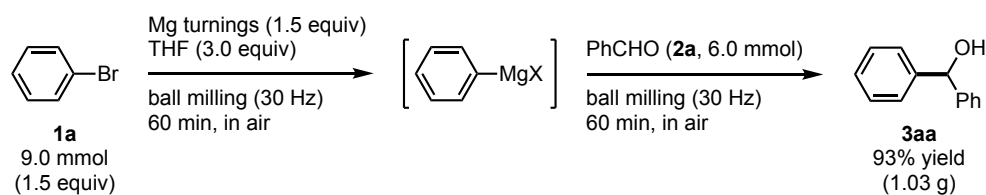
Table 3-1. Optimization of reaction conditions for the formation of magnesium-based carbon nucleophiles under mechanochemical conditions.



entry	additive (3.0 equiv)	yield of 3aa
1	-	6
2	THF 123 μ L	94
3	Et ₂ O 155 μ L	79
4	CPME 175 μ L	87
5	1,4-dioxane 128 μ L	5
6	toluene 160 μ L	<1
7	hexane 200 μ L	1



A stainless-steel milling jar (5 mL) and stainless-steel ball (diameter: 10 mm) were used.



Scheme 3-4. Gram-scale preparation of magnesium-based carbon nucleophile and reaction with aldehyde under the mechanochemical condition. A stainless-steel milling jar (25 mL) and two stainless-steel balls (diameter: 10 mm) were used.

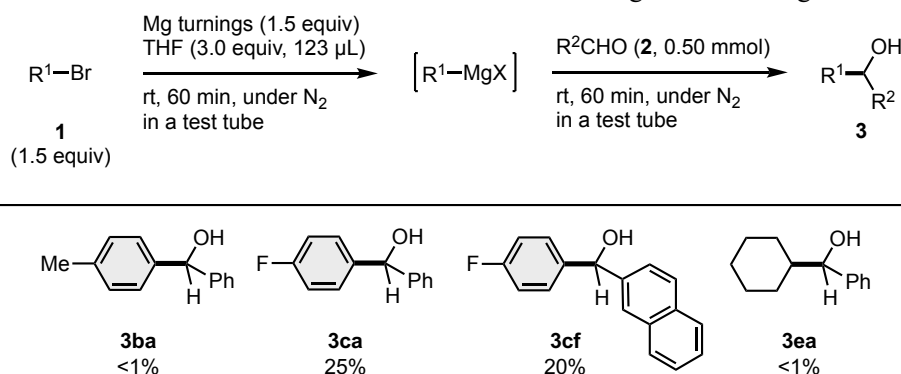
With the optimized conditions (conditions A) in hand, I investigated the substrate scope for the nucleophilic addition to aldehydes and ketones (Table 3-2). The results show that this method is characterized by a broad substrate scope that encompasses aromatic and aliphatic bromides (**1a–1e**), aldehydes (**2a–2c**, and **2f**), and ketones (**2d** and **2e**) to give the desired alcohols (**3aa–3ef**) in moderate to high yields. Furthermore, this method was also applicable to aryl halides that bear various substituents, such as methoxy-, chlorine, and dimethylamino groups in *para*-position and methyl, methoxy-, and phenyl groups in *ortho*-position (for details, see the experimental section). To improve the yield of **3**, the use of an excess of magnesium (5.0 equiv) or organic halide (2.0 equiv) were tested (conditions B). Although conditions B generally provided product yields comparable to those achieved using conditions A, conditions B improved the efficiency of the reactions using secondary alkyl bromide **1e**, affording the products **3ea–3ef** in moderate to good yields. The addition of lithium salts such as lithium chloride and lithium bromide was slightly improved the yields of the reactions using **1a** and **1c** as the substrates (for details, see the experimental section). I also attempted the reactions using the liquid substrates in a test tube with efficient mixing by magnetic stirring under the optimized conditions, but these reactions resulted in poor or almost no product formation (Table 3-3). These results suggest that strong mechanical agitation in the ball mill is crucial for the formation of the magnesium-based carbon nucleophiles.³⁰

Table 3-2. Scope of the mechanochemical synthesis of magnesium-based carbon nucleophiles and their nucleophilic addition to aldehydes and ketones.

		$\text{R}^1\text{-Br} \xrightarrow[\text{60 min, in air}]{\text{Mg turnings, THF, ball milling (30 Hz)}} \left[\text{R}^1\text{-MgBr} \right] \xrightarrow[\text{60 min, in air}]{\text{R}^2\text{-C(=O)-R}^3 \text{ (2, 0.50 mmol), ball milling (30 Hz)}} \text{R}^1\text{-C(OH)(R}^2\text{)(R}^3\text{)}$				
		conditions A electrophile (1.0 equiv), halide (1.5 equiv) Mg (1.5 equiv), and THF (3.0 equiv)				
		conditions B electrophile (1.0 equiv), halide (2.0 equiv) Mg (5.0 equiv), and THF (3.0 equiv)				
$\text{R}^1\text{-Br}$	$\text{R}^2\text{-C(=O)-R}^3$	1a	1b	1c	1d	1e
2a		3aa A: 84% (94%) B: 64% (75%) with LiBr	3ba A: 86% (91%) B: 56% (78%)	3ca A: 77% (81%) B: 67% (75%) with LiCl	3da A: 73% (90%) B: 77% (92%)	3ea A: (24%) B: 58% (74%)
2b		3ab A: 70% (84%) B: 63% with LiBr	3bb A: 70% (86%) B: 42% (61%)	3cb A: 70% (81%) B: 61% with LiCl	3db A: 46% (62%) B: 62%	3eb A: 40% B: 42% (50%)
2c		3ac A: 73% (75%) B: 58% (67%) with LiCl	3bc A: 62% (66%) B: 55% (68%)	3cc A: 62% (70%) B: 55% (62%) with LiCl	3dc A: 67% (70%) B: 55% (67%)	3ec A: (26%) B: 43% (44%)
2d		3ad A: 82% (88%) B: 45% (63%) with LiBr	3bd A: 74% (80%) B: 64% (70%)	3cd A: 71% (71%) B: 61% (74%) with LiCl	3dd A: (58%) B: 60% (71%)	3ed A: (33%) B: 30% (41%)
2e		3ae A: 79% (83%) B: 69% (82%) with LiBr	3be A: 69% (72%) B: 60% (85%)	3ce A: (54%) B: 72% with LiCl	3de A: (66%) B: 63% (77%)	3ee A: 15% B: 22% (38%)
2f		3af A: 73% (83%) B: 73% (82%)	3bf A: 72% (81%) B: 68% (75%)	3cf A: (48%) B: 65% (72%)	3df A: 68% (73%) B: 99%	3ef A: (19%) B: 50% (51%)

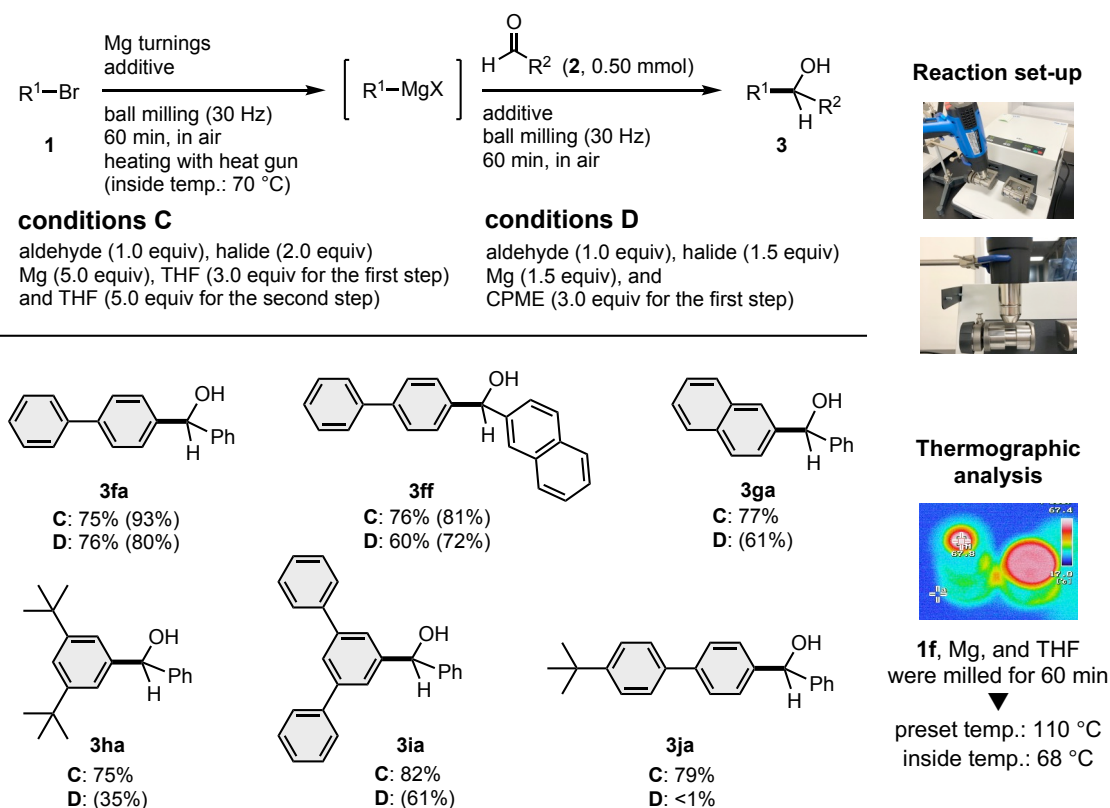
A stainless-steel milling jar (5 mL) and stainless-steel ball (diameter: 10 mm) were used. Isolated yields are reported as percentages. Proton NMR integrated yields are shown in parentheses. For details, see the Supplementary Information.

Table 3-3. Reactions under solvent-less conditions without strong mechanical agitation.



An attempts to react magnesium and solid aryl halides such as 4-bromobiphenyl (**1f**) for the subsequent nucleophilic addition to benzaldehyde (**2a**) resulted in almost no reaction under the optimized conditions A or B. Neither prolonging the reaction time nor using liquid additives improved the yield of the product (**3fa**). To promote the formation of magnesium-based nucleophiles from the solid aryl halides, I decided to carry out the reaction at higher temperature. In one of the previous studies reported by Ito, Kubota, and co-workers, the authors revealed that external heating enables poorly soluble aryl halides to react in solid-state cross-coupling reactions.³¹ In that case, external heating may help to weaken the intermolecular interactions of solid substrates, which would improve the mixing efficiency and promote chemical reactions. Specifically, I placed a commercially available, temperature-controllable heat gun directly above the ball-milling jar.³¹ The mechanochemical reactions between magnesium and the solid aryl halides were conducted while applying hot air to the outside of the milling jar. I set the temperature of the heat gun to 110 °C in order to ensure an internal reaction temperature of 70 °C, which was confirmed by thermography immediately after opening the milling jar (Table 3-4). The reaction between magnesium and **1f** in the presence of THF (3.0 equiv) was complete within 1 hour and formed the desired nucleophilic addition product (**3fa**) in high yield (75% yield). In this procedure, the addition of THF (5.0 equiv) was also needed for the nucleophilic addition step, which improved the yield of **3fa**. These high-temperature ball-milling conditions (conditions C) were applied to various solid bromides (**1f–1j**) and afforded the corresponding alcohols (**3ff–3ja**) in high yield. The use of CPME instead of THF provided comparable yields of the addition products (conditions D).

Table 3-4. Scope of the mechanochemical synthesis of magnesium-based carbon nucleophiles from solid aryl halides via high-temperature ball-milling.

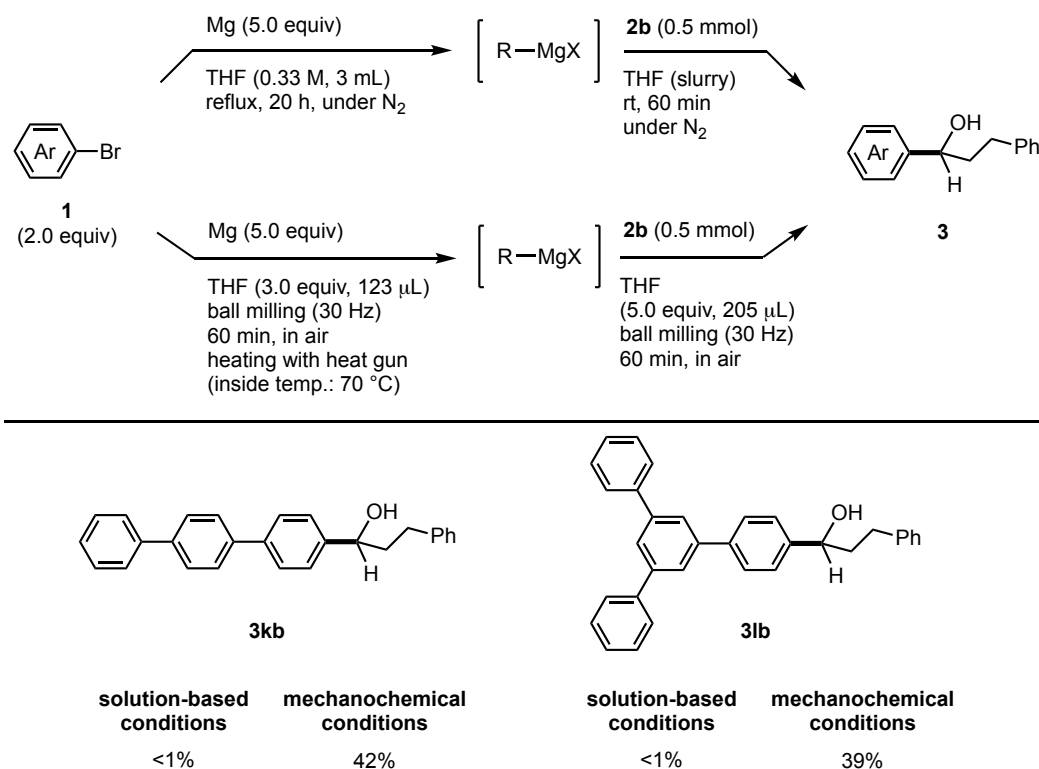


A stainless-steel milling jar (5 mL) and stainless-steel ball (diameter: 10 mm) were used. Isolated yields are reported as percentages. Proton NMR integrated yields are shown in parentheses. For details, see the Supplementary Information.

Reactions of Mg metal with poorly soluble aryl halides under conventional solution-based conditions are often inefficient. For example, the reaction of poorly soluble 4-bromoterphenyl (**1k**) under reflux conditions (309.2 mg of **1k** in 3 mL of THF, 0.33 M, a slurry, for 20 hours) did not afford any nucleophilic addition product and the starting material **1k** remained (Table 3-5). I also attempted using more dilute conditions (309.2 mg of **1k** in 15 mL of THF, 0.067 M, a clear solution, for 20 hours), albeit that **3kb** was still not obtained. In contrast, the developed mechanochemical conditions provided the corresponding magnesium-based carbon nucleophile from **1k** via high-temperature ball milling within 60 minutes, and the desired nucleophilic addition product (**3kb**) was obtained in moderate yield (42% yield). Furthermore, poorly soluble **1l** was also reactive under the mechanochemical conditions and formed the desired nucleophilic addition product (**3lb**) in 39% yield, while **3lb** was not obtained under solution-based conditions. These results demonstrate the potential of this mechanochemical protocol as an

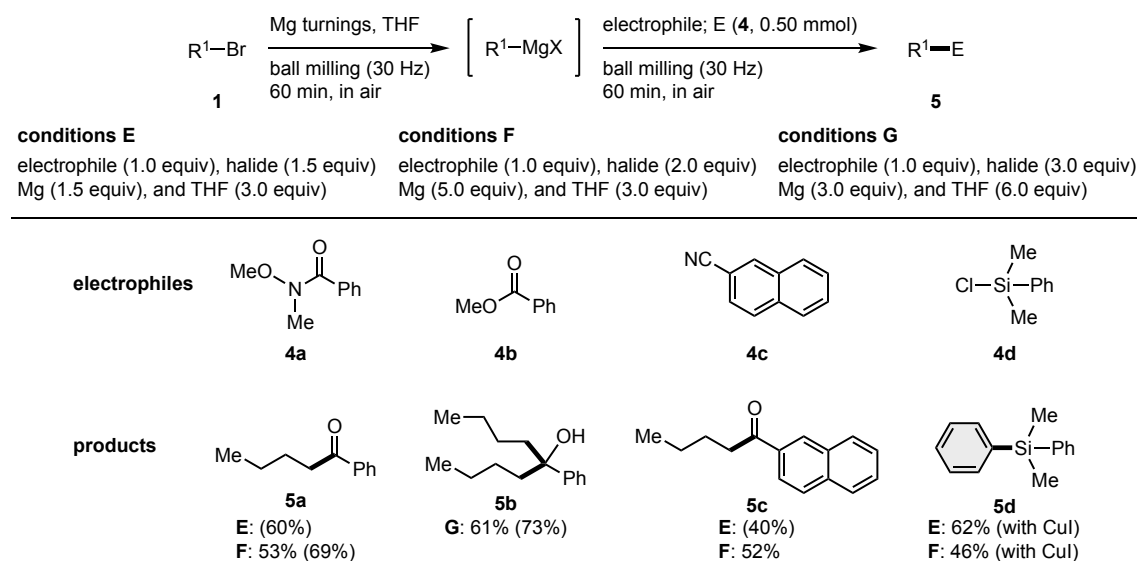
operationally simple and efficient route to synthesize novel magnesium-based carbon nucleophiles from poorly soluble substrates that are incompatible with conventional solution-based conditions.

Table 3-5. Mechanochemical synthesis of magnesium-based carbon nucleophiles from poorly soluble aryl halides.



A stainless-steel milling jar (5 mL) and stainless-steel ball (diameter: 10 mm) were used. Isolated yields are reported as percentages. For details, see the Supplementary Information.

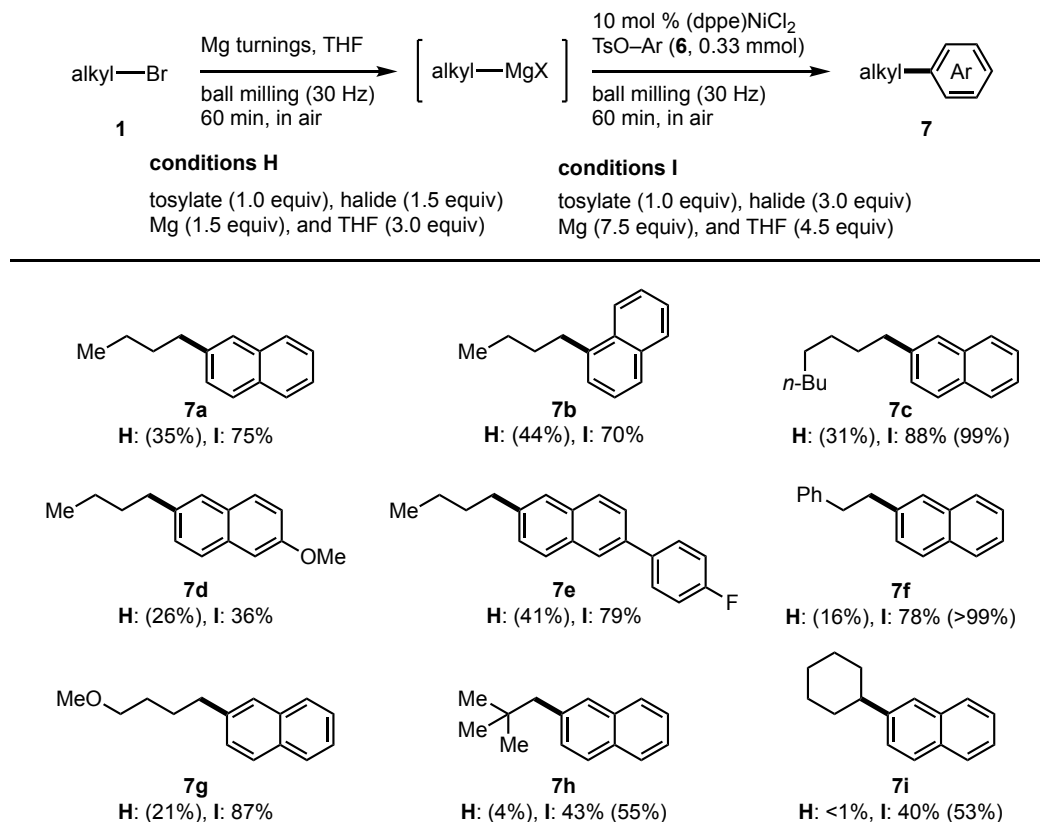
The mechanochemically synthesized organomagnesium nucleophiles were applicable to reactions with various organic electrophiles (Table 3-6). A Weinreb amide (**4a**) and ester (**4b**) were converted to the corresponding ketone (**5a**) and tertiary alcohol (**5b**) in good yield. Nitrile (**4c**) reacted with the organomagnesium nucleophile derived from **1d** even at room temperature to provide the corresponding ketone (**5c**) in moderate yield (52% yield). Other C–C-bond-forming reactions with carbon dioxide, epoxides, and amides afforded the corresponding products in low to good yield (for details, see the experimental section). In addition, the organomagnesium reagents were applicable to not only C–C-bond-formation reactions, but also Si–C-bond-formation reactions with chlorosilane (**4d**) in the presence of a catalytic amount of copper iodide.³²

Table 3-6. Nucleophilic addition to various electrophiles under mechanochemical conditions.

A stainless-steel milling jar (5 mL) and stainless-steel ball (diameter: 10 mm) were used. Isolated yields are reported as percentages. Proton NMR integrated yields are shown in parentheses. For details, see the Supplementary Information.

Next, I investigated nickel-catalyzed Kumada–Tamao–Corriu coupling reactions between the mechanochemically synthesized magnesium-based carbon nucleophiles and aryl tosylates under ball-milling conditions (Table 3-7).³³ After the reaction between **1d** and magnesium, the jar was opened in air and 2-naphthyl tosylate (**6a**) and 10 mol% of (dppe)NiCl₂ were quickly added. The subsequent ball-milling reaction afforded the cross-coupling product **7a** in 35% NMR yield (conditions H). I found that increasing the amounts of **1d**, magnesium, and THF improved the yield of **7a** to 75% (conditions I). Under conditions I, reactions with simple naphthyl tosylates gave the desired products (**7b** and **7c**) in high yield (70% and 88% yield, respectively). However, **7d**, i.e., the product derived from naphthyl tosylate bearing a methoxy group (**6c**), was obtained in relatively low yield (36% yield), while the product bearing a fluoride atom (**7e**) was obtained in good yield (79% yield). A variety of primary and secondary alkyl bromides were applicable to this mechanochemical cross-coupling reactions (**7f–7i**). This is the first example of Kumada–Tamao–Corriu cross-coupling reactions under mechanochemical conditions.

Table 3-7. Nickel-catalyzed Kumada–Tamao–Corriu coupling reaction under mechanochemical conditions.

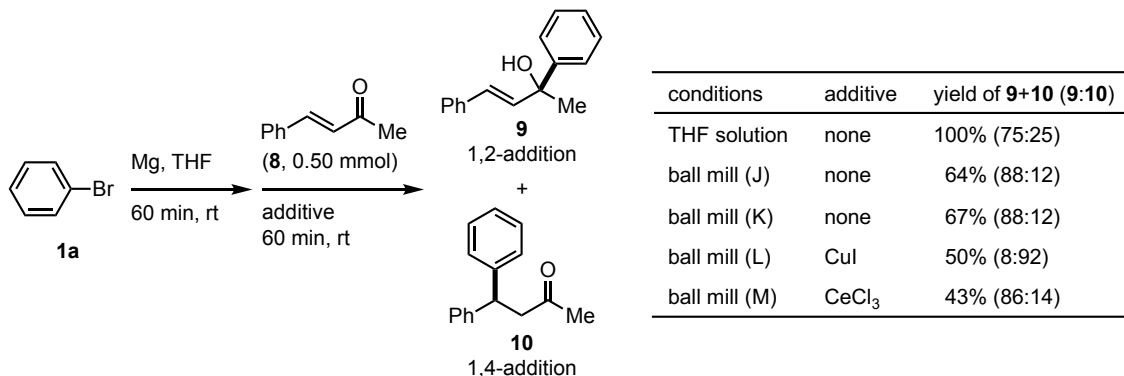


A stainless-steel milling jar (5 mL) and stainless-steel ball (diameter: 10 mm) were used. Isolated yields are reported as percentages. Proton NMR integrated yields are shown in parentheses. For details, see the Supplementary Information.

Nucleophilic addition reactions of the mechanochemically synthesized magnesium-based carbon nucleophiles to conjugated enone **8** were also examined (Table 3-8). The reaction of the phenyl magnesium reagent with benzylidene acetone (**8**) in THF solution at room temperature afforded a mixture of the 1,2-addition product (**9**) and the 1,4-addition product (**10**) (**9/10** = 75:25). Interestingly, the selectivity toward 1,2-addition increased under the mechanochemical conditions (**9/10** = 88:12). Furthermore, the mechanochemical nucleophilic addition in the presence of copper iodide afforded the 1,4-addition product (**10**) with high selectivity (50% yield, **9/10** = 8:92), suggesting that the corresponding cuprate might be formed even under the mechanochemical conditions. The addition of CeCl_3 did not influence the selectivity under the mechanochemical conditions (43% yield, **9/10** = 86:14), while Imamoto and co-workers reported that CeCl_3 improved the selectivity toward the 1,2-addition product under the corresponding solution-based

conditions.^{34, 35}

Table 3-8. Metal-mediated nucleophilic addition to conjugated enone **8**.



conditions J: enone (1.0 equiv), halide (1.5 equiv), Mg (1.5 equiv), and THF (3.0 equiv)

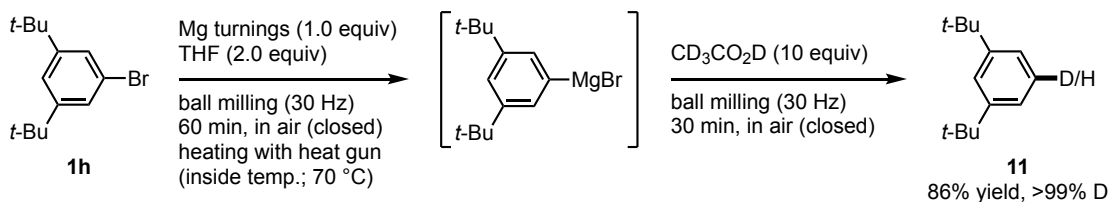
conditions K: enone (1.0 equiv), halide (2 equiv), Mg (5 equiv), and THF (3 equiv)

conditions L: enone (1.0 equiv), halide (4.0 equiv), Mg (4.0 equiv), CuI (2.0 equiv), and THF (8.0 equiv)

conditions M: enone (1.0 equiv), halide (1.5 equiv), Mg (1.5 equiv), CeCl₃ (1.5 equiv), and THF (3.0 equiv)

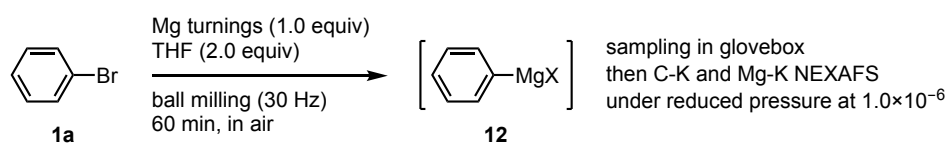
A stainless-steel milling jar (5 mL) and stainless-steel ball (diameter: 10 mm) were used. Isolated yields are reported as percentages. Proton NMR integrated yields are shown in parentheses. For details, see the Supplementary Information.

In order to confirm the generation of magnesium-based carbon nucleophiles under ball-milling conditions, a deuterium-labeling experiment was conducted (Scheme 3-5). 3,5-Di-tert-butylphenyl bromide (**1h**) was treated with magnesium under the optimized conditions, the jar was opened, and CD₃CO₂D was added quickly. The subsequent ball-milling reaction furnished deuterium-labeled 1,3-di-tert-butylbenzene **11** (>99% D), which suggests that the corresponding magnesium-based carbon nucleophile is formed.



Scheme 3-5. Deuterium-labeling experiment of mechanochemically-generated magnesium-based carbon nucleophile. A stainless-steel milling jar (5 mL) and stainless-steel ball (diameter: 10 mm) were used. Proton NMR integrated yield is reported as percentages. For details, see the Supplementary Information.

Furthermore, near edge X-ray absorption fine structure (NEXAFS) spectroscopy was used to analyze the generation of magnesium-based carbon nucleophiles under mechanochemical conditions. The NEXAFS measurements were carried out at UVSOR synchrotron facility (Japan) using the magnesium-based carbon nucleophile **12**, which was prepared by ball milling and transferred into the soft X-ray optics under an argon atmosphere (Scheme 3-6). The formation of the divalent cationic Mg^{2+} species was unequivocally confirmed by the high-energy shift of the Mg K-absorption edge (1307.4 eV) relative to the Mg^0 edge (1302.6 eV) of a standard magnesium flake (Figure 1a).³⁶ The high similarity of Mg-K and C-K NEXAFS spectra of mechanochemically-prepared **12** and PhMgBr prepared in solution (Figures 1a and 1b) supports the formation of similar organomagnesium species that possess a carbon–magnesium bond under both ball-milling and solution conditions in THF. The intense $1s-\pi^*$ transition peaks³⁷ at 285.7 and 287.7 eV in the C-K NEXAFS spectra also support the formation of a carbon–magnesium bond resulting from the transformation of the C–Br bond of the starting bromobenzene (for details, see the experimental section).



Scheme 3-6. Preparation of a sample **12** for NEXAFS analysis.

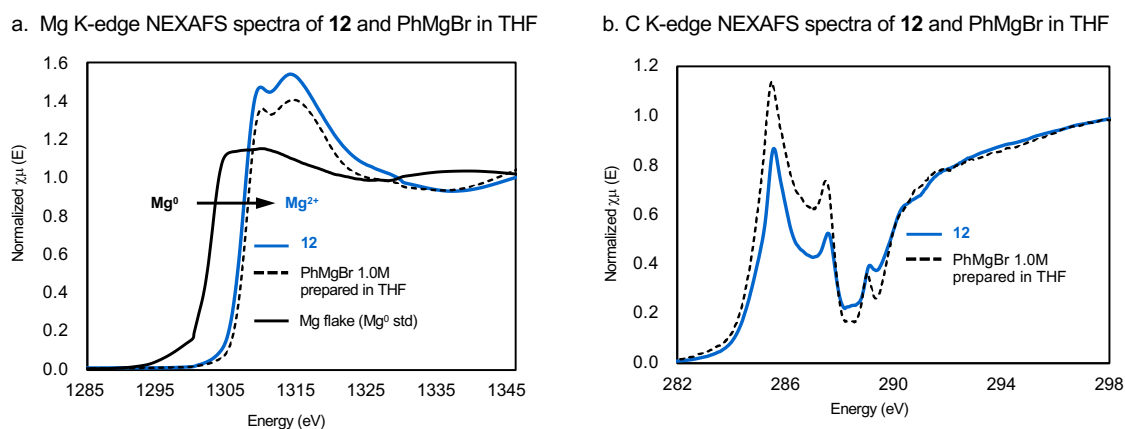


Figure 1. NEXAFS analysis of a magnesium-based carbon nucleophile prepared under mechanochemical conditions. **a**, Mg K-edge NEXAFS spectra of mechanochemically-prepared **12**, PhMgBr prepared in THF solution, and a Mg turnings of a $\text{Mg}(0)$ standard. **b**, C K-edge NEXAFS spectra of mechanochemically-prepared **12**, and PhMgBr prepared in THF solution.

Summary

The present mechanochemical synthesis of magnesium-based carbon nucleophiles and their reactions with various electrophiles can be carried out in air without the need for large amounts of dry and degassed solvent(s), special precautions, or synthetic techniques. In addition to these advantages, solid-state ball-milling conditions enabled the synthesis of novel magnesium-based carbon nucleophiles from poorly soluble aryl halides that are incompatible with conventional solution-based conditions. This can expand the utility of Grignard reagents. Direct spectroscopic evidence for the formation of magnesium-based carbon nucleophiles under mechanochemical conditions was obtained using NEXAFS spectroscopy. Given the widespread use of Grignard reagents in modern organic chemistry, I anticipate that this new approach will inspire the development of attractive synthetic applications to complement existing solution-based technologies.^{38–40}

Reference

- 1) Grignard, V. C. *R. Acad. Sci.* **1900**, *130*, 1322.
- 2) *Handbook of Grignard Reagents*; Silverman, G. S., Rakita, P. E., Eds.; Marcel Dekker, 1996.
- 3) *Grignard Reagents: New Developments*; Richey, H. G., Jr., Ed.; John Wiley & Sons, 1999.
- 4) Banno, T.; Hayakawa, Y.; Umeno, M. *J. Organomet. Chem.* **2002**, *653*, 288.
- 5) *Handbook of Functionalized Organometallics: Applications in Synthesis*; Knochel, P. Ed.; Wiley-VCH: Weinheim, 2005.
- 6) Seyferth, D. *Organometallics* **2009**, *28*, 1598.
- 7) Knochel, P. Organomagnesium and Organozinc Chemistry. In *Organometallics in Synthesis—Third Manual*; Schlosser, M. Ed.; John Wiley & Sons, 2013; pp. 223–372.
- 8) Nagaki, A.; Yoshida, J. Preparation and Use of Organolithium and Organomagnesium Species in Flow. In *Organometallic Flow Chemistry*; Noël, T. Ed.; Springer, 2016; pp. 137–175.
- 9) Trost, B. M. *Science* **1991**, *254*, 1471.
- 10) Teerlinck, C. E.; Bowyer, W. J. *J. Org. Chem.* **1996**, *61*, 1059.
- 11) Einhorn, C.; Einhorn, J.; Luche, J.-L. *Synthesis* **1989**, *11*, 787.
- 12) Gold, H.; Larhed, M.; Nilsson, P. *Synlett* **2005**, *10*, 1596.
- 13) Lai, Y.-H. *Synthesis* **1981**, *8*, 585.
- 14) Tilstam, U.; Weinmann, H. *Org. Process Res. Dev.* **2002**, *6*, 906.
- 15) Piller, F. M.; Appukkuttan, P.; Gavryushin, A.; Helm, M.; Knochel, P. *Angew. Chem., Int. Ed.* **2008**, *47*, 6802.

- 16) James, S. L.; Adams, C. J.; Bolm, C.; Braga, D.; Collier, P.; Friščić, T.; Grepioni, F.; Harris, K. D. M.; Hyett, G.; Jones, W.; Krebs, A.; Mack, J.; Maini, L.; Orpen, A. G.; Parkin, I. P.; Shearouse, W. C.; Steed, J. W.; Waddell, D. C. *Chem. Soc. Rev.* **2012**, *41*, 413.
- 17) Do, J.-L.; Friščić, T. *ACS Cent. Sci.* **2017**, *3*, 13.
- 18) Hernández, J. G.; Bolm, C. *J. Org. Chem.* **2017**, *82*, 4007.
- 19) Kubota, K.; Ito, H. *Trends Chem.* **2020**, *2*, 1066.
- 20) Howard, J. L.; Cao, Q.; Browne, D. L. *Chem. Sci.* **2018**, *9*, 3080.
- 21) Tan, D.; García, F. *Chem. Soc. Rev.* **2019**, *48*, 2274.
- 22) Bolm, C.; Hernández, J. G. *Angew. Chem., Int. Ed.* **2019**, *58*, 3285.
- 23) Porcheddu, A.; Colacino, E.; De Luca, L.; Delogu, F. *ACS Catal.* **2020**, *10*, 8344.
- 24) Kaupp, G. *CrystEngComm.* **2009**, *11*, 388.
- 25) Harrowfield, J. M.; Hart, R. J.; Whitaker, C. R. *Aust. J. Chem.* **2001**, *54*, 423.
- 26) Birke, V.; Schütt, C.; Burmeier, H.; Ruck, W. K. L. *Fresenius Environ. Bull.* **2011**, *20*, 2794.
- 27) Speight, I. R.; Hanusa, T. P. *Molecules* **2020**, *25*, 570.
- 28) Chen, H.; Fan, J.; Fu, Y.; Do-Thanh, C.-L.; Suo, X.; Wang, T.; Popovs, I.; Jiang, D.-e.; Yuan, Y.; Yang, Z.; Dai, S. *Adv. Mater.* **2021**, *33*, 2008685.
- 29) Cao, Q.; Howard, J. L.; Wheatley, E.; Browne, D. L. *Angew. Chem., Int. Ed.* **2018**, *57*, 11339.
- 30) Waddell, D. C.; Clark, T. D.; Mack, J. *Tetrahedron Lett.* **2012**, *53*, 4510.
- 31) Seo, T.; Toyoshima, N.; Kubota, K.; Ito, H. *J. Am. Chem. Soc.* **2021**, *143*, 6165.
- 32) Morita, E.; Murakami, K.; Iwasaki, M.; Hirano, K.; Yorimitsu, H.; Oshima, K. *Bull. Chem. Soc. Jpn.* **2009**, *82*, 1012.
- 33) Piontek, A.; Ochędzan-Siodłak, W.; Bisz, E.; Szostak, M. *Adv. Synth. Catal.* **2019**, *361*, 2329.
- 34) Imamoto, T.; Takiyama, N.; Nakamura, K. *Tetrahedron Lett.* **1985**, *26*, 4763.
- 35) Imamoto, T.; Takiyama, N.; Nakamura, K.; Hatojima, T.; Kamiya, Y. *J. Am. Chem. Soc.* **1989**, *111*, 4392.
- 36) Witte, K.; Streeck, C.; Mantouvalou, I.; Suchkova, S. A.; Lokstein, H.; Grötzsch, D.; Martyanov, W.; Weser, J.; Kanngießner, B.; Beckhoff, B.; Stiel, H. *J. Phys. Chem. B* **2016**, *120*, 11619.
- 37) Cooney, R. R.; Urquhart, S. G. *J. Phys. Chem. B* **2004**, *108*, 18185.
- 38) A preliminary theoretical study was also carried out to predict the structure of the magnesium-based carbon nucleophiles prepared by ball-milling (for details, see Figure S11).

- 39) The Bolm group reported mechanochemical Grignard reactions with gaseous CO₂, which afford the corresponding carboxylic acids in moderate to good yield, in pre-print form. Pfennig, V. S.; Vilella, R. C.; Nikodemus, J.; Bolm, C. *ChemRxiv* **2021**, DOI: 10.33774/chemrxiv-2021-r0xdb.
- 40) The development of Minisci-type reactions using magnesium under ball-milling conditions, which is related to our present study, has been reported: Wu, C.; Ying, T.; Yang, X.; Su, W.; Dushkin, A. V.; Yu, J. *Org. Lett.* **2021**, *23*, 6423.

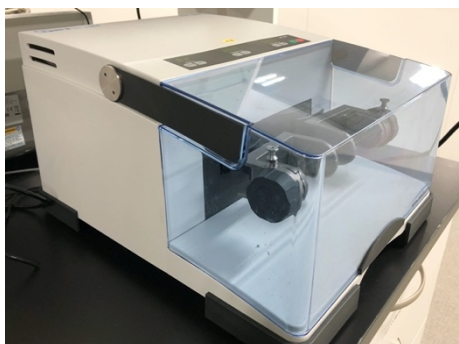
Experimental Section

Table of Contents

Instrumentation and Chemicals	104
General Procedures	106
Air Stability of the Grignard Reagent Prepared by Ball Mill	114
Substrates Preparations	115
Thermography Measurements for Reaction Temperature inside Ball Milling Jars	116
Gram-Scale Reaction Procedures	117
Optimization Studies	118
Reactions under the Solvent-less Conditions in a Test Tube	122
Scope of Organic Halides and Electrophiles	123
Radical Clock Experiments	125
Deuteration Experiments	126
X-ray Absorption Fine Structure (XAFS) Analysis of 12	127
Theoretical Study to Predict Structures of Magnesium-Based Carbon Nucleophiles	128
Product Characterizations	130
References	153

Instrumentation and Chemicals

Materials were obtained from commercial suppliers and purified using standard procedures, unless otherwise noted. Solvents were purchased from commercial suppliers and further dried over molecular sieve (MS 4Å). Magnesium turnings ($\geq 99.5\%$, product no. 137-06041) and Mg powder (99%, product no. 135-00062) were purchased from Wako Pure Chemical Industries, Co., Ltd. All reactions were performed using grinding vessels in the Retsch MM 400 (Supplementary Figure 1). Both jars and balls were made of stainless steel (Supplementary Figure 2). The jars were heated using a heat gun with a temperature control function (EARTH MAN HG-1450B, TAKAGI Co., Ltd.). NMR spectra were recorded on JEOL JNM-ECX400P and JNM-ECS400 spectrometers (^1H : 392, 396, 400, or 401 MHz, ^{13}C : 99, 100, or 101 MHz). Tetramethylsilane (^1H) and CDCl_3 (^{13}C) were employed as external standards, respectively. Multiplicity was recorded as follows: s = singlet, brs = broad singlet, d = doublet, t = triplet, q = quartet, quint = quintet, sex = sextet, sept = septet, and m = multiplet. Dibromomethane was used as an internal standard to determine the NMR yields. Thermographic images were obtained using the InfRec Thermo GEAR (NEC Avio Infrared Technologies Co., Ltd.). Recycling preparative gel permeation chromatography (GPC) was conducted with the JAI LC-9101 using CHCl_3 as the eluent with the JAIGEL-1H. High-resolution mass spectra were recorded at the Global Facility Center, Hokkaido University.



Supplementary Figure 1. Retsch MM400 used in this study.



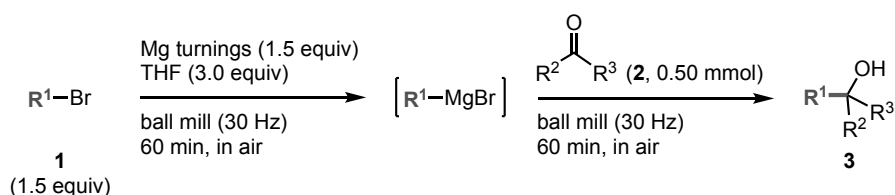
Supplementary Figure 2. Stainless jars and balls used in this study.



Supplementary Figure 3. Temperature-controllable heat gun used in this study.

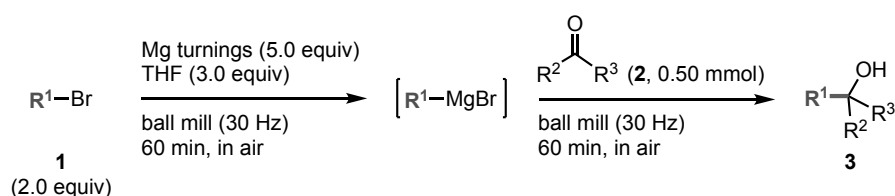
General Procedures

Conditions A: Reactions using liquid bromides



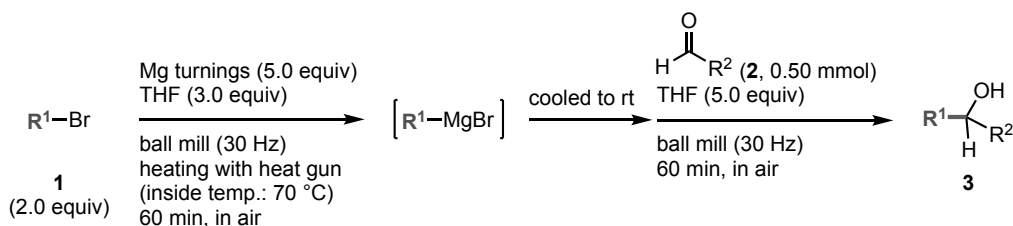
Mg turnings (0.75 mmol, 1.5 equiv) were placed in a milling jar (5 mL) with a ball (10 mm, diameter) in air. An organic bromide (**1**, 0.75 mmol, 1.5 equiv) and THF (123 μL , 1.5 mmol, 3.0 equiv) were added to the jar using a syringe. After the jar was closed without purging with inert gas, the jar was placed in the ball mill (Retsch MM 400, 1 h, 30 Hz). After grinding for 1 h, the jar was opened in air and charged with a distilled aldehyde (**2a–2c** and **2f**, 0.50 mmol, distilled before use) or a ketone (**2d** and **2e**, 0.50 mmol). The jar was then closed without purging with inert gas, and was placed in the ball mill (Retsch MM 400, 1 h, 30 Hz). After grinding for 1 h, the reaction mixture was quenched with a saturated aqueous solution of NH_4Cl and extracted with CH_2Cl_2 (30 mL \times 3). The solution was washed with brine and dried over Na_2SO_4 . After the removal of the solvents under reduced pressure, the crude material was purified by flash column chromatography (SiO_2 , hexane/ethyl acetate, 100:0 to 80:20) to give the corresponding product **3**.

Conditions B: Reactions using liquid bromides



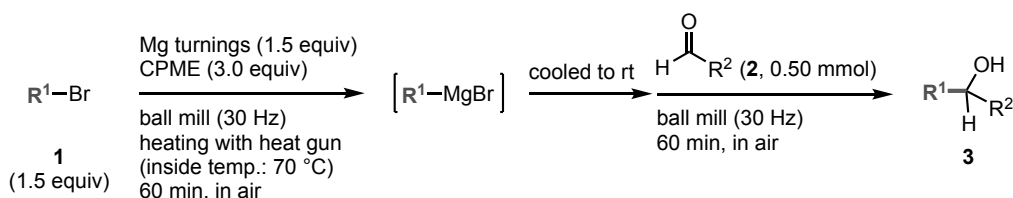
Mg turnings (2.5 mmol, 5.0 equiv) were placed in a milling jar (5 mL) with a ball (10 mm, diameter) in air. An organic bromide (**1**, 1.0 mmol, 2.0 equiv) and THF (123 μL , 1.5 mmol, 3.0 equiv) were added to the jar using a syringe. After the jar was closed without purging with inert gas, the jar was placed in a ball mill (Retsch MM 400, 1 h, 30 Hz). After grinding for 1 h, the jar was opened in air and charged with a distilled aldehyde (**2a–2c** and **2f**, 0.50 mmol, distilled before use) or a ketone (**2d** and **2e**, 0.50 mmol). The jar was then closed without purging with inert gas, and was placed in the ball mill (Retsch MM 400, 1 h, 30 Hz). After grinding for 1 h, the reaction mixture was quenched with a saturated aqueous solution of NH_4Cl and extracted with CH_2Cl_2 (30 mL \times 3). The solution was washed with brine and dried over Na_2SO_4 . After the removal of the solvents under reduced pressure, the crude material was purified by flash column chromatography (SiO_2 , hexane/ethyl acetate, 100:0 to 80:20) to give the corresponding product **3**. In some cases, the product **3** was further purified by recycling GPC.

Conditions C: Reactions using solid aryl bromides



Mg turnings (2.5 mmol, 5.0 equiv) and an aryl bromide (**1**, 1.0 mmol, 2.0 equiv) were placed in a milling jar (5 mL) with a ball (10 mm, diameter) in air. THF (123 μL , 1.5 mmol, 3.0 equiv) was added to the jar using a syringe. After the jar was closed without purging with inert gas, the jar was placed in the ball mill (Retsch MM 400, 1 h, 30 Hz). A heat gun was set approximately 1 cm above the jar and was turned on (preset temperature: 110 $^\circ\text{C}$, internal temperature: *ca.* 70 $^\circ\text{C}$). After grinding for 1 h, the jar was cooled to room temperature, opened in air, and charged with a distilled aldehyde (**2**, 0.50 mmol) and THF (204 μL , 2.5 mmol, 5.0 equiv). The jar was then closed without purging with inert gas, and was placed in a ball mill (Retsch MM 400, 1 h, 30 Hz). After grinding for 1 h, the reaction mixture was quenched with a saturated aqueous solution of NH_4Cl and extracted with CH_2Cl_2 (30 mL \times 3). The solution was washed with brine and dried over Na_2SO_4 . After the removal of the solvents under reduced pressure, the crude material was purified by flash column chromatography (SiO_2 , hexane/ethyl acetate, 100:0 to 80:20) to give the corresponding product **3**. In some cases, the product **3** was further purified by recycling GPC.

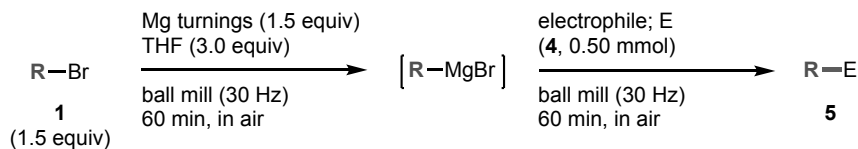
Conditions D: Reactions using solid aryl bromides



Mg turnings (0.75 mmol, 1.5 equiv) and an aryl bromide (**1**, 0.75 mmol, 1.5 equiv) were placed in a milling jar (5 mL) with a ball (10 mm, diameter) in air. CPME (175 μL , 1.5 mmol, 3.0 equiv) was added to the jar using a syringe. After the jar was closed without purging with inert gas, the jar was placed in the ball mill (Retsch MM 400, 1 h, 30 Hz). A heat gun was set in a downward direction approximately 1 cm above the jar and was turned on (preset temperature: 110 $^\circ\text{C}$, internal temperature: *ca.* 70 $^\circ\text{C}$). After grinding for 1 h, the jar was cooled to room temperature, opened in air, and charged with a distilled aldehyde (**2**, 0.50 mmol). The jar was then closed without purging with inert gas, and was placed in the ball mill (Retsch MM 400, 1 h, 30 Hz). After grinding for 1 h, the reaction mixture was quenched with a saturated aqueous solution of NH_4Cl and extracted with CH_2Cl_2 (30 mL \times 3). The solution was washed with brine and dried over Na_2SO_4 . After the removal of the solvents under reduced pressure, the crude material was purified by flash column chromatography (SiO_2 ,

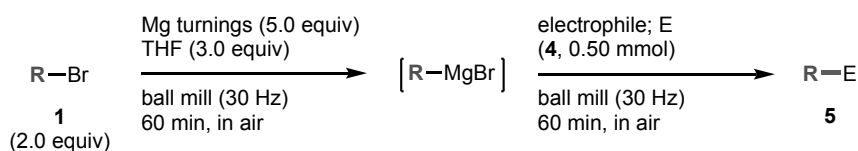
hexane/ethyl acetate, 100:0 to 80:20) to give the corresponding product **3**.

Conditions E: Nucleophilic addition to various electrophiles



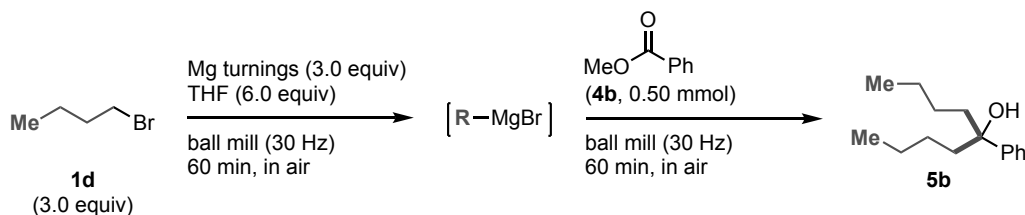
Mg turnings (0.75 mmol, 1.5 equiv) were placed in a milling jar (5 mL) with a ball (10 mm, diameter) in air. An organic bromide (**1**, 0.75 mmol, 1.5 equiv) and THF (123 μ L, 1.5 mmol, 3.0 equiv) were added to the jar using a syringe. After the jar was closed without purging with inert gas, the jar was placed in the ball mill (Retsch MM 400, 1 h, 30 Hz). After grinding for 1 h, the jar was opened in air, and charged with an electrophile (**4**, 0.50 mmol). The jar was then closed without purging with inert gas, and was placed in the ball mill (Retsch MM 400, 1 h, 30 Hz). After grinding for 1 h, the reaction mixture was quenched with a saturated aqueous solution of NH_4Cl and extracted with CH_2Cl_2 (30 mL \times 3). The solution was washed with brine and dried over Na_2SO_4 . After the removal of the solvents under reduced pressure, the crude material was purified by flash column chromatography (SiO_2 , hexane/ethyl acetate, 100:0 to 80:20) to give the corresponding product **5**. In some cases, the product **5** was further purified by recycling GPC.

Conditions F: Nucleophilic addition to various electrophiles



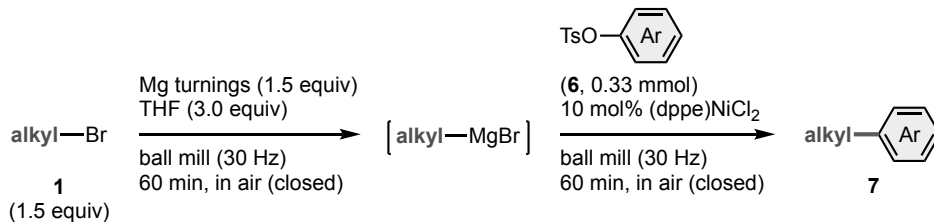
Mg turnings (2.5 mmol, 5.0 equiv) were placed in a milling jar (5 mL) with a ball (10 mm, diameter) in air. An organic bromide (**1**, 1.0 mmol, 2.0 equiv) and THF (123 μ L, 1.5 mmol, 3.0 equiv) were added to the jar using a syringe. After the jar was closed without purging with inert gas, the jar was placed in the ball mill (Retsch MM 400, 1 h, 30 Hz). After grinding for 1 h, the jar was opened in air and charged with an electrophile (**4**, 0.50 mmol). The jar was then closed without purging with inert gas and was placed in the ball mill (Retsch MM 400, 1 h, 30 Hz). After grinding for 1 h, the reaction mixture was quenched with a saturated aqueous solution of NH_4Cl and extracted with CH_2Cl_2 (30 mL \times 3). The solution was washed with brine and dried over Na_2SO_4 . After the removal of the solvents under reduced pressure, the crude material was purified by flash column chromatography (SiO_2 , hexane/ethyl acetate, 100:0 to 80:20) to give the corresponding product **5**. In some cases, the product **5** was further purified by recycling GPC.

Conditions G: Nucleophilic addition to ester



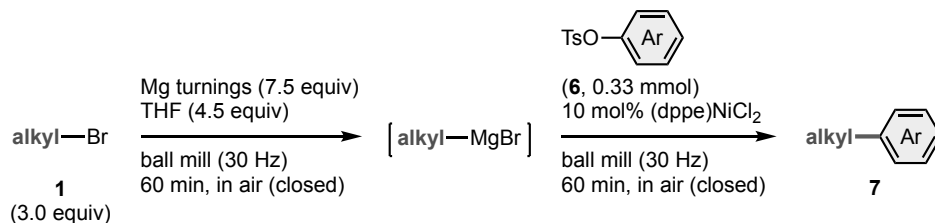
Mg turnings (1.0 mmol, 3.0 equiv) were placed in a milling jar (5 mL) with a ball (10 mm, diameter) in air. Then 1-bromobutane (**1d**, 1.0 mmol, 3.0 equiv) and THF (164 μ L, 2.0 mmol, 6.0 equiv) were added to the jar using a syringe. After the jar was closed without purging with inert gas, the jar was placed in the ball mill (Retsch MM 400, 1 h, 30 Hz). After grinding for 1 h, the jar was opened in air and charged with methyl benzoate (**4b**, 0.33 mmol). The jar was then closed without purging with inert gas and was placed in the ball mill (Retsch MM 400, 1 h, 30 Hz). After grinding for 1 h, the reaction mixture was quenched with a saturated aqueous solution of NH_4Cl and extracted with CH_2Cl_2 (30 mL \times 3). The solution was washed with brine and dried over Na_2SO_4 . After the removal of the solvents under reduced pressure, the crude material was purified by flash column chromatography (SiO_2 , hexane/ethyl acetate, 100:0 to 80:20) to give the corresponding product **5b**.

Conditions H: Kumada-Tamao-Corriu coupling reactions



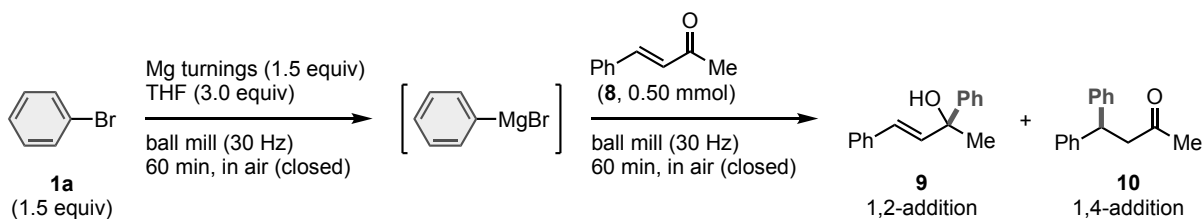
Mg turnings (0.50 mmol, 1.5 equiv) were placed in a milling jar (5 mL) with a ball (10 mm, diameter) in air. An alkyl bromide (**1**, 0.50 mmol, 1.5 equiv) and THF (82 μ L, 1.0 mmol, 3.0 equiv) were added to the jar using a syringe. After the jar was closed without purging with inert gas, the jar was placed in the ball mill (Retsch MM 400, 1 h, 30 Hz). After grinding for 1 h, the jar was opened in air and was charged with $(dppe)NiCl_2$ (0.033 mmol, 0.10 equiv) and an aryl tosylate (**6**, 0.33 mmol). The jar was then closed without purging with inert gas and was placed in the ball mill (Retsch MM 400, 1 h, 30 Hz). After grinding for 1 h, the reaction mixture was quenched with 1.0 M HCl and extracted with CH_2Cl_2 (30 mL \times 3). The solution was dried over Na_2SO_4 and the solvents were removed under reduced pressure. The crude material was purified by flash column chromatography (SiO_2 , hexane/ CH_2Cl_2 , 97:3) to give the corresponding product **7**. In some cases, the product **7** was further purified by recycling GPC.

Conditions I: Kumada-Tamao-Corriu coupling reactions



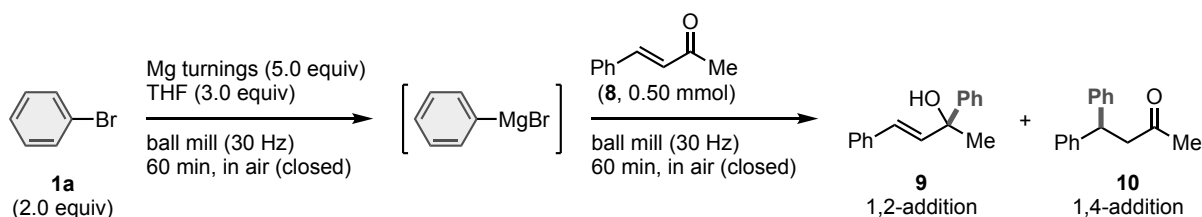
Mg turnings (2.5 mmol, 7.5 equiv) were placed in a milling jar (5 mL) with a ball (10 mm, diameter) in air. An alkyl bromide (**1**, 1.0 mmol, 3.0 equiv) and THF (123 μ L, 1.5 mmol, 4.5 equiv) were added to the jar using a syringe. After the jar was closed without purging with inert gas, the jar was placed in the ball mill (Retsch MM 400, 1 h, 30 Hz). After grinding for 1 h, the jar was opened in air and was charged with (dppe)NiCl₂ (0.033 mmol, 0.10 equiv) and an aryl tosylate (**6**, 0.33 mmol). The jar was then closed without purging with inert gas and was placed in the ball mill (Retsch MM 400, 1 h, 30 Hz). After grinding for 1 h, the reaction mixture was quenched with 1.0 M HCl and extracted with CH₂Cl₂ (30 mL \times 3). The solution was dried over Na₂SO₄ and the solvents were removed under reduced pressure. The crude material was purified by flash column chromatography (SiO₂, hexane/CH₂Cl₂, 97:3) to give the corresponding product **7**. In some cases, the product **7** was further purified by recycling GPC.

Conditions J: Nucleophilic addition to enone



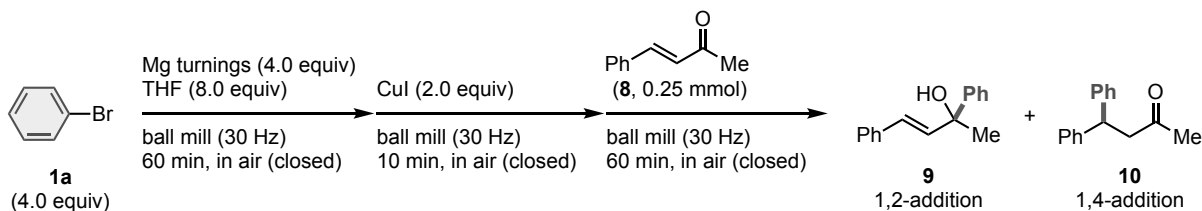
Mg turnings (0.75 mmol, 1.5 equiv) were placed in a milling jar (5 mL) with a ball (10 mm, diameter) in air. Bromobenzene (**1a**, 0.75 mmol, 1.5 equiv) and THF (123 μ L, 1.5 mmol, 3.0 equiv) were added to the jar using a syringe. After the jar was closed without purging with inert gas, the jar was placed in the ball mill (Retsch MM 400, 1 h, 30 Hz). After grinding for 1 h, the jar was opened in air and was charged with (*E*)-4-phenylbut-3-en-2-one (**8**, 0.50 mmol). The jar was then closed without purging with inert gas and was placed in the ball mill (Retsch MM 400, 1 h, 30 Hz). After grinding for 1 h, the reaction mixture was quenched with a saturated aqueous solution of NH₄Cl and extracted with CH₂Cl₂ (30 mL \times 3). The solution was washed with brine and dried over Na₂SO₄. After the removal of the solvents under reduced pressure, ¹H NMR analysis of the resulting crude mixture was conducted to determine the yields of the 1,2-addition product **9** and the 1,4-addition product **10**.

Conditions K: Nucleophilic addition to enone



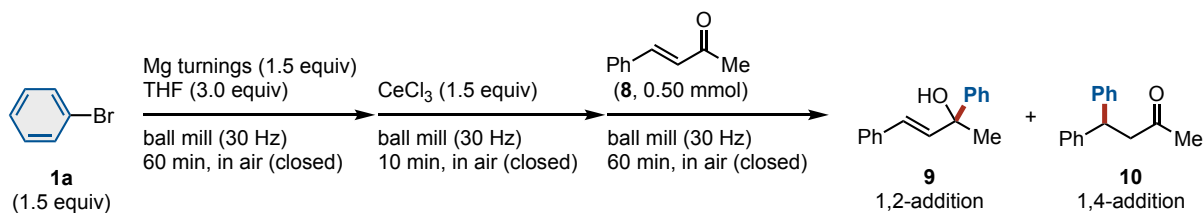
Mg turnings (2.5 mmol, 5.0 equiv) were placed in a milling jar (5 mL) with a ball (10 mm, diameter) in air. Bromobenzene (**1a**, 1.0 mmol, 2.0 equiv) and THF (123 μ L, 1.5 mmol, 3.0 equiv) were added to the jar using a syringe. After the jar was closed without purging with inert gas, the jar was placed in the ball mill (Retsch MM 400, 1 h, 30 Hz). After grinding for 1 h, the jar was opened in air and was charged with (*E*)-4-phenylbut-3-en-2-one (**8**, 0.50 mmol). The jar was then closed without purging with inert gas and was placed in the ball mill (Retsch MM 400, 1 h, 30 Hz). After grinding for 1 h, the reaction mixture was quenched with a saturated aqueous solution of NH_4Cl and extracted with CH_2Cl_2 (30 mL \times 3). The solution was washed with brine and dried over Na_2SO_4 . After the removal of the solvents under reduced pressure, ^1H NMR analysis of the resulting crude mixture was conducted to determine the yields of the 1,2-addition product **9** and the 1,4-addition product **10**.

Conditions L: Nucleophilic addition to enone in the presence of copper iodide



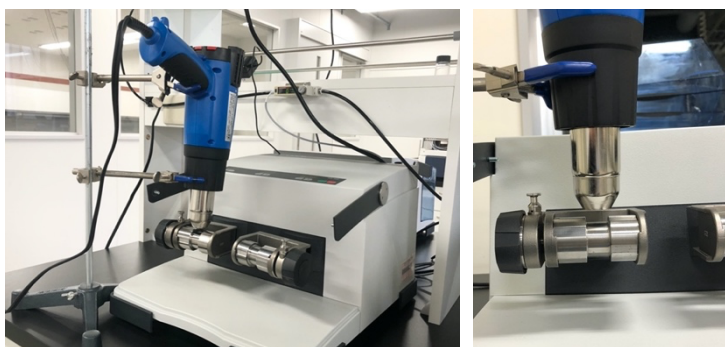
Mg turnings (1.0 mmol, 4.0 equiv) were placed in a milling jar (5 mL) with a ball (10 mm, diameter) in air. Bromobenzene (**1a**, 1.0 mmol, 4.0 equiv) and THF (164 μ L, 2.0 mmol, 8.0 equiv) were added to the jar using a syringe. After the jar was closed without purging with inert gas, the jar was placed in the ball mill (Retsch MM 400, 1 h, 30 Hz). After grinding for 1 h, the jar was opened in air and was charged with copper iodide (0.50 mmol, 2.0 equiv). The jar was then closed without purging with inert gas and was placed in the ball mill (Retsch MM 400, 10 min, 30 Hz). After grinding for 10 min, the jar was opened in air and was charged with (*E*)-4-phenylbut-3-en-2-one (**8**, 0.25 mmol). The jar was then closed without purging with inert gas and was placed in the ball mill (Retsch MM 400, 1 h, 30 Hz). After grinding for 1 h, the reaction mixture was quenched with a saturated aqueous solution of NH_4Cl and extracted with CH_2Cl_2 (30 mL \times 3). The solution was washed with brine and dried over Na_2SO_4 . After the removal of the solvents under reduced pressure, ^1H NMR analysis of the resulting crude mixture was conducted to determine the yields of the 1,2-addition product **9** and the 1,4-addition product **10**.

Conditions M: Nucleophilic addition to enone in the presence of cerium chloride

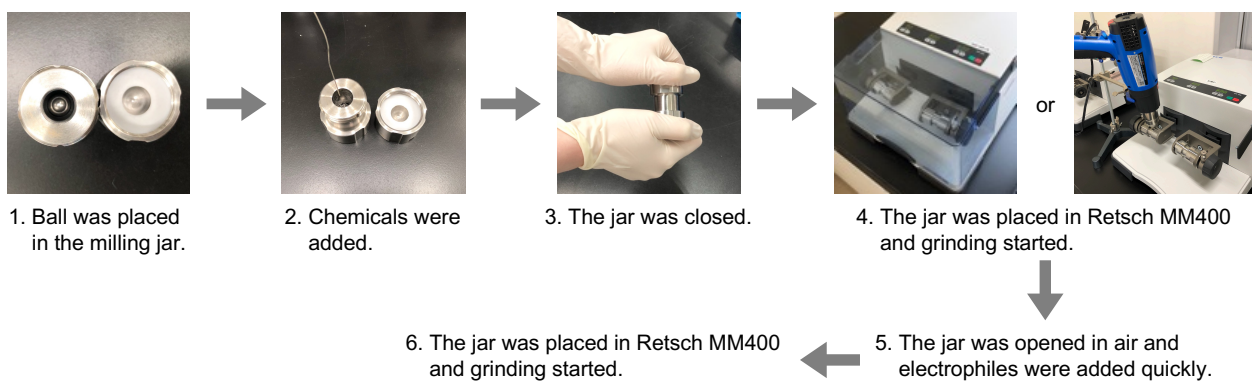


Mg turnings (0.75 mmol, 1.5 equiv) were placed in a milling jar (5 mL) with a ball (10 mm, diameter) in air. Bromobenzene (**1a**, 0.75 mmol, 1.5 equiv) and THF (123 μL , 1.5 mmol, 3.0 equiv) were added to the jar using a syringe. After the jar was closed without purging with inert gas, the jar was placed in the ball mill (Retsch MM 400, 1 h, 30 Hz). After grinding for 1 h, the jar was opened in air and was charged with cerium chloride (0.75 mmol, 1.5 equiv). The jar was then closed without purging with inert gas and was placed in the ball mill (Retsch MM 400, 10 min, 30 Hz). After grinding for 10 min, the jar was opened in air and was charged with (*E*)-4-phenylbut-3-en-2-one (**8**, 0.50 mmol). The jar was then closed without purging with inert gas and was placed in the ball mill (Retsch MM 400, 1 h, 30 Hz). After grinding for 1 h, the reaction mixture was quenched with a saturated aqueous solution of NH_4Cl and extracted with CH_2Cl_2 (30 mL \times 3). The solution was washed with brine and dried over Na_2SO_4 . After the removal of the solvents under reduced pressure, ^1H NMR analysis of the resulting crude mixture was conducted to determine the yields of the 1,2-addition product **9** and the 1,4-addition product **10**.

The representative procedure is shown in below pictures (Supplementary Figures 4 and 5).



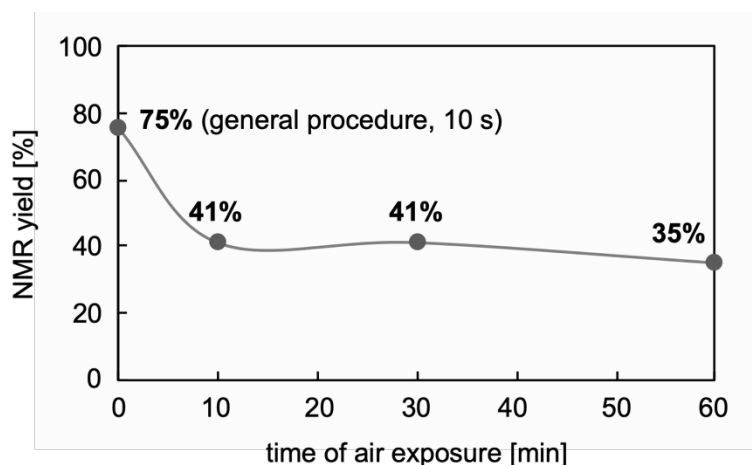
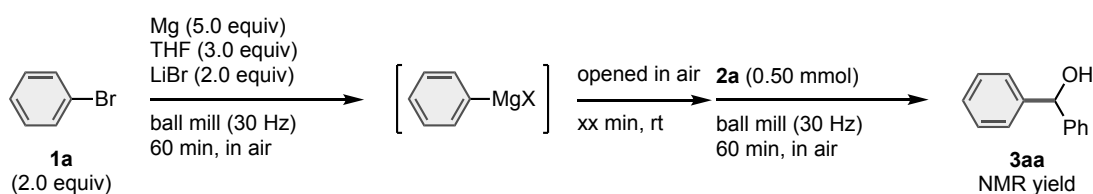
Supplementary Figure 4. Setting of the heat gun for conditions C and D. The heat gun was fixed with clamps and placed directly above the ball milling jar (distance between the heat gun and ball milling jar: *ca.* 1 cm).



Supplementary Figure 5. Procedure of setting up the mechanochemical reactions.

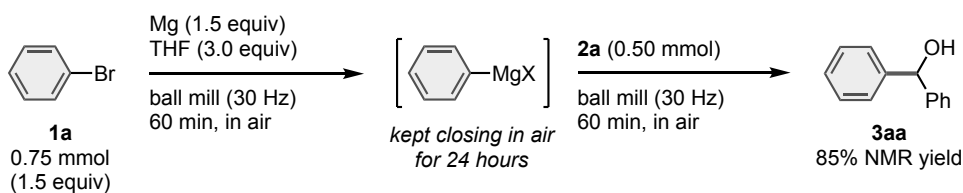
Air Stability of the Grignard Reagent Prepared by Ball Mill

Electrophiles should be added as soon as possible after opening the jar. I conducted nucleophilic addition reactions after exposing the mechanochemically synthesized organomagnesium species to the air for 10–60 min, as shown below. The results showed that the yield of **3aa** decreased when the synthesized organomagnesium species were exposed to the air for 10 min or more. While benzene was detected after the exposure of the synthesized organomagnesium species to the air, byproducts derived from oxygen or carbon dioxide, such as phenol and benzoic acid, were not detected under the mechanochemical conditions. This result suggests that the decreased yield of the organomagnesium nucleophile is mainly caused by protonation by moisture during the exposure to air.

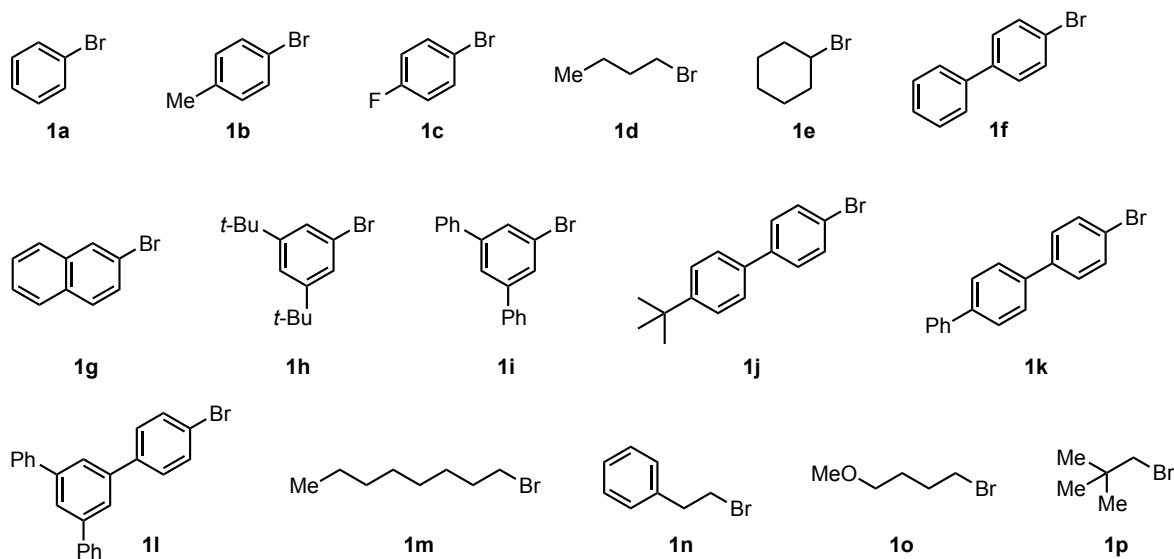


Supplementary Figure 6. Decreased yield of the nucleophilic addition product **3aa** after exposure of the mechanochemically synthesized organomagnesium species to the air.

I also examined the nucleophilic addition reactions when the mechanochemically synthesized organomagnesium species in the ball milling jar was kept closed in air at room temperature for 24 hours. This result showed that the organomagnesium reagents could be retained for several hours after their preparation if the jar was kept closed.

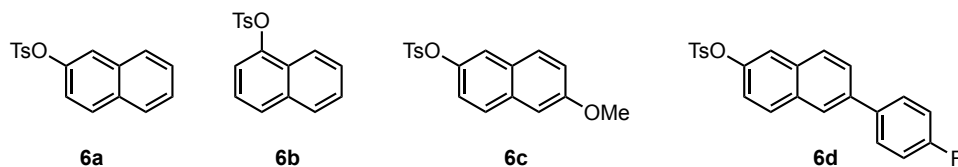


Substrate Preparations



Supplementary Figure 7. List of organic bromides used in this study. All organic bromides were obtained from commercial suppliers and were used as received.

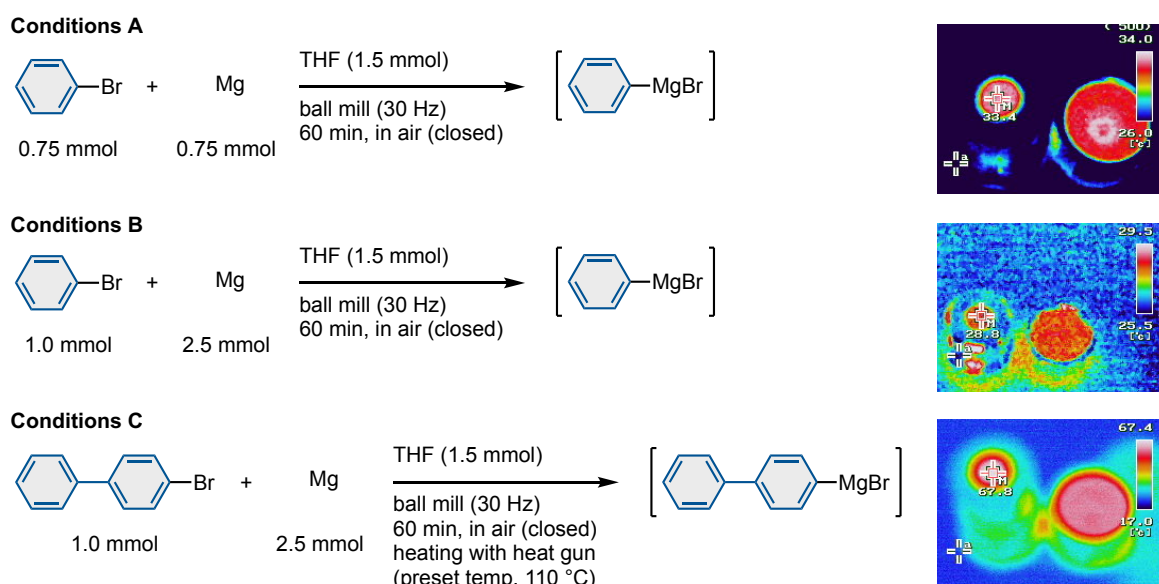
All aryl tosylates (**6a–6d**) were synthesized from the corresponding naphthols according to the reported procedure.^[1] To a solution of naphthol (2.0 mmol) in THF (0.6 mL) was added 10wt% K_2CO_3 (3.8 mmol) or 15wt% NaOH (6.6 mmol) as an aqueous solution. After the resulting solution was cooled to 0 °C, a solution of TsCl (458 mg, 2.4 mmol for 10% K_2CO_3 or 385 mg, 2.02 mmol for 15% NaOH) in THF (1.4 mL) was slowly added over 15 min at 0 °C. After the addition of TsCl, the reaction mixture was stirred for 2 h at room temperature. EtOAc (8 mL) was added to the reaction mixture and the two-phase mixture was separated. The organic layer was washed with H_2O (3 mL) and dried over Na_2SO_4 . The removal of the solvents under reduced pressure gave the corresponding pure aryl tosylate **6**. Trace amounts of TsCl were removed by washing the product with hexanes.



Supplementary Figure 8. List of aryl tosylates used in this study.

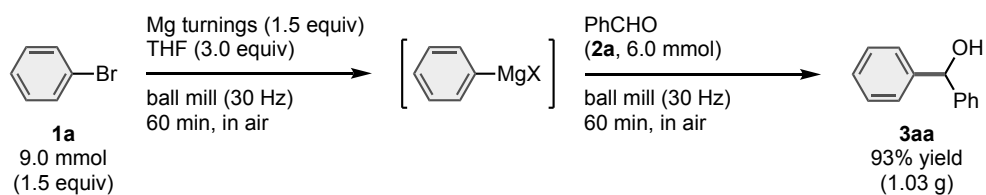
Thermography Measurements for Reaction Temperature inside Ball Milling Jars

The temperature inside the milling jar of the mechanochemical reaction was immediately confirmed by thermography after opening the jar. The crude mixtures were prepared under the following conditions: (A) 0.75 mmol of **1a**; 0.75 mmol of Mg turnings; 1.5 mmol of THF in a stainless-steel ball milling jar (5 mL) with a stainless-steel ball (10 mm); 30Hz; 1 h; (B) 1.0 mmol of **1a**; 2.5 mmol of Mg turnings; 1.5 mmol of THF in a stainless-steel ball milling jar (5 mL) with a stainless-steel ball (10 mm); 30Hz; 1 h; (C) 1.0 mmol of **1f**; 2.5 mmol of Mg turnings; 1.5 mmol of THF in a stainless-steel ball milling jar (5 mL) with a stainless-steel ball (10 mm); 30Hz; 1 h; preset temperature of heat gun: 110 °C. The obtained images (Fig. S9) showed that the temperatures were 33 °C, 29 °C, and 68 °C for the conditions A, B, and C, respectively.



Supplementary Figure 9. Thermography measurements for temperature inside the milling jar after the reaction of organic halides and Mg.

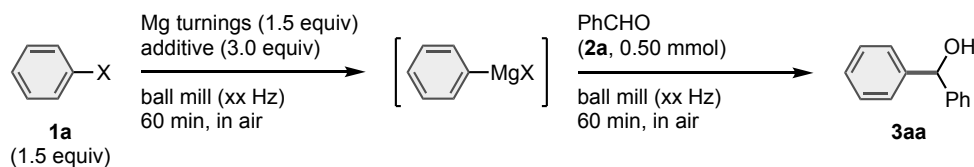
Gram-Scale Reaction Procedures



Mg turnings (216.1 mg, 9.0 mmol) were placed in a milling jar (10 mL) with two balls (15 mm, diameter) in air. Bromobenzene (**1a**, 1.424 g, 9.0 mmol) and THF (1.44 mL, 18 mmol) were added to the jar using a syringe. The jar was then closed without purging with inert gas, the jar was placed in the ball mill (Retsch MM 400, 60 min, 30 Hz). After grinding for 1 h, the jar was opened in air and was charged with a distilled benzaldehyde (**2a**, 636.7 mg, 6.0 mmol). The jar was then closed without purging with inert gas and was placed in the ball mill (Retsch MM 400, 60 min, 30 Hz). After grinding for 1 h, the reaction mixture was quenched with a saturated aqueous solution of NH_4Cl and extracted with CH_2Cl_2 . The solution was dried over Na_2SO_4 and the solvents were removed under reduced pressure. The crude material was purified by flash column chromatography (SiO_2 , hexane/ethyl acetate) to give the corresponding product **3aa** as a white powder (1.03 g, 5.6 mmol, 93% yield).

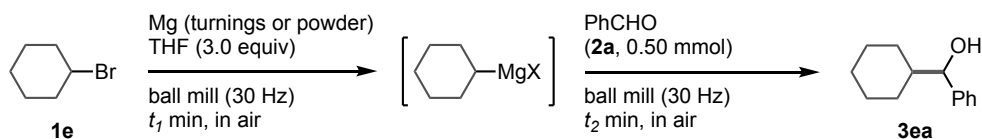
Optimization Studies

Supplementary Table 1. Optimization of the reaction conditions using aryl halides^a



entry	halide	additive (volume)	milling frequency (Hz)	ball size (Φ mm)	yield (%)
1	1a (X = Br)	-	30	10	6
2	1a	THF (123 μ L)	30	10	94
3	1a	Et ₂ O (155 μ L)	30	10	79
4	1a	CPME (175 μ L)	30	10	87
5	1a	MTBE (176 μ L)	30	10	57
6	1a	1,4-dioxane (128 μ L)	30	10	5
7	1a	hexane (200 μ L)	30	10	<1
8	1a	toluene (160 μ L)	30	10	1
9	1a	THF (61 μ L)	30	10	47
10	1a	THF (183 μ L)	30	10	90
11 ^b	1a	THF (123 μ L)	30	10	92
12	1a	THF (123 μ L)	25	10	90
13	1a	THF (123 μ L)	30	5	91
14 ^c	1a	THF (123 μ L)	30	5	52
15	1a' (X = I)	THF (123 μ L)	30	10	14
16 ^d	1a'	THF (123 μ L)	30	10	74
17	1a'' (X = Cl)	THF (123 μ L)	30	10	84

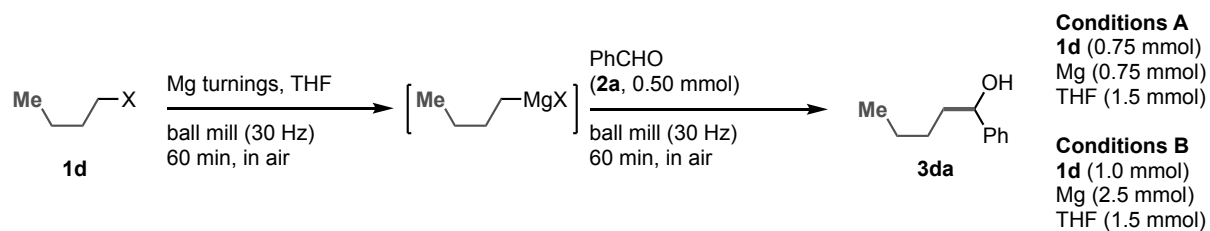
^aReactions performed using Retsch MM400, stainless-steel milling jar (5 mL) and a stainless-steel ball. Conditions: **1a** (0.75 mmol), Mg (0.75 mmol), **2a** (0.50 mmol). Yields were determined by ¹H NMR analysis with dibromomethane as an internal standard. ^bUndistilled THF (purchased from FUJIFILM Wako Chemicals; product no. 206-05106; BHT is included as a stabilizer) was used. ^cReactions performed using Retsch MM400, stainless-steel milling jar (1.5 mL) and a stainless-steel ball (diameter: 5 mm). ^dConditions: **1a'** (1.0 mmol), Mg (2.5 mmol), **2a** (0.50 mmol).

Supplementary Table 2. Optimization of reaction using secondly alkyl bromide^a

entry	1e (equiv)	Mg (equiv)	reaction time (min)		yield (%)
			first step	second step	
1	1.5	1.5 (turnings)	60	60	24
2	1.5	1.5 (powder)	60	60	30
3	1.5	1.5 (turnings)	60	60	26
4	1.8	2.5 (turnings)	60	60	23
5	1.8	2.5 (turnings)	90	60	53
6	1.8	2.5 (turnings)	120	60	43
7	2.0	2.5 (turnings)	90	60	74
8	2.0	2.5 (powder)	60	60	62
9	2.0	2.5 (powder)	90	60	56

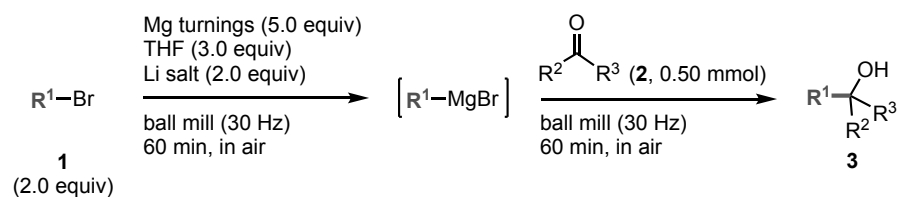
^aReactions performed using Retsch MM400, stainless-steel milling jar (5 mL) and a stainless-steel ball (10 mm, diameter). Yields were determined by ¹H NMR analysis with dibromomethane as an internal standard.

Supplementary Table 3. Effect of halides^a



entry	halide	conditions	yield (%)
1	1d (X = Br)	A	90
2	1d	B	92
3	1d' (X = I)	A	45
4	1d'	B	68
5	1d'' (X = Cl)	A	82
6	1d''	B	84

^aReactions performed using Retsch MM400, stainless-steel milling jar (5 mL) and a stainless-steel ball (10 mm, diameter). Conditions A: **1d** (0.75 mmol), Mg (0.75 mmol), THF (1.5 mmol), **2d** (0.50 mmol). Conditions B: **1d** (1.0 mmol), Mg (2.5 mmol), THF (1.5 mmol), **2d** (0.50 mmol). Yields were determined by ¹H NMR analysis with dibromomethane as an internal standard.

Supplementary Table 4. Effect of the addition of lithium salts^a

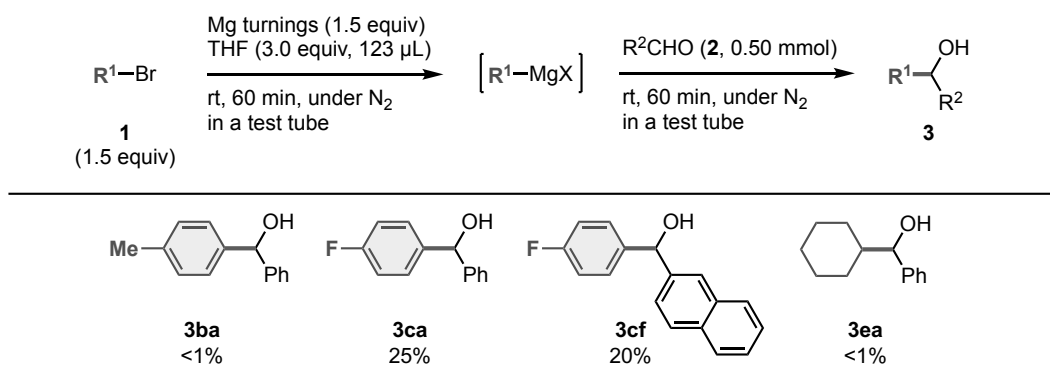
entry	halide	electrophile	Li salt	yield (%)
1	1a	2e	-	68
2	1a	2e	LiBr	82
3	1b	2a	-	70
4	1b	2a	LiBr	65
5	1c	2a	LiBr	40
6	1c	2a	LiCl	81
7	1d	2a	-	92
8	1d	2a	LiBr	28

^aReactions performed using Retsch MM400, stainless-steel milling jar (5 mL) and a stainless-steel ball (10 mm, diameter). Lithium salts were dried under reduced pressure at 150 °C for 3 hours before use. Yields were determined by ¹H NMR analysis with dibromomethane as an internal standard.

Reactions Under the Solvent-less Conditions in a Test Tube

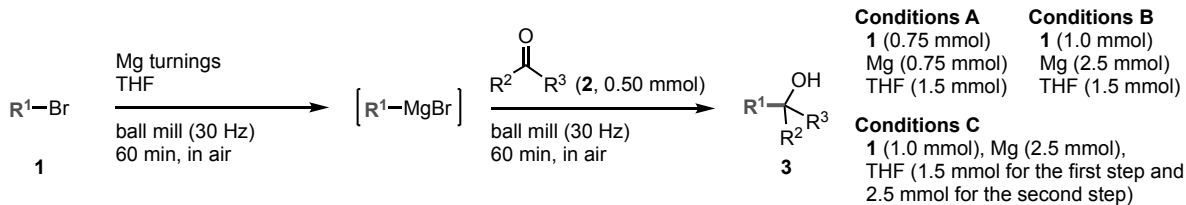
Mg turnings (18.2 mg, 0.75 mmol) were placed in an oven-dried reaction vial. After being sealed with a screw cap containing a Teflon-coated rubber septum, the vial was connected to a nitrogen line through a needle. An organic bromide (**1**, 0.75 mmol) and THF (123 μ L, 1.5 mmol) were added to the vial and then the reaction mixture was stirred at room temperature. After 1 h, a distilled aldehyde (**2a** or **2f**, 0.50 mmol) was added and the reaction mixture was stirred for 1 h at room temperature. The reaction mixture was quenched with a saturated aqueous solution of NH_4Cl and extracted with CH_2Cl_2 (30 mL \times 3). The solution was washed with brine and dried over Na_2SO_4 . After the removal of the solvents under reduced pressure, the resulting crude mixture was analyzed by ^1H NMR with dibromomethane as an internal standard to determine the NMR yield of the product **3**.

Even though the reaction mixtures are liquid, I confirmed that the organomagnesium nucleophiles were not generated efficiently in a test tube using magnetic stirring under the optimized conditions shown in Figure S10. These results suggest that activation of magnesium metal by strong mechanical agitation in a ball mill seems to be essential for the efficient formation of the organomagnesium species.

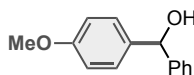


Supplementary Figure 10. Reactions under solvent-less conditions without strong mechanical agitation.

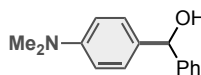
Scope of Organic Halides and Electrophiles



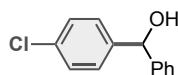
substituents in *para*-position



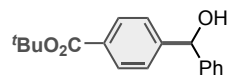
A: 56% (62%)



A: (74%)

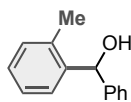


C: 58% (60%)

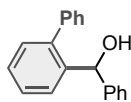


A: complex mixture

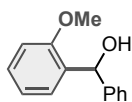
substituents in *ortho*-position



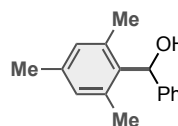
A: 85% (90%)



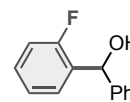
A: 82% (88%)



A: 80%

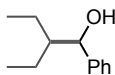


A: 72% (80%)



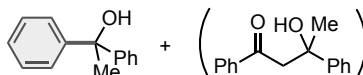
A: complex mixture

secondary alkyl halides



B: (14%)

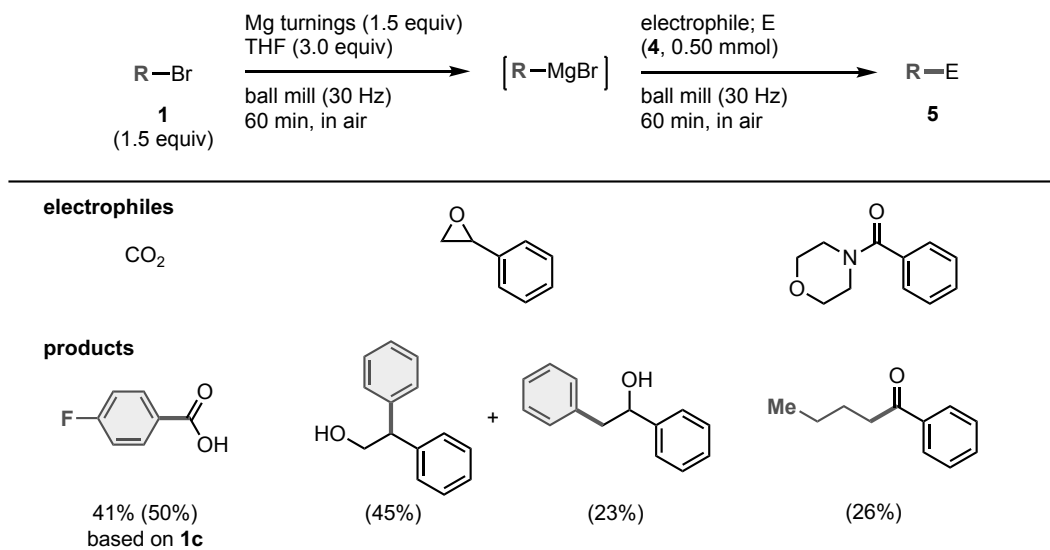
addition to ketones



B: (57%)

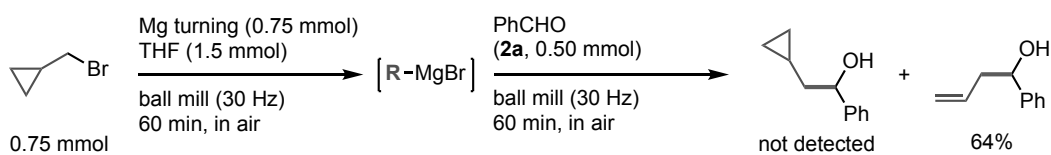
(4%)

Supplementary Figure 11. Scope of the mechanochemical synthesis of organomagnesium nucleophiles from various organic bromides and their nucleophilic addition to aldehydes and ketones. Isolated yields are reported as percentages. Proton NMR integrated yields are shown in parentheses.



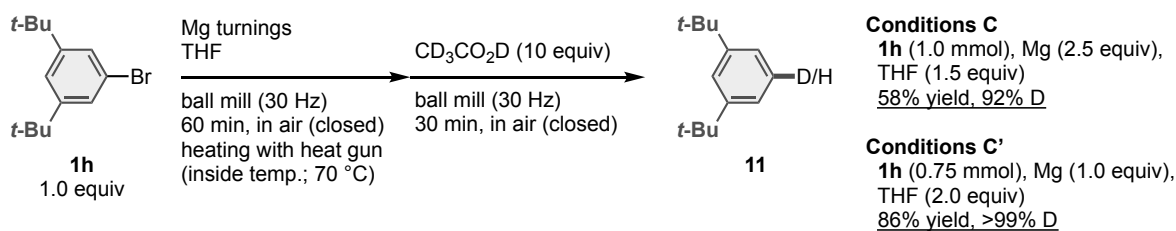
Supplementary Figure 12. Nucleophilic addition to various electrophiles under the optimized conditions E. Isolated yields are reported as percentages. Proton NMR integrated yields are shown in parentheses.

Radical Clock Experiments



Mg turnings (18.3 mg, 0.75 mmol) and (bromomethyl)cyclopropane (100.5 mg, 0.75 mmol) were placed in a milling jar (5 mL) with a ball (diameter: 10 mm) in air. THF (123 μ L, 1.5 mmol) was added to the jar using a syringe. After the jar was closed without purging with inert gas, the jar was placed in the ball mill (Retsch MM 400, 60 min, 30 Hz). After grinding for 1 h, the jar was opened in air, and charged with benzaldehyde (53.2 mg, 0.50 mmol). The jar was then closed without purging with inert gas and placed in the ball mill (Retsch MM 400, 60 min, 30 Hz). After grinding for 60 min, the reaction mixture was quenched with a saturated aqueous solution of NH_4Cl and extracted with CH_2Cl_2 (3×30 mL). The solution was washed with brine and dried over Na_2SO_4 . After the removal of the solvents under reduced pressure, the resulting crude mixture was analyzed by ^1H NMR spectroscopy with 4-dimethylaminopyridine as an internal standard to determine the NMR yield.

Deuteration Experiments



Mg turnings and 1-bromo-3,5-di-*tert*-butylbenzene (**1h**) were placed in a milling jar (5 mL) with a ball (diameter: 10 mm) in air. THF was added to the jar using a syringe. After the jar was closed without purging with inert gas, the jar was placed in the ball mill (Retsch MM 400, 60 min, 30 Hz). A heat gun was set approximately 1 cm above the jar and was turned on (preset temperature: 110 °C, internal temperature: *ca.* 70 °C). After grinding for 1 h, the jar was cooled to room temperature for 20 minutes, opened in air, and charged with acetic acid-*d*₄ (10 equiv). The jar was then closed without purging with inert gas and was placed in the ball mill (Retsch MM 400, 30 min, 30 Hz). After grinding for 30 min, the reaction mixture was quenched with a saturated aqueous solution of NaHCO₃ and extracted with CH₂Cl₂ (30 mL×3). The solution was washed with brine and dried over Na₂SO₄. After the removal of the solvents under reduced pressure, the resulting crude mixture was analyzed by ¹H NMR with dibromomethane as an internal standard to determine the NMR yield of 1,3-di-*tert*-butylbenzene (**11**).

X-Ray Absorption Fine Structure (XAFS) Analysis of 12

Mg K-edge NEXAFS measurements were performed at the soft X-ray beamline BL2A of UVSOR-III synchrotron.^[2] The mechanochemically-prepared gummy organomagnesium sample of **12** was pasted on high purity indium foil and fixed onto a copper sample holder. For the sample preparation of solution-phase-prepared **12**, 1.0 M of THF solution of **12**^[3] without MgBr₂ precipitation dropped and dried on high purity indium foil. The sample holder was fixed on a linear and rotatable manipulator and then installed into a vacuum chamber, which was evacuated to a pressure of less than 1×10^{-6} Pa. The sample preparation and install processes were carefully performed under argon or nitrogen atmospheres. The Mg K-edge NEXAFS spectra (1250–1400 eV) were taken in total electron yields (TEYs) by measuring a sample drain current. The energy resolution of the incident soft X-rays at the Mg K-edge is set to 0.2 eV in the range from 1300 to 1330 eV and 1.0 eV in the range from 1250 to 1300 eV and from 1330 to 1400 eV.

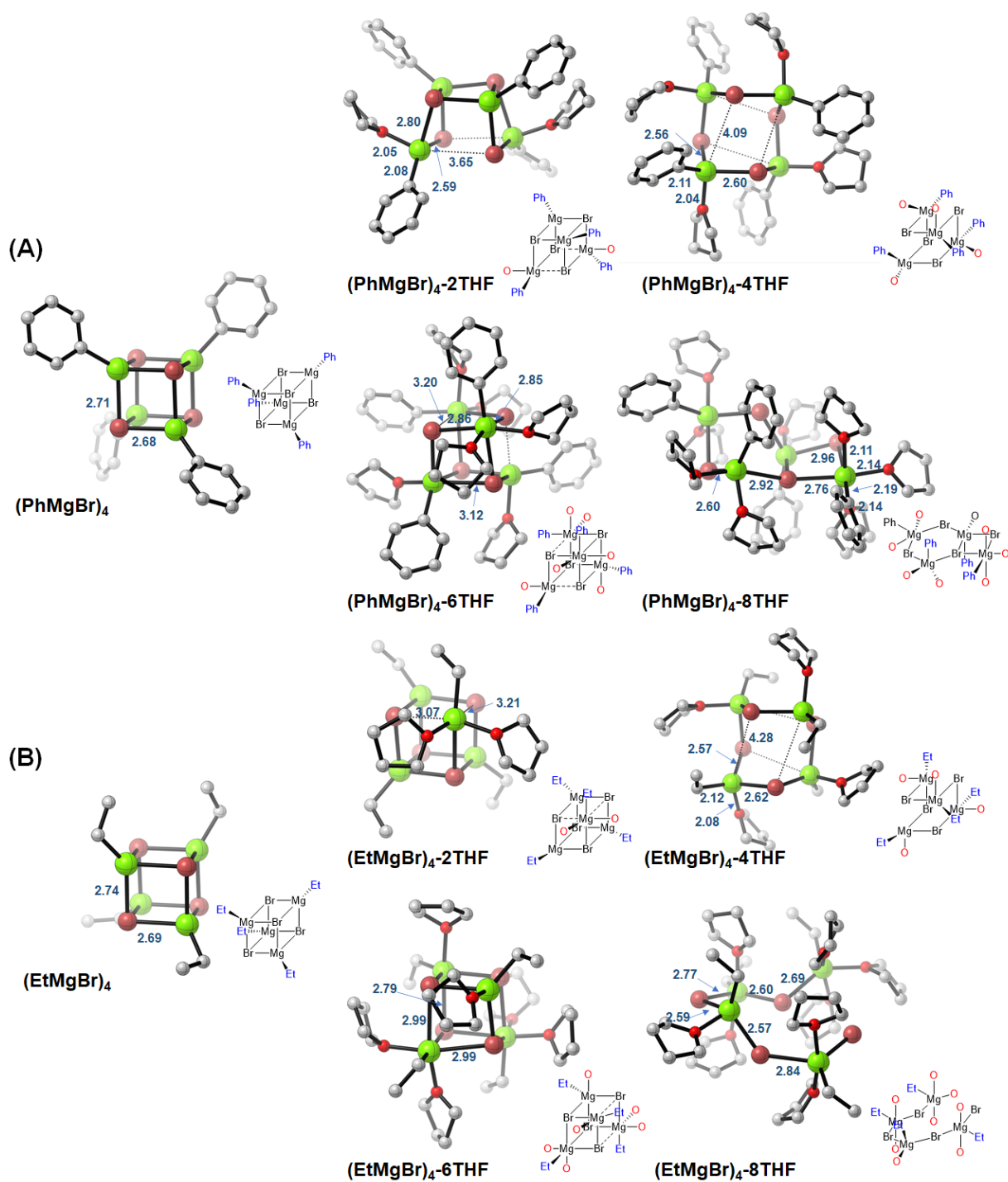
C K-edge NEXAFS measurements were performed at the soft X-ray beamline BL3U of the UVSOR-III synchrotron.^[4] All the organomagnesium samples were fixed onto a stainless sample holder and installed into a vacuum chamber 1×10^{-6} Pa in the same manner as for the Mg K-edge NEXAFS measurement. The C K-edge NEXAFS spectra (280–300 eV) were taken in total electron yields (TEYs) by measuring a sample drain current. The energy resolution of the incident soft X-rays at the C K-edge is set to 0.05 eV in the range from 283 to 293 eV and 0.2 eV in the range from 280 to 283 eV and from 293 to 300 eV.

The data processing for the subtraction of background of indium foil, baseline correction, and normalization of the resulting spectra were performed by using Athena program.^[5]

Theoretical Study to Predict Structures of Magnesium-Based Carbon Nucleophiles

Experimentally, 2.0 equivalents of THF for aryl halides was added to the reaction system as an additive. Though the ligation of solvent molecule to Mg atom is known for the Grignard reagent in solution,^[6-8] how does the existence of THF affect the structure of the Grignard reagent in solid-state remains unclear so far. To understand the impact of the THF addition, a theoretical study using model complexes (RMgBr)_{4-n}THF (of which R = Phenyl (Ph) and Ethyl (Et) groups and *n* = 0, 2, 4, 6 and 8) was performed. To locate the most stable structures of these complexes, minimum-only sampling calculations were conducted using the SC-AFIR method^[9, 10] at the GFN-xTB^[11, 12] level of theory under the ORCA environment,^[13, 14] where the model collision energy parameter Gamma of the AFIR method was set as 200 kJ/mol. As the results, 1623 and 1420 local minimum structures were obtained for (PhMgBr)₄ and (EtMgBr)₄, respectively. The most stable structures were then selected for the second round of sampling calculations by adding 2, 4, 6 and 8 THF molecules, respectively. For (PhMgBr)_{4-n}THF, 1511, 1426, 948 and 750 local minimum structures were eventually provided for *n* = 2, 4, 6, and 8 respectively. In the case of (EtMgBr)_{4-n}THF, 1786, 1501, 1065 and 837 local minimum structures were located. Stable structures acquired in the sampling calculations were subsequently fully re-optimized at B3LYP-D3/Def2SVP level of theory^[15-20] using the RIJCOSX approximation^[21, 22] (as implemented in the ORCA package). An auxiliary basis set, named def2/J,^[20] was employed in the RIJCOSX approximation. Frequency calculations were also carried out at the same level of theory to confirm that all the optimized structures were minima. Since the reaction was conducted in the solid state, no solvation model is adopted in this work. All the Gibbs energies quoted below were evaluated at 298.15 K and 1 atm.

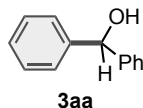
As shown in Figure S11, the most stable (PhMgBr)₄ and (EtMgBr)₄ isomers were found to have cubic structures. In both R = Ph and Et cases, the additional THF molecules coordinated to the Mg atoms, and such a coordination eventually induced the scission of Mg-Br bonds in the cubic structure. In other words, the coordination of THF molecules transformed the cubic structures into the more opened ones. Given that, it is supposed that one of the impacts of the THF addition is to transform the (RMgBr)_{*m*} species from an unreactive, closed form to the more reactive and open form. Further exploration of the stable structures of (RMgBr)_{*m-n*}THF (for *m* = 6 and more) are currently under progress in our laboratory, aiming at providing a better understanding of the structures of the Grignard reagents in solid-state through the comparisons between the theoretical study and the experimental NEXAFS spectra.



Supplementary Figure 13. Optimized structures of $(\text{PhMgBr})_4-n\text{THF}$ (A) and $(\text{EtMgBr})_4-n\text{THF}$ (B) at the B3LYP-D3/Def2SVP level, where $n = 0, 2, 4, 6$ and 8 (note that all H atoms are omitted for clarity). The addition of THF molecules transformed the cubic structures obtained at $n = 0$ to the more opened structures by the coordination to Mg atoms and the Mg-Br bond scission associated.

Product Characterizations

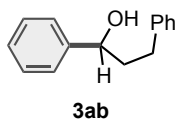
Diphenylmethanol (**3aa**).



Conditions A: The reaction was conducted with **1a** (79 μ L, 0.75 mmol) and **2a** (53.7 mg, 0.50 mmol). The product **3aa** was obtained in 84% yield (77.9 mg, 0.42 mmol) as a white powder.

Conditions B: The reaction was conducted with **1a** (105 μ L, 1.0 mmol), lithium bromide (86.9 mg, 1.0 mmol), and **2a** (53.2 mg, 0.50 mmol). The product **3aa** was obtained in 64% yield (59.1 mg, 0.32 mmol) as a white powder. ^1H and ^{13}C NMR of the product **3aa** were in agreement with the literature.^[23] ^1H NMR (400 MHz, CDCl_3 , δ): 2.22 (d, $J = 3.6$ Hz, 1H), 5.86 (d, $J = 3.6$ Hz, 1H), 7.27 (tt, $J = 1.7, 7.1$ Hz, 2H), 7.31–7.41 (m, 8H). ^{13}C NMR (101 MHz, CDCl_3 , δ): 76.1 (CH), 126.5 (CH), 127.5 (CH), 128.4 (CH), 143.7 (C). HRMS-EI (m/z): $[\text{M}]^+$ calcd for $\text{C}_{13}\text{H}_{12}\text{O}$, 184.0888; found, 184.0885.

1,3-Diphenylpropan-1-ol (**3ab**).

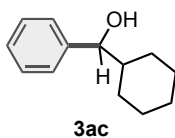


Conditions A: The reaction was conducted with **1a** (79 μ L, 0.75 mmol) and **2b** (68.9 mg, 0.51 mmol). The product **3ab** was obtained in 70% yield (76.5 mg, 0.36 mmol) as a colorless oil.

Conditions B: The reaction was conducted with **1a** (105 μ L, 1.0 mmol), lithium bromide (86.9 mg, 1.0 mmol for the first step), and **2b** (66.9 mg, 0.50 mmol). The product **3ab** was obtained in 63% yield (66.8 mg, 0.32 mmol) as a colorless oil. ^1H and ^{13}C NMR of the product **3ab** were in agreement with the literature.^[23]

^1H NMR (400 MHz, CDCl_3 , δ): 1.83 (d, $J = 3.2$ Hz, 1H), 1.99–2.20 (m, 2H), 2.62–2.81 (m, 2H), 4.68–4.72 (m, 1H), 7.17–7.32 (m, 6H), 7.36 (d, $J = 4.4$ Hz, 4H). ^{13}C NMR (100 MHz, CDCl_3 , δ): 32.0 (CH_2), 40.4 (CH_2), 73.8 (CH), 125.8 (CH), 125.9 (CH), 127.6 (CH), 128.3 (CH), 128.39 (CH), 128.45 (CH), 141.7 (C), 144.5 (C). HRMS-EI (m/z): $[\text{M}]^+$ calcd for $\text{C}_{15}\text{H}_{16}\text{O}$, 212.1201; found, 212.1204.

Cyclohexyl(phenyl)methanol (**3ac**).

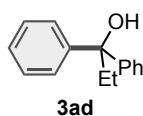


Conditions A: The reaction was conducted with **1a** (79 μ L, 0.75 mmol) and **2c** (56.8 mg, 0.51 mmol). The product **3ac** was obtained in 73% yield (70.6 mg, 0.37 mmol) as a white powder.

Conditions B: The reaction was conducted with **1a** (105 μ L, 1.0 mmol), lithium chloride (42.6 mg, 1.0 mmol for the first step), and **2c** (56.3 mg, 0.50 mmol). The product **3ac** was obtained in 58% yield (55.7 mg, 0.29 mmol) as a white powder. ^1H and ^{13}C NMR of the product **3ac** were in agreement with the literature.^[23]

^1H NMR (392 MHz, CDCl_3 , δ): 0.87–1.29 (m, 5H), 1.34–1.41 (m, 1H), 1.55–1.70 (m, 3H), 1.73–1.80 (m, 1H), 1.81 (d, $J = 3.1$ Hz, 1H), 1.95–2.03 (m, 1H), 4.37 (dd, $J = 2.7, 7.1$ Hz, 1H), 7.24–7.37 (m, 5H). ^{13}C NMR (101 MHz, CDCl_3 , δ): 25.96 (CH_2), 26.04 (CH_2), 26.4 (CH_2), 28.8 (CH_2), 29.2 (CH_2), 44.9 (CH), 79.3 (CH), 126.6 (CH), 127.4 (CH), 128.1 (CH), 143.6 (C). HRMS-EI (m/z): $[\text{M}]^+$ calcd for $\text{C}_{13}\text{H}_{18}\text{O}$, 190.1358; found, 190.1360.

1,1-Diphenylpropan-1-ol (**3ad**).

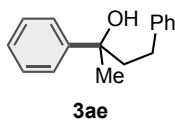


Conditions A: The reaction was conducted with **1a** (79 μ L, 0.75 mmol) and **2d** (67.3 mg, 0.50 mmol). The product **3ad** was obtained in 82% yield (87.7 mg, 0.41 mmol) as a white powder.

Conditions B: The reaction was conducted with **1a** (105 μ L, 1.0 mmol), lithium bromide (87.0 mg, 1.0 mmol for the first step), and **2d** (66.8 mg, 0.50 mmol). The product **3ad** was obtained in 45% yield (47.8 mg, 0.23 mmol) as a white powder. ^1H and ^{13}C NMR of the product **3ad** were in agreement with the literature.^[24]

^1H NMR (400 MHz, CDCl_3 , δ): 0.89 (t, $J = 7.4$ Hz, 3H), 2.06 (s, 1H), 2.33 (q, $J = 7.3$ Hz, 2H), 7.22 (tt, $J = 1.5, 7.3$ Hz, 2H), 7.31 (t, $J = 7.4$ Hz, 4H), 7.40–7.44 (m, 4H). ^{13}C NMR (101 MHz, CDCl_3 , δ): 8.1 (CH_3), 34.4 (CH_2), 78.4 (C), 126.0 (CH), 126.7 (CH), 128.1 (CH), 146.8 (C). HRMS-ESI (m/z): $[\text{M}-\text{H}]^+$ calcd for $\text{C}_{15}\text{H}_{15}\text{O}$, 211.1128; found, 211.1126.

2,4-Diphenylbutan-2-ol (**3ae**).



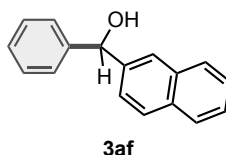
Conditions A: The reaction was conducted with **1a** (79 μ L, 0.75 mmol) and **2e** (74.1 mg, 0.50 mmol). The product **3ae** was obtained in 79% yield (89.5 mg, 0.40 mmol) as a white powder.

Conditions B: The reaction was conducted with **1a** (105 μ L, 1.0 mmol), lithium bromide (86.8 mg, 1.0 mmol for the first step), and **2e** (74.2 mg, 0.50 mmol). The product **3ae** was obtained in 69% yield (77.7 mg, 0.34 mmol) as a white powder. ^1H and ^{13}C NMR of the product **3ae** were in agreement with the literature.^[25]

^1H NMR (401 MHz, CDCl_3 , δ): 1.62 (s, 3H), 1.73 (s, 1H), 2.07–2.20 (m, 2H), 2.40–2.49 (m, 1H),

2.58–2.67 (m, 1H), 7.12 (d, $J = 7.2$ Hz, 2H), 7.16 (dt, $J = 1.7, 7.3$ Hz, 1H), 7.22–7.29 (m, 3H), 7.34–7.40 (m, 2H), 7.45–7.51 (m, 2H). ^{13}C NMR (101 MHz, CDCl_3 , δ): 30.38 (CH_2), 30.43 (CH_3), 45.9 (CH_2), 74.6 (C), 124.7 (CH), 125.7 (CH), 126.6 (CH), 128.19 (CH), 128.24 (CH), 128.3 (CH), 142.2 (C), 147.5 (C). HRMS-EI (m/z): $[\text{M}]^+$ calcd for $\text{C}_{16}\text{H}_{18}\text{O}$, 226.1358; found, 226.1358.

Naphthalen-2-yl(phenyl)methanol (**3af**).

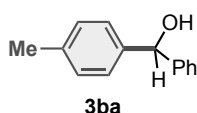


Conditions A: The reaction was conducted with **1a** (79 μL , 0.75 mmol) and **2f** (78.1 mg, 0.50 mmol). The product **3af** was obtained in 73% yield (86.0 mg, 0.37 mmol) as a white powder.

Conditions B: The reaction was conducted with **1a** (157.4 mg, 1.0 mmol) and **2f** (78.1 mg, 0.50 mmol). The product **3af** was obtained in 73% yield (85.1 mg, 0.36 mmol) as a white powder. ^1H and ^{13}C NMR of the product **3af** were in agreement with the literature.^[23]

^1H NMR (400 MHz, CDCl_3 , δ): 2.54 (d, $J = 3.2$ Hz, 1H), 5.90 (d, $J = 2.8$ Hz, 1H), 7.23 (tt, $J = 1.9, 7.1$ Hz, 1H), 7.27–7.33 (m, 2H), 7.34–7.40 (m, 3H), 7.41–7.49 (m, 2H), 7.74 (d, $J = 8.8$ Hz, 1H), 7.75–7.81 (m, 2H), 7.83 (s, 1H). ^{13}C NMR (101 MHz, CDCl_3 , δ): 76.2 (CH), 124.7 (CH), 124.9 (CH), 125.9 (CH), 126.1 (CH), 126.6 (CH), 127.59 (CH), 127.61 (CH), 128.0 (CH), 128.2 (CH), 128.5 (CH), 132.8 (C), 133.2 (C), 141.0 (C), 143.5 (C). HRMS-EI (m/z): $[\text{M}]^+$ calcd for $\text{C}_{17}\text{H}_{14}\text{O}$, 234.1045; found, 234.1037.

Phenyl(*p*-tolyl)methanol (**3ba**).

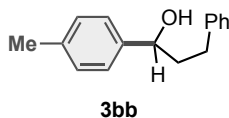


Conditions A: The reaction was conducted with **1b** (128.3 mg, 0.75 mmol) and **2a** (53.5 mg, 0.50 mmol). The product **3ba** was obtained in 86% yield (86.1 mg, 0.43 mmol) as a white powder.

Conditions B: The reaction was conducted with **1b** (170.5 mg, 1.0 mmol), THF (1.5 mmol for the first step, 0.5 mmol for the second step), and **2a** (53.2 mg, 0.50 mmol). The product **3ba** was obtained in 56% yield (55.4 mg, 0.28 mmol) as a white powder. ^1H and ^{13}C NMR of the product **3ba** were in agreement with the literature.^[23]

^1H NMR (400 MHz, CDCl_3 , δ): 2.15 (d, $J = 3.6$ Hz, 1H), 2.33 (s, 3H), 5.83 (d, $J = 3.6$ Hz, 1H), 7.15 (d, $J = 7.6$ Hz, 2H), 7.23–7.29 (m, 3H), 7.31–7.40 (m, 4H). ^{13}C NMR (100 MHz, CDCl_3 , δ): 21.1 (CH_3), 76.0 (CH), 126.4 (CH), 126.5 (CH), 127.4 (CH), 128.4 (CH), 129.1 (CH), 137.2 (C), 140.9 (C), 143.9 (C). HRMS-EI (m/z): $[\text{M}]^+$ calcd for $\text{C}_{14}\text{H}_{14}\text{O}$, 198.1045; found, 198.1048.

3-Phenyl-1-(*p*-tolyl)propan-1-ol (**3bb**).

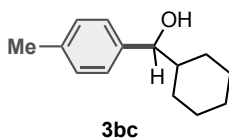


Conditions A: The reaction was conducted with **1b** (128.3 mg, 0.75 mmol) and **2b** (67.8 mg, 0.51 mmol). The product **3bb** was obtained in 70% yield (80.5 mg, 0.36 mmol) as a colorless oil.

Conditions B: The reaction was conducted with **1b** (171.0 mg, 1.0 mmol) and **2b** (67.3 mg, 0.50 mmol). The product **3bb** was obtained in 42% yield (48.1 mg, 0.21 mmol) as a colorless oil. ^1H and ^{13}C NMR of the product **3bb** were in agreement with the literature.^[26]

^1H NMR (392 MHz, CDCl_3 , δ): 1.77 (d, $J = 3.1$ Hz, 1H), 1.97–2.19 (m, 2H), 2.35 (s, 3H), 2.61–2.79 (m, 2H), 4.66 (sept, $J = 2.7$ Hz, 1H), 7.14–7.31 (m, 9H). ^{13}C NMR (99 MHz, CDCl_3 , δ): 21.1 (CH_3), 32.0 (CH_2), 40.3 (CH_2), 73.7 (CH), 125.8 (CH), 125.9 (CH), 128.3 (CH), 128.4 (CH), 129.1 (CH), 137.3 (C), 141.5 (C), 141.8 (C). HRMS-EI (m/z): $[\text{M}]^+$ calcd for $\text{C}_{16}\text{H}_{18}\text{O}$, 226.1358; found, 226.1361.

Cyclohexyl(*p*-tolyl)methanol (**3bc**).

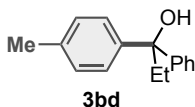


Conditions A: The reaction was conducted with **1b** (128.3 mg, 0.75 mmol) and **2c** (56.4 mg, 0.50 mmol). The product **3bc** was obtained in 62% yield (64.0 mg, 0.31 mmol) as a white powder.

Conditions B: The reaction was conducted with **1b** (172.0 mg, 1.0 mmol), THF (1.5 mmol for the first step, 0.5 mmol for the second step), and **2c** (56.3 mg, 0.50 mmol). The product **3bc** was obtained in 55% yield (56.8 mg, 0.28 mmol) as a white powder. ^1H and ^{13}C NMR of the product **3bc** were in agreement with the literature.^[27]

^1H NMR (400 MHz, CDCl_3 , δ): 0.86–1.28 (m, 5H), 1.33–1.40 (m, 1H), 1.57–1.69 (m, 3H), 1.73–1.81 (m, 2H), 1.97–2.03 (m, 1H), 2.34 (s, 3H), 4.33 (dd, $J = 3.0, 7.0$ Hz, 1H), 7.13–7.21 (m, 4H). ^{13}C NMR (100 MHz, CDCl_3 , δ): 21.1 (CH_3), 26.0 (CH_2), 26.1 (CH_2), 26.4 (CH_2), 28.9 (CH_2), 29.3 (CH_2), 44.8 (CH), 79.2 (CH), 126.5 (CH), 128.8 (CH), 136.9 (C), 140.6 (C). HRMS-EI (m/z): $[\text{M}]^+$ calcd for $\text{C}_{14}\text{H}_{20}\text{O}$, 204.1514; found, 204.1513.

1-Phenyl-1-(*p*-tolyl)propan-1-ol (**3bd**).

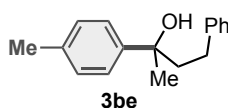


Conditions A: The reaction was conducted with **1b** (128.3 mg, 0.75 mmol) and **2d** (67.5 mg, 0.50 mmol). The product **3bd** was obtained in 74% yield (84.0 mg, 0.37 mmol) as a colorless oil.

Conditions B: The reaction was conducted with **1b** (171.2 mg, 1.0 mmol) and **2d** (67.0 mg, 0.50 mmol). The product **3bd** was obtained in 64% yield (72.3 mg, 0.32 mmol) as a colorless oil. ^1H and ^{13}C NMR of the product **3bd** were in agreement with the literature.^[24]

^1H NMR (400 MHz, CDCl_3 , δ): 0.88 (t, $J = 7.6$ Hz, 3H), 2.03 (s, 1H), 2.31 (q, $J = 7.3$ Hz, 2H), 2.32 (s, 3H), 7.12 (d, $J = 8.4$ Hz, 2H), 7.21 (t, $J = 7.2$ Hz, 1H), 7.28–7.33 (m, 4H), 7.41 (d, $J = 7.2$ Hz, 2H). ^{13}C NMR (101 MHz, CDCl_3 , δ): 8.1 (CH_3), 20.9 (CH_3), 34.4 (CH_2), 78.3 (C), 126.0 (CH), 126.6 (CH), 128.0 (CH), 128.7 (CH), 136.3 (C), 144.0 (C), 147.0 (C). HRMS-ESI (m/z): $[\text{M}-\text{H}]^+$ calcd for $\text{C}_{16}\text{H}_{17}\text{O}$, 225.1285; found, 225.1284.

4-Phenyl-2-(*p*-tolyl)butan-2-ol (**3be**).

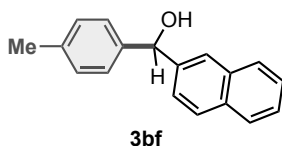


Conditions A: The reaction was conducted with **1b** (128.3 mg, 0.75 mmol) and **2e** (74.4 mg, 0.50 mmol). The product **3be** was obtained in 69% yield (83.7 mg, 0.35 mmol) as a colorless oil.

Conditions B: The reaction was conducted with **1b** (170.1 mg, 1.0 mmol) and **2e** (73.9 mg, 0.50 mmol). The product **3be** was obtained in 60% yield (71.9 mg, 0.30 mmol) as a colorless oil.

^1H NMR (400 MHz, CDCl_3 , δ): 1.60 (s, 3H), 1.72 (s, 1H), 2.04–2.18 (m, 2H), 2.36 (s, 3H), 2.41–2.49 (m, 1H), 2.56–2.66 (m, 1H), 7.10–7.20 (m, 5H), 7.24 (d, $J = 7.2$ Hz, 2H), 7.36 (dt, $J = 2.1, 8.5$ Hz, 2H). ^{13}C NMR (101 MHz, CDCl_3 , δ): 20.9 (CH_3), 30.4 (CH_3), 30.4 (CH_2), 45.8 (CH_2), 74.6 (C), 124.6 (CH), 125.7 (CH), 128.26 (CH), 128.29 (CH), 128.9 (CH), 136.1 (C), 142.3 (C), 144.5 (C). HRMS-EI (m/z): $[\text{M}]^+$ calcd for $\text{C}_{17}\text{H}_{20}\text{O}$, 240.1514; found, 240.1515.

Naphthalen-2-yl(*p*-tolyl)methanol (**3bf**).



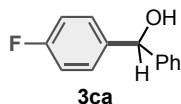
Conditions A: The reaction was conducted with **1b** (128.3 mg, 0.75 mmol) and **2f** (78.1 mg, 0.50 mmol). The product **3bf** was obtained in 72% yield (89.8 mg, 0.36 mmol) as a white powder.

Conditions B: The reaction was conducted with **1b** (173.4 mg, 1.0 mmol) and **2f** (78.2 mg, 0.50 mmol). The product **3bf** was obtained in 68% yield (84.0 mg, 0.34 mmol) as a white powder. ^1H and ^{13}C NMR of the product **3bf** were in agreement with the literature.^[28]

^1H NMR (400 MHz, CDCl_3 , δ): 2.30 (s, 3H), 2.43 (s, 1H), 5.90 (s, 1H), 7.11 (d, $J = 8.0$ Hz, 2H), 7.26 (d, $J = 8.0$ Hz, 2H), 7.38 (d, $J = 8.4$ Hz, 1H), 7.40–7.50 (m, 2H), 7.74 (d, $J = 8.8$ Hz, 1H), 7.76–7.82 (m, 2H), 7.85 (s, 1H). ^{13}C NMR (101 MHz, CDCl_3 , δ): 21.1 (CH_3), 76.1 (CH), 124.7 (CH), 124.8 (CH), 125.8 (CH), 126.1 (CH), 126.6 (CH), 127.6 (CH), 128.0 (CH), 128.2 (CH), 129.2 (CH), 132.8 (C),

133.2 (C), 137.3 (C), 140.7 (C), 141.2 (C). HRMS-EI (m/z): [M]⁺ calcd for C₁₈H₁₆O, 248.1201; found, 248.1198.

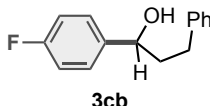
(4-Fluorophenyl)(phenyl)methanol (3ca).



Conditions A: The reaction was conducted with **1c** (82 μ L, 0.75 mmol) and **2a** (53.5 mg, 0.50 mmol). The product **3ca** was obtained in 77% yield (73.8 mg, 0.36 mmol) as a white powder.

Conditions B: The reaction was conducted with **1c** (109 μ L, 1.0 mmol), lithium chloride (42.4 mg, 1.0 mmol), and **2a** (53.1 mg, 0.50 mmol). The product **3ca** was obtained in 67% yield (68.0 mg, 0.34 mmol) as a white powder. ¹H and ¹³C NMR of the product **3ca** were in agreement with the literature.^[23] ¹H NMR (401 MHz, CDCl₃, δ): 2.19 (d, J = 3.2 Hz, 1H), 5.84 (d, J = 3.6 Hz, 1H), 7.02 (tt, J = 2.2, 8.9 Hz, 2H), 7.27–7.39 (m, 7H). ¹³C NMR (101 MHz, CDCl₃, δ): 75.5 (CH), 115.2 (d, J_{C-F} = 22.1 Hz, CH), 126.4 (CH), 127.7 (CH), 128.2 (d, J_{C-F} = 8.0 Hz, CH), 128.5 (CH), 139.5 (d, J_{C-F} = 3.0 Hz, C), 143.6 (C), 162.1 (d, J_{C-F} = 245.7 Hz, C). HRMS-ESI (m/z): [M–H]⁺ calcd for C₁₃H₁₀FO, 201.0721; found, 201.0717.

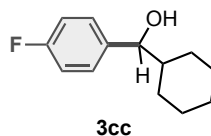
1-(4-Fluorophenyl)-3-phenylpropan-1-ol (3cb).



Conditions A: The reaction was conducted with **1c** (82 μ L, 0.75 mmol) and **2b** (67.0 mg, 0.50 mmol). The product **3cb** was obtained in 70% yield (80.2 mg, 0.35 mmol) as a colorless oil.

Conditions B: The reaction was conducted with **1c** (109 μ L, 1.0 mmol), lithium chloride (42.4 mg, 1.0 mmol) and **2b** (66.9 mg, 0.50 mmol). The product **3cb** was obtained in 61% yield (70.3 mg, 0.31 mmol) as a colorless oil. ¹H and ¹³C NMR of the product **3cb** were in agreement with the literature.^[26] ¹H NMR (392 MHz, CDCl₃, δ): 1.82 (d, J = 3.1 Hz, 1H), 1.95–2.18 (m, 2H), 2.61–2.79 (m, 2H), 4.68 (sept, J = 2.7 Hz, 1H), 7.04 (tt, J = 2.5, 9.1 Hz, 2H), 7.19 (t, J = 6.3 Hz, 3H), 7.26–7.36 (m, 4H). ¹³C NMR (101 MHz, CDCl₃, δ): 31.9 (CH₂), 40.5 (CH₂), 73.2 (CH), 115.3 (d, J_{C-F} = 22.1 Hz, CH), 125.9 (CH), 127.5 (d, J_{C-F} = 7.7 Hz, CH), 128.37 (CH), 128.40 (CH), 140.2 (C), 141.5 (C), 162.2 (d, J_{C-F} = 245.7 Hz, C). HRMS-ESI (m/z): [M–H]⁺ calcd for C₁₅H₁₄FO, 229.1034; found, 229.1032.

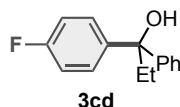
Cyclohexyl(4-fluorophenyl)methanol (**3cc**).



Conditions A: The reaction was conducted with **1c** (82 μ L, 0.75 mmol) and **2c** (55.9 mg, 0.50 mmol). The product **3cc** was obtained in 62% yield (64.8 mg, 0.31 mmol) as a yellow oil.

Conditions B: The reaction was conducted with **1c** (109 μ L, 1.0 mmol), lithium chloride (42.4 mg, 1.0 mmol) and **2c** (55.4 mg, 0.50 mmol). The product **3cc** was obtained in 55% yield (56.9 mg, 0.27 mmol) as a yellow oil. ^1H and ^{13}C NMR of the product **3cc** were in agreement with the literature.^[29] ^1H NMR (400 MHz, CDCl_3 , δ): 0.84–1.29 (m, 5H), 1.32–1.39 (m, 1H), 1.52–1.71 (m, 3H), 1.74–1.82 (m, 2H), 1.93–2.00 (m, 1H), 4.36 (dd, $J = 3.0, 7.0$ Hz, 1H), 7.02 (tt, $J = 2.3, 9.0$ Hz, 2H), 7.24–7.29 (m, 2H). ^{13}C NMR (101 MHz, CDCl_3 , δ): 25.9 (CH_2), 26.0 (CH_2), 26.3 (CH_2), 28.8 (CH_2), 29.1 (CH_2), 45.0 (CH), 78.6 (CH), 114.9 (d, $J_{\text{C-F}} = 21.2$ Hz, CH), 128.1 (d, $J_{\text{C-F}} = 7.7$ Hz, CH), 139.2 (d, $J_{\text{C-F}} = 2.8$ Hz, C), 162.0 (d, $J_{\text{C-F}} = 244.7$ Hz, C). HRMS-EI (m/z): $[\text{M}]^+$ calcd for $\text{C}_{13}\text{H}_{17}\text{FO}$, 208.1263; found, 208.1263.

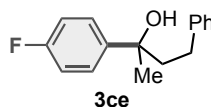
1-(4-Fluorophenyl)-1-phenylpropan-1-ol (**3cd**).



Conditions A: The reaction was conducted with **1c** (82 μ L, 0.75 mmol) and **2d** (67.5 mg, 0.50 mmol). The product **3cd** was obtained in 71% yield (82.0 mg, 0.36 mmol) as a colorless oil.

Conditions B: The reaction was conducted with **1c** (175.0 mg, 1.0 mmol), lithium chloride (42.4 mg, 1.0 mmol) and **2d** (67.2 mg, 0.50 mmol). The product **3cd** was obtained in 61% yield (70.1 mg, 0.30 mmol) as a colorless oil. ^1H and ^{13}C NMR of the product **3cd** were in agreement with the literature.^[24] ^1H NMR (400 MHz, CDCl_3 , δ): 0.88 (t, $J = 7.4$ Hz, 3H), 2.04 (s, 1H), 2.30 (q, $J = 7.2$ Hz, 2H), 6.98 (tt, $J = 2.3, 9.0$ Hz, 2H), 7.23 (tt, $J = 1.5, 7.1$ Hz, 1H), 7.29–7.42 (m, 6H). ^{13}C NMR (101 MHz, CDCl_3 , δ): 8.1 (CH_3), 34.5 (CH_2), 78.1 (C), 114.7 (d, $J_{\text{C-F}} = 21.2$ Hz, CH), 126.0 (CH), 126.9 (CH), 127.8 (d, $J_{\text{C-F}} = 7.7$ Hz, CH), 128.2 (CH), 142.7 (d, $J_{\text{C-F}} = 2.9$ Hz, C), 146.7 (C), 161.5 (d, $J_{\text{C-F}} = 245.6$ Hz, C). HRMS-ESI (m/z): $[\text{M}-\text{H}]^+$ calcd for $\text{C}_{15}\text{H}_{14}\text{FO}$, 229.1034; found, 229.1031.

2-(4-Fluorophenyl)-4-phenylbutan-2-ol (**3ce**).

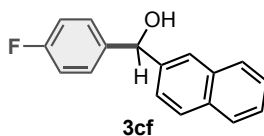


Conditions A: The reaction was conducted with **1c** (82 μ L, 0.75 mmol) and **2e** (74.4 mg, 0.50 mmol). The product **3ce** was obtained in 54% NMR yield.

Conditions B: The reaction was conducted with **1c** (109 μ L, 1.0 mmol), lithium chloride (42.4 mg, 1.0 mmol), and **2e** (73.9 mg, 0.50 mmol). The product **3ce** was obtained in 72% yield (87.9 mg, 0.36 mmol) as a white powder.

^1H NMR (392 MHz, CDCl_3 , δ): 1.60 (s, 3H), 1.71 (s, 1H), 2.06–2.16 (m, 2H), 2.37–2.49 (m, 1H), 2.55–2.66 (m, 1H), 7.04 (tt, $J = 2.4, 9.2$ Hz, 2H), 7.11 (d, $J = 6.7$ Hz, 2H), 7.16 (tt, $J = 1.6, 7.4$ Hz, 1H), 7.22–7.28 (m, 2H), 7.40–7.48 (m, 2H). ^{13}C NMR (101 MHz, CDCl_3 , δ): 30.4 (CH_2), 30.5 (CH_3), 46.0 (CH_2), 74.4 (C), 114.9 (d, $J_{\text{C-F}} = 21.2$ Hz, CH), 125.8 (CH), 126.4 (CH), 126.5 (CH), 128.3 (d, $J_{\text{C-F}} = 13.5$ Hz, CH), 142.0 (C), 143.2 (d, $J_{\text{C-F}} = 2.9$ Hz, C), 161.6 (d, $J_{\text{C-F}} = 245.6$ Hz, C). HRMS-EI (m/z): $[\text{M}]^+$ calcd for $\text{C}_{16}\text{H}_{17}\text{FO}$, 224.1263; found, 224.1267.

(4-Fluorophenyl)(naphthalen-2-yl)methanol (3cf).

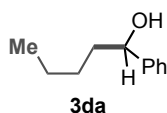


Conditions A: The reaction was conducted with **1c** (82 μ L, 0.75 mmol) and **2f** (78.1 mg, 0.50 mmol). The product **3cf** was obtained in 48% NMR yield.

Conditions B: The reaction was conducted with **1c** (174.4 mg, 109 μ L, 1.0 mmol) and **2f** (78.1 mg, 0.50 mmol). The product **3cf** was obtained in 65% yield (82.5 mg, 0.33 mmol) as pale-yellow oil. ^1H and ^{13}C NMR of the product **3cf** were in agreement with the literature.^[28]

^1H NMR (400 MHz, CDCl_3 , δ): 2.55–2.64 (m, 1H), 5.88 (s, 1H), 6.97 (tt, $J = 2.3, 9.1$ Hz, 2H), 7.27–7.36 (m, 3H), 7.42–7.50 (m, 2H), 7.75 (d, $J = 8.4$ Hz, 1H), 7.77–7.84 (m, 3H). ^{13}C NMR (101 MHz, CDCl_3 , δ): 75.6 (CH), 115.3 (d, $J_{\text{C-F}} = 21.2$ Hz, CH), 124.5 (CH), 124.9 (CH), 126.1 (CH), 126.3 (CH), 127.6 (CH), 128.0 (CH), 128.3 (d, $J_{\text{C-F}} = 7.6$ Hz, CH), 128.4 (CH), 132.8 (C), 133.1 (C), 139.3 (d, $J_{\text{C-F}} = 2.8$ Hz, C), 140.9 (C), 162.1 (d, $J_{\text{C-F}} = 245.6$ Hz, C). HRMS-EI (m/z): $[\text{M}]^+$ calcd for $\text{C}_{17}\text{H}_{13}\text{FO}$, 252.0950; found, 252.0946.

1-Phenylpentan-1-ol (3da).



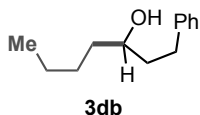
Conditions A: The reaction was conducted with **1d** (81 μ L, 0.75 mmol) and **2a** (53.4 mg, 0.50 mmol). The product **3da** was obtained in 73% yield (60.2 mg, 0.37 mmol) as a colorless oil.

Conditions B: The reaction was conducted with **1d** (107 μ L, 1.0 mmol) and **2a** (53.3 mg, 0.50 mmol). The product **3da** was obtained in 77% yield (63.7 mg, 0.39 mmol) as a colorless oil. ^1H and ^{13}C NMR of the product **3da** were in agreement with the literature.^[30]

^1H NMR (400 MHz, CDCl_3 , δ): 0.89 (t, $J = 7.0$ Hz, 3H), 1.21–1.45 (m, 4H), 1.66–1.88 (m, 2H), 1.79

(d, $J = 3.2$ Hz, 1H), 4.64–4.70 (m, 1H), 7.27–7.31 (m, 1H), 7.35–7.36 (m, 4H). ^{13}C NMR (101 MHz, CDCl_3 , δ): 14.0 (CH_3), 22.5 (CH_2), 27.9 (CH_2), 38.7 (CH_2), 74.6 (CH), 125.8 (CH), 127.4 (CH), 128.3 (CH), 144.9 (C). HRMS-EI (m/z): $[\text{M}]^+$ calcd for $\text{C}_{11}\text{H}_{16}\text{O}$, 164.1201; found, 164.1200.

1-Phenylheptan-3-ol (**3db**).

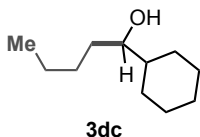


Conditions A: The reaction was conducted with **1d** (81 μL , 0.75 mmol) and **2b** (67.0 mg, 0.50 mmol). The product **3db** was obtained in 46% yield (44.6 mg, 0.23 mmol) as pale-yellow oil.

Conditions B: The reaction was conducted with **1d** (136.0 mg, 1.0 mmol) and **2b** (67.2 mg, 0.50 mmol). The product **3db** was obtained in 62% yield (60.1 mg, 0.31 mmol) as pale-yellow oil. ^1H and ^{13}C NMR of the product **3db** were in agreement with the literature.^[26]

^1H NMR (400 MHz, CDCl_3 , δ): 0.90 (t, $J = 6.8$ Hz, 3H), 1.21–1.61 (m, 7H), 1.66–1.87 (m, 2H), 2.59–2.72 (m, 1H), 2.74–2.86 (m, 1H), 3.61 (sept, $J = 4.0$ Hz, 1H), 7.14–7.23 (m, 3H), 7.28 (t, $J = 7.6$ Hz, 2H). ^{13}C NMR (101 MHz, CDCl_3 , δ): 14.0 (CH_3), 22.7 (CH_2), 27.8 (CH_2), 32.0 (CH_2), 37.2 (CH_2), 39.0 (CH_2), 71.3 (CH), 125.7 (CH), 128.3 (CH), 128.4 (CH), 142.2 (C). HRMS-EI (m/z): $[\text{M}]^+$ calcd for $\text{C}_{13}\text{H}_{20}\text{O}$, 192.1514; found, 192.1511.

1-Cyclohexylpentan-1-ol (**3dc**).

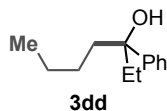


Conditions A: The reaction was conducted with **1d** (81 μL , 0.75 mmol) and **2c** (55.8 mg, 0.50 mmol). The product **3dc** was obtained in 67% yield (57.0 mg, 0.33 mmol) as a pale-yellow oil.

Conditions B: The reaction was conducted with **1d** (137.2 mg, 1.0 mmol) and **2c** (56.6 mg, 0.50 mmol). The product **3dc** was obtained in 55% yield (47.2 mg, 0.28 mmol) as a pale-yellow oil. ^1H and ^{13}C NMR of the product **3dc** were in agreement with the literature.^[31]

^1H NMR (400 MHz, CDCl_3 , δ): 0.91 (t, $J = 6.8$ Hz, 3H), 0.97–1.57 (m, 13H), 1.60–1.70 (m, 2H), 1.72–1.88 (m, 3H), 3.29–3.45 (m, 1H). ^{13}C NMR (101 MHz, CDCl_3 , δ): 14.1 (CH_3), 22.8 (CH_2), 26.2 (CH_2), 26.4 (CH_2), 26.5 (CH_2), 27.6 (CH_2), 28.1 (CH_2), 29.2 (CH_2), 33.8 (CH_2), 43.5 (CH), 76.2 (CH). HRMS-ESI (m/z): $[\text{M}-\text{H}]^+$ calcd for $\text{C}_{11}\text{H}_{21}\text{O}$, 169.1598; found, 169.1594.

3-Phenylheptan-3-ol (3dd).

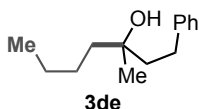


Conditions A: The reaction was conducted with **1d** (80 μ L, 0.75 mmol) and **2d** (67.4 mg, 0.50 mmol). The product **3dd** was obtained in 58% NMR yield.

Conditions B: The reaction was conducted with **1d** (107 μ L, 1.0 mmol) and **2d** (73.4 mg, 0.55 mmol). The product **3dd** was obtained in 60% yield (62.6 mg, 0.32 mmol) as a pale-yellow oil. ^1H and ^{13}C NMR of the product **3dd** were in agreement with the literature.^[32]

^1H NMR (400 MHz, CDCl_3 , δ): 0.75 (t, $J = 7.4$ Hz, 3H), 0.83 (t, $J = 7.4$ Hz, 3H), 0.94–1.11 (m, 1H), 1.16–1.34 (m, 3H), 1.69 (s, 1H), 1.72–1.92 (m, 4H), 7.22 (tt, $J = 1.8, 7.0$ Hz, 1H), 7.30–7.40 (m, 4H). ^{13}C NMR (101 MHz, CDCl_3 , δ): 7.8 (CH_3), 14.0 (CH_3), 23.1 (CH_2), 25.6 (CH_2), 35.4 (CH_2), 42.3 (CH_2), 77.2 (C), 125.3 (CH), 126.2 (CH), 127.9 (CH), 146.1 (C). HRMS-ESI (m/z): $[\text{M}+\text{Na}]^+$ calcd for $\text{C}_{13}\text{H}_{20}\text{ONa}$, 215.1412; found, 215.1409.

3-Methyl-1-phenylheptan-3-ol (3de).

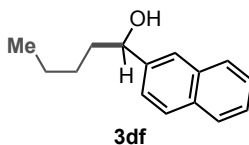


Conditions A: The reaction was conducted with **1d** (80 μ L, 0.75 mmol) and **2e** (74.0 mg, 0.50 mmol). The product **3de** was obtained in 66% NMR yield.

Conditions B: The reaction was conducted with **1d** (137.0 mg, 1.0 mmol) and **2e** (74.8 mg, 0.50 mmol). The product was **3de** obtained in 63% yield (65.6 mg, 0.32 mmol) as a yellow oil. ^1H and ^{13}C NMR of the product **3de** were in agreement with the literature.^[33]

^1H NMR (400 MHz, CDCl_3 , δ): 0.92 (t, $J = 7.0$ Hz, 3H), 1.23 (s, 3H), 1.28–1.41 (m, 5H), 1.45–1.61 (m, 2H), 1.69–1.82 (m, 2H), 2.61–2.72 (m, 2H), 7.12–7.22 (m, 3H), 7.28 (t, $J = 7.4$ Hz, 2H). ^{13}C NMR (101 MHz, CDCl_3 , δ): 14.1 (CH_3), 23.2 (CH_2), 26.1 (CH_2), 26.9 (CH_3), 30.3 (CH_2), 41.7 (CH_2), 43.7 (CH_2), 72.6 (C), 125.7 (CH), 128.27 (CH), 128.34 (CH), 142.6 (C). HRMS-ESI (m/z): $[\text{M}-\text{H}]^+$ calcd for $\text{C}_{14}\text{H}_{21}\text{O}$, 205.1598; found, 205.1595.

1-(Naphthalen-2-yl)pentan-1-ol (3df).

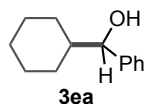


Conditions A: The reaction was conducted with **1d** (80 μ L, 0.75 mmol) and **2f** (78.1 mg, 0.50 mmol). The product **3df** was obtained in 68% yield (73.1 mg, 0.34 mmol) as a white solid.

Conditions B: The reaction was conducted with **1d** (137.0 mg, 1.0 mmol) and **2f** (78.2 mg, 0.50 mmol). The product **3df** was obtained in 99% yield (107.3 mg, 0.50 mmol) as a white solid. ^1H and ^{13}C NMR of the product **3df** were in agreement with the literature.^[30]

^1H NMR (400 MHz, CDCl_3 , δ): 0.86 (t, $J = 7.0$ Hz, 3H), 1.17–1.45 (m, 4H), 1.69–1.90 (m, 2H), 2.21 (s, 1H), 4.76 (t, $J = 6.6$ Hz, 1H), 7.39–7.50 (m, 3H), 7.72 (s, 1H), 7.76–7.84 (m, 3H). ^{13}C NMR (101 MHz, CDCl_3 , δ): 14.0 (CH_3), 22.6 (CH_2), 27.9 (CH_2), 38.6 (CH_2), 74.6 (CH), 124.1 (CH), 124.5 (CH), 125.7 (CH), 126.0 (CH), 127.6 (CH), 127.8 (CH), 128.1 (CH), 132.8 (C), 133.2 (C), 142.2 (C). HRMS-EI (m/z): $[\text{M}]^+$ calcd for $\text{C}_{15}\text{H}_{18}\text{O}$, 214.1358; found, 214.1355.

Cyclohexyl(phenyl)methanol (**3ea**).

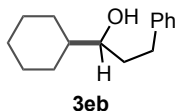


Conditions A: The reaction was conducted with **1e** (92 μL , 0.75 mmol) and **2a** (53.5 mg, 0.50 mmol). The product **3ea** was obtained in 24% NMR yield.

Conditions B: The reaction was conducted with **1e** (123 μL , 1.0 mmol) and **2a** (52.9 mg, 0.50 mmol). The reaction time of the first step was extended to 90 minutes. The product **3ea** was obtained in 58% yield (55.2 mg, 0.29 mmol) as a colorless oil. ^1H and ^{13}C NMR of the product **3ea** were in agreement with the literature.^[23]

^1H NMR (392 MHz, CDCl_3 , δ): 0.87–1.29 (m, 5H), 1.34–1.42 (m, 1H), 1.57–1.71 (m, 3H), 1.73–1.82 (m, 1H), 1.80 (d, $J = 3.6$ Hz, 1H), 1.95–2.03 (m, 1H), 4.37 (dd, $J = 2.8, 7.6$ Hz, 1H), 7.24–7.37 (m, 5H). ^{13}C NMR (101 MHz, CDCl_3 , δ): 25.95 (CH_2), 26.04 (CH_2), 26.4 (CH_2), 28.8 (CH_2), 29.2 (CH_2), 44.9 (CH), 79.3 (CH), 126.6 (CH), 127.3 (CH), 128.1 (CH), 143.6 (C). HRMS-EI (m/z): $[\text{M}]^+$ calcd for $\text{C}_{13}\text{H}_{18}\text{O}$, 190.1358; found, 190.1351.

1-Cyclohexyl-3-phenylpropan-1-ol (**3eb**).



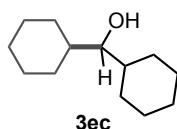
Conditions A: The reaction was conducted with **1e** (92 μL , 0.75 mmol) and **2b** (67.1 mg, 0.50 mmol). The product **3eb** was obtained in 40% yield (43.8 mg, 0.20 mmol) as a white solid.

Conditions B: The reaction was conducted with **1e** (162.8 mg, 1.0 mmol) and **2b** (67.2 mg, 0.50 mmol). The reaction time of the first step was extended to 90 minutes. The product **3eb** was obtained in 42% yield (45.9 mg, 0.21 mmol) as a white solid. ^1H and ^{13}C NMR of the product **3eb** were in agreement with the literature.^[26]

^1H NMR (400 MHz, CDCl_3 , δ): 0.94–1.39 (m, 6H), 1.42 (s, 1H), 1.60–1.87 (m, 7H), 2.58–2.72 (m, 1H), 2.78–2.89 (m, 1H), 3.34–3.43 (m, 1H), 7.14–7.23 (m, 3H), 7.24–7.32 (m, 2H). ^{13}C NMR (101

MHz, CDCl₃, δ): 26.1 (CH₂), 26.3 (CH₂), 26.5 (CH₂), 27.8 (CH₂), 29.1 (CH₂), 32.3 (CH₂), 35.9 (CH₂), 43.7 (CH), 75.6 (CH), 125.7 (CH), 128.3 (CH), 128.4 (CH), 142.4 (C). HRMS-ESI (m/z): [M+Na]⁺ calcd for C₁₅H₂₂ONa, 241.1563; found, 241.1562.

Dicyclohexylmethanol (**3ec**).

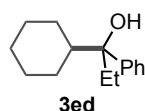


Conditions A: The reaction was conducted with **1e** (92 μL, 0.75 mmol) and **2c** (56.5 mg, 0.50 mmol). The product **3ec** was obtained in 26% NMR yield.

Conditions B: The reaction was conducted with **1e** (123 μL, 1.0 mmol) and **2c** (56.2 mg, 0.50 mmol). The reaction time of the first step was extended to 90 minutes. The product **3ec** was obtained in 43% yield (42.0 mg, 0.21 mmol) as a white solid. ¹H and ¹³C NMR of the product **3ec** were in agreement with the literature.^[34]

¹H NMR (400 MHz, CDCl₃, δ): 0.94–1.32 (m, 11H), 1.37–1.49 (m, 2H), 1.52–1.60 (m, 2H), 1.62–1.70 (m, 2H), 1.71–1.87 (m, 6H), 2.99–3.10 (m, 1H). ¹³C NMR (101 MHz, CDCl₃, δ): 26.1 (CH₂), 26.46 (CH₂), 26.52 (CH₂), 27.3 (CH₂), 30.0 (CH₂), 39.8 (CH), 80.4 (CH). HRMS-ESI (m/z): [M+Na]⁺ calcd for C₁₃H₂₄ONa, 219.1725; found, 219.1729.

1-Cyclohexyl-1-phenylpropan-1-ol (**3ed**).

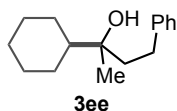


Conditions A: The reaction was conducted with **1e** (97 μL, 0.79 mmol) and **2d** (67.5 mg, 0.50 mmol). The product **3ed** was obtained in 33% NMR yield.

Conditions B: The reaction was conducted with **1e** (163.7 mg, 1.0 mmol) and **2d** (67.4 mg, 0.50 mmol). The reaction time of the first step was extended to 90 minutes. The product **3ed** was obtained in 30% yield (33.3 mg, 0.15 mmol) as a colorless oil. ¹H and ¹³C NMR of the product **3ed** were in agreement with the literature.^[35]

¹H NMR (400 MHz, CDCl₃, δ): 0.69 (t, *J* = 7.4 Hz, 3H), 0.87–1.29 (m, 5H), 1.38–1.46 (m, 1H), 1.56–1.70 (m, 4H), 1.73–1.81 (m, 1H), 1.89 (q, *J* = 7.3 Hz, 2H), 1.92–1.95 (m, 1H), 7.19–7.24 (m, 1H), 7.29–7.38 (m, 4H). ¹³C NMR (101 MHz, CDCl₃, δ): 7.8 (CH₃), 26.4 (CH₂), 26.6 (CH₂), 26.67 (CH₂), 26.69 (CH₂), 27.4 (CH₂), 31.6 (CH₂), 47.9 (CH), 79.2 (C), 125.9 (CH), 126.0 (CH), 127.7 (CH), 145.1 (C). HRMS-ESI (m/z): [M-H]⁺ calcd for C₁₅H₂₁O, 217.1598; found, 217.1598.

2-Cyclohexyl-4-phenylbutan-2-ol (**3ee**).

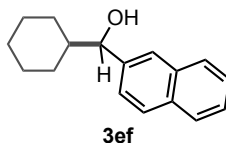


Conditions A: The reaction was conducted with **1e** (97 μ L, 0.79 mmol) and **2e** (75.1 mg, 0.51 mmol). The product **3ee** was obtained in 15% yield (17.1 mg, 0.073 mmol) as a pale-yellow oil.

Conditions B: The reaction was conducted with **1e** (163.7 mg, 1.0 mmol) and **2e** (73.2 mg, 0.49 mmol). The reaction time of the first step was extended to 90 minutes. The product **3ee** was obtained in 22% yield (25.7 mg, 0.11 mmol) as a pale-yellow oil. ^1H and ^{13}C NMR of the product **3ee** were in agreement with the literature.^[36]

^1H NMR (401 MHz, CDCl_3 , δ): 0.95–1.31 (m, 9H), 1.39 (tt, $J = 2.4, 11.8$ Hz, 1H), 1.61–1.90 (m, 7H), 2.68 (q, $J = 7.7$ Hz, 2H), 7.14–7.23 (m, 3H), 7.24–7.32 (m, 2H). ^{13}C NMR (101 MHz, CDCl_3 , δ): 23.8 (CH_3), 26.5 (CH_2), 26.7 (CH_2), 26.8 (CH_2), 26.9 (CH_2), 27.6 (CH_2), 29.8 (CH_2), 41.9 (CH_2), 47.6 (CH), 74.4 (C), 125.7 (CH), 128.3 (CH), 128.4 (CH), 142.9 (C). HRMS-ESI (m/z): $[\text{M}+\text{Na}]^+$ calcd for $\text{C}_{16}\text{H}_{24}\text{ONa}$, 255.1719; found, 255.1718.

Cyclohexyl(naphthalen-2-yl)methanol (**3ef**).

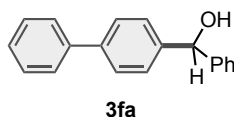


Conditions A: The reaction was conducted with **1e** (97 μ L, 0.79 mmol) and **2f** (78.1 mg, 0.50 mmol). The product **3ef** was obtained in 19% NMR yield.

Conditions B: The reaction was conducted with **1e** (130 μ L, 1.1 mmol), Mg (48.6 mg, 2.0 mmol), and **2f** (78.1 mg, 0.50 mmol). The product **3ef** was obtained in 50% yield (59.9 mg, 0.25 mmol) as a white solid. ^1H and ^{13}C NMR of the product **3ef** were in agreement with the literature.^[30]

^1H NMR (400 MHz, CDCl_3 , δ): 0.98 (dq, $J = 3.4, 10.1$ Hz, 1H), 1.05–1.31 (m, 4H), 1.34–1.45 (m, 1H), 1.53–1.82 (m, 4H), 1.98 (s, 1H), 2.02 (d, $J = 12.8$ Hz, 1H), 4.53 (d, $J = 7.2$ Hz, 1H), 7.40–7.51 (m, 3H), 7.72 (s, 1H), 7.78–7.87 (m, 3H). ^{13}C NMR (101 MHz, CDCl_3 , δ): 26.0 (CH_2), 26.1 (CH_2), 26.4 (CH_2), 28.8 (CH_2), 29.4 (CH_2), 44.9 (CH), 79.5 (CH), 124.7 (CH), 125.5 (CH), 125.7 (CH), 126.0 (CH), 127.6 (CH), 127.88 (CH), 127.92 (CH), 132.9 (C), 133.1 (C), 141.0 (C). HRMS-EI (m/z): $[\text{M}]^+$ calcd for $\text{C}_{17}\text{H}_{20}\text{O}$, 240.1514; found, 240.1510.

(1,1'-Biphenyl)-4-yl(phenyl)methanol (**3fa**).

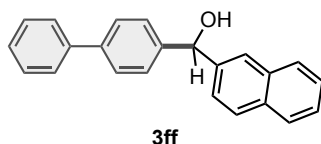


Conditions C: The reaction was conducted with **1f** (233.9 mg, 1.0 mmol), THF (1.5 mmol for the first step, 2.5 mmol for the second step) and **2a** (54.1 mg, 0.51 mmol). The product **3fa** was obtained in 75% yield (99.3 mg, 0.38 mmol) as a white solid.

Conditions D: The reaction was conducted with **1f** (174.9 mg, 0.75 mmol) and **2a** (53.3 mg, 0.50 mmol). The product **3fa** was obtained in 76% yield (99.8 mg, 0.38 mmol) as a white solid. ^1H and ^{13}C NMR of the product **3fa** were in agreement with the literature.^[23]

^1H NMR (400 MHz, CDCl_3 , δ): 2.47 (s, 1H), 5.81 (s, 1H), 7.25 (tt, $J = 1.8, 7.2$ Hz, 1H), 7.29–7.35 (m, 3H), 7.36–7.43 (m, 6H), 7.50–7.57 (m, 4H). ^{13}C NMR (101 MHz, CDCl_3 , δ): 75.9 (CH), 126.5 (CH), 126.9 (CH), 127.0 (CH), 127.17 (CH), 127.23 (CH), 127.6 (CH), 128.5 (CH), 128.7 (CH), 140.4 (C), 140.7 (C), 142.7 (C), 143.7 (C). HRMS-EI (m/z): $[\text{M}]^+$ calcd for $\text{C}_{19}\text{H}_{16}\text{O}$, 260.1201; found, 260.1205.

(1,1'-Biphenyl)-4-yl(naphthalen-2-yl)methanol (3ff**).**

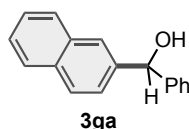


Conditions C: The reaction was conducted with **1f** (233.7 mg, 1.0 mmol), THF (1.5 mmol for the first step, 2.5 mmol for the second step) and **2f** (78.3 mg, 0.50 mmol). The product **3ff** was obtained in 76% yield (118.4 mg, 0.38 mmol) as a white solid.

Conditions D: The reaction was conducted with **1f** (174.4 mg, 0.75 mmol) and **2f** (78.0 mg, 0.50 mmol). The product **3ff** was obtained in 60% yield (92.4 mg, 0.30 mmol) as a white solid. ^1H and ^{13}C NMR of the product **3ff** were in agreement with the literature.^[37]

^1H NMR (400 MHz, CDCl_3 , δ): 2.43 (d, $J = 3.6$ Hz, 1H), 6.01 (d, $J = 2.4$ Hz, 1H), 7.32 (tt, $J = 1.5, 7.4$ Hz, 1H), 7.38–7.50 (m, 7H), 7.52–7.58 (m, 4H), 7.77–7.87 (m, 3H), 7.91 (s, 1H). ^{13}C NMR (101 MHz, CDCl_3 , δ): 76.1 (CH), 124.7 (CH), 125.0 (CH), 126.0 (CH), 126.2 (CH), 127.06 (CH), 127.11 (CH), 127.3 (CH), 127.7 (CH), 128.1 (CH), 128.4 (CH), 128.7 (CH), 132.9 (C), 133.2 (C), 140.5 (C), 140.7 (C), 141.0 (C), 142.6 (C). HRMS-EI (m/z): $[\text{M}]^+$ calcd for $\text{C}_{23}\text{H}_{18}\text{O}$, 310.1358; found, 310.1350.

Naphthalen-2-yl(phenyl)methanol (3ga**).**



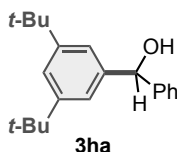
Conditions C: The reaction was conducted with **1g** (207.2 mg, 1.0 mmol), THF (1.5 mmol for the first step, 2.5 mmol for the second step) and **2a** (53.9 mg, 0.51 mmol). The product **3ga** was obtained in 77% yield (91.7 mg, 0.39 mmol) as a white solid. ^1H and ^{13}C NMR of the product **3ga** were in agreement with the literature.²³

Conditions D: The reaction was conducted with **1g** (156.0 mg, 0.75 mmol) and **2a** (52.6 mg, 0.50

mmol). The product **3ga** was obtained in 61% NMR yield.

¹H NMR (400 MHz, CDCl₃, δ): 2.32 (d, *J* = 3.6 Hz, 1H), 6.01 (d, *J* = 3.6 Hz, 1H), 7.25–7.30 (m, 1H), 7.34 (tt, *J* = 1.7, 7.3 Hz, 2H), 7.40–7.45 (m, 3H), 7.47 (quint, *J* = 3.1 Hz, 2H), 7.77–7.86 (m, 3H), 7.90 (s, 1H). ¹³C NMR (101 MHz, CDCl₃, δ): 76.3 (CH), 124.7 (CH), 125.0 (CH), 125.9 (CH), 126.2 (CH), 126.7 (CH), 127.6 (CH), 128.0 (CH), 128.3 (CH), 128.5 (CH), 132.8 (C), 133.2 (C), 141.0 (C), 143.6 (C). HRMS-EI (*m/z*): [*M*]⁺ calcd for C₁₇H₁₄O, 234.1045; found, 234.1046.

(3,5-Di-*tert*-butylphenyl)(phenyl)methanol (**3ha**).

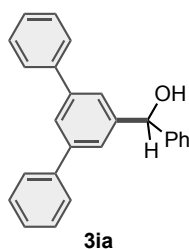


Conditions C: The reaction was conducted with **1h** (269.8 mg, 1.0 mmol), THF (1.5 mmol for the first step, 2.5 mmol for the second step) and **2a** (53.8 mg, 0.51 mmol). The product **3ha** was obtained in 75% yield (112.4 mg, 0.38 mmol) as a white solid.

Conditions D: The reaction was conducted with **1h** (201.9 mg, 0.75 mmol) and **2a** (52.3 mg, 0.49 mmol). The product **3ha** was obtained in 35% NMR yield.

¹H NMR (400 MHz, CDCl₃, δ): 1.30 (s, 18H), 2.19 (d, *J* = 3.2 Hz, 1H), 5.84 (d, *J* = 3.6 Hz, 1H), 7.23 (d, *J* = 1.2 Hz, 2H), 7.24–7.29 (m, 1H), 7.31–7.37 (m, 3H), 7.38–7.43 (m, 2H). ¹³C NMR (101 MHz, CDCl₃, δ): 31.4 (CH₃), 34.9 (C), 76.9 (CH), 120.8 (CH), 121.6 (CH), 126.5 (CH), 127.3 (CH), 128.3 (CH), 142.9 (C), 143.9 (C), 150.8 (C). HRMS-EI (*m/z*): [*M*]⁺ calcd for C₂₁H₂₈O, 296.2140; found, 296.2135.

(1,1':3',1''-Terphenyl)-5'-yl(phenyl)methanol (**3ia**).



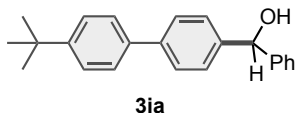
Conditions C: The reaction was conducted with **1i** (309.2 mg, 1.0 mmol), THF (1.5 mmol for the first step, 2.5 mmol for the second step) and **2a** (53.8 mg, 0.51 mmol). The product **3ia** was obtained in 82% yield (139.4 mg, 0.41 mmol) as a white solid.

Conditions D: The reaction was conducted with **1i** (231.6 mg, 0.75 mmol) and **2a** (53.6 mg, 0.50 mmol). The product **3ia** was obtained in 61% NMR yield.

¹H NMR (400 MHz, CDCl₃, δ): 2.43 (s, 1H), 5.92 (s, 1H), 7.25 (tt, *J* = 1.7, 7.3 Hz, 1H), 7.30–7.36 (m, 4H), 7.39–7.45 (m, 6H), 7.56–7.60 (m, 4H), 7.61 (t, *J* = 1.8 Hz, 2H), 7.69 (t, *J* = 1.6 Hz, 1H). ¹³C

NMR (101 MHz, CDCl₃, δ): 76.3 (CH), 124.3 (CH), 125.4 (CH), 126.5 (CH), 127.3 (CH), 127.5 (CH), 127.7 (CH), 128.6 (CH), 128.7 (CH), 140.9 (C), 142.0 (C), 143.6 (C), 144.8 (C). HRMS-EI (m/z): [M]⁺ calcd for C₂₅H₂₀O, 336.1514; found, 336.1503.

[4'-(*tert*-Butyl)-(1,1'-biphenyl)-4-yl](phenyl)methanol (3ja).

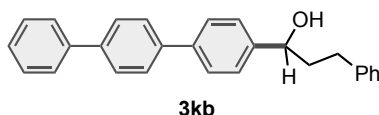


Conditions C: The reaction was conducted with **1j** (289.5 mg, 1.0 mmol), THF (1.5 mmol for the first step, 2.5 mmol for the second step) and **2a** (52.7 mg, 0.50 mmol). The product was obtained in 79% yield (124.8 mg, 0.39 mmol) as a white solid.

Conditions D: The reaction was conducted with **1j** (217.1 mg, 0.75 mmol) and **2a** (53.5 mg, 0.50 mmol). The product **3ja** was not detected by ¹H NMR.

¹H NMR (400 MHz, CDCl₃, δ): 1.35 (s, 9H), 2.29 (s, 1H), 5.87 (s, 1H), 7.27 (tt, *J* = 1.7, 7.2 Hz, 1H), 7.32–7.38 (m, 2H), 7.39–7.47 (m, 6H), 7.51 (dt, *J* = 2.0, 8.7 Hz, 2H), 7.55 (dt, *J* = 1.8, 8.1 Hz, 2H). ¹³C NMR (101 MHz, CDCl₃, δ): 31.3 (CH₃), 34.5 (C), 76.0 (CH), 125.7 (CH), 126.5 (CH), 126.7 (CH), 126.9 (CH), 127.1 (CH), 127.6 (CH), 128.5 (CH), 137.8 (C), 140.3 (C), 142.5 (C), 143.7 (C), 150.3 (C). HRMS-EI (m/z): [M]⁺ calcd for C₂₃H₂₄O, 316.1827; found, 316.1816.

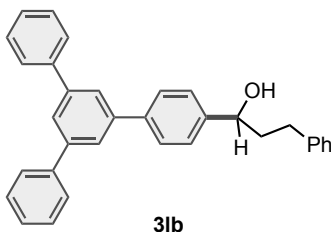
(1,1':3',1''-Terphenyl)-5'-yl(phenyl)methanol (3kb).



Conditions C: The reaction was conducted with **1k** (309.6 mg, 1.0 mmol), THF (1.5 mmol for the first step, 2.5 mmol for the second step) and **2b** (68.7 mg, 0.51 mmol). The product **3kb** was obtained in 42% yield (72.4 mg, 0.20 mmol) as a white solid.

¹H NMR (392 MHz, CDCl₃, δ): 1.87 (d, *J* = 3.5 Hz, 1H), 2.03–2.25 (m, 2H), 2.67–2.85 (m, 2H), 4.73–4.80 (m, 1H), 7.17–7.24 (m, 3H), 7.27–7.32 (m, 2H), 7.34–7.39 (m, 1H), 7.43–7.49 (m, 4H), 7.62–7.66 (m, 4H), 7.68 (s, 4H). ¹³C NMR (99 MHz, DMSO-d₆, 70 °C, δ): 31.3 (CH₂), 40.5 (CH₂), 71.2 (CH), 125.2 (CH), 125.9 (CH), 126.19 (CH), 126.21 (CH), 126.7 (CH), 126.8 (CH), 127.1 (CH), 127.9 (CH), 128.6 (CH), 137.8 (C), 138.7 (C), 138.9 (C), 139.5 (C), 141.8 (C), 145.2 (C). HRMS-EI (m/z): [M]⁺ calcd for C₂₇H₂₄O, 364.1827; found, 364.1825.

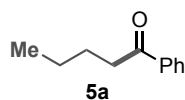
3-Phenyl-1-[5'-phenyl-(1,1':3',1''-terphenyl)-4-yl]propan-1-ol (**3lb**)



Conditions C: The reaction was conducted with **11** (384.7 mg, 1.0 mmol), THF (1.5 mmol for the first step, 2.5 mmol for the second step) and **2b** (66.9 mg, 0.50 mmol). The product **3lb** was obtained in 39% yield (85.9 mg, 0.19 mmol) as a white solid.

^1H NMR (392 MHz, CDCl_3 , δ): 1.89 (d, $J = 3.5$ Hz, 1H), 2.04–2.28 (m, 2H), 2.67–2.87 (m, 2H), 4.74–4.81 (m, 1H), 7.18–7.33 (m, 5H), 7.37–7.43 (m, 2H), 7.45–7.52 (m, 6H), 7.68–7.73 (m, 6H), 7.79 (s, 3H). ^{13}C NMR (99 MHz, CDCl_3 , δ): 32.0 (CH_2), 40.4 (CH_2), 73.5 (CH), 125.0 (CH), 125.1 (CH), 125.8 (CH), 126.4 (CH), 127.3 (CH), 127.4 (CH), 127.5 (CH), 128.36 (CH), 128.41 (CH), 128.8 (CH), 140.3 (C), 141.0 (C), 141.7 (C), 141.8 (C), 142.3 (C), 143.8 (C). HRMS-EI (m/z): $[\text{M}+\text{Na}]^+$ calcd for $\text{C}_{33}\text{H}_{28}\text{ONa}$, 463.2032; found, 463.2033.

1-Phenylpentan-1-one (**5a**).

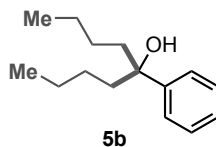


Conditions E: The reaction was conducted with **1d** (102.3 mg, 0.75 mmol) and **4a** (86.8 mg, 0.53 mmol). The product **5a** was obtained in 60% NMR yield and 44% isolated yield (37.7 mg, 0.23 mmol) as a pale-yellow oil.

Conditions F: The reaction was conducted with **1d** (107 μL , 1.0 mmol) and **4a** (82.5 mg, 0.50 mmol). The product **5a** was obtained in 53% yield (43.3 mg, 0.27 mmol) as a pale-yellow oil. ^1H and ^{13}C NMR of the product **5a** were in agreement with the literature.^[38]

^1H NMR (400 MHz, CDCl_3 , δ): 0.96 (t, $J = 7.4$ Hz, 3H), 1.42 (sex, $J = 7.4$ Hz, 2H), 1.73 (quint, $J = 7.4$ Hz, 2H), 2.97 (t, $J = 7.6$ Hz, 2H), 7.46 (t, $J = 7.4$ Hz, 2H), 7.56 (tt, $J = 1.7, 7.3$ Hz, 1H), 7.95–7.99 (m, 2H). ^{13}C NMR (100 MHz, CDCl_3 , δ): 13.9 (CH_3), 22.5 (CH_2), 26.4 (CH_2), 38.3 (CH_2), 128.0 (CH), 128.5 (CH), 132.8 (CH), 137.0 (C), 200.6 (C). HRMS-EI (m/z): $[\text{M}]^+$ calcd for $\text{C}_{11}\text{H}_{14}\text{O}$, 162.1045; found, 162.1044.

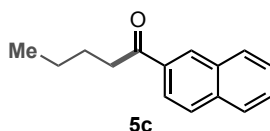
5-Phenylnonan-5-ol (5b).



Conditions G: The reaction was conducted with **1d** (136.1 mg, 1.0 mmol) and **4b** (45.5 mg, 0.33 mmol). The product **5b** was obtained in 61% yield (44.7 mg, 0.20 mmol) as a colorless oil. ^1H and ^{13}C NMR of the product **5b** were in agreement with the literature.^[32]

^1H NMR (400 MHz, CDCl_3 , δ): 0.83 (t, $J = 7.2$ Hz, 6H), 0.96–1.08 (m, 2H), 1.18–1.33 (m, 6H), 1.67 (s, 1H), 1.72–1.88 (m, 4H), 7.22 (t, $J = 7.2$ Hz, 1H), 7.31–7.40 (m, 4H). ^{13}C NMR (100 MHz, CDCl_3 , δ): 14.0 (CH_3), 23.1 (CH_2), 25.6 (CH_2), 42.7 (CH_2), 125.2 (CH), 126.2 (CH), 128.0 (CH), 146.5 (C). HRMS-ESI (m/z): $[\text{M}-\text{H}]^+$ calcd for $\text{C}_{15}\text{H}_{23}\text{O}$, 219.1754; found, 219.1752.

1-(Naphthalen-2-yl)pentan-1-one (5c).

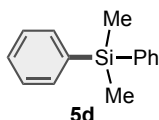


Conditions E: The reaction was conducted with **1d** (102.4 mg, 0.75 mmol) and **4c** (76.6 mg, 0.50 mmol). The product **5c** was obtained in 40% NMR yield.

Conditions F: The reaction was conducted with **1d** (136.8 mg, 1.0 mmol) and **4c** (76.8 mg, 0.50 mmol). The product **5c** was obtained in 52% yield (55.5 mg, 0.26 mmol) as a yellow solid. ^1H and ^{13}C NMR of the product **5c** were in agreement with the literature.^[38]

^1H NMR (400 MHz, CDCl_3 , δ): 0.99 (t, $J = 7.2$ Hz, 3H), 1.46 (sex, $J = 7.4$ Hz, 2H), 1.79 (quint, $J = 7.5$ Hz, 2H), 3.11 (t, $J = 7.2$ Hz, 2H), 7.53–7.63 (m, 2H), 7.89 (t, $J = 7.8$ Hz, 2H), 7.98 (d, $J = 8.0$ Hz, 1H), 8.04 (dd, $J = 1.8, 8.6$ Hz, 1H), 8.48 (s, 1H). ^{13}C NMR (100 MHz, CDCl_3 , δ): 14.0 (CH_3), 22.5 (CH_2), 26.6 (CH_2), 38.4 (CH_2), 123.9 (CH), 126.6 (CH), 127.7 (CH), 128.26 (CH), 128.32 (CH), 129.47 (CH), 129.54 (CH), 132.5 (C), 134.3 (C), 135.4 (C), 200.5 (C). HRMS-EI (m/z): $[\text{M}]^+$ calcd for $\text{C}_{15}\text{H}_{16}\text{O}$, 212.1201; found, 212.1201.

Dimethyldiphenylsilane (5d).



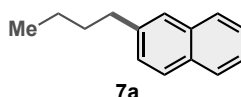
Conditions E: The reaction was conducted with **1a** (118.4 mg, 0.75 mmol), **4d** (85 mg, 0.50 mmol), and CuI (23.6 mg, 0.13 mmol). The product **5d** was obtained in 62% yield (66.0 mg, 0.31 mmol) as a colorless oil.

Conditions F: The reaction was conducted with **1a** (157.0 mg, 1.0 mmol), **4d** (85.5 mg, 0.50 mmol),

and CuI (23.8 mg, 0.13 mmol). The product **5d** was obtained in 46% yield (49.4 mg, 0.23 mmol) as a colorless oil. ¹H and ¹³C NMR of the product **5d** were in agreement with the literature.^[39]

¹H NMR (400 MHz, CDCl₃, δ): 0.55 (s, 6H), 7.32–7.41 (m, 6H), 7.48–7.55 (m, 4H). ¹³C NMR (100 MHz, CDCl₃, δ): –2.4 (CH₃), 127.8 (CH), 129.1 (CH), 134.2 (CH), 138.2 (C). HRMS-EI (m/z): [M]⁺ calcd for C₁₄H₁₆Si, 212.1021; found, 212.1018.

2-Butylnaphthalene (**7a**).

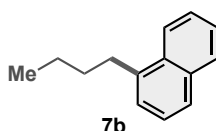


Conditions H: The reaction was conducted with **1d** (69.8 mg, 0.50 mmol) and **6a** (98.8 mg, 0.33 mmol). The product **7a** was obtained in 35% NMR yield.

Conditions I: The reaction was conducted with **1d** (136.8 mg, 1.0 mmol) and **6a** (98.6 mg, 0.33 mmol). The reaction time of the second step was shortened to 30 minutes. The product **7a** was obtained in 75% yield (45.6 mg, 0.25 mmol) as a colorless oil. ¹H and ¹³C NMR of the product **7a** were in agreement with the literature.^[40]

¹H NMR (400 MHz, CDCl₃, δ): 0.95 (t, *J* = 7.4 Hz, 3H), 1.40 (sex, *J* = 7.4 Hz, 2H), 1.65–1.73 (m, 2H), 2.78 (t, *J* = 7.6 Hz, 2H), 7.34 (dd, *J* = 1.8, 8.4 Hz, 1H), 7.42 (dq, *J* = 1.6, 7.3 Hz, 2H), 7.61 (s, 1H), 7.73–7.82 (m, 3H). ¹³C NMR (99 MHz, CDCl₃, δ): 14.0 (CH₃), 22.4 (CH₂), 33.5 (CH₂), 35.8 (CH₂), 124.9 (CH), 125.8 (CH), 126.3 (CH), 127.36 (CH), 127.44 (CH), 127.6 (CH), 127.7 (CH), 131.9 (C), 133.6 (C), 140.4 (C). HRMS-EI (m/z): [M]⁺ calcd for C₁₄H₁₆, 184.1252; found, 184.1250.

1-Butylnaphthalene (**7b**).



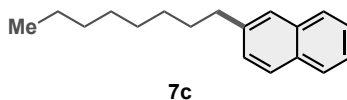
Conditions H: The reaction was conducted with **1d** (69.1 mg, 0.50 mmol) and **6b** (98.6 mg, 0.33 mmol). The product **7b** was obtained in 44% NMR yield.

Conditions I: The reaction was conducted with **1d** (136.5 mg, 1.0 mmol) and **6b** (98.6 mg, 0.33 mmol). The reaction time of the second step was shortened to 30 minutes. The product **7b** was obtained in 70% yield (42.6 mg, 0.23 mmol) as a colorless oil. ¹H and ¹³C NMR of the product **7b** were in agreement with the literature.^[40]

¹H NMR (400 MHz, CDCl₃, δ): 0.97 (t, *J* = 7.4 Hz, 3H), 1.46 (sex, *J* = 7.4 Hz, 2H), 1.51–1.70 (m, 2H), 3.07 (t, *J* = 8.0 Hz, 2H), 7.32 (d, *J* = 6.8 Hz, 1H), 7.39 (t, *J* = 7.6 Hz, 1H), 7.44–7.53 (m, 2H), 7.70 (d, *J* = 8.0 Hz, 1H), 7.85 (d, *J* = 7.6 Hz, 1H), 8.05 (d, *J* = 8.4 Hz, 1H). ¹³C NMR (100 MHz, CDCl₃, δ): 14.0 (CH₃), 22.9 (CH₂), 32.8 (CH₂), 33.0 (CH₂), 123.9 (CH), 125.3 (CH), 125.50 (CH),

125.57 (CH), 125.8 (CH), 126.3 (CH), 128.7 (CH), 131.9 (C), 133.9 (C), 139.0 (C). HRMS-EI (m/z): [M]⁺ calcd for C₁₄H₁₆, 184.1252; found, 184.1252.

2-Octylnaphthalene (7c).

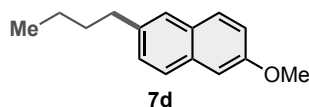


Conditions H: The reaction was conducted with **1m** (96.0 mg, 0.50 mmol) and **6a** (98.8 mg, 0.33 mmol). The product **7c** was obtained in 31% NMR yield.

Conditions I: The reaction was conducted with **1m** (193.7 mg, 1.0 mmol) and **6a** (98.5 mg, 0.33 mmol). The product **7c** was obtained in 88% yield (69.7 mg, 0.29 mmol) as a colorless oil. ¹H and ¹³C NMR of the product **7c** were in agreement with the literature.^[40]

¹H NMR (400 MHz, CDCl₃, δ): 0.88 (t, *J* = 6.8 Hz, 3H), 1.18–1.42 (m, 10H), 1.70 (quint, *J* = 7.5 Hz, 2H), 2.76 (t, *J* = 7.6 Hz, 2H), 7.33 (dd, *J* = 1.8, 8.6 Hz, 1H), 7.42 (dq, *J* = 1.4, 6.8 Hz, 2H), 7.61 (s, 1H), 7.73–7.83 (m, 3H). ¹³C NMR (101 MHz, CDCl₃, δ): 14.1 (CH₃), 22.7 (CH₂), 29.3 (CH₂), 29.4 (CH₂), 29.5 (CH₂), 31.4 (CH₂), 31.9 (CH₂), 36.1 (CH₂), 124.9 (CH), 125.8 (CH), 126.3 (CH), 127.37 (CH), 127.43 (CH), 127.6 (CH), 127.7 (CH), 131.9 (C), 133.6 (C), 140.4 (C). HRMS-EI (m/z): [M]⁺ calcd for C₁₈H₂₄, 240.1878; found, 240.1876.

2-Butyl-6-methoxynaphthalene (7d).

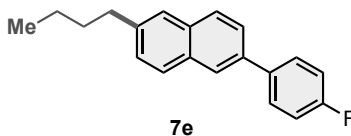


Conditions H: The reaction was conducted with **1d** (67.7 mg, 0.50 mmol) and **6c** (108.4 mg, 0.33 mmol). The product **7d** was obtained in 26% NMR yield.

Conditions I: The reaction was conducted with **1d** (107 μL, 1.0 mmol) and **6c** (108.2 mg, 0.33 mmol). The product **7d** was obtained in 36% yield (25.7 mg, 0.12 mmol) as a white solid. ¹H and ¹³C NMR of the product **7d** were in agreement with the literature.^[41]

¹H NMR (400 MHz, CDCl₃, δ): 0.94 (t, *J* = 7.2 Hz, 3H), 1.33–1.44 (m, 2H), 1.63–1.72 (m, 2H), 2.74 (t, *J* = 7.6 Hz, 2H), 3.91 (s, 3H), 7.10–7.13 (m, 2H), 7.30 (dd, *J* = 2.0, 8.6 Hz, 1H), 7.54 (s, 1H), 7.64–7.69 (m, 2H). ¹³C NMR (99 MHz, CDCl₃, δ): 14.0 (CH₃), 22.4 (CH₂), 33.6 (CH₂), 35.6 (CH₂), 55.2 (CH₃), 105.6 (CH), 118.5 (CH), 126.1 (CH), 126.6 (CH), 127.9 (CH), 128.8 (CH), 129.1 (C), 132.8 (C), 138.1 (C), 157.0 (C). HRMS-EI (m/z): [M]⁺ calcd for C₁₅H₁₈O, 214.1358; found, 214.1358.

2-Butyl-6-(4-fluorophenyl)naphthalene (7e).

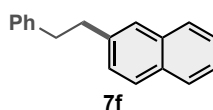


Conditions H: The reaction was conducted with **1d** (69.2 mg, 0.50 mmol) and **6d** (129.2 mg, 0.33 mmol). The product **7d** was obtained in 41% NMR yield.

Conditions I: The reaction was conducted with **1d** (137.0 mg, 1.0 mmol) and **6d** (129.7 mg, 0.33 mmol). The product **7d** was obtained in 79% yield (72.4 mg, 0.26 mmol) as a white solid.

^1H NMR (396 MHz, CDCl_3 , δ): 0.96 (t, $J = 7.3$ Hz, 3H), 1.41 (sex, $J = 7.4$ Hz, 2H), 1.65–1.75 (m, 2H), 2.79 (t, $J = 7.7$ Hz, 2H), 7.16 (tt, $J = 2.5, 9.1$ Hz, 2H), 7.37 (dd, $J = 1.4, 8.5$ Hz, 1H), 7.61–7.69 (m, 4H), 7.81 (d, $J = 8.3$ Hz, 1H), 7.84 (d, $J = 8.3$ Hz, 1H), 7.94 (s, 1H). ^{13}C NMR (100 MHz, CDCl_3 , δ): 14.0 (CH_3), 22.4 (CH_2), 33.5 (CH_2), 35.8 (CH_2), 115.6 (d, $J = 21.0$ Hz, CH), 125.3 (CH), 125.4 (CH), 126.0 (CH), 127.9 (CH), 127.99 (CH), 128.01 (CH), 128.8 (d, $J = 7.6$ Hz, CH), 132.1 (C), 132.7 (C), 136.7 (C), 137.4 (d, $J = 2.9$ Hz, C), 140.7 (C), 162.4 (d, $J = 247.0$ Hz, CH). HRMS-EI (m/z): $[\text{M}]^+$ calcd for $\text{C}_{20}\text{H}_{19}\text{F}$, 278.1471; found, 278.1465.

2-Phenethylnaphthalene (7f).

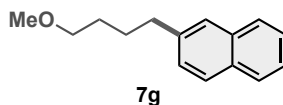


Conditions H: The reaction was conducted with **1n** (93.2 mg, 0.50 mmol) and **6a** (98.4 mg, 0.33 mmol). The product **7f** was obtained in 16% NMR yield.

Conditions I: The reaction was conducted with **1n** (185.5 mg, 1.0 mmol) and **6a** (98.6 mg, 0.33 mmol). The product **7f** was obtained in 78% yield (59.6 mg, 0.26 mmol) as a white solid. ^1H and ^{13}C NMR of the product **7f** were in agreement with the literature.^[42]

^1H NMR (400 MHz, CDCl_3 , δ): 2.96–3.03 (m, 2H), 3.04–3.12 (m, 2H), 7.16–7.23 (m, 3H), 7.24–7.30 (m, 2H), 7.32 (dd, $J = 1.6, 8.4$ Hz, 1H), 7.37–7.47 (m, 2H), 7.60 (s, 1H), 7.72–7.84 (m, 3H). ^{13}C NMR (101 MHz, CDCl_3 , δ): 37.8 (CH_2), 38.1 (CH_2), 125.1 (CH), 125.85 (CH), 125.92 (CH), 126.4 (CH), 127.3 (CH), 127.4 (CH), 127.6 (CH), 127.8 (CH), 128.3 (CH), 128.5 (CH), 132.0 (C), 133.6 (C), 139.2 (C), 141.7 (C). HRMS-EI (m/z): $[\text{M}]^+$ calcd for $\text{C}_{18}\text{H}_{16}$, 232.1252; found, 232.1244.

2-(4-methoxybutyl)naphthalene (7g).

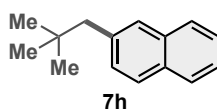


Conditions H: The reaction was conducted with **1o** (83.8 mg, 0.50 mmol) and **6a** (98.4 mg, 0.33 mmol). The product **7g** was obtained in 21% NMR yield.

Conditions I: The reaction was conducted with **1o** (167.7 mg, 1.0 mmol) and **6a** (98.6 mg, 0.33 mmol). The product **7g** was obtained in 87% yield (61.8 mg, 0.29 mmol) as a colorless oil. ¹H and ¹³C NMR of the product **7g** were in agreement with the literature.^[42]

¹H NMR (400 MHz, CDCl₃, δ): 1.61–1.70 (m, 2H), 1.73–1.83 (m, 2H), 2.80 (t, *J* = 7.4 Hz, 2H), 3.33 (s, 3H), 3.41 (t, *J* = 6.5 Hz, 2H), 7.34 (dd, *J* = 1.6, 8.2 Hz, 1H), 7.43 (dq, *J* = 1.2, 6.8 Hz, 2H), 7.62 (s, 1H), 7.75–7.82 (m, 3H). ¹³C NMR (99 MHz, CDCl₃, δ): 27.8 (CH₂), 29.3 (CH₂), 35.8 (CH₂), 58.5 (CH₃), 72.6 (CH₂), 125.0 (CH), 125.8 (CH), 126.3 (CH), 127.31 (CH), 127.35 (CH), 127.5 (CH), 127.7 (CH), 131.9 (C), 133.6 (C), 139.9 (C). HRMS-EI (*m/z*): [M]⁺ calcd for C₁₅H₁₈O, 214.1358; found, 214.1357.

2-Neopentyl-naphthalene (**7h**).

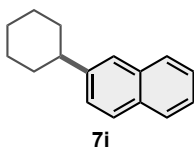


Conditions H: The reaction was conducted with **1p** (75.5 mg, 0.50 mmol) and **6a** (98.3 mg, 0.33 mmol). The product **7h** was obtained in 4% NMR yield.

Conditions I: The reaction was conducted with **1p** (151.5 mg, 1.0 mmol) and **6a** (98.4 mg, 0.33 mmol). The reaction time of the second step was 30 minutes. The product **7h** was obtained in 43% yield (27.9 mg, 0.25 mmol) as a white solid. ¹H and ¹³C NMR of the product **7h** were in agreement with the literature.^[43]

¹H NMR (400 MHz, CDCl₃, δ): 0.95 (s, 9H), 2.65 (s, 2H), 7.28 (d, *J* = 8.4 Hz, 1H), 7.42 (quint, *J* = 6.9 Hz, 2H), 7.56 (s, 1H), 7.73 (d, *J* = 8.4 Hz, 1H), 7.79 (t, *J* = 8.2 Hz, 2H). ¹³C NMR (101 MHz, CDCl₃, δ): 29.5 (CH₃), 32.1 (C), 50.3 (CH₂), 125.0 (CH), 125.7 (CH), 126.8 (CH), 127.50 (CH), 127.52 (CH), 128.6 (CH), 129.5 (CH), 131.9 (C), 133.2 (C), 137.4 (C). HRMS-EI (*m/z*): [M]⁺ calcd for C₁₅H₁₈, 198.1409; found, 198.1412.

2-Cyclohexyl-naphthalene (**7i**).



Conditions H: The reaction was conducted with **1e** (82.7 mg, 0.50 mmol) and **6a** (98.4 mg, 0.33 mmol). The product **7i** was not obtained.

Conditions I: The reaction was conducted with **1e** (164.0 mg, 1.0 mmol) and **6a** (98.5 mg, 0.33 mmol). The reaction time was 90 minutes for the first step and 30 minutes for the second step. The product **7i** was obtained in 40% yield (27.5 mg, 0.13 mmol) as a pale orange oil. ¹H and ¹³C NMR of the product **7i** were in agreement with the literature.^[40]

¹H NMR (400 MHz, CDCl₃, δ): 1.29 (tq, *J* = 4.0, 12.5 Hz, 1H), 1.38–1.60 (m, 4H), 1.74–1.82 (m, 1H), 1.84–1.92 (m, 2H), 1.93–2.01 (m, 2H), 2.66 (tt, *J* = 3.3, 11.5 Hz, 1H), 7.35–7.48 (m, 3H), 7.63 (s, 1H), 7.74–7.83 (m, 3H). ¹³C NMR (101 MHz, CDCl₃, δ): 26.2 (CH₂), 26.9 (CH₂), 34.4 (CH₂), 44.6 (CH), 124.5 (CH), 125.0 (CH), 125.7 (CH), 126.2 (CH), 127.51 (CH), 127.55 (CH), 127.7 (CH), 132.1 (C), 133.6 (C), 145.5 (C). HRMS-EI (*m/z*): [M] calcd for C₁₆H₁₈, 210.1409; found, 210.1403.

References

1. Lei, X.; Jalla, A.; Shama, M. A. A.; Stafford, J. M.; Cao, B. *Synthesis* **2015**, *47*, 2578–2585.
2. Hiraya, A.; Watanabe, M.; Sham, T. K. *Rev. Sci. Instrum.* **1995**, *66*, 1528–1530.
3. A 1.0 M THF solution of phenylmagnesium bromide (Cat. No. 32141-25) was purchase from TCI and used after sonication to completely dissolve the precipitation of magnesium halide.
4. Hatsui, T.; Shigemasa, E.; Kosugi, N. *AIP Conf. Proc.* **2004**, *705*, 921–924.
5. Ravel, B.; Newville, M. *J. Synchrotron Radiat.* **2005**, *12*, 537–541.
6. Mori, T.; Kato, S. *J. Phys. Chem. A* **2009**, *113*, 6158–6165.
7. Peltzer, R. M.; Eisenstein, O.; Nova, A.; Cascella, M. *J. Phys. Chem. B* **2017**, *121*, 4226–4237.
8. Peltzer, R. M.; Gauss, J.; Eisenstein, O.; Cascella, M. *J. Am. Chem. Soc.* **2020**, *142*, 2984–2994.
9. Maeda, S.; Harabuchi, Y.; Takagi, M.; Taketsugu, T.; Morokuma, K. *Chem. Rec.* **2016**, *16*, 2232–2248.
10. Maeda, S.; Harabuchi, Y.; Takagi, M.; Saita, K.; Suzuki, K.; Ichino, T.; Sumiya, T.; Sugiyama, K.; Ono, Y. *J. Comput. Chem.* **2018**, *39*, 233–251.
11. Grimme, S.; Bannwarth, C.; Shushkov, P. *J. Chem. Theory Comput.* **2017**, *13*, 1989–2009.
12. Bursch, M.; Neugebauer, H.; Grimmer, S. *Angew. Chem., Int. Ed.* **2019**, *58*, 11078–11087.
13. Neese, F. *WIREs Comput. Mol. Sci.* **2012**, *2*, 73–78.
14. Neese, F. *WIREs Comput. Mol. Sci.* **2018**, *8*, e1327.
15. Becke, A. D. *Phys. Rev. A* **1988**, *38*, 3098–3100.
16. Becke, A. D. *J. Chem. Phys.* **1933**, *98*, 1372–1377.
17. Lee, C.; Yang, W.; Parr, R. G. *Phys. Rev. B* **1988**, *37*, 785–789.
18. Grimme, S.; Antony, J.; Ehrlich, S.; Krieg, H. *J. Chem. Phys.* **2010**, *132*, 154104.
19. Weigend, F.; Ahlrichs, R. *Phys. Chem. Chem. Phys.* **2005**, *7*, 3297–3305.
20. Weigend, F. *Phys. Chem. Chem. Phys.* **2006**, *8*, 1057–1065.
21. Neese, F.; Wennmohs, F.; Hansen, A.; Becker, U. *Chem. Phys.* **2009**, *356*, 98–109.
22. Izsák, R.; Neese, F. *J. Chem. Phys.* **2011**, *135*, 144105.
23. Gaykar, R. N.; Bhunia, A.; Biju, A. T. *J. Org. Chem.* **2018**, *83*, 11333–11340.
24. Liao, Y.-X.; Xing, C.-H.; Hu, Q.-S. *Org. Lett.* **2012**, *14*, 1544–1547.
25. Zhu, Q.; He, Z.; Wang, L.; Hu, Y.; Xia, C.; Liu, C. *Chem. Commun.* **2019**, *55*, 11884–11887.
26. Ng, T. W.; Liao, G.; Lau, K. K.; Pan, H.-J.; Zhao, Y. *Angew. Chem., Int. Ed.* **2020**, *59*, 11384–11389.
27. Shen, Z.-L.; Yeo, Y.-L.; Loh, T.-P. *J. Org. Chem.* **2008**, *73*, 3922–3924.
28. Yamamoto, T.; Ohta, T.; Ito, Y. *Org. Lett.* **2005**, *7*, 4153–4155.
29. Polidano, K.; Reed-Berendt, B. G.; Basset, A.; Watson, A. J. A.; Williams, J. M. J.; Morrill, L. C. *Org. Lett.* **2017**, *19*, 6716–6719.

30. Wu, X.; Li, X.; Huang, W.; Wang, Y.; Xu, H.; Cai, L.; Qu, J.; Chen, Y. *Org. Lett.* **2019**, *21*, 2453–2458.
31. Fernández-Mateos, E.; Maciá, B.; Yus, M. *Adv. Synth. Catal.* **2013**, *355*, 1249–1254.
32. Chen, D.; Zhang, Y.; Pan, X.; Wang, F.; Huang, S. *Adv. Synth. Catal.* **2018**, *360*, 3607–3612.
33. Too, P. C.; Tnay, Y. L.; Chiba, S. *Beilstein J. Org. Chem.* **2013**, *9*, 1217–1225.
34. Tamang, S. R.; Findlater, M. *J. Org. Chem.* **2017**, *82*, 12857–12862.
35. Bagutski, V.; French, R. M.; Aggarwal, V. K. *Angew. Chem., Int. Ed.* **2010**, *49*, 5142–5145.
36. Bieszczad, B.; Gilheany, D. G. *Angew. Chem., Int. Ed.* **2017**, *56*, 4272–4276.
37. Li, K.; Hu, N.; Luo, R.; Yuan, W.; Tang, W. A. *J. Org. Chem.* **2013**, *78*, 6350–6355.
38. Xia, Y.; Wang, J.; Dong, G. *J. Am. Chem. Soc.* **2018**, *140*, 5347–5351.
39. Morita, E.; Murakami, K.; Iwasaki, M.; Hirano, K.; Yorimitsu, H.; Oshima, K. *Bull. Chem. Soc. Jpn.* **2009**, *82*, 1012–1014.
40. Sumida, Y.; Sumida, T.; Hosoya, T. *Synthesis* **2017**, *49*, 3590–3601.
41. Agrawal, T.; Cook, S. P. *Org. Lett.* **2013**, *15*, 96–99.
42. Tobisu, M.; Takahira, T.; Morioka, T.; Chatani, N. *J. Am. Chem. Soc.* **2016**, *138*, 6711–6714.
43. Tobisu, M.; Takahira, T.; Chatani, N. *Org. Lett.* **2015**, *17*, 4352–4355.

List of Publications

Chapter 1.

Mechanochemistry Allows Carrying Out Sensitive Organometallic Reactions in Air: Glove-Box-and-Schlenk-Line-Free Synthesis of Oxidative Addition Complexes from Aryl Halides and Palladium(0)

Kubota, K.; Takahashi, R.; Ito, H.

Chem. Sci. **2019**, *10*, 5837–5842.

Chapter 2.

Air- and Moisture-Stable Xantphos-ligated Palladium Dialkyl Complex as a Precatalyst for Cross-Coupling Reactions

Takahashi, R.; Kubota, K.; Ito, H.

Chem. Commun. **2020**, *56*, 407–410.

Chapter 3.

Mechanochemical synthesis of magnesium-based carbon nucleophiles in air and their use in organic synthesis

Takahashi, R.; Hu, A.; Gao, P.; Gao, Y.; Pang, Y.; Seo, T.; Jiang, J.; Maeda, S.; Takaya, H.; Kubota, K.; Ito, H.

Nat. Commun. **2021**, *12*, 6691.

Other Publications

1. Synthesis of Acylborons by Ozonolysis of Alkenylboronates: Preparation of an Enantioenriched Amino Acid Acylboronate

Taguchi, J.; Ikeda, T.; Takahashi, R.; Sasaki, I.; Ogasawara, Y.; Dairi, T.; Kato, N.; Yamamoto, Y.; Bode, J. W.; Ito, H.

Angew. Chem. Int. Ed. **2017**, *56*, 13847–13851.

2. Concise Synthesis of Potassium Acyltrifluoroborates from Aldehydes by a Cu(I)-catalyzed Borylation/Oxidation Protocol

Taguchi, J.; Takeuchi, T.; Takahashi, R.; Masero, F.; Ito, H.

Angew. Chem. Int. Ed. **2019**, *58*, 7299–7303.

Acknowledgements

The Studies presented in this thesis have been carried out under the direction of Professor Doctor Hajime Ito at the *Faculty of Engineering, Hokkaido University* and *Institute for Chemical Reaction Design and Discovery (WPI-ICReDD), Hokkaido University* during 2016–2022. The studies are concerned with the development of novel organic transformations using mechanochemistry.

At first and foremost, I would like to express his deepest gratitude to Prof. Hajime Ito, whose constant guidance, enormous supports and insightful comments were invaluable during his study. I also would like to thank Associate Prof. Koji Kubota for his sound advice, insightful suggestions, and encouragement in the course of this study. I would also like to express my great appreciation to Takaki Mashimo, Toshiki Sumitani, and Assistant Prof. Tomohiro Seki for their help in analyzing the X-ray crystallography data, and to Prof. Hikaru Takaya, Prof. Satoshi Maeda, and Assistant Prof. Julong Jiang for their help in confirming the structure of organomagnesium reagents by X-ray absorption fine structure analysis and theoretical studies. I am indebted to Prof. Tsuneo Imamoto, Associate Prof. Tatsuo Ishiyama and Assistant Prof. Mingoo Jin for their helpful advice and stimulating discussions.

I am grateful to thank Dr. Anqi Hu, Dr. Yadong Pang, Dr. Pan Gao, Dr. Yunpeng Gao, and other members of the Prof. Ito's research group for their good collaboration and for providing a good working atmosphere. This work supported by the Ambitious Leader's Program of Hokkaido University and JSPS.

Rina Takahashi

Graduate School of Chemical Sciences and Engineering
Hokkaido University
March, 2022